Fall 2020

Distributed Cooperative Control of Multi-Agent Systems Under Detectability and Communication Constraints

Himadri Basu
University of New Hampshire, Durham

Distributed Cooperative Control of Multi-Agent Systems Under Detectability and Communication Constraints

By

Himadri Basu

Baccalaureate Degree (B. Tech), West Bengal University of Technology, 2013

Master's Degree (M.E.), Jadavpur University, 2015

DISSERTATION

Submitted to the University of New Hampshire

in Partial Fulfillment of

the Requirements for the Degree of

Doctor of Philosophy

in

Electrical and Computer Engineering

September 2020

THESIS COMMITTEE PAGE

This thesis has been examined and approved in partial fulfillment of the requirements for the degree of Doctorate of Philosophy in Electrical and Computer Engineering by:

- Thesis Director, Se Young Yoon, Assistant Professor at the Department of Electrical and Computer Engineering
- Francesco Ferrante, Assistant Professor of Control Systems at Université Grenoble Alpes
- Michael Carter, Associate Professor at the Department of Electrical and Computer Engineering
- May-Win Thein, Associate Professor at the Department of Mechanical Engineering
- Edward Song, Assistant Professor at the Department of Electrical and Computer Engineering

On September 1, 2020

Original approval signatures are on file with the University of New Hampshire Graduate School.

Abstract

Cooperative control of multi-agent systems has recently gained widespread attention from the scientific communities due to numerous applications in areas such as the formation control in unmanned vehicles, cooperative attitude control of spacecrafts, clustering of micro-satellites, environmental monitoring and exploration by mobile sensor networks, etc. The primary goal of a cooperative control problem for multi-agent systems is to design a decentralized control algorithm for each agent, relying on the local coordination of their actions to exhibit a collective behavior. Common challenges encountered in the study of cooperative control problems are unavailable group-level information, and limited bandwidth of the shared communication. In this dissertation, we investigate one of such cooperative control problems, namely cooperative output regulation, under various local and global level constraints coming from physical and communication limitations.

The objective of the cooperative output regulation problem (CORP) for multi-agent systems is to design a distributed control strategy for the agents to synchronize their state with an external system, called the leader, in the presence of disturbance inputs. For the problem at hand, we additionally consider the scenario in which none of the agents can independently access the synchronization signal from their view of the leader, and therefore it is not possible for the agents to achieve the group objective by themselves unless they cooperate among members. To this end, we devise a novel distributed estimation algorithm to collectively gather the leader states under the discussed detectability constraint, and then use this estimation to synthesize a distributed control solution to the problem.

Next, we extend our results in CORP to the case with uncertain agent dynamics arising from modeling errors. In addition to the detectability constraint, we also assumed that the local regulated error signals are not available to the agents for feedback, and thus none of the agents have all the required measurements to independently synthesize a control solution. By combining the distributed observer and a control law based on the internal model principle for the agents, we offer a solution to the robust CORP under these added constraints.

In practical applications of multi-agent systems, it is difficult to consistently maintain a reliable communication between the agents. By considering such challenge in the communication, we study the CORP for the case when agents are connected through a time-varying communication topology. Due to the presence of the detectability constraint that none of the agents can independently access all the leader states at any switching instant, we devise a distributed estimation algorithm for the agents to collectively reconstruct the leader states. Then by using this estimation, a distributed dynamic control solution is offered to solve the CORP under the added communication constraint. Since the fixed communication network is a special case of this time-varying counterpart, the offered control solution can be viewed as a generalization of the former results.

For effective validation of previous theoretical results, we apply the control algorithms to a practical case study problem on synchronizing the position of networked motors under time-varying communication. Based on our experimental results, we also demonstrate the uniqueness of derived control solutions.

Another communication constraint affecting the cooperative control performance is the presence of network delays. To this regard, first we study the distributed state estimation problem of an autonomous plant by a network of observers under

heterogeneous time-invariant delays and then extend to the time-varying counterpart. With the use of a low gain based estimation technique, we derive a sufficient stability condition in terms of the upper bound of the low gain parameter or the time delay to guarantee the convergence of estimation errors. Additionally, when the plant measurements are subject to bounded disturbances, we find that that the local estimation errors also remain bounded. Lastly, by using this estimation, we present a distributed control solution for a leader-follower synchronization problem of a multi-agent system.

Next, we present another case study concerning a synchronization control problem of a group of distributed generators in an islanded microgrid under unknown time-varying latency. Similar to the case of delayed communication in aforementioned works, we offer a low gain based distributed control protocol to synchronize the terminal voltage and inverter operating frequency.

Contents

List of Tables

List of Figures

Nomenclature

Control Theory

MAS	Multi-agent system
ORP	Output regulation problem
CORP	Cooperative output regulation problem

Chapter 1

Introduction

1.1 Cooperative Control of Multi-Agent Systems

Social behavior in animal groups are among the most remarkable phenomena observed in nature. A flock of birds wheeling and turning in unison, and a school of fish gliding spontaneously, are a few examples. These collective groups can achieve goals, like migrating or avoiding predators and obstacles, that are beyond the potential of the individual members. Such synchronized group behaviors emerge from instantaneous decisions made by independent members of the group. Thus, for the group to behave as a single entity, the actions of the agents must be coordinated through shared information between local neighbors. These collective behaviors observed in nature often serve as inspiration to engineers in the design of collaborating teams of mobile robots and autonomous unmanned vehicles, which have made ways to the arenas of air, sea, and space in support of missions pertaining to national defense, surveillance, and environmental monitoring.

Multi-agent systems (MASs) refer to a group of simple subsystems, called agents, with limited processing capabilities, locally sensed information, and limited inter-agent communications. The Cooperative control problems are defined for these MASs, and aims to design control strategies for agents to achieve a collective objective of the system. A MAS through cooperative control can perform complex tasks by coordinated actions, which may be otherwise impossible by a single agent, thus offering several advantages such as flexibility, reliability, improved efficiency and reduced cost. Because of the great interdisciplinary interest, cooperative control problem of networked MAS has attracted a great deal of attention in various fields of physics, mathematics, biology, engineering and control theory.

The cooperative control of MAS finds applications in the areas of unmanned vehicles, mobile robot systems, microsatellite clustering and sensor networks [4]. As a consequence to the growing research interest in these areas, the various aspects of the cooperative control problem actively studied in the literature include consensus [5], formation control [4,6], leader tracking or synchronization [7], and coverage control [8,9]. While each of these areas of cooperative control problem offers a unique set of challenges, the underlying goal of designing a decentralized control scheme for agents utilizing the local interaction is common to all of them.

Consensus is one of the fundamental issues in cooperative control problem in which the objective is to design a distributed control policy for each agent based on the local information, such that all of them agree upon certain states of interest. For example, such states may represent position, velocity, acceleration, or motor voltage of dynamic mobile robots as shown in Fig. 1.1, in which they agree on a direction and heading velocity to move with as a group. Surveys of the recent results can be found in the works of [10–13] and the references therein. The consensus problem has been studied under time-invariant communication networks in [14] and time-varying counterpart in [15, 16] and time-delay in [17–20].

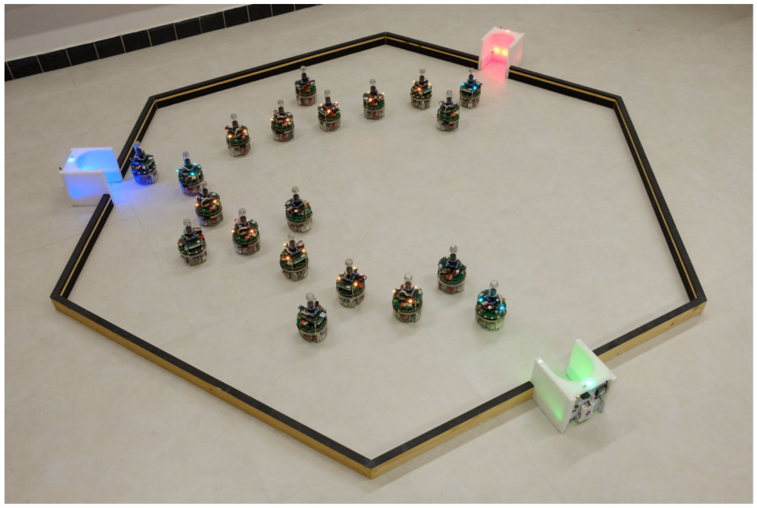

Figure 1.1: Swarm of mobile robots [1]

1.2 Cooperative Output Regulation

In this dissertation we study another important class of cooperative control problems, namely cooperative output regulation problem (CORP), which is an extension of the classical output regulation problem (ORP) to the multi-agent framework. The objective of the ORP is to regulate a prescribed output signal to zero, while keeping all the trajectories of the system bounded. The external signals affecting the system are assumed to belong to a certain class of functions generated by an exosystem. These exogenous signals generated by exosystem includes both the reference signals to be tracked and the disturbances to be rejected. The ORP was first formulated for linear systems in [21] and for nonlinear systems in [22, 23].

The goal of the CORP is to design a control strategy for the follower agents to synchronize their states with the exosystem, also referred to as leader in [24, 25], in the presence of environmental disturbances. Therefore, CORP generalizes the leader-follower tracking problems studied in [26, 27]. Various other cooperative control problems, such as output synchronization and leader tracking can also be formulated in terms of the CORP.

The MAS in the CORP may include agents which may not have direct access to the leader information. In this case, the agents are required to cooperatively estimate the leader states, and propagate this information to the rest of the group through a communication network to achieve the control objectives. The solution to the CORP must therefore incorporate information of the communication protocol to ensure the propagation of estimated leader information among all the agents in the system.

A typical scenario of the CORP, as given in [28], is motivated by a practical example where a group of tanks in a parading team is tasked to maintain a prescribed formation relative to a leader tank. While some tanks, being near, can directly sense the absolute position information from the leader, the others cannot. The tanks which have a direct access to the leader tank position, are referred to as "informed" agents in [29, 30]. The control challenge in this problem is to derive a distributed control law for the agents such that the absolute leader position is properly disseminated among the tank platoons while being subjected to noisy communication.

1.3 State of the Art in Cooperative Output Regulation Problem

Traditionally the CORP for MAS has been handled by either a feedforward approach or an internal model-based control. A preliminary form of the CORP, called synchronized output regulation problem [31, 32], was solved using a feedforward control approach for homogeneous linear MASs. Based on this feedforward control structure, the seminal works in [29, 30] proposed respectively a distributed state feedback and an output feedback control solutions for CORP.

On the other hand, the idea of classical internal model based control (IMC) was extended for MASs, and a distributed IMC approach was adopted in [28, 33] to solve the robust CORP by an eigenstructure assignment. Since the nominal system is stabilized by an eigenvalue placement method in both these papers, the IMC approach can tolerate only small variations of the uncertain parameters. The control solution offered in these papers also rely on the assumption that a specific “virtual error signal” is available to the agents for feedback. Additionally, in [28], a “no-cycle” assumption on the communication topology was considered, while [33] replaced this constraint by assuming instead identical nominal dynamics of the follower agents. In [34], authors employed a new class of internal models to solve the robust CORP for linear MAS using distributed output feedback control. For linear MAS with uniform and non-uniform relative degrees respectively, the robust CORP was studied in [35, 36]. Recently, the IMC approach was also adapted to solve robust CORP for nonlinear agents in [33]. The same problem was considered in [37] for known leader dynamics, and in [38] for unknown leaders.

The structure of the controller in all the above works exploits knowledge of the global communication structure of the MASs. Based on an adaptive distributed state estimation to reconstruct the leader states, a distributed control solution that is independent of any global information on the communication graph was proposed in [39].

A practical challenge of implementing a MAS is in maintaining a reliable communication between the agents of the system. Interruption in the communication links between agents can be caused due to noise, link failures/reconstructions, range limitations, etc. The limited bandwidth of shared communication channels by the agents can also cause problems like packet drop outs and network congestion [40]. Under a switching communication network, the CORP was studied for non-singular MAS in [41] and for singular MAS in [42].

Although the aforementioned works implicitly consider that the agents in a multi-agent framework coordinate in an instanteneous manner, the presence of latency in the communication networks however is unavoidable. Therefore, various cooperative control problems have been studied over the last decade under time-invariant or time-varying communication delays. Distributed estimation problem with multiple stochastic communication delays appears in [43]. The consensus problem for first-order agents with a time-varying communication delay was studied in [20], while the same problem for second-order agents with nonlinear dynamics was investigated in [44] with a fixed communication delay. For higher-order systems, the consensus problem was studied in [19, 45] for fixed input and communication delays, and in [18] for unknown communication delays.

1.4 Motivation

The solutions to the CORP proposed so far in the literature, build upon the assumption that at least one of the agents in the system can independently estimate the leader states from its own measurements. This decentralized estimation of the leader states is then propagated to neighboring agents, until the entire system is synchronized. This assumption can be a limitation in applications, where simple agents do not have the sensing and computational resources required to estimate the full dynamics of a complex leader. For example, in the case where the leader dynamics are spatially distributed and follower agents can only collect localized measurements, the information collected by individual agents may not be sufficient to reconstruct the leader states. The information gathered by followers thus need to be integrated for the reconstruction of leader states. In view of this application, the assumption on independent estimation of leader states by an agent in [29, 30] appears restrictive. With this as motivation, in the following section we briefly outline the objectives of this dissertation.

1.5 Objectives of This Thesis

The primary objective of this dissertation is to address the central question: "is it possible to solve the CORP in case when none of the follower agents receives sufficient information to independently reconstruct the leader states?" The CORP with the relaxed detectability requirement resulting from the above research question is defined as "generalized CORP". Motivated by the example in Section 1.4, our first task is to derive a distributed estimation algorithm, differently from the works of [29, 30], to collectively reconstruct the leader states, and use this estimation to design a distributed control algorithm for solving the CORP. The results of this study are reported in Chapter 2. Given the relaxed detectability assumption, next we aim to extend the study of CORP for MAS by considering additional physical restrictions such as uncertainty in the agent dynamics, actuator saturation and communication constraints such as time-varying topology and network delay. The objectives of this thesis are summarized below.

- Extend the solution to the CORP for nominal MAS to the case when agent dynamics is associated with the parametric uncertainty resulting from modeling error. This study is aimed at generalizing the results in [28, 33], where a specific "virtual error" signal was assumed to be available to the agents for feedback. Since the access of the "virtual error" signal may not always be possible in a given application, from the distributed state estimation of the nominal case we instead construct an estimate of the "regulated error" signal to use it as a feedback to the control. Then, by deriving a distributed control algorithm based on the internal model principle, we derive a solution to the robust CORP. The results are presented in Chapter 3.
- Next, we will study the CORP under the time-varying communication topology for the agents. The goal here is to derive a control solution to the CORP

based on the distributed estimation of the leader states in case when the agents group cannot independently solve the generalized CORP at any single switching configuration. The results of this study will be reported in Chapter 4.

- For validating the effectiveness of the derived theoretical algorithms, we pursue a case study where we implement the results on an experimental platform to solve for a position synchronization problem of networked motors. The testing platform is a network of motors, and the goal is to synchronize the motor shafts positions to a prescribed signal provided by an external leader. Constraints such as restricted access to the leader signal, and intermittent communication between the agents, are added to the problem. Work is currently underway to extend the experimental validation work to a leader-follower formation control using a robotic platform with a couple of quadcopters and ground robots. This experimental testing is reported in Chapter 5.

- We study the distributed state estimation/sensing problem for a network of observer agents under time-invariant communication delays in Chapter 6. Compared to the distributed observers in [46], which was formulated based on the solution to a parametric Riccati equation, the results in our current work offer a more general Hurwitz condition for the convergence of the state estimation. This generalization is achieved by offering an alternative formulation and proof of the main results. The new formulation also allows for the derivation of a closed-form solution to the upper bound of the low-gain control parameter, while the same parameter may only be searched numerically in [46]. The design of the feedback correction gains for the distributed observers have also been streamlined with the generalized stability condition, reducing the number of design parameters, and presenting analytical methods for their selections. Finally, this work also investigates the effect of external disturbances on the convergence of the observer error dynamics, and evaluates the distributed observer solution for the leader-follower synchronization problem under measurement and inter-agent communication delays. An extension of this result to the time-varying counterpart is given in Chapter 7.

- Next, we pursue another case study where we extend the results of the cooperative sensing problem to a practical control application problem with an aim to synchronize a network of distributed generators (DG) in an islanded microgrid under communication latencies. The objective is to synchronize the voltage and frequency of a group of DGs over a time-delayed communication network. When the microgrid is islanded from the utility grid, the transient voltage and frequency instability is further worsened by the presence of a large time delay in the network. As a means to achieve stability and satisfactory synchronization control for the group of DGs within the MG, this work presents a consensus based distributed voltage and frequency control protocol, in which the effects of time delays associated with the exchange of information through the communication network is considered. By using the low gain methodology, sufficient delay dependent stability conditions and an upper bound for the low gain parameter were derived to ensure the stability of the synchronization in the face of communication delays. With the low gain parameter being selected from the derived bounds, we also show that the control protocol can always achieve this synchronization for any arbitrarily large delays. The results of this work are reported in Chapter 8.

- The future works of this dissertation, given in Chapter 9 are aimed at addressing the CORP for multi-agent systems with intermittent outputs.

Chapter 2

Cooperative Output Regulation of Multi-Agent Systems under Exosystem Detectability Constraint

2.1 Introduction

In this chapter, the CORP for linear MASs is investigated for the case when none of the agents can estimate the exosystem states from its measurement. Due to this detectability constraint, the agents cannot independently synchronize themselves with the exosystem and the output regulation problem is not directly solvable. To address this problem, we first develop a novel distributed estimation algorithm to reconstruct the exosystem states from the collective measurements of the agents. Stability conditions for the exosystem state estimation error dynamics are derived using Lyapunov analysis. Then, from the estimation of the exosystem states by the agents, distributed state feedback and output feedback control solutions are proposed.

Numerical simulations are given to illustrate the theoretical analysis. A leader-follower consensus problem is considered as a special case of this study.

The rest of the chapter is organized as follows. Some preliminaries are presented in Section 2.2 with relevant terminologies on information graphs. In Section 2.3 we formulate our control problem, and give necessary assumptions. The main results of this chapter are derived in the subsequent sections. State feedback control solution is proposed for the MAS in Section 2.4, and measurement feedback solutions are provided in Section 2.5. The proposed solutions to the CORPs are validated with an illustrative example in Section 2.6. Finally some concluding remarks are presented in Section 2.7.

Throughout the text, the following notations are frequently used: $\otimes$ denotes the Kronecker product of two matrices, I_r denotes an identity matrix of dimension $r \times r$, $\mathbf{1}_{N\times 1}$ denotes an N column vector with all elements being equal to 1 and $0_{m\times n}$ denotes a zero matrix with dimension $m \times n$.

2.2 Preliminaries

2.2.1 System Model

Consider the following system group, consisting of N linear subsystems with dynamics

$$
\begin{aligned}
\dot{x}_i &= A_i x_i + B_i u_i + E_i w, \\
e_i &= C_i x_i + D_i u_i + F_i w, \\
y_{mi} &= C_{w_i} w, \;\; i \;= 1, 2, 3, \cdots, N,
\end{aligned}
\tag{2.1}
$$

where $x_i \in \mathbb{R}^{n_i}, u_i \in \mathbb{R}^{m_i}$ are the state and control input vectors, respectively, of the i^{th} subsystem. Signal $e_i \in \mathbb{R}^p$ is the regulated output, i.e. the output that is to be regulated to the origin, while $y_{mi} \in \mathbb{R}^{\mathbf{p}_i}$ is an information signal that each subsystem receives from the exosystem to formulate the control. The external signal $w \in \mathbb{R}^q$ in (2.1) represents both the reference input to be tracked and the disturbance input to be rejected by the subsystems. The external signal is generated by the exosystem

$$\dot{w} = Sw. \tag{2.2}$$

The control objective of the CORP is to design a distributed dynamic feedback control law, such that the regulated output e_i of each subsystem in (2.1) asymptotically approaches zero for any arbitrary initial conditions. To achieve this, we decouple our problem into two parts: the asymptotic stabilization of the nominal subsystem dynamics, and the output regulation of the combined system (2.1) - (2.2). Before we get into the assumptions regarding the network connections, some basic graph terminologies are given below.

2.2.2 Information Graph

A digraph or a directed graph $\mathcal{G} = (\mathcal{V}, \mathcal{E})$ is a set of finite nodes $\mathcal{V}$ and edges $\mathcal{E}$, where $\mathcal{V} = \{0, 1, 2, \cdots, N\}$ and $\mathcal{E} \subseteq \mathcal{V} \times \mathcal{V}$. An edge directed from the i^{th} node to the j^{th} node is given by (i, j), where i and j are the parent node and the child node, respectively. The node i is also termed the neighbouring node of j. The neighbouring set of node i, $\mathcal{N}_i \subseteq \mathcal{V}$, is the set of all its parent nodes.

A digraph is a directed tree if it has all nodes with a single parent, except for a root node that has no parent and can reach any other node in the digraph. A subgraph $\mathcal{G}_s = (\mathcal{V}_\int, \mathcal{E}_\int)$ of a digraph $\mathcal{G} = (\mathcal{V}, \mathcal{E})$ is a directed spanning tree if $\mathcal{G}_s$ is a directed tree with $\mathcal{V}_\int = \mathcal{V}$ and $\mathcal{E}_\int \subseteq \mathcal{E} \bigcap (\mathcal{V}_\int \times \mathcal{V}_\int)$.

The adjacency matrix $\mathcal{A} = [a_{ij}] \in \mathbb{R}^{(N+1)\times(N+1)}$ of a digraph is a non-negative matrix with $a_{ij} > 0$ when there is a directed edge from j to i, $(j, i) \in \mathcal{E}$, and $a_{ij} = 0$ when $(j, i) \notin \mathcal{E}$. The Laplacian matrix $L = [l_{ij}] \in \mathbb{R}^{(N+1)\times(N+1)}$ is a zero row sum matrix with elements

$$l_{ij} = -a_{ij}, \quad \text{if } j \neq i,$$
$$l_{ii} = \sum_{j=1}^{N} a_{ij}, \quad \text{if } j = i.$$

2.3 Problem Formulation

Similarly to the formulation of the CORP in [30], the system composed of (2.1) and (2.2) is viewed as a MAS with leader agent (2.2) and N follower agents (2.1). We also classify the follower agents (2.1) into two subgroups. For some integer l, $0 < l \leq N$, let the subsystems corresponding to $i = l+1, l+2, \cdots, N$ form a subgroup of passive agents with $C_{w_i} = 0$. On the other hand, subsystems with $i = 1, 2, \cdots, l$ form the subgroup of active agents. An active agent i is in the neighbouring set of the leader if $C_{w_i} \neq 0$.

Let $\mathcal{G} = (\mathcal{V}, \mathcal{E})$ be the digraph representing the MAS composed by (2.1) and (2.2), where $\mathcal{V} = \{0, 1, \cdots, N\}$. Without loss of generality, we let node 0 to be the exosystem (2.2). Nodes 1 to l are the active agents, and nodes $(l+1)$ to N correspond to the passive agents.

Remark 2.3.1. *Note here that our definition of the active subgroup is modified from that of informed agents in [30], as it may include subsystems i with $C_{w_i} = 0$. Assumptions 2.3.4 and 2.3.5 to be introduced later in this section will make evident that our definition of active agents includes all subsystems that actively participate in the estimation of the exosystem states, rather than only based on the agents' measurement signal y_{mi}. We also note that similarly to the uninformed agents in [29, 30], passive agents rely on the collective estimation of the exosystem states by active agents for control.*

The following assumptions are commonly considered in the literature to guarantee the solvability of the output regulation problem.

Assumption 2.3.1. *S has all eigenvalues on the imaginary axis.*

Assumption 2.3.2. *The pair (A_i, B_i) in (2.1) is stabilizable.*

Assumption 2.3.3. *For all $\lambda \in \sigma(S)$, where $\sigma(S)$ is the spectrum of S,*

$$rank \begin{bmatrix} A_i - \lambda I & B_i \\ C_i & D_i \end{bmatrix} = n_i + p, i = 1, 2, \cdots, N.$$

Remark 2.3.2. *By Theorem 3.2 in [23], for any matrices E_i and F_i, the regulator equations*

$$\begin{aligned} X_i S &= A_i X_i + B_i U_i + E_i, \\ 0 &= C_i X_i + D_i U_i + F_i, \; i = 1, 2, 3, \cdots, N. \end{aligned} \tag{2.3}$$

admit a unique solution pair (X_i, U_i) if and only if the Assumption 2.3.3 is satisfied.

The assumption on the exosystem dynamics in Assumption 2.3.1 does not pose a stringent requirement on the implementability of our results since exponentially increasing disturbance/reference signals are rare in practical applications. We also neglect exponentially stable modes of the exosystem dynamics as they would result in a trivial solution to the output regulation problem. Equation (2.3) is commonly referred to as the regulator equation in the literature, solvability of which is necessary and sufficient to achieve output regulation as stated in [23].

The solution to the CORP in [30] also requires all agents i in the "informed" group to be able to reconstruct the exosystem states from their own measurement y_{mi}. In other words, this is equivalent to (S, C_{w_i}) being detectable for some agent i. Here, we aim to extend the results in [30] by relaxing this detectability requirement, and we consider the case where (S, C_{w_i}) is not detectable for any agent i, i.e. no agent can estimate the exosystem trajectory from the individual measurements. Instead, agents reach a consensus on the exosystem states from their combined individual measurement y_{mi}'s, and the connectivity properties among the active agents. The above discussion is summarized in the next two assumptions.

Assumption 2.3.4. *Let the matrix* $\bar{C}_{w_a} = col(C_{w_1}, C_{w_2}, C_{w_3}, \cdots, C_{w_l})$ *and* l *be the number of active followers, where* $col(C_{w_1}, C_{w_2}, C_{w_3}, \ldots, C_{w_l}) = [C_{w_1}^T \; C_{w_2}^T \cdots \; C_{w_l}^T]^T$ *for* C_{w_i}*'s with appropriate dimensions. The pair* $(S, \bar{C}_{w_a})$ *is detectable.*

Remark 2.3.3. *This assumption is referred to as the combined detectability property throughout the text. Unlike [29, 30], which require at least an agent* i *such that* y_{mi} *is sufficient to reconstruct* $w(t)$*, Assumption 2.3.4 states that the combined output* $y_m = col(y_{m1}, y_{m2}, \cdots, y_{ml})$ *must be sufficient to estimate the exosystem trajectory* $w(t)$*. The price of the relaxed detectability assumption comes as an added connectivity requirement in Assumption 2.3.5.*

Assumption 2.3.5. *All the active followers form a strongly connected partition of the digraph* $\mathcal{G}$*, and at least one active follower is a child of node 0.*

Remark 2.3.4. *Due to the relaxed detectability assumption in Assumption 2.3.4, active agents must rely on other active agents to complement their local measurement in estimating* $w(t)$*. This leads to the above connectivity assumption. Active agents with output matrix* $C_{w_i} = 0$ *can be viewed as agents that are not in the vicinity of the leader to obtain direct measurement, but they contribute by permitting communication between other active agents in the network. On the other hand, passive agents do not have computational and sensing abilities to estimate* $w(t)$ *themselves, and they are primarily dependent on the estimation by the active agents. Note that by Assumption 2.3.5, agents in the active subgroup cannot be children nodes of passive agents.*

To illustrate further on the classification among agents, we consider for example the digraph in Figure 2.1 where agents $1, 2$ and 3 are active agents and 4 is a passive agent. Consider that agents 2 and 3 cannot individually estimate the full state vector w from the information relayed by the leader. Even though $C_{w_3} = 0$ since agent 3 is not a child node of the leader, it actively takes part in the estimation process by allowing the agent 2 to retrieve the missing exosystem information from agent 1 through the network. Thus active agents work as a group to propagate the necessary information in the strongly connected network so that all agents can arrive at a consensus with the complementing information.

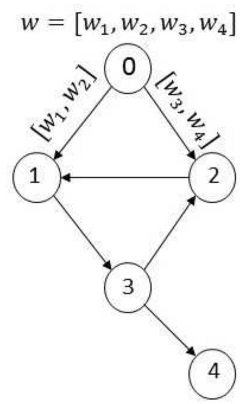

Figure 2.1: The network topology for the example (node 0 as leader)

Remark 2.3.5. *In the case where there is only one agent in an active subgroup, Assumptions 2.3.4, 2.3.5, and the definition of active agents reduce to equivalent assumptions and the definition of informed agents in [29, 30].*

In order to reconstruct the leader dynamics from the available measurements to the followers, we now introduce the distributed dynamic compensator for active agents as follows

$$\dot{\eta}_i = S\eta_i + \mu \left(\sum_{j \in \mathcal{N}_i} a_{ij}(\eta_j - \eta_i) + a_{i0}G_i(y_{mi} - C_{w_i}\eta_i) \right), \tag{2.4}$$

for a real scalar $\mu > 0$ and measured output signal y_{mi} for a follower agent i being defined in (2.1). Here G_i is the observer gain for the partial estimation of the leader states by the i^{th} node, η_j is the state vector of the dynamic compensator of the neighbouring agent $j \in \mathcal{N}_i$. The last two terms in the right side of (2.4) correspond to the correction terms where the first one is derived from the relative difference of inter-agent estimated information while the second term is the error between the measured output and estimated output of an active agent i. Unlike [29,30] where w is directly available to an agent i from its measurement y_{mi}, we need an observer with gain G_i to drive η_i in the direction guided by the estimation error of an agent's own output.

For passive followers, the proposed distributed dynamic compensator takes the form

$$\dot{\eta}_i = S\eta_i + \mu\left(\sum_{j\in\mathcal{N}_i} a_{ij}(\eta_j - \eta_i)\right). \tag{2.5}$$

Finally we define the CORP for MAS with follower agents' dynamics (2.1) as follows:

Problem 2.3.1. *CORP*-Given the MAS with agent dynamics (2.1), exosystem (2.2) and communication graph $\mathcal{G}$ find a distributed dynamic feedback control law u_i, $i = 1,2,\cdots,N$, such that

1. the subsystem (2.1) under the control u_i is asymptotically stable when $w = 0$,
2. for any arbitrary initial conditions $x_i(0), \eta_i(0)$, and $w(0)$, the regulated output satisfies $\lim_{t\to\infty} e_i(t) = 0$.

The following notation practices are introduced here, and they will be followed throughout the remainder of this chapter unless specified otherwise. For a group of vectors $\xi_i, i = 1,2,\cdots,N$,

$$\begin{aligned} \xi &= \mathrm{col}(\xi_1,\xi_2,\cdots,\xi_N), \\ \xi_a &= \mathrm{col}(\xi_1,\xi_2,\cdots,\xi_l), \\ \xi_p &= \mathrm{col}(\xi_{l+1},\xi_{l+2},\cdots,\xi_N). \end{aligned} \tag{2.6}$$

For a group of matrices $\Xi_i, i = 1, 2, \cdots, N$,

$$
\begin{aligned}
\Xi &= \text{blk diag}(\Xi_1, \Xi_2, \cdots, \Xi_N),\ \bar{\Xi} = \text{col}(\Xi_1, \Xi_2, \cdots, \Xi_N), \\
\Xi_a &= \text{blk diag}(\Xi_1, \Xi_2, \cdots, \Xi_l),\ \bar{\Xi}_a = \text{col}(\Xi_1, \Xi_2, \cdots, \Xi_l), \\
\Xi_p &= \text{blk diag}(\Xi_{l+1}, \Xi_{l+2}, \cdots, \Xi_N),\ \bar{\Xi}_p = \text{col}(\Xi_{l+1}, \Xi_{l+2}, \cdots, \Xi_N),
\end{aligned} \tag{2.7}
$$

where matrix Ξ is a block diagonal matrix with i^{th} diagonal block Ξ_i. The identity matrix and the all-ones matrix will be expressed as $I_a \in \mathbb{R}^{a\times a}$ and $\mathbf{1}_{a\times b} \in \mathbb{R}^{a\times b}$, respectively.

2.4 Distributed State Feedback Control

Based on the compensator equations (2.4) and (2.5), the control law for the follower agent i is given as

$$u_i = K_{1_i} x_i + K_{2_i} \eta_i, \tag{2.8}$$

where x_i is the state vector of the agent i. Feedback gain matrix $K_{1_i} \in \mathbb{R}^{m_i \times n_i}$ is selected such that $(A_i + B_i K_{1_i})$ is Hurwitz and $K_{2_i} \in \mathbb{R}^{m_i \times q}$ is obtained from the solution pair to the regulator equation (2.3),

$$K_{2_i} = U_i - K_{1_i} X_i. \tag{2.9}$$

For the digraph $\mathcal{G}$ corresponding to the MAS (2.1) with leader (2.2), let $\mathcal{A} = [a_{ij}]$ be its adjacency matrix, and let L be the Laplacian matrix,

$$L = \left[\begin{array}{c|cc} 0 & 0 & 0 \\ \hline \alpha_{21} & \alpha_{22} & \alpha_{23} \\ \alpha_{31} & \alpha_{32} & \alpha_{33} \end{array}\right],$$

where $\alpha_{21} \in \mathbb{R}^l$, $\alpha_{31} \in \mathbb{R}^{(N-l)}$, $\alpha_{22} \in \mathbb{R}^{l\times l}$ and $\alpha_{33} \in \mathbb{R}^{(N-l)\times(N-l)}$. By definition, passive agents cannot be a child node of the leader, which yields that $\alpha_{31} = 0$. The Laplacian matrix for the considered network can then be rewritten as

$$L = \left[\begin{array}{c|cc} 0 & 0 & 0 \\ \hline \alpha_{21} & \alpha_{22} & \alpha_{23} \\ 0 & \alpha_{32} & \alpha_{33} \end{array}\right] = \left[\begin{array}{c|c} 0 & 0 \\ \hline \nabla \mathbf{1}_N & \mathcal{H} \end{array}\right],$$

where ∇ is an $N \times N$ diagonal matrix with elements $-a_{i0}$ along the diagonal and $\mathbf{1}_N$ is an N dimensional column vector whose elements are all 1. The zero row sum property of the Laplacian matrix yields $\nabla \mathbf{1}_N = \mathcal{H}\mathbf{1}_N$. By Assumption 2.3.5, $\mathcal{L} = \alpha_{22} + \mathrm{diag}(\alpha_{21})$ corresponds to a strongly connected digraph $\mathcal{G}_1$ of $\mathcal{G}$, where $\mathrm{diag}(\alpha_{21})$ denotes a diagonal matrix with the diagonal entries being the elements of α_{21}.

Lemma 2.4.1. *$\mathcal{H}$ is nonsingular if and only if the digraph contains a directed spanning tree with node 0 as the root. Additionally, if $\mathcal{H}$ is nonsingular, then the eigenvalues of α_{22} and α_{33} have positive real parts.*

Proof. By Lemma A in [30], $\mathcal{H}$ is nonsingular if and only if it is embedded with a directed spanning tree with node zero as the root. Furthermore, the eigenvalues of $\mathcal{H}$ have positive real parts when $\mathcal{H}$ is nonsingular. The second part of the lemma can be shown by noting from Remark 2.3.4 that $\alpha_{23} = 0$. Hence $\mathcal{H}$ nonsigular implies that α_{22} and α_{33} are nonsingular, and they have eigenvalues with positive real parts. □

Lemma 2.4.2. *(Lemma 2.12 of [47]) Let $\mathcal{L}$ be a Laplacian matrix corresponding to a strongly connected digraph. There exists a vector of positive numbers $\zeta = \left[\zeta_1, \zeta_2, \cdots, \zeta_l\right]^T$ such that $\mathbf{1}_l^T\zeta = 1$, and $\zeta^T\mathcal{L} = 0$. In addition, for the positive definite diagonal matrix $\Sigma = diag(\zeta)$ with the elements of ζ along its diagonal, the matrix $\hat{\mathcal{L}} = \Sigma\mathcal{L} + \mathcal{L}^T\Sigma$ is a symmetric matrix with zero row and column sums.*

We note that $\hat{\mathcal{L}}$ is the Laplacian matrix corresponding to an undirected graph. Then from [17], $\hat{\mathcal{L}}$ is a positive semi-definite matrix with a simple zero eigenvalue and corresponding eigenvector $\mathbf{1}_l$.

Lemma 2.4.3. *Consider the dynamic compensator* (2.4) *and* (2.5) *with digraph* $\mathcal{G}$ *satisfying Assumption 2.3.5, gains* G_i*, scaling factor* $\mu > 0$ *and a positive definite* P *such that the matrix* $P(S-\mu G_i C_{w_i}) + (S-\mu G_i C_{w_i})^T P$ *has non-positive eigenvalues for all follower agents* i *and*

$$\mathcal{R} = \left(lS - \mu \sum_{i=1}^{l} G_i' C_{w_i} \right)$$

is Hurwitz, where $G_i' = \zeta_i G_i$ *and* ζ_i *is the* i^{th} *element of the left eigenvector* ζ *of* $\mathcal{L}$ *corresponding to the eigenvalue* 0*. Then the compensator states* η_i *asymptotically approaches the exosystem states,*

$$\lim_{t\to\infty} (\eta_i(t) - w(t)) = 0, \; i = 1,2,3,\cdots,N,$$

if and only if the digraph $\mathcal{G}$ *contains a directed spanning tree with node 0 as the root.*

Proof. (If part.) Let $\tilde{\eta}_i = \eta_i - w, i = 1,2,3,\cdots,N$, and the combined vectors $\tilde{\eta}_a, \tilde{\eta}_p$ as defined in (2.6). The convergence of the dynamic compensator states will be proven first for the active agents, and later for the passive agents.

From dynamic compensator for the active agents (2.4) and exosystem (2.2), we obtain

$$\dot{\tilde{\eta}}_a = [(I_l \otimes S) - \mu(G_a C_{w_a}) - \mu(\mathcal{L} \otimes I_q)] \; \tilde{\eta}_a = [\rho - \mu(\mathcal{L} \otimes I_q)] \; \tilde{\eta}_a, \tag{2.10}$$

where $\rho = \text{blk diag}(\rho_1, \rho_2, \cdots, \rho_l)$, and $\rho_i = S - \mu G_i C_{w_i}$. Consider the Lyapunov function $V = \tilde{\eta}_a^{\mathrm{T}} (\Sigma \otimes P) \tilde{\eta}_a$, where a positive definite matrix P is the unique solution of

$$P\mathcal{R}^{\mathrm{T}} + \mathcal{R}P < 0. \tag{2.11}$$

The existence and uniqueness of P is guaranteed since $\mathcal{R}$ is a Hurwitz matrix. Then by differentiating the Lyapunov function we obtain

$$\begin{aligned}\dot{V} &= \tilde{\eta}_a^{\mathrm{T}} \left(\rho^{\mathrm{T}} (\Sigma \otimes P) + (\Sigma \otimes P)\rho\right) \tilde{\eta}_a - \mu \tilde{\eta}_a^{\mathrm{T}} \left(\left(\mathcal{L}^{\mathrm{T}}\Sigma + \Sigma\mathcal{L}\right) \otimes P\right) \tilde{\eta}_a \\ &= \tilde{\eta}_a^{\mathrm{T}} \left(\rho^{\mathrm{T}} (\Sigma \otimes P) + (\Sigma \otimes P)\rho\right) \tilde{\eta}_a - \mu \tilde{\eta}_a^{\mathrm{T}} \left(\hat{\mathcal{L}} \otimes P\right) \tilde{\eta}_a. \end{aligned} \tag{2.12}$$

Since the matrix $(P\rho_i + \rho_i^{\mathrm{T}} P)$ is negative semi-definite by assumption and $(\hat{\mathcal{L}} \otimes P)$ is positive semi-definite by virtue of Lemma 2.4.2, then from (2.12) we obtain, $\dot{V} \leq 0$. In addition $\tilde{\eta}_a^{\mathrm{T}} \left(\mathcal{L}^{\mathrm{T}} \otimes P\right) \tilde{\eta}_a = 0$ only when $\tilde{\eta}_1 = \tilde{\eta}_2 = \cdots = \tilde{\eta}_l$. By virtue of (2.11), $\dot{V}$ in (2.12) reduces to

$$\dot{V} = \tilde{\eta}_a^{\mathrm{T}} \left(\rho^{\mathrm{T}} (\Sigma \otimes P) + (\Sigma \otimes P)\rho\right) \tilde{\eta}_a = \tilde{\eta}_1^{\mathrm{T}} \left(P\mathcal{R}^{\mathrm{T}} + \mathcal{R}P\right) \tilde{\eta}_1 < 0. \tag{2.13}$$

Therefore $\dot{V} < 0$ for all $\tilde{\eta}_a \neq 0$, and (2.10) is asymptotically stable.

Similarly, from the dynamic compensator (2.5) for passive agents, we obtain

$$\begin{aligned}\dot{\tilde{\eta}}_p &= -\mu(\alpha_{32} \otimes I_q)\tilde{\eta}_a + [(I_{N-l} \otimes S) - \mu(\alpha_{33} \otimes I_q)]\tilde{\eta}_p, \\ &= -\mu(\alpha_{32} \otimes I_q)\tilde{\eta}_a + \mathcal{P}\tilde{\eta}_p, \end{aligned} \tag{2.14}$$

where $\mathcal{P} = (I_{N-l} \otimes S) - \mu(\alpha_{33} \otimes I_q)$. The eigenvalues of $\mathcal{P}$ are $\lambda_i(S) - \mu\lambda_j(\alpha_{33}) : i \in 1, 2, \cdots, q, j \in 1, 2, \cdots, N-l$, where $\lambda_i(S)$ and $\lambda_j(\alpha_{33})$ are respectively the eigenvalues of S and α_{33}. Lemma 2.4.1 then yields that $\mathcal{P}$ is Hurwitz for $\mu > 0$ and (2.14) is asymptotically stable.

(Only if part.) Suppose the digraph $\mathcal{G}$ does not have a spanning tree with node 0 as the root, then $\mathcal{H}$ is singular and either of α_{22} or α_{33} have a zero eigenvalue. Let

$$\mathcal{L}_s = \begin{bmatrix} 0 & 0_{1\times l} \\ \alpha_{21} & \alpha_{22} \end{bmatrix}$$

be a Laplacian matrix corresponding to a subgraph $\mathcal{G}_s$ of $\mathcal{G}$, obtained by deleting passive agent nodes. Then, $-\mathcal{L}_s$ is a Metzler matrix with zero row sum. Recall that active agents, corresponding to nodes $i = 1, 2, 3, \cdots, l$, form a strongly connected partition of $\mathcal{G}$ with at least one child node of the node 0. Thus by the proof of Lemma 1 in [30], α_{22} is nonsingular, which yields that α_{33} has to be singular. As a result, $\mathcal{P}$ in (2.14) is not Hurwitz, since all of its eigenvalues do not have strictly negative real parts, and $\lim_{t\to\infty} \tilde{\hat{\eta}} \neq 0$. □

Remark 2.4.1. *$\mathcal{R}$ can be rewritten in the matrix form as*

$$\mathcal{R} = lS - \mu \mathbf{G} \bar{C}_{w_a}, \tag{2.15}$$

where $\mathbf{G} = [G_1' \; G_2' \; \cdots \; G_l']$ and $\bar{C}_{w_a}$ is defined in Assumption 2.3.4. By Assumption 2.3.4, there is always a matrix $\mathbf{G}$ such that $\mathcal{R}$ is Hurwitz. The design procedure for the distributed observer gain matrix G_i (2.4) *is summarized as follows. Select G_i in such a way that*

- *the matrix $\mathcal{R}$* (2.15) *is Hurwitz and as a result there exists a unique positive definite solution P to equation* (2.11)*.*
- *the matrix $P\rho_i + \rho_i^T P$ is negative semi-definite.*

Remark 2.4.2. *Lemma 2.4.3 shows that the distributed dynamic compensator* (2.4) *can lead to a consensus on the exosystem states, even when none of the agents in the system can reconstruct the exosystem states from local measurements. Additionally,* *for the particular case where the pairs (S, C_{w_i}) are detectable for some active agent i, the results in Lemma 2.4.3 and Assumptions 2.3.4 and 2.3.5 are equivalent to results presented in [29].*

Using the notation in (2.6) and (2.7), define the system state and the regulated output of the overall system be $x_c = \mathrm{col}(x_a, x_p, \tilde{\eta}_a, \tilde{\eta}_p)$ and $e = \mathrm{col}(e_a, e_p)$. The overall closed-loop system under the control (2.4), (2.5) and (2.8) is represented by the following state equations

$$\begin{aligned} \dot{x}_c =& \mathbf{A}_c x_c + \mathbf{B}_c w, \\ e =& \mathbf{C}_c x_c + \mathbf{D}_c w, \end{aligned} \tag{2.16}$$

with the system matrices being

$$\mathbf{A}_c = \left[\begin{array}{c|c} \mathbf{A}_{c_1} & \mathbf{A}_{c_2} \\ \hline 0 & \mathbf{A}_{c_4} \end{array}\right], \ \mathbf{A}_{c_1} = \left[\begin{array}{c|c} A_a + B_a K_{1_a} & 0 \\ \hline 0 & A_p + B_p K_{1_p} \end{array}\right],$$

$$\mathbf{A}_{c_2} = \left[\begin{array}{c|c} B_a K_{2_a} & 0 \\ \hline 0 & B_p K_{2_p} \end{array}\right], \ \mathbf{A}_{c_4} = \left[\begin{array}{c|c} \rho - \mu(\mathcal{L} \otimes I_q) & 0 \\ \hline -\mu(\alpha_{32} \otimes I_q) & \mathcal{P} \end{array}\right].$$

The input matrix is given by $\mathbf{B}_c = \mathrm{col}(\mathbf{B}_{c_1}, \mathbf{B}_{c_2})$, where

$$\mathbf{B}_{c_1} = \mathrm{col}(\bar{E}_a + B_a \bar{K}_{2_a}, \bar{E}_p + B_p \bar{K}_{2_p}), \ \mathbf{B}_{c_2} = 0.$$

The output matrix

$$\mathbf{C}_c = \left[\begin{array}{cc|cc} C_a + D_a K_{1_a} & 0 & D_a K_{2_a} & 0 \\ \hline 0 & C_p + D_p K_{1_p} & 0 & D_p K_{2_p} \end{array}\right],$$

The static gain matrix $\mathbf{D}_c$ is

$$\mathbf{D}_c = \mathrm{col}(\bar{F}_a + D_a \bar{K}_{2_a}, \bar{F}_p + D_p \bar{K}_{2_p}).$$

Remark 2.4.3. *The block diagonal components of A_{c_1} can be made Hurwitz by Assumption 2 and the selection of suitable feedback gain K_{1_i}. Similarly, the block diagonal terms in A_{c_4} can be made Hurwitz by a gain G_i satisfying the necessary conditions in Lemma 2.*

Theorem 2.4.4. *Under Assumptions 2.3.1 to 2.3.5, the CORP is solvable by the feedback control law* (2.8)*, with suitable gains G_i's and K_{1_i}'s as described in Remarks 2.4.1 and 2.4.3, and scaling factor $\mu > 0$, if and only if the digraph $\mathcal{G}$ contains a directed spanning tree with node* 0 *as the root.*

Proof. (If part). The linear regulator equation in (2.3) corresponding to the active and passive agents can be rewritten as

$$\begin{aligned} \bar{X}_a S &= (A_a + B_a K_{1_a})\bar{X}_a + B_a \bar{K}_{2_a} + \bar{E}_a, \\ 0 &= (C_a + D_a K_{1_a})\bar{X}_a + D_a \bar{K}_{2_a} + \bar{F}_a, \\ \bar{X}_p S &= (A_p + B_p K_{1_p})\bar{X}_p + B_p \bar{K}_{2_p} + \bar{E}_p, \\ 0 &= (C_p + D_p K_{1_p})\bar{X}_p + D_p \bar{K}_{2_p} + \bar{F}_p, \end{aligned} \tag{2.17}$$

where $\bar{X}_a$ and $\bar{X}_p$ follow the notation in (2.7). Let us define a new state variable in the form $\tilde{x}_i = x_i - \bar{X}_i w, i = 1, 2, \cdots, N$. Then by (2.17) we get the following state equation for the active agents

$$\dot{\tilde{x}}_a = \dot{x}_a - \bar{X}_a \dot{w} \ = (A_a + B_a K_{1_a})\tilde{x}_a + B_a K_{2_a} \tilde{\eta}_a. \tag{2.18}$$

Similarly for the passive agents

$$\dot{\tilde{x}}_p = \dot{x}_p - \bar{X}_p \dot{w} = (A_p + B_p K_{1_p})\tilde{x}_p + B_p K_{2_p} \tilde{\eta}_p. \tag{2.19}$$

By combining (2.18) and (2.19), the overall state space equation for the follower agents can be rewritten as $\dot{x}_e = \mathbf{A}_c x_e$, where $x_e = \mathrm{col}(\tilde{x}_a, \tilde{x}_p, \tilde{\eta}_a, \tilde{\eta}_p)$. Since the system matrix $\mathbf{A}_c$ is Hurwitz, we obtain that $\lim_{t\to\infty} x_e(t) = 0$.

Now, it yields from (2.17) that the regulated output for the active agents equals

$$\begin{aligned} e_a =&(C_a + D_a K_{1_a})x_a + D_a K_{2_a}\tilde{\eta}_a + (\tilde{F}_a + D_a \tilde{K}_{2_a})w, \\ =&(C_a + D_a K_{1_a})\tilde{x}_a + D_a K_{2_a}\tilde{\eta}_a. \end{aligned} \tag{2.20}$$

Similarly, for passive agents, the regulated error output become

$$\begin{aligned} e_p =&(C_p + D_p K_{1_p})\tilde{x}_p + D_p K_{2_p}\tilde{\eta}_p + (\tilde{F}_p + D_p \tilde{K}_{2_p})w, \\ =&(C_p + D_p K_{1_p})\tilde{x}_p + D_p K_{2_p}\tilde{\eta}_p. \end{aligned} \tag{2.21}$$

Therefore the regulated output of the follower agents can be combined as $e = \mathbf{C}_c x_e$. Since x_e asymptotically converges to zero, $\lim_{t\to\infty} e_i(t) = 0$ for all agent i. Thus the CORP is solved.

(Only if part) Suppose the digraph $\mathcal{G}$ does not contain a spanning tree with node 0 as the root. Therefore from Lemma 2.4.3, $\lim_{t\to\infty} \eta_i(t) - w(t) \neq 0$ for any follower i. Hence, $\mathbf{A}_{c_4}$ is not Hurwitz and as a result, $\mathbf{A}_c$ is not Hurwitz as well. Thus, the output regulation problem is not solvable by the control law (2.8). □

Remark 2.4.4. *The solution to the CORP proposed in this work relies on the communication network between the active agents to complement the incomplete measurement y_{mi}. Under Assumptions 2.3.4 and 2.3.5, a path between the active agents is guaranteed so that the incomplete measurements of one agent are complemented by the information shared within the active subgroup. Indeed, the dynamic compensator in* (2.4) *can be seen as a cooperative observer of the exosystem states from the local measurement y_{mi} and the observation η_j by neighbouring agent j.*

2.5 Distributed Output Feedback Control

We now propose a measurement output feedback solution to Problem 2.3.1.. Let the measured output $y_i \in \mathbb{R}^{\mathbf{p}_i}$ for the i^{th} subsystem is given by

$$y_i = C_{x_i} x_i,\ i = 1, 2, 3, ..., N. \tag{2.22}$$

Assumption 2.5.1. *The pairs (A_i, C_{x_i}) are detectable, $i = 1, 2, \cdots, N$.*

Additionally, we note that the signal y_{mi} from the exosystem is available to agent i through their communication to determine their cooperative estimation $\eta_i(t)$ (2.4) and (2.5) of the leader's state $w(t)$ in (2.2). For the MAS satisfying the above assumptions, we consider the distributed dynamic measurement output feedback controller as

$$u_i = K_{1_i} \hat{x}_i + K_{2_i} \eta_i,\ i = 1, 2, 3, ..., N, \tag{2.23}$$

where $\hat{x}_i \in \mathbb{R}^{n_i}$ is the estimation of the state vector x_i for the i^{th} agent, $\eta_i(t)$ is defined for active agents in (2.4) and for passive agents in (2.5), and controller gain matrices K_{1_i} and K_{2_i} are given in (2.8) and (2.9). For agents $i = 1, 2, \cdots, N$, $\hat{x}_i$ is defined as

$$\dot{\hat{x}}_i = A_i \hat{x}_i + B_i u_i + E_i \eta_i + H_i (C_{x_i} \hat{x}_i - y_i), \tag{2.24}$$

where the observer gain matrix $H_i \in \mathbb{R}^{n_i \times p_i}$ is selected such that $(A_i + H_i C_{x_i})$ is a Hurwitz matrix. The error equation corresponding to (2.24) can be found as

$$\dot{\tilde{\hat{x}}}_i = (A_i + H_i C_{x_i})\, \tilde{x}_i + E_i \tilde{\eta}_i, \tag{2.25}$$

where $\tilde{\hat{x}}_i = \hat{x}_i - x_i, i = 1, 2, \cdots, N$. Since $\lim_{t\to\infty} \tilde{\eta}_i(t) = 0$ by Lemma 2.4.3, then $\lim_{t\to\infty} \tilde{\hat{x}}_i(t) = 0$ by virtue of $(A_i + H_i C_{x_i})$ being a Hurwitz matrix.

Under the measurement feedback distributed control (2.23), define the overall closed-loop system state as $x_c = \mathrm{col}(x, \tilde{\hat{x}}, \tilde{\eta})$ and $e = \mathrm{col}(e_a, e_p)$. The dynamics of the overall closed-loop system then follows the state space equation (2.16) with

$$\mathbf{A}_c = \left[\begin{array}{c|c} A + BK_1 & BK_c \\ \hline 0 & \mathbf{A}_{c3} \end{array}\right], \; K_c = \begin{bmatrix} K_1 & K_2 \end{bmatrix}$$

$$\mathbf{A}_{c3} = \left[\begin{array}{c|c} A + HC_x & E \\ \hline 0 & \mathbf{A}_{c4} \end{array}\right], \; \mathbf{A}_{c4} = \begin{bmatrix} \rho - \mu(\mathcal{L} \otimes I_q) & 0 \\ -\mu(\alpha_{32} \otimes I_q) & \mathcal{P} \end{bmatrix},$$

$$\mathbf{B}_c = \mathrm{col}(\mathbf{B}_{c_1}, 0), \; \mathbf{B}_{c_1} = \mathrm{col}(\bar{E} + B\bar{K}_2),$$

$$\mathbf{C}_c = \begin{bmatrix} C + DK_1 & DK \end{bmatrix}, \; \mathbf{D}_c = \mathrm{col}(\bar{F} + D\bar{K}_2).$$

Remark 2.5.1. *From the proof of Lemma 2.4.3, the matrix $\mathbf{A}_{c_4}$ is Hurwitz and so is $\mathbf{A}_{c_3}$ by the suitable selection of observer gain H. Similarly from Assumption 2.3.2, the choice of K_1 makes the matrix $A + BK_1$ Hurwitz and as a result $\mathbf{A}_c$ is also Hurwitz. Therefore, the overall undisturbed $(w = 0)$ closed-loop system matrix $\mathbf{A}_c$ is stable if and only if Lemma 2.4.3 is satisfied and the controller and observer gains K_{1i}, K_{2i}, H_i in* (2.23) *are properly selected.*

Theorem 2.5.1. *Under Assumptions 2.3.1-2.5.1, the CORP is solvable by the distributed dynamic measurement output feedback control law* (2.23) *with suitable controller and observer gains as described in Remark 2.5.1, and a scaling factor $\mu > 0$, if and only if the digraph $\mathcal{G}$ contains a directed spanning tree with node 0 as the root.*

Proof. (If part.) We define a state variable of the form $\tilde{x}_i = x_i - X_i w, i = 1, 2, \cdots, N$, and thereby we get the following state equations using (2.17)

$$\dot{\tilde{x}} = (A + BK_1)\tilde{x} + BK_1\tilde{\hat{x}} + BK_2\tilde{\eta}. \tag{2.26}$$

The overall state space equation with state $x_e = \mathrm{col}(\tilde{x}, \tilde{\hat{x}}, \tilde{\eta})$ can be rewritten in the form as $\dot{x}_e = \mathbf{A}_c x_e$. It follows from Remark 2.5.1 that the system matrix $\mathbf{A}_c$ is Hurwitz and hence $\lim_{t\to\infty} x_e(t) = 0$.

The regulated output of the agents, obtained using (2.17), reduce to the form

$$e = (C+DK_1)\tilde{x} + DK_1\tilde{\hat{x}} + DK_2\tilde{\eta} = \mathbf{C}_c x_e.$$

Since x_e asymptotically converges to zero, $\lim_{t\to\infty} e_i(t) = 0, i = 1, 2, \cdots, N$ and thus the output regulation problem is solved.

(Only if part.) Suppose the digraph $\mathcal{G}$ does not have a directed spanning tree with node 0 as the root. Then there exists at least one node, which is not reachable from node 0, implying that node must be a passive one because otherwise all the active agents are strongly connected and by Assumption 2.3.5, all the active agents are reachable from node 0. Therefore α_{33} is singular from Lemma 1 and $\lim_{t\to\infty} \tilde{\eta}_p \neq 0$ by Assumption 2.3.1. Thus $\mathbf{A}_{c_4}$ can not be made Hurwitz and as a result $\mathbf{A}_c$ is also not Hurwitz. Thus the output regulation problem is not solvable by the control law (2.23). This concludes the proof. □

2.6 Illustrative Example

In this section we present a numerical example to illustrate the design process of our proposed solution. The follower agents are considered to be double integrator systems, and the exosystem is assumed to be an unforced dual-frequency harmonic oscillator. The system dynamics as given in (2.1) have the following state space matrices

$$A_i = \begin{bmatrix} 0 & 1 \\ 0 & 0 \end{bmatrix}, B_i = \begin{bmatrix} 0 \\ 1 \end{bmatrix}, E_i = \begin{bmatrix} 0 & 0 & 0 & 0 \\ 1 & 0 & 1 & 0 \end{bmatrix},$$
$$C_i = \begin{bmatrix} 1 & 0 \end{bmatrix}, D_i = 0, F_i = \begin{bmatrix} 0 & 1 & 0 & 1 \end{bmatrix}, \ i = 1, 2, 3, 4.$$

The dynamics of the exosystem are captured by (2.2) with

$$S = \text{blk diag}(S_1, S_2), \; S_1 = \begin{bmatrix} 0 & -1 \\ 1 & 0 \end{bmatrix}, \; S_2 = \begin{bmatrix} 0 & -2 \\ 2 & 0 \end{bmatrix}.$$

The communication network between the subsystems and the exosystem is illustrated in Fig. 2.1. The active followers $i = 1$, 2, and 3 form a strongly connected network as in Assumption 2.3.5, while $i = 4$ corresponds to a passive agent. Subsystems 1 and 2 are children nodes of the exosystem, and agent 3 is a child node of agent 2 and the Laplacian matrix corresponding to Fig. 2.1 is found to be

$$L = \begin{bmatrix} 0 & 0 & 0 & 0 & 0 \\ -1 & 2 & -1 & 0 & 0 \\ -1 & 0 & 2 & -1 & 0 \\ 0 & -1 & 0 & 1 & 0 \\ 0 & 0 & 0 & -1 & 1 \end{bmatrix},$$

which satisfies the connectivity requirement in Assumption 2.3.5. The strongly-connected graph Laplacian matrix $\mathcal{L}$ for the active agents is given as

$$\mathcal{L} = \begin{bmatrix} 1 & -1 & 0 \\ 0 & 1 & -1 \\ -1 & 0 & 1 \end{bmatrix},$$

which has the left eigenvector $\zeta = \begin{bmatrix} 1/3 & 1/3 & 1/3 \end{bmatrix}^{\mathrm{T}}$.

The measured output matrices are given as

$$C_{w_1} = \begin{bmatrix} 1 & 0 & 0 & 0 \\ 0 & 1 & 0 & 0 \end{bmatrix}, \; C_{w_2} = \begin{bmatrix} 0 & 0 & 1 & 0 \\ 0 & 0 & 0 & 1 \end{bmatrix}, \; C_{w_3} = 0.$$

It is easy to check that the pair $(S,\bar{C}_{w_a})$ is detectable, and thus Assumption 2.3.4 is satisfied. Given the measurement output matrices $C_{w_i}, i=1,2,3$, the pair of matrices (S,C_{w_i}) is not detectable and thus the control algorithms developed in [29,30] do not apply to the current problem, i.e. from $y_1 = \begin{bmatrix} w_1, w_2 \end{bmatrix}^{\mathrm{T}}$, $y_2 = \begin{bmatrix} w_3, w_4 \end{bmatrix}^{\mathrm{T}}$ and $w_3 = 0$, it is not possible for any active follower $i = 1,2,3$ to independently estimate the complete exosystem state vector w. We choose the observer gain matrices G_i as follows

$$G_1 = \begin{bmatrix} 1 & 0 & 1 & 0 \\ 0 & 1 & 0 & 0 \end{bmatrix}, G_2 = \begin{bmatrix} 0 & 0 & 1 & 0 \\ 0 & 0 & 0 & 1 \end{bmatrix}, G_3 = 0,$$

which satisfy the conditions in Lemma 2, i.e, $\mathcal{R} = 3S - \mu\sum_{i=1}^{3} G_i' C_{w_i}$ is a Hurwitz matrix. Then from (2.11), we find $P = 1.5I_4$ which renders $(P\rho_i + \rho_i^{\mathrm{T}} P),\ i = 1,2,3$ a negative semi-definite matrix. By selecting $\mu = 1$, the eigenvalues of matrix $\mathcal{R}$ can be placed at $-0.33 \pm j3, -0.33 \pm j6$. For further increment of μ, the eigenvalues can be moved further to the left half plane, assuring faster tracking of exosystem signal (2.2) by the dynamic compensator states (2.4), (2.5).

The distributed control law yields the form (2.8) with

$$K_{1_i} = \begin{bmatrix} -8 & -4 \end{bmatrix}, K_{2_i} = \begin{bmatrix} -5 & -7 & -9 & -4 \end{bmatrix},$$

for $i = 1,2,3$ and 4.

Applying the control law (2.8), we obtain the simulation result in Figure 2.2, which shows the regulated output of the follower agents asymptotically converging to zero. Figure 2.3 shows that all the followers' estimation $\eta_{ij},\ i = 1,2,3,4$ of exosystem state component w_j successfully track the leader's trajectory.

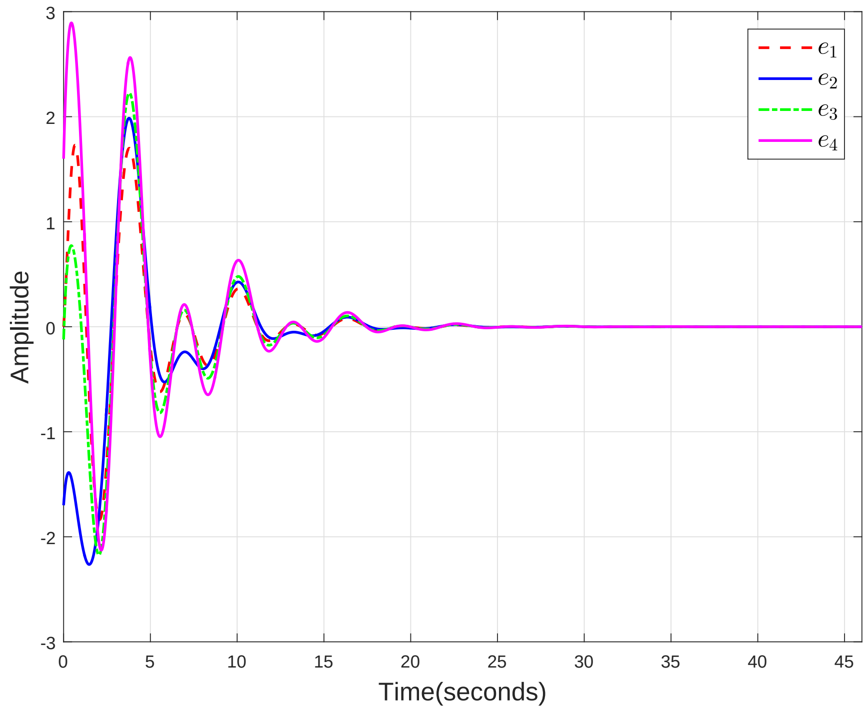

Figure 2.2: Regulated error output of the overall system under the distributed state feedback control

Next, we approach the same problem using distributed output feedback control law (2.23) where

$$K_{1_i} = \begin{bmatrix} -8 & -4 \end{bmatrix}, K_{2_i} = \begin{bmatrix} -5 & -7 & -9 & -4 \end{bmatrix}, H_i = \begin{bmatrix} -8 & -4 \end{bmatrix}^{\mathrm{T}}.$$

It is easy to verify that Assumptions 2.3.1-2.5.1 hold and thus it is possible to solve the problem by using distributed output feedback control (2.23).

Applying the control law (2.23) we obtain the simulation result in Fig. 2.4, which presents the regulated output of the follower agents as they converge to zero asymptotically.

2.7 Conclusion

In this chapter, the CORP for linear MASs is considered. In particular, we investigate the case where the agents in the system only receive limited information about the

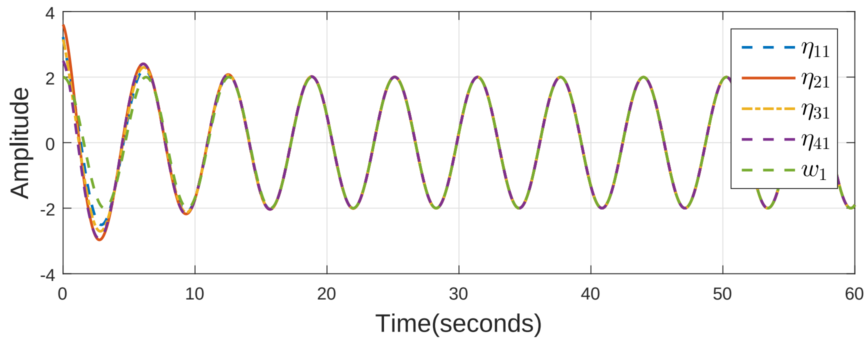

(a) w_1

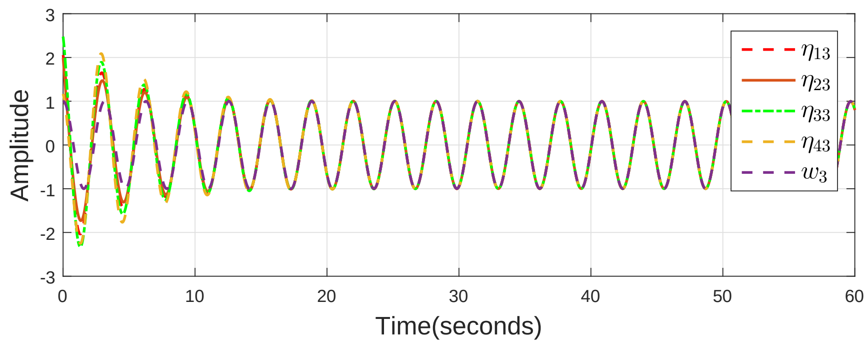

(b) w_3

Figure 2.3: Tracking of the exosystem states w_1, w_3 by the follower agents under distributed state feedback control law

exosystem states. The proposed solution to the regulation problem is a distributed control law that incorporates a decentralized observation method to collectively estimate the exosystem dynamics. Compared to previous works in the literature, cooperative output regulation is achieved here under relaxed detectability assumption.

An illustrative example was offered to verify the theoretical results developed in this chapter. Simulation results show that the regulated error outputs of the MAS are synchronized and converges to zero. It is also seen in the illustrative example that the distributed exosystem observer provides accurate estimations of the leader dynamics to all follower agents in the system.

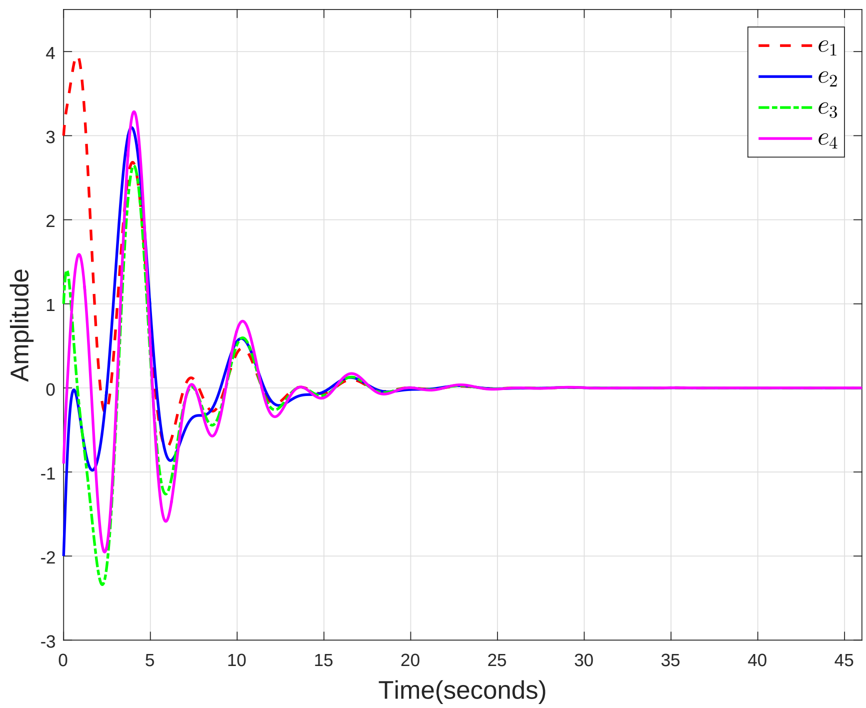

Figure 2.4: Regulated error output of the overall system under the distributed output feedback control

Chapter 3

Robust Cooperative Output Regulation of Multi-Agent Systems

3.1 Introduction

In this chapter, robust CORP for a class of linear uncertain MASs is studied under the assumption that none of the agents can access sufficient exosystem measurements and local regulated error signals for control. Due to these constraints, the agents in the system cannot independently reconstruct the exosystem dynamics, or rely on their own local measurements to achieve the objectives of the ORP. The solution to the regulation problem proposed in this work is a distributed dynamic control law that reconstructs the exosystem states, given a mild collective detectability assumption. Furthermore, the proposed distributed control law incorporates an internal model of the exosystem to allow for uncertain dynamics of the MAS A numerical example is offered to illustrate the effectiveness of the proposed control solution.

The rest of the chapter is organized in the following way. Some preliminaries on the MAS dynamics are presented in Section 3.2. In Section 3.2.1 we formulate our control problem and introduce the problem objective. The state feedback control solutions are derived in Section 3.4 while the output feedback counterpart in Section 3.5. These results are validated with an illustrative example in Section 3.6. Finally, some concluding remarks are presented in Section 3.7. Unless mentioned otherwise, the symbol $\|.\|$ in this chapter denotes the infinity norm of a vector.

3.2 Preliminaries

3.2.1 System Model

Consider the following system group, consisting of N linear subsystems with dynamics

$$\begin{aligned} \dot{x}_i &= A_i^* x_i + B_i^* u_i + E_i^* w, \\ e_i &= C_i x_i + D_i u_i + F_i w, \\ y_{mi} &= C_{w_i} w, \;\; i = 1, 2, 3, \cdots, N, \end{aligned} \tag{3.1}$$

where $x_i \in \mathbb{R}^{n_i}, u_i \in \mathbb{R}^{m_i}, e_i \in \mathbb{R}^p$ and $y_{mi} \in \mathbb{R}^{\mathbf{p}_i}$ are respectively the state, control input, regulated output and measurement output vectors of the i^{th} subsystem as noted in Chapter 2. We assume that the matrix C_{w_i} is known, but the matrices A_i^*, B_i^* and E_i^* are uncertain and defined as

$$\begin{aligned} A_i^* &= A_i + \delta A_i, \\ B_i^* &= B_i + \delta B_i, \\ E_i^* &= E_i + \delta E_i, \end{aligned} \tag{3.2}$$

where A_i, B_i and E_i are known nominal values, and $\delta A_i, \delta B_i$ and δE_i are perturbations from their respective nominal values. For convenience, define a row vector d_w as

$$\begin{aligned} d_w =[&\text{vec}(\delta A_1) \quad \text{vec}(\delta A_2) \quad \cdots \quad \text{vec}(\delta A_N) \\ &\text{vec}(\delta B_1) \quad \text{vec}(\delta B_2) \quad \cdots \quad \text{vec}(\delta B_N) \end{aligned}$$

$$\operatorname{vec}(\delta E_1) \quad \operatorname{vec}(\delta E_2) \quad \cdots \quad \operatorname{vec}(\delta E_N)] \in \mathbb{R}^{\sum_{i=1}^{N} n_i(n_i+m_i+q)}, \tag{3.3}$$

where $\operatorname{vec}(\Lambda) = \begin{bmatrix} \Lambda_1 & \Lambda_2 & \cdots & \Lambda_{m_1} \end{bmatrix}$ with Λ_i being the i^{th} row of $\Lambda \in \mathbb{R}^{m_1 \times m_2}$, and $d_w = 0$ corresponds to a nominal system. The external signal $w \in \mathbb{R}^q$ in (3.1), generated by the exosystem (2.2) represents both the reference input to be tracked and the disturbance input to be rejected by the subsystems.

The control objective of the considered problem is to design a robust distributed dynamic feedback control law, such that the regulated output e_i of each subsystem in (3.1) asymptotically approaches zero for a small parameter perturbation d_w. Similar to Chapter 2, we decouple our problem into two parts: the asymptotic stabilisation of the nominal subsystem dynamics, and the output regulation of the combined system (3.1), (2.2) under perturbation d_w. Next we mathematically formulate the proposed problem with necessary underlying assumptions and define the problem objective.

3.3 Problem Formulation

Similar to the nominal case, we consider that the Assumptions 2.3.1-2.5.1 hold. With the communication network between the follower agents captured by the digraph $\mathcal{G}$ and the distributed observer dynamics (2.4) and (2.5), we introduce the current problem objective.

Problem 3.3.1. *Robust CORP* - Given the MAS with agent dynamics (3.1), exosystem (2.2) and communication graph $\mathcal{G}$ find a robust dynamic feedback control law u_i, $i = 1, 2, \cdots, N$, such that

1. the subsystem (3.1) under the control u_i is asymptotically stable when $w = 0$,

2. for any arbitrary initial conditions $x_i(0), \eta_i(0)$, and $w(0)$, the regulated output satisfies $\lim_{t\to\infty} e_i(t) = 0$.

3.4 Distributed State Feedback Control

Consider the case when $d_w \neq 0$ and we propose a solution to Problem 3.3.1 as follows

$$\begin{aligned} u_i &= K_{1_i} x_i + K_{2_i} z_i, \\ \dot{z}_i &= T_1 z_i + T_2 \hat{e}_i, i = 1, 2, \cdots, N, \end{aligned} \tag{3.4}$$

where x_i is the state vector of the agent, $z_i \in \mathbb{R}^{n_z}$, and the pair of matrices (T_1, T_2) is a p-copy internal model of S. The matrices of the pair (T_1, T_2) [23] are defined as follows

$$\begin{aligned} T_1 &= \text{blk diag} \underbrace{[\gamma, \gamma, ..., \gamma]}_{p\text{-tuple}}, \\ T_2 &= \text{blk diag} \overbrace{[\beta, \beta, ..., \beta]}, \end{aligned} \tag{3.5}$$

where γ is a square matrix and β is a column vector so that (γ, β) is controllable and the characteristic polynomial of γ equals the minimal polynomial of S. The local regulated error $e_i, i = 1, 2, \cdots, l$ is assumed not to be available through feedback in our work, we instead make use of an estimated error variable $\hat{e}_i, i = 1, 2, \cdots, N$ defined as

$$\hat{e}_i = C_i x_i + D_i u_i + F_i \eta_i, \tag{3.6}$$

where η_i is obtained from (2.4) and (2.5). The appropriate selection of control gain matrices $K_{1_i} \in \mathbb{R}^{m_i \times n_i}$, and $K_{2_i} \in \mathbb{R}^{m_i \times n_z}$ is noted in the next remark.

Remark 3.4.1. *From the definition of internal model and Assumption 2.3.3, T_1 satisfies*

$$\mathit{rank} \begin{bmatrix} A_i - \lambda I & B_i \\ C_i & D_i \end{bmatrix} = n_i + p, \forall \lambda \in \bar{\sigma}(T_1), i = 1, 2, \cdots, N, \tag{3.7}$$

where $\bar{\sigma}(T_1)$ denotes the eigenspectrum of T_1. Furthermore, Lemma 1.26 from [23] yields that the pairs

$$\left(\begin{bmatrix} A_i & 0 \\ T_2C_i & T_1 \end{bmatrix}, \begin{bmatrix} B_i \\ T_2D_i \end{bmatrix}\right), i = 1, 2, \cdots, N,$$

are stabilizable, and there exists $\begin{bmatrix} K_{1_i} & K_{2_i} \end{bmatrix}$ such that

$$\begin{aligned} A_{nc_i} &= \begin{bmatrix} A_i & 0 \\ T_2C_i & T_1 \end{bmatrix} + \begin{bmatrix} B_i \\ T_2D_i \end{bmatrix} \begin{bmatrix} K_{1_i} & K_{2_i} \end{bmatrix}, \\ &= \left[\begin{array}{c|c} A_i + B_iK_{1_i} & B_iK_{2_i} \\ \hline T_2(C_i + D_iK_{1_i}) & T_1 + T_2D_iK_{2_i} \end{array}\right], i = 1, 2, \cdots, N, \end{aligned} \tag{3.8}$$

is Hurwitz.

With a slight abuse of notation, we redefine the overall closed-loop state vector as $x_c = \mathrm{col}(x, z, \tilde{\eta})$ and $e = \mathrm{col}(e_a, e_p)$. The overall closed-loop dynamics of the MAS (3.1) and (2.2) under the control (2.4), (2.5) and (3.4) then follows the state equation (2.16) with the system matrices

$$\mathbf{A}_c = \left[\begin{array}{c|c} \mathbf{A}_{c_1} & \mathbf{A}_{c_2} \\ \hline 0 & \mathbf{A}_{c_4} \end{array}\right],$$

where

$$\mathbf{A}_{c_1} = \left[\begin{array}{c|c} A^* + B^*K_1 & B^*K_2 \\ \hline (I_N \otimes T_2)(C + DK_1) & (I_N \otimes T_1) + (I_N \otimes T_2)DK_2 \end{array}\right],$$

$$\mathbf{A}_{c_2} = \left[\begin{array}{c} 0 \\ \hline (I_N \otimes T_2)F \end{array}\right], \mathbf{A}_{c_4} = \left[\begin{array}{c|c} \rho - \mu(\mathcal{L} \otimes I_q) & 0 \\ \hline -\mu(\alpha_{32} \otimes I_q) & \mathcal{P} \end{array}\right],$$

$$\mathbf{B}_c = \mathrm{col}(\mathbf{B}_{c_1}, 0), \mathbf{B}_{c_1} = \mathrm{col}(\bar{E}^*, (I_N \otimes T_2)\bar{F}),$$
$$\mathbf{C}_c = \begin{bmatrix} \mathbf{C}_{c_1} & 0 \end{bmatrix}, \mathbf{C}_{c_1} = \begin{bmatrix} C + DK_1 & DK_2 \end{bmatrix},$$
$$\mathbf{D}_c = \mathrm{col}(\bar{F}_a, \bar{F}_p).$$

It was noted in the proof of Lemma 2.4.3 that matrices $\rho - \mu(\mathcal{L} \otimes I_q)$ and $\mathcal{P}$ are Hurwitz and so is $\mathbf{A}_{c_4}$. Therefore, the overall closed-loop system matrix $\mathbf{A}_c$ is Hurwitz if $\mathbf{A}_{c_1}$ or equivalently the matrices

$$A_{c_i} = \left[\begin{array}{c|c} A_i^* + B_i^* K_{1_i} & B_i^* K_{2_i} \\ \hline T_2(C_i + D_i K_{1_i}) & T_1 + T_2 D_i K_{2_i} \end{array}\right], i = 1, 2, \cdots, N, \tag{3.9}$$

can be made Hurwitz. Let $\mathbf{x}_c = \mathrm{col}(x, z)$ define states associated with $\mathbf{A}_{c_1}$. The regulation problem in (2.16) thus reduces to the regulation with reduced system

$$\begin{aligned} \dot{\mathbf{x}}_c &= \mathbf{A}_{c_1}\mathbf{x}_c + \mathbf{B}_c w + \mathbf{A}_{c_2}\tilde{\eta}, \\ e &= \mathbf{C}_{c_1}\mathbf{x}_c + \mathbf{D}_c w. \end{aligned} \tag{3.10}$$

Remark 3.4.1 also states that A_{nc_i} and the nominal value of $\mathbf{A}_{c_1}$, given as

$$\mathbf{A}_{nc_1} = \left[\begin{array}{c|c} A + BK_1 & BK_2 \\ \hline (I_N \otimes T_2)(C + DK_1) & (I_N \otimes T_1) + (I_N \otimes T_2)DK_2 \end{array}\right], \tag{3.11}$$

can be made Hurwitz by the selection of control gains K_1 and K_2 and block diagonal matrices A and B are defined in (2.7).

Lemma 3.4.1. *Under Assumption 2.3.1, consider the controller* (3.4) *incorporating an internal model of the exosystem* (2.2), *so that the closed-loop system* (3.10) *has asymptotically stable nominal dynamics. There exists an open neighbourhood W of the origin such that A_{c_i}, $i = 1, 2, \cdots, N$ is Hurwitz for $d_w \in W$. Furthermore, there* *exists a unique matrix X_{c_i} that satisfies*

$$\begin{aligned} X_{c_i}S &= A_{c_i}X_{c_i} + B_{c_i}, \\ 0 &= C_{c_i}X_{c_i} + F_i. \end{aligned} \tag{3.12}$$

where

$$B_{c_i} = \begin{bmatrix} E_i^* \\ T_2F_i \end{bmatrix}, C_{c_i} = \begin{bmatrix} C_i + D_iK_{1_i} & D_iK_{2_i} \end{bmatrix}.$$

Proof. By Remark 3.4.1 and internal model (T_1, T_2) in (3.4), there exists $\begin{bmatrix} K_{1_i} & K_{2_i} \end{bmatrix}$, $i = 1, 2, \cdots, N$, such that $A_{nc_i}, i = 1, 2, \cdots, N$ are Hurwitz. In addition, there exists an open neighbourhood W around the origin such that for any $d_w \in W$, (3.9) and $\mathbf{A}_{c_1}$ are also Hurwitz. It follows from Lemma 1.27 of [23] and Assumption 2.3.1 that, if A_{c_i} and $\mathbf{A}_{c_1}$ are Hurwitz, then for any E_i^* and F_i with appropriate dimensions, there exist unique solutions X_i and $Z_i, i = 1, 2, \cdots, N$ satisfying

$$\begin{aligned} X_iS &= (A_i^* + B_i^*K_{1_i})X_i + B_i^*K_{2_i}Z_i + E_i^*, \\ Z_iS &= T_1Z_i + T_2((C_i + D_iK_{1_i})X_i + D_iK_{2_i}Z_i + F_i), \\ 0 &= (C_i + D_iK_{1_i})X_i + D_iK_{2_i}Z_i + F_i. \end{aligned} \tag{3.13}$$

Let $X_{c_i} = \mathrm{col}(X_i, Z_i), i = 1, 2, \cdots, N$. Then (3.13) implies (3.12), which concludes the proof. □

Theorem 3.4.2. *For MAS* (3.1) *and* (2.2)*, let Assumptions 2.3.1-2.3.5 be satisfied, and its connectivity digraph contains a directed spanning tree with node* 0 *as the root. The robust CORP is solvable by a p-copy internal model* (T_1, T_2) *in* (3.5) *and a distributed dynamic feedback control law* (3.4)*, if the conditions in Lemma 3 are satisfied.*

Proof. Let system (3.1) and (2.2) satisfy Assumptions 2.3.4 and 2.3.5, and digraph $\mathcal{G}$ contain a directed spanning tree. Then by Lemma 2, there exist G_i's such that $\lim_{t\to\infty}\tilde{\eta}_i(t)=0$. Additionally, the regulation of the overall system (2.16) reduces to the regulation of (3.10). We transform the coordinates of the state variables (x_i, z_i) as follows.

$$\begin{aligned}\tilde{x}_i &= x_i - X_i w,\\ \tilde{z}_i &= z_i - Z_i w, i=1,2,\cdots,N.\end{aligned} \tag{3.14}$$

Then (3.14) in combination with (3.12) yields the state equations

$$\dot{\tilde{x}}_i = (A_i^* + B_i^* K_{1_i})\tilde{x}_i + B_i^* K_{2_i}\tilde{z}_i, \tag{3.15}$$

$$\dot{\tilde{z}}_i = T_2(C_i + D_i K_{1_i})\tilde{x}_i + (T_1 + T_2 D_i K_{2_i})\tilde{z}_i + T_2 F_i \tilde{\eta}_i. \tag{3.16}$$

The error equation in (3.10), combined with (3.12) and (3.14), can be rewritten to the following form,

$$e_i = (C_i + D_i K_{1_i})\tilde{x}_i + (D_i K_{2_i})\tilde{z}_i. \tag{3.17}$$

Let $\mathbf{x}_{c_i} = \mathrm{col}(x_i, z_i), \tilde{\mathbf{x}}_{c_i} = \mathrm{col}(\tilde{x}_i, \tilde{z}_i)$. Then (3.15), (3.16), and (3.17) yield that

$$\begin{aligned}\dot{\tilde{\mathbf{x}}}_{c_i} &= A_{c_i}\tilde{\mathbf{x}}_{c_i} + \begin{bmatrix} 0 \\ T_2 F_i \end{bmatrix}\tilde{\eta}_i,\\ e_i &= C_{c_i}\tilde{\mathbf{x}}_{c_i},\end{aligned} \tag{3.18}$$

and $\tilde{\eta}_i(t) \to 0$ as $t \to \infty$. By Lemma 3, there exists an open neighbourhood W such that A_{c_i} is Hurwitz for $d_w \in W$. Therefore $\lim_{t\to\infty} e_i(t) = 0$. This concludes the proof. □

Remark 3.4.2. *Our solution to the robust CORP takes advantage of the estimation of the leader states by the active agent group as in Lemma 2.4.3 to reconstruct the local* *regulated error signals, rather than requiring specific structure for the local feedback measurement. This extends the results presented in [33] to systems with arbitrary local feedback measurements, as long as the assumptions of the control problem are satisfied.*

Remark 3.4.3. *The design procedure for the distributed feedback control law* (3.4) *is summarized as follows:*

- *select* (T_1, T_2) *as a p-copy internal model of* S*;*
- *select* K_{1_i} *and* K_{2_i} *such that* A_{nc_i} *in* (3.8) *is Hurwitz;*
- *choose an observer gain vector* G_i *which satisfies the conditions of Lemma 2.4.3 and* $\mathcal{R}$ *is Hurwitz;*
- *select the real positive valued parameter* μ *to regulate the convergence rate of* $\tilde{\eta}$*.*

3.5 Distributed Output Feedback Control

We now present the measurement feedback solution to Problem 3.3.1 for the uncertain MAS with $d_w \neq 0$. Let the measured output $y_i \in \mathbb{R}^{\mathbf{p}_i}$ for the i^{th} subsystem be given by

$$y_i = C_i x_i, \; i = 1, 2, 3, \ldots, N.$$

The definition of the measurement signal is narrower than that in the nominal case because the uncertainty in the measurement signal adds error to the state observation of the subsystems, which then propagates to the regulation signal e_i. Additionally, we also note that the exosystem measurement $y_{mi} = C_{w_i} w(t)$ is available to the active agents through their communication to determine their cooperative estimation of the leader's state η_i (2.4).

Assumption 3.5.1. *The pairs* (A_i, C_i) *are detectable,* $i = 1, 2, \cdots, N$*.*

For the MAS satisfying the Assumptions 2.3.1-2.3.5, 3.5.1, we consider the distributed dynamic measurement output feedback control law for $i = 1, 2, \cdots, N$ as

$$\begin{aligned}
u_i &= \begin{bmatrix} K_{1_i} & K_{2_i} \end{bmatrix} z_i, \\
\dot{z}_i &= \begin{bmatrix} A_i + B_i K_{1_i} + J_i C_i & B_i K_{2_i} \\ 0 & T_1 \end{bmatrix} z_i + \begin{bmatrix} -J_i \\ T_2 \end{bmatrix} \hat{e}_i + \begin{bmatrix} 0 \\ T_2 D_i \end{bmatrix} u_i + \begin{bmatrix} E_i \\ 0 \end{bmatrix} \eta_i, \\
\hat{e}_i &= y_i + F_i \eta_i, \ i = 1, 2, \cdots, N,
\end{aligned} \tag{3.19}$$

where $\eta_i \in \mathbb{R}^q$ are given in (2.4), (2.5), and $K_{1_i} \in \mathbb{R}^{m_i \times n_i}$ and $K_{2_i} \in \mathbb{R}^{m_i \times n_z}$ are the controller gains to be defined later. The estimation of regulated error $\hat{e}_i$ is obtained by the measurement output y_i and the distributed observer state η_i. The matrix J_i is found such that $A_i + J_i C_i$ is Hurwitz based on Assumption 3.5.1.

Remark 3.5.1. *The selection of the measurement signals in this section is inspired by [48], and it is needed to prevent the error caused by the uncertainty in the local state equations to propagate to the regulated error signal. Differently from [48], the control solution presented in this section incorporates the cooperative estimation of the exosystem state vector w to allow for system with milder detectability properties as in Assumption 2.3.4.*

Under the measurement feedback distributed control law (3.19), and with a slight abuse of notation as in previous sections, the state equations of the overall uncertain closed-loop system yield the form (2.16) with $x_c = \mathrm{col}(x, z, \tilde{\eta}), \tilde{\eta}_i = \eta_i - w, e = \mathrm{col}(e_a, e_p)$ and the state space matrices

$$\mathbf{A}_c = \left[\begin{array}{c|c} \mathbf{A}_{c_1} & \mathbf{A}_{c_2} \\ \hline 0 & \mathbf{A}_{c_4} \end{array}\right],$$

$$\mathbf{A}_{c_1} = \left[\begin{array}{c|cc} A^* & B^*K_1 & B^*K_2 \\ \hline -JC & A+BK_1+JC & BK_2 \\ (I_N \otimes T_2)C & (I_N \otimes T_2)DK_1 & (I_N \otimes T_1)+(I_N \otimes T_2)DK_2 \end{array}\right],$$

$$\mathbf{A}_{c_2} = \left[\begin{array}{c} 0 \\ \hline E-JF \\ (I_N \otimes T_2)F \end{array}\right],\ \mathbf{A}_{c_4} = \begin{bmatrix} \rho-\mu(\mathcal{L}\otimes I_q) & 0 \\ -\mu(\alpha_{32}\otimes I_q) & \mathcal{P} \end{bmatrix},$$

$$\mathbf{B}_c = \mathrm{col}(\mathbf{B}_{c_1}, 0),\ \mathbf{B}_{c_1} = \mathrm{col}(\bar{E}^*, \bar{E}-J\bar{F}, (I_N \otimes T_2)\bar{F}),$$

$$\mathbf{C}_c = \begin{bmatrix} \mathbf{C}_{c_1} & 0 \end{bmatrix},\ \mathbf{C}_{c_1} = \begin{bmatrix} C & DK_1 & DK_2 \end{bmatrix},$$

$$\mathbf{D}_c = \mathrm{col}(\bar{F}_a, \bar{F}_p).$$

It is noted in the proof of Lemma 2.4.3 that $\rho-\mu(\mathcal{L}\otimes I_q)$ and $\mathcal{P}$ are Hurwitz, and so $\mathbf{A}_{c_4}$ is Hurwitz. Therefore the overall closed-loop system matrix $\mathbf{A}_c$ is Hurwitz if $\mathbf{A}_{c_1}$ can be made Hurwitz, or

$$A_{c_i} = \left[\begin{array}{c|cc} A_i^* & B_i^*K_{1_i} & B_i^*K_{2_i} \\ \hline -J_iC_i & A_i+B_iK_{1_i}+J_iC_i & B_iK_{2_i} \\ T_2C_i & T_2D_iK_{1_i} & T_1+T_2D_iK_{2_i} \end{array}\right], \tag{3.20}$$

is Hurwitz for all $i = 1, 2, \cdots, N$.

Let $\mathbf{x}_c = \mathrm{col}(x, z)$ define the states associated with $\mathbf{A}_{c_1}$. The regulation problem in (2.16) then simplifies to the regulation of reduced system

$$\begin{aligned} \dot{\mathbf{x}}_c &= \mathbf{A}_{c_1}\mathbf{x}_c + \mathbf{A}_{c_2}\tilde{\eta} + \mathbf{B}_{c_1}w, \\ e &= \mathbf{C}_{c_1}\mathbf{x}_c + \mathbf{D}_c w. \end{aligned} \tag{3.21}$$

By the transformation matrix

$$T = \begin{bmatrix} I_{N_s} & 0 & 0 \\ 0 & 0 & I_{N_z} \\ -I_{N_s} & I_{N_s} & 0 \end{bmatrix}, N_s = \sum_{i=1}^{N} n_i, N_z = Nn_z,$$

the nominal value of $\mathbf{A}_{c_1}$ is similar to

$$T\mathbf{A}_{nc_1}T^{-1} = \left[\begin{array}{cc|c} A+BK_1 & BK_2 & BK_1 \\ (I_N \otimes T_2)(C+DK_1) & (I_N \otimes T_1) & (I_N \otimes T_2)DK_1 \\ & +(I_N \otimes T_2)DK_2 & \\ \hline 0 & 0 & A+JC \end{array}\right], \tag{3.22}$$

which is Hurwitz by the selection of K_1 and K_2 as in Remark 3.4.1, and the selection of J_i by Assumption 3.5.1.

Lemma 3.5.1. *Under Assumption 2.3.1, consider the controller* (3.19) *incorporating an internal model of the exosystem* (2.2)*, so that the closed-loop system* (3.21) *has asymptotically stable nominal dynamics. There exists an open neighbourhood W of the origin such that $A_{c_i}, i = 1, 2, \cdots, N$ is Hurwitz for $d_w \in W$. Furthermore, there exists a unique matrix X_{c_i} that satisfies*

$$\begin{aligned} X_{c_i}S &= A_{c_i}X_{c_i} + B_{c_i}, \\ 0 &= C_{c_i}X_{c_i} + F_i, \end{aligned} \tag{3.23}$$

where

$$B_{c_i} = col(E_i^*, E_i - J_iF_i, T_2F_i),\ C_{c_i} = \begin{bmatrix} C_i & D_iK_{1_i} & D_iK_{2_i} \end{bmatrix}.$$

Proof. By Remark 3.4.1 and internal model (T_1, T_2) in (3.19), there exists $\begin{bmatrix} K_{1_i} & K_{2_i} \end{bmatrix}$, and $J_i,\ i = 1,2,\cdots,N$, such that the nominal value of $\mathbf{A}_{c_1}$ (3.22) is Hurwitz. In addition there exists an open neighbourhood W around the origin such that for any $d_w \in W$, $\mathbf{A}_{c_1}$ and (3.20) are also Hurwitz. It follows from Lemma 1.27 of [23] and Assumption 2.3.1 that, if $\mathbf{A}_{c_1}$ and A_{c_i} are Hurwitz, then for any E_i^* and F_i with appropriate dimensions, there exist unique solutions X_i and $Z_i, i = 1,2,\cdots,N$ satisfying

$$\begin{aligned} X_i S &= A_i^* X_i + B_i^* \begin{bmatrix} K_{1_i} & K_{2_i} \end{bmatrix} Z_i + E_i^*, \\ Z_i S &= \begin{bmatrix} A_i + B_i K_{1_i} + J_i C_i & B_i K_{2_i} \\ 0 & T_1 \end{bmatrix} Z_i + \begin{bmatrix} -J_i C_i \\ T_2 C_i \end{bmatrix} X_i \\ &\quad + \begin{bmatrix} 0 & 0 \\ T_2 D_i K_{1_i} & T_2 D_i K_{2_i} \end{bmatrix} Z_i + \begin{bmatrix} E_i - J_i F_i \\ T_2 F_i \end{bmatrix}, \\ 0 &= C_i X_i + \begin{bmatrix} D_i K_{1_i} & D_i K_{2_i} \end{bmatrix} Z_i + F_i. \end{aligned} \tag{3.24}$$

Let $X_{c_i} = \mathrm{col}(X_i, Z_i), i = 1,2,\cdots,N$. Then (3.24) implies (3.23) which concludes the proof. □

Theorem 3.5.2. *For MAS* (3.1) *and* (2.2)*, let Assumptions 2.3.1-2.3.5 and 3.5.1 be satisfied, and its connectivity digraph contains a directed spanning tree with node* 0 *as the root. The robust CORP is solvable by a p-copy internal model* (T_1, T_2) *in* (3.5) *and a distributed dynamic output feedback control law* (3.19)*, if the conditions in Lemma 3.5.1 are satisfied.*

Proof. Let system (3.1) and (2.2) satisfy Assumptions 2.3.4 and 2.3.5, and let digraph $\mathcal{G}$ contain a directed spanning tree. Then by Lemma 2.4.3, there exists G_i's such that $\lim_{t\to\infty} \tilde{\eta}_i(t) = 0$. Additionally, the regulation of the overall system (2.16) reduces to the regulation of (3.21). Using the same coordinate transformation of the state variables (x_i, z_i) as in (3.14) results in

$$\dot{\tilde{\mathbf{x}}}_{c_i} = A_{c_i}\tilde{\mathbf{x}}_{c_i} + \begin{bmatrix} 0 \\ E_i - J_i F_i \\ T_2 F_i \end{bmatrix} \tilde{\eta}_i, \qquad e_i = C_{c_i}\tilde{\mathbf{x}}_{c_i}. \tag{3.25}$$

where $\tilde{\mathbf{x}}_{c_i} = \mathrm{col}(\tilde{x}_i, \tilde{z}_i)$, and $\tilde{\eta}_i(t) \to 0$ as $t \to \infty$. From Lemma 3.5.1, there exists an open neighbourhood W such that A_{c_i} (3.25) is Hurwitz for $d_w \in W$. Therefore $\lim_{t\to\infty} e_i(t) = 0$. This concludes the proof. □

Remark 3.5.2. *The design procedure for the distributed output feedback control law* (3.19) *is summarized as follows:*

- *select* (T_1, T_2) *as a p-copy internal model of* S*;*
- *select* K_{1_i} *and* K_{2_i} *such that the nominal form of subsystem matrix* A_{nc_i} *in* (3.8) *is Hurwitz;*
- *choose an observer gain vector* G_i *which satisfies the conditions of Lemma 2.4.3 and* $\mathcal{R}$ (2.15) *is Hurwitz;*
- *select the real positive valued parameter* μ *to regulate the convergence rate of* $\tilde{\eta}$*.*

So far we have considered that the measurement output y_i and regulated output e_i do not have uncertainties in their equations. We now briefly investigate the effect of uncertain parameters in the error equation, i.e, $e_i^* = C_i^* x_i + D_i^* u_i + F_i^* w$, where C_i^*, D_i^*, F_i^* are defined in a similar manner as (3.2), and $\delta C_i, \delta D_i, \delta F_i$ are perturbations from their respective nominal values C_i, D_i, F_i. The measurement output and the estimated regulated error are defined as $y_i = C_i^* x_i$ and $\hat{e}_i = y_i + F_i \eta_i$, respectively.

Following the same procedure as presented earlier in this section, it can be shown that Lemma 3.5.1 still holds in the presence of the measurement and regulated error uncertainties. In addition, following the proof of Theorem 3.5.2 it can be shown that the regulated error signal e_i will approach

$$e_i = (\begin{bmatrix} \delta D_i K_{1_i} & \delta D_i K_{2_i} \end{bmatrix} Z_i + \delta F_i) w, \tag{3.26}$$

as time approaches infinity, where Z_i is the new solution to (3.23). The residual error in (3.26) is expected as it represents the difference between the estimated regulated error $\hat{e}_i$ in the control and its actual value.

3.6 Illustrative Example

To illustrate the design process of our proposed solution we now present a numerical example in this section. With the same nominal system matrices and exosystem as in Section 2.6 and the communication digraph between the followers as in Fig. 2.1, we now introduce the uncertainty to the follower subsystems as follows

$$\delta A_i = \begin{bmatrix} 0 & 0 \\ 0.1i & 0.2i \end{bmatrix}, \delta B_i = \begin{bmatrix} 0 \\ 0.2i \end{bmatrix}, \delta E_i = \begin{bmatrix} 0 & 0 & 0 & 0 \\ 0.2i & 0 & 0.2i & 0 \end{bmatrix}, i = 1,2,3,4. \tag{3.27}$$

The distributed control law yields the form (3.4) with

$$K_{1_i} = \begin{bmatrix} -40 & -13 \end{bmatrix}, K_{2_i} = \begin{bmatrix} -14 & -39 & -27 & -36 \end{bmatrix}, \; i = 1,2,3,4.$$

To solve the robust output regulation problem, we define the 1-copy internal model satisfying (3.7) as

$$G_1 = \left[\begin{array}{c|c} 0 & I_3 \\ \hline -4 & Q \end{array}\right], \; G_2 = \begin{bmatrix} 0_{3\times 1} \\ 1 \end{bmatrix}, \; Q = \begin{bmatrix} 0 & -5 & 0 \end{bmatrix}. \tag{3.28}$$

From (3.8) we verify that the nominal subsystem matrix A_{nc_i} is Hurwitz. Applying the control law (3.4), we obtain the simulation result in Figure 3.1, which shows the regulated output of the follower agents asymptotically converging to zero.

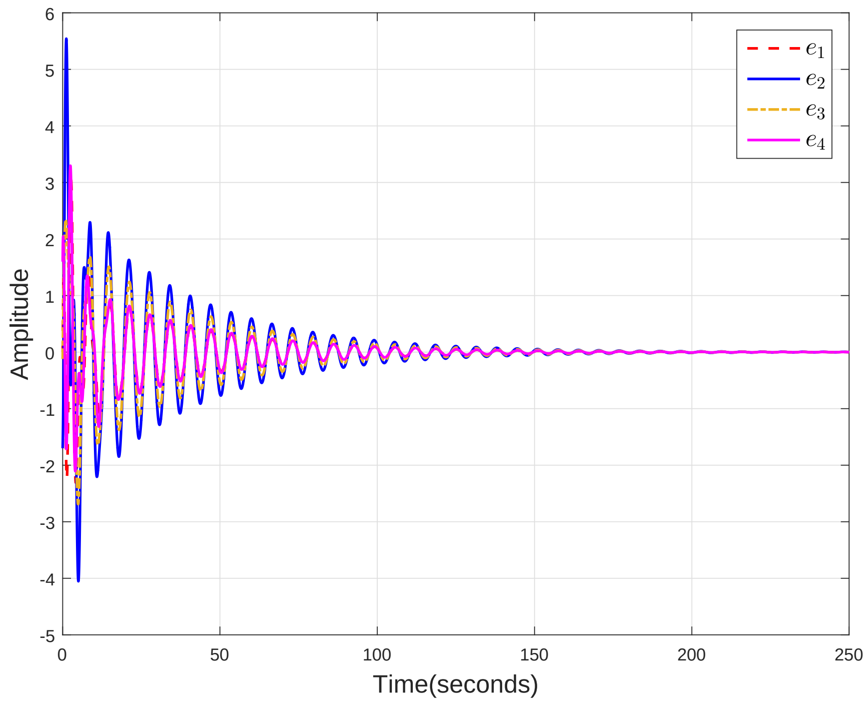

Figure 3.1: Regulated error output of the overall system under the distributed state feedback control

Next, we approach the same problem using distributed output feedback control law (3.19) where $J_i = \begin{bmatrix} -8 & -4 \end{bmatrix}^{\mathrm{T}}$, K_{1_i} and K_{2_i} are the same as the state feedback case. It is easy to verify that Assumptions 2.3.1-2.3.5, 3.5.1 hold and thus it is possible to solve the problem by using distributed output feedback control (3.19) incorporating an internal model, the values of which are given in (3.28). We verify that the nominal form of (3.21) is stable, and so there exists an open neighbourhood W of the origin such that $\mathbf{A}_{c_1}$ is Hurwitz when the uncertainties (3.27) are introduced into the system. Applying the control law (3.19) we obtain the simulation result in Fig. 3.2, which presents the regulated output of the follower agents as they converge to zero asymptotically. Furthermore, we consider the uncertain measurement outputs

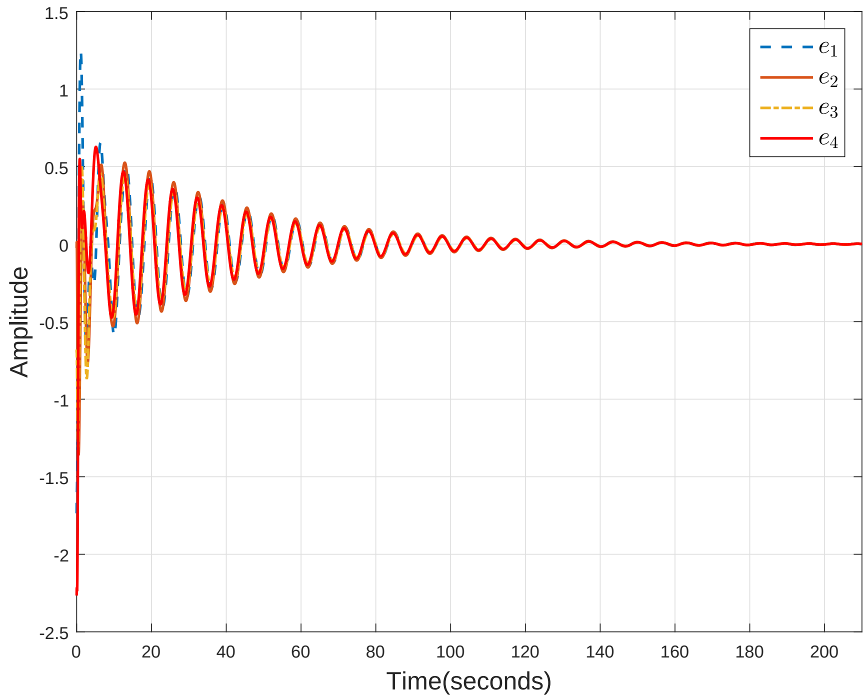

Figure 3.2: Regulated error output of the overall system under the distributed output feedback control

y_i and regulated outputs $e_i, i = 1,2,3,4$ with

$$\delta C_i = \begin{bmatrix} 0.1i & 0 \end{bmatrix}, \delta D_i = 0.1i, \delta F_i = \begin{bmatrix} 0 & 0.1i & 0 & 0.1i \end{bmatrix}, \ i = 1,2,3,4,$$

which when substituted in (3.26) yield

$$\|e_1\| = 0.789, \|e_2\| = 1.4, \|e_3\| = 1.913, \|e_4\| = 2.367.$$

3.7 Conclusion

In this chapter, the CORP for uncertain MASs is considered. In particular, we investigate the case where the agents in the system are unable to access their local regulated error signals as feedback measurements, and all agents receive limited information about the exosystem states. The proposed solution to the regulation problem is a distributed control law that incorporates an internal model of the exosystem, and a decentralized observation method to collectively estimate the exosystem dynamics. Compared to previous works in the literature, robust CORP is achieved here under relaxed requirement on the feedback error signal needed for control. We also derived the maximum bounds on the error regulated signal when it was subjected to uncertainty.

An illustrative example was offered to verify the theoretical results developed in this chapter. Simulation results show that the regulated error outputs of the MAS are synchronized and converges to zero. It is also seen in the illustrative example that the decentralized exosystem observer provides accurate estimations of the leader dynamics to all follower agents in the system.

Chapter 4

Coperative Output Regulation under Switching Communication and Detectability Constraints

In this chapter we study the CORP of linear MASs under switching communication topology and exosystem detectability constraints. As compared to similar works in the literature, we consider the problem scenario in which none of the agents can estimate the exosystem states from their individual measurements on any of the switching configurations of the system. In other words, no agent in the system can solve the output regulation problem independently. Consensus and output regulation problems for MASs with time-varying communication topologies are studied for time delayed systems in [17, 25, 49, 50], and systems without delay in [41, 51]. Synchronization problems for homogeneous nonlinear agents over switching networks is studied in [52]. However the cooperative control problem with the considered detectability constraint has not yet been addressed for the switching communication topology in the earlier works, to the best of authors' knowledge.

By devising a distributed observer to reconstruct the exosystem states based on the collective measurements available to the followers over a certain switching time-intervals, we synthesize a distributed control solution to the output regulation problem. The rest of the chapter is organized in the following way. System dynamics and relevant terminologies of information graphs are presented in Section 4.1. In Section 4.2 we formulate our control problem, and provide necessary assumptions. Next, we derive the main theoretical results of this work, and offer a state feedback distributed control solution in Section 4.3, and measurement output feedback control solution in Section 4.4. These results are further validated with the help of an illustrative example in Section 4.5. Finally some conclusions are reported in Section 4.6.

Notation. We now briefly introduce the most frequently used notations through the rest of the chapter. The symbol $\|.\|$ denotes the Euclidean norm of a vector/matrix unless otherwise mentioned, and $\lambda_i(\mathcal{X})$ denotes the i^{th} eigenvalue of a matrix $\mathcal{X}$. For two symmetric matrices A and B, $A < (\leq) B$ implies that the matrix $A - B$ is negative (semi-) definite.

4.1 Preliminaries

4.1.1 System Model

Consider the system group consisting of N linear subsystems in (2.1) and an exosystem in (2.2) with the measurement signal y_{mi} for the i^{th} subsystem redefined as

$$y_{mi} = C_{w_i}(\sigma(t), t)w, \ y_{mi} \in \mathbb{R}^{p_{m_i}}, \tag{4.1}$$

where $\sigma(t)$ is the switching signal corresponding to the switching communication topology to be introduced next.

4.1.2 Information Graph

Given a set of r digraphs $\mathcal{G}_i = (\mathcal{V}, \mathcal{E}_i), i = 1, 2, 3, \cdots, r$, which has the same node set as the digraph $\mathcal{G} = (\mathcal{V}, \mathcal{E})$ and $\mathcal{E} = \cup_{i=1}^{r} \mathcal{E}_i$, then $\mathcal{G} = \cup_{i=1}^{r} \mathcal{G}_i$ is said to be the union of digraphs $\mathcal{G}_i$.

Let us assume an infinite sequence of switching instants $\{t_i : i \in \mathbb{Z}^+ \cup \{0\}$ and $t_0 = 0\}$, which satisfies $t_{k+1} - t_k \geq \boldsymbol{\tau}^* > 0$, where $\boldsymbol{\tau}^*$ is called the dwell time and $\mathbb{Z}^+$ is the set of positive integers. We define $\sigma(t)$ to denote a piecewise constant switching signal such that $\sigma(t) \in \mathcal{P} = \{1, 2, \cdots, \rho\}$ where $\rho \in \mathbb{Z}^+$ is a switching index set. Define switching graph $\mathcal{G}_{\sigma(t)} = (\mathcal{V}, \mathcal{E}_{\sigma(t)}), \mathcal{E}_{\sigma(t)} \subseteq (\mathcal{V} \times \mathcal{V}), \mathcal{V} = \{0, 1, 2, \cdots, N\}$, for the switching signal $\sigma(t)$. The neighboring set of node j, $\mathcal{N}_{j,\sigma(t)} \subseteq \mathcal{V}$, is the set of all its parent nodes in the digraph $\mathcal{G}_{\sigma(t)}$. The weighted adjacency matrix $\mathcal{A}_{\sigma(t)} = [a_{ij}(\sigma(t), t)] \in \mathbb{R}^{(N+1)\times(N+1)}$ of a digraph is a non-negative matrix with $a_{ij}(\sigma(t), t) > 0$ when there is a directed edge from j to i, $(j, i) \in \mathcal{E}_{\sigma(t)}$, and $a_{ij}(\sigma(t), t) = 0$ when $(j, i) \notin \mathcal{E}_{\sigma(t)}$. The Laplacian matrix $L_{\sigma(t)} = [l_{ij}(\sigma(t), t)] \in \mathbb{R}^{(N+1)\times(N+1)}$ is a zero row sum matrix with elements

$$\begin{aligned} l_{ij}(\sigma(t), t) &= -a_{ij}(\sigma(t), t), && \text{if } j \neq i, \\ l_{ii}(\sigma(t), t) &= \sum_{j=1}^{N} a_{ij}(\sigma(t), t), && \text{if } j = i. \end{aligned}$$

4.2 Problem Formulation

The system composed of (2.1) with redefined measurement signal (4.1) and (2.2) is viewed as a MAS with the exosystem (2.2) as the leader and all the subsystems in (2.1) as the followers. Let $\mathcal{G}_{\sigma(t)} = (\mathcal{V}, \mathcal{E}_{\sigma(t)}), \mathcal{V} = \{0, 1, 2, \cdots, N\}$ be the digraph representing the dynamic interconnections among the subsystems of the MAS composed of (2.1) and (2.2). Without loss of generality, we let the node 0 be the exosystem. From the definition of $\mathcal{A}_{\sigma(t)}$, weights $a_{i0}(\sigma(t), t) > 0$ if and only if the i^{th} subsystem has the exosystem (2.2) in its neighboring set at the instant t with communication graph $\mathcal{G}_{\sigma(t)}$.

Moreover $C_{w_i}(\sigma(t),t)=0$ when the i^{th} subsystem is not a child node of the exosystem in $\mathcal{G}_{\sigma(t)}$.

Similar to the case for static communication network, we consider the Assumptions 2.3.1-2.3.3, which are required to guarantee the solvability of any traditional CORP.

The solutions to the CORP for time-varying communication topology in [25, 41, 49, 51] either explicitly or implicitly require that at least one of the agents can independently access the complete state vector of exosystem dynamics from the measurement signal y_{mi} at some switching instants $t_j, j\in\mathbb{Z}^+\cup\{0\}$ when $C_{w_i}(\sigma(t),t)\neq 0$. In other words, this is equivalent to $(S, C_{w_i}(\sigma(t_j),t_j))$ being detectable for a child agent i of the exosystem with the communication network topology being represented by the digraph $\mathcal{G}_{\sigma(t_j)}$.

Building upon the results of [41], here we aim to relax the detectability requirement on individual agents of the exosystem, and we consider the case where no agent have access to enough information to independently reconstruct the leader states at any switching instant. Instead, agents reach a consensus on the exosystem states from their combined measurement y_{mi}'s over a series of switching instants and the joint connectivity property among agents. The above discussion is summarized in the next assumption.

Assumption 4.2.1. *There exists a subsequence $\{i_k\}$ of $\{i : i=0,1,2,\cdots\}$ with uniformly bounded time intervals $[t_{i_k}, t_{i_{k+1}})$, $t_{i_{k+1}}-t_{i_k}<v$ for some positive v, such that the following hold.*

- *All the followers form a strongly connected partition in the "joint communication network" $\cup_{j=i_k}^{i_{k+1}-1}\mathcal{G}_{\sigma(t_j)}$.*
- *The pair $(S, \int_{t_{i_k}}^{t_{i_{k+1}}}\bar{C}_w(\sigma(t),t)\;dt)$ is detectable where $\bar{C}_w = col(C_{w_1}, C_{w_2}, \cdots, C_{w_N})$. This condition is referred to as the combined detectability property.*

Remark 4.2.1. *The need for Assumption 4.2.1 can be justified as follows. Because* $(S, C_{w_i}(\sigma, t_j))$ *is not required to be detectable at any time instance* t_j*, the solutions in [41, 49] are not applicable here. A practical alternative solution is to introduce additional comunication between follower agents to share their view of the exosystem, and complement the incomplete measurements. These requirements are met with the connecitivity property and the detectability condition in Assumption 4.2.1. In the case where there is only one agent connected to the leader during the time interval* $[t_{i_k}, t_{i_{k+1}})$*, Assumption 4.2.1 can be viewed as an equivalent to the connectivity requirement and individual observability condition in [41, 49].*

Finally we define the CORP under switching communication networks as follows.

Definition 4.2.1. *CORP* - Given the MAS comprising of the agent dynamics (2.1) with y_{mi} in (4.1), exosystem (2.2), and communication graph $\mathcal{G}_{\sigma(t)}$, find a distributed control law u_i, $i = 1, 2, \cdots, N$ such that:

1. when $w = 0$, the subsystem (2.1) under the control $u_i = u_i(\sigma(t), t)$ is exponentially stable,
2. for any arbitrary initial conditions $x_i(0)$, and $w(0)$, the regulated output satisfies $\lim_{t\to\infty} e_i(t) = 0$.

In the following sections, we will introduce our control law to achieve the objectives of the CORP as prescribed in Definition 4.2.1.

4.3 Distributed State Feedback Control

The distributed dynamic compensator for the followers is defined as

$$\begin{aligned}
\dot{\eta}_i &= f_i(\sigma(t), t) + \mu a_{i0}(\sigma(t), t) G_i C_{w_i}(\sigma(t), t)(w - \eta_i), \\
f_i &= S\eta_i + \mu \left(\sum_{j \in \mathcal{N}_i(\sigma(t), t)} a_{ij}(\sigma(t), t)(\eta_j - \eta_i) \right),
\end{aligned} \tag{4.2}$$

where $\mu > 0$ is a scalar gain, G_i is the observer gain, and η_j is the state vector of the dynamic compensator of the neighboring agent $j \in \mathcal{N}_i(\sigma(t),t)$ and $(j,i) \in \mathcal{E}_{\sigma(t)} \subseteq (\mathcal{V} \times \mathcal{V})$. Since $a_{i0}(\sigma(t),t)$ in (4.2) is a scalar quantity, it can be absorbed into the matrix $C_{w_i}(\sigma(t),t)$ without loss of generality, such that $C_{w_i}(\sigma(t),t) = 0$ when $a_{i0}(\sigma(t),t) = 0$, and $C_{w_i}(\sigma(t),t) \neq 0$ when $a_{i0}(\sigma(t),t) \neq 0$. Based on the above compensator equation, the control law for the follower agent i is given as

$$u_i = K_{1_i} x_i + K_{2_i} \eta_i, i = 1, 2, \cdots, N, \tag{4.3}$$

where x_i is the agent state vector, and η_i comes from the dynamic compensator (4.2) of agent i. Feedback gain matrix $K_{1_i} \in \mathbb{R}^{m_i \times n_i}$ is chosen such that $(A_i + B_i K_{1_i})$ is Hurwitz from Assumption 2.3.2, and $K_{2_i} \in \mathbb{R}^{m_i \times q}$ is obtained from the solution pair to the regulator equations (2.3),

$$K_{2_i} = U_i - K_{1_i} X_i. \tag{4.4}$$

For the digraph $\mathcal{G}_{\sigma(t)}$ corresponding to the MAS (2.1) with leader (2.2), let $\mathcal{A}_{\sigma(t)} = [a_{ij}(\sigma(t),t)]$ be the adjacency matrix and $L_{\sigma(t)}$ be the Laplacian matrix

$$L_{\sigma(t)} = \left[\begin{array}{c|c} 0 & 0 \\ \hline \nabla_{\sigma(t)} \mathbf{1}_N & \mathcal{H}_{\sigma(t)} \end{array}\right]$$

where ∇ is an $N \times N$ diagonal matrix with the diagonal elements $-a_{i0}(\sigma(t),t)$. Zero row sum property of $L_{\sigma(t)}$ yields $\mathcal{H}_{\sigma(t)} \mathbf{1}_N = -\nabla_{\sigma(t)} \mathbf{1}_N$.

Let $\tilde{\eta}_i = \eta_i - w$, and therefore the dynamic compensator in (4.2) yields

$$\dot{\tilde{\eta}} = \left[\rho(\sigma(t),t) - \mu(\mathcal{L}_{\sigma(t)} \otimes I_q)\right] \tilde{\eta}, \tag{4.5}$$

where $\rho(\sigma(t),t) = (I_N \otimes S) - \mu G C_w(\sigma(t),t)$, $\mathcal{L}_{\sigma(t)}$ is the Laplacian matrix of all the follower subsystems (2.1), obtained from $L_{\sigma(t)}$ by deleting the edges incoming from or outgoing to the leader. Before we present our main result, we first establish a lemma on the consensus of the dynamic compensator states $\eta_i,\ i = 1,2,\cdots,N$.

Consider a Lyapunov function for $Q > 0$,

$$V_1 = \tilde{\eta}^{\mathrm{T}} Q \tilde{\eta}, \tag{4.6}$$

where $\tilde{\eta}$ is a solution of (4.5). To avoid notational complexity, we will use $\rho_{\sigma,t} = \rho(\sigma(t),t), C_{w_{\sigma,t}} = C_w(\sigma(t),t)$ in the current discussion. Since the switching signal $\sigma(t)$ is piecewise constant, so are $\rho_{\sigma,t}$ and $C_{w_{\sigma,t}}$. Therefore, $V_1(t)$ is continuously differentiable at any time except for the switching instants. Differentiation of V_1 at non-switching instants yields

$$\dot{V}_1 = \tilde{\eta}^{\mathrm{T}} \Big[\Big(\rho_{\sigma,t} - \mu \mathcal{L}_{\sigma(t)} \otimes I_q \Big)^{\mathrm{T}} Q + Q \Big(\rho_{\sigma,t} - \mu \mathcal{L}_{\sigma(t)} \otimes I_q \Big) \Big] \tilde{\eta}.$$

With the help of a numerical example such as in [53], it can be shown that $V_1(t)$ may not decrease uniformly. Therefore, Barbalat's Lemma as in [51] may not be applicable for the stability analysis of (4.5). Instead we use the following stability theorem from [54].

Lemma 4.3.1. *Consider a function $V_1 : W \times \mathbb{R} \to \mathbb{R}$, with $W \subset \mathbb{R}^{Nq}$ an open neighborhood of 0. Let the following conditions on V_1 be satisfied.*

- *There exist strictly positive numbers λ_{min} and λ_{max} such that*

$$\forall \tilde{\eta} \in W : \lambda_{min} \|\tilde{\eta}\|^2 \leq V_1(\tilde{\eta},t) \leq \lambda_{max} \|\tilde{\eta}\|^2 \text{ and } V_1(0,t) = 0, \forall t.$$

- *There exists an increasing sequence of time $\{t_{i_k}\}$, with $t_{i_k} \to \infty$ as $i_k \to \infty$, and a finite $v > 0$, $v_1 > 0$ such that $\forall i_k \in \mathbb{Z}^+$, $t_{i_{k+1}} - t_{i_k} < v$, and $\forall \tilde{\eta}(t_{i_k}) \in W \backslash \{0\}$,*

$V_1(\tilde{\eta}, t)$ *satisfies*

$$V_1(\tilde{\eta}(t_{i_{k+1}}), t_{i_{k+1}}) - V_1(\tilde{\eta}(t_{i_k}), t_{i_k}) \leq -v_1 \|\tilde{\eta}(t_{i_k})\|^2 < 0,$$

where $\tilde{\eta}(t_{i_{k+1}})$ *is the solution of* (4.5) *at* $t_{i_{k+1}}$ *with the initial condition* $\tilde{\eta}(t_{i_k})$ *at* t_{i_k}*.*

Then the equilibrium point $\tilde{\eta}(t) = 0$ *of* (4.5) *is exponentially stable.*

Proof. The observer error dynamics in (4.5) can be rewritten in the form as

$$\dot{\tilde{\eta}}(t) = g(\tilde{\eta}(t), t), \tag{4.7}$$

with $g : W \times \mathbb{R} \to \mathbb{R}^{Nq}$, for an open neighborhood of the origin W, and measurable function $g(\tilde{\eta}, t)$ such that $g(0, t) = 0$, $\forall t \in \mathbb{R}$. Additionally, the function $g(\tilde{\eta}(t), t)$ is locally Lipschitz on W, which implies that there exists a unique solution to equation (4.7) for all $\tilde{\eta} \in W$. The proof of this theorem with (4.7) then mirrors the equivalent results for exponential stability in [54]. $\square$

From the choice of our Lyapunov function (4.6), it is evident that

$$V_1(0, t) = 0, \forall t \geq 0,$$
$$\lambda_{\min}(Q)\|\tilde{\eta}\|^2 \leq V_1(\tilde{\eta}, t) \leq \lambda_{\max}\|\tilde{\eta}\|^2.$$

Thus $V_1(\tilde{\eta}, t)$ satisfies the first condition of Lemma 4.3.1. In the following lemma, we present conditions to ensure the negative definiteness requirement on the difference of the Lyapunov function measured over the time sequence $\{t_{i_k}\}$, which in turn will prove the exponential stability of $\tilde{\eta}(t)$ by Lemma 4.3.1.

Lemma 4.3.2. *Consider the dynamic compensator* (4.2) *with digraph* $\mathcal{G}_{\sigma(t)}$ *and time sequence* $\{t_{i_k}\}$ *satisfying Assumption 4.2.1. Let the scaling factor* μ*, observer gains* G_i

and a positive definite matrix P such that the matrix $P(S-\mu G_i\int_{t_{i_k}}^{t_{i_{k+1}}} C_{w_i}(\sigma(t),t)\ dt)+(S-\mu G_i\int_{t_{i_k}}^{t_{i_{k+1}}} C_{w_i}(\sigma(t),t)\ dt)^T P$ has non-positive eigenvalues for all follower agents i and

$$\boldsymbol{\mathcal{R}} = NvS-\mu\mathbf{G}\int_{t_{i_k}}^{t_{i_{k+1}}} \bar{C}_w(\sigma(t),t)\ dt \tag{4.8}$$

is Hurwitz with $\mathbf{G}=[G_1'\ G_2'\ \cdots\ G_l']$, $G_i'=\zeta_i G_i$, where ζ_i is the i^{th} element of the left eigenvector $\zeta=\left[\zeta_1,\zeta_2,\cdots,\zeta_l\right]^T$ of the matrix $\left[\int_{t_{i_k}}^{t_{i_{k+1}}} \mathcal{L}_{\sigma(t)}\ dt\right]$ corresponding to the zero eigenvalue. The compensator states η_i then exponentially approaches the exosystem states,

$$\lim_{t\to\infty}(\eta_i(t)-w(t))=0, i=1,2,\cdots,N.$$

Proof. For a non-switching communication digraph $\mathcal{G}=\mathcal{G}_{\sigma(t)}$, the above lemma results in Lemma 2 of [2]. For the case of switching communication digraph, the difference $\Delta V_1 = V_1(\tilde{\eta}(t_{i_{k+1}}),t_{i_{k+1}})-V_1(\tilde{\eta}(t_{i_k}),t_{i_k})$, with V_1 being defined in (4.6) reduces to

$$\Delta V_1 = \tilde{\eta}^{\mathrm{T}}(t_{i_{k+1}})Q\tilde{\eta}(t_{i_{k+1}})-\tilde{\eta}^{\mathrm{T}}(t_{i_k})Q\tilde{\eta}(t_{i_k}), \tag{4.9}$$

where $\tilde{\eta}(t_{i_{k+1}})=\Phi(t_{i_{k+1}},t_{i_k})\tilde{\eta}(t_{i_k})$ and $\Phi(t,t_{i_k})$ is the state transition matrix of system (4.5). Please note that the notations $\mathcal{L}_{\sigma(t)}$ and $\mathcal{L}_\sigma$ are used interchangeably throughout the text. Assume that the number of switches occurring within the time interval $[t_{i_k},t_{i_{k+1}})$ is m, and denote the switching time instants as $t_{i_k}+\delta_1, t_{i_k}+\delta_2, t_{i_k}+\delta_3,\cdots,t_{i_k}+\delta_m$. By using the properties of state transition matrix $\Phi(\cdot)$ of (4.5), $\tilde{\eta}(t_{i_{k+1}})$ in (4.9) can be expressed by the following product of $\tilde{\eta}(t_{i_k})$

$$\tilde{\eta}(t_{i_{k+1}}) = \prod_{j=1}^{m+1}\Phi(t_{i_k}+\delta_j, t_{i_k}+\delta_{j-1})\tilde{\eta}(t_{i_k}), \tag{4.10}$$

with $\delta_{m+1}=t_{i_{k+1}}-t_{i_k}$, $\delta_0=0$. As noted earlier, the error dynamics in (4.5) remains time-invariant during a non-switching time interval, and thus $\Phi(\cdot)$ in (4.10) yields as follows

$$\Phi(t_{i_k}+\delta_{j+1},t_{i_k}+\delta_j)=e^{M_{\sigma,t_{i_k}+\delta_j}(\delta_{j+1}-\delta_j)}, \tag{4.11}$$

where $M_{\sigma,t}=\rho_{\sigma,t}-\mu\mathcal{L}_\sigma\otimes I_q$. For small enough $\mu>0$, the Baker-Campbell-Hausdorff formula for the product of matrix exponentials in (4.10) gives

$$V_1(\tilde{\eta}(t_{i_{k+1}}),t_{i_{k+1}})=\tilde{\eta}^{\mathrm{T}}(t_{i_k})\left[e^{\mathbf{M}^{\mathrm{T}}}Qe^{\mathbf{M}}\right]\tilde{\eta}(t_{i_k}),\ \mathbf{M}=\int_{t_{i_k}}^{t_{i_{k+1}}}M_{\sigma,t_{i_k}+\delta_j}\ dt. \tag{4.12}$$

By assumption $\boldsymbol{\mathcal{R}}$ is Hurwitz and consequently there exists a unique positive definite solution P to the inequality

$$P\boldsymbol{\mathcal{R}}^{\mathrm{T}}+\boldsymbol{\mathcal{R}}P<0. \tag{4.13}$$

Furthermore, since $P(S-\mu G_i\int_{t_{i_k}}^{t_{i_{k+1}}}C_{w_i}(\sigma(t),t)\ dt)+(S-\mu G_i\int_{t_{i_k}}^{t_{i_{k+1}}}C_{w_i}(\sigma(t),t)\ dt)^{\mathrm{T}}P$ is assumed to be negative semi-definite, then the stability results of Lemma 2.4.3 yield that $\mathbf{M}$ is Hurwitz and as a result for a positive definite matrix Q

$$\mathbf{M}^{\mathrm{T}}Q+Q\mathbf{M}<0. \tag{4.14}$$

Thus, from Theorem A.5 of [55], $e^{\mathbf{M}^{\mathrm{T}}}Qe^{\mathbf{M}}<Q$, which gives $V_1(\tilde{\eta}(t_{i_{k+1}}),t_{i_{k+1}})-V_1(\tilde{\eta}(t_{i_k}),t_{i_k})<0$. Therefore the second condition of Lemma 4.3.1 is satisfied, *i.e.*, $\tilde{\eta}=0$ of (4.5) is exponentially stable. In other words, $\lim_{t\to\infty}(\eta_i(t)-w(t))=0, i=1,2,\cdots,N$. This concludes the proof. □

Remark 4.3.1. $\boldsymbol{\mathcal{R}}$ *can be rewritten in the matrix form*

$$\boldsymbol{\mathcal{R}}=NvS-\mu\mathbf{G}C_w^*,\ \textit{where}\ C_w^*\ =\int_{t_{i_k}}^{t_{i_{k+1}}}\bar{C}_w(\sigma(\tau),\tau)\ dt. \tag{4.15}$$

By the detectability condition in Assumption 4.2.1, there is always a matrix $\mathbf{G}$ *and a positive scalar* μ *such that* $\boldsymbol{\mathcal{R}}$ *is Hurwitz. In the case when the switching sequence* $\sigma(t)$

is periodic, matrix C_w^* can be uniquely determined and used in deriving the observer gains G_i.

Using the notations in (2.6) and (2.7), define the system state and the regulated output of the overall system be $x_c = \mathrm{col}(x, \tilde{\eta})$ and e. The overall closed-loop system under the control (4.2), (4.3) is represented by the following state equations

$$\begin{aligned} \dot{x}_c &= \mathbf{A}_{c_{\sigma(t)}} x_c + \mathbf{B}_c w, \\ e &= \mathbf{C}_c x_c + \mathbf{D}_c w, \end{aligned} \tag{4.16}$$

with the system matrix being

$$\mathbf{A}_{c_{\sigma(t)}} = \left[\begin{array}{c|c} \mathbf{A}_{c_1} & \mathbf{A}_{c_2} \\ \hline 0 & M_{\sigma,t} \end{array}\right],$$

where

$$\mathbf{A}_{c_1} = A + BK_1, \mathbf{A}_{c_2} = BK_2,$$

and A, B, K_1 and K_2 are defined as in (2.7). The remaining matrices are given by $\mathbf{B}_c = \mathrm{col}(\bar{E} + B\bar{K}_2, 0)$, $\mathbf{C}_c = \begin{bmatrix} C + DK_1 & DK_2 \end{bmatrix}$, $\mathbf{D}_c = \bar{F} + D\bar{K}_2$.. We now introduce the following lemma to carry out the stability analysis of (4.16).

Lemma 4.3.3. *Consider the closed-loop system* (4.16)*. Under Assumptions 2.3.1, 2.3.2 and 4.2.1, the origin of the unperturbed linear switched system*

$$\dot{x}_c = \mathbf{A}_{c_{\sigma(t)}} x_c \tag{4.17}$$

can be made exponentially stable by the selection of K_{1_i} if $\tilde{\eta}_i$'s are exponentially stable.

Proof. The block diagonal components of $\mathbf{A}_{c_1}$ can be made Hurwitz by Assumption 2.3.2 and the selection of suitable gain matrix K_{1_i}, $i = 1, 2, \cdots, N$. From Lemma 4.3.1, the exponential stability of $\tilde{\eta}(t)$ implies that there exists strictly positive constants ε_1

and δ_1 such that

$$\|\tilde{\eta}(t)\| \leq \varepsilon_1 e^{-\delta_1(t-t_0)}\|\tilde{\eta}(t_0)\|. \tag{4.18}$$

Since $\mathbf{A}_{c_1}$ and $\mathbf{A}_{c_2}$ are time-invariant, then for any initial states $x(t_0), \tilde{\eta}(t_0)$ and $\forall t_0$, the solution $x(t)$ of the linear switched system $\dot{x}(t) = \mathbf{A}_{c_1}x(t) + \mathbf{A}_{c_2}\tilde{\eta}(t)$ satisfies

$$x(t) = e^{\mathbf{A}_{c_1}(t-t_0)}x(t_0) + \int_{t_0}^{t} e^{\mathbf{A}_{c_1}(t-\tau)}\mathbf{A}_{c_2}\tilde{\eta}(\tau)d\tau. \tag{4.19}$$

Given $\mathbf{A}_{c_1}$ is Hurwitz, there exists strictly positive constants ε_2 and δ_2 such that

$$\|e^{\mathbf{A}_{c_1}t}\| \leq \varepsilon_2 e^{-\delta_2 t}. \tag{4.20}$$

By (4.18) and (4.20), the norm bound on equation (4.19) can be rewritten as follows

$$\begin{aligned}\|x(t)\| &\leq \varepsilon_2 e^{-\delta_2(t-t_0)}\|x(t_0)\| + \varepsilon_1\varepsilon_2\|\mathbf{A}_{c_2}\|\|\tilde{\eta}(t_0)\|\frac{e^{\delta_2 t_0}}{\delta_2 - \delta_1}\left[e^{-\delta_1(t-t_0)} - e^{-\delta_2(t-t_0)}\right], \\ &\leq \varepsilon_2 e^{-\delta_2(t-t_0)}\|x(t_0)\| + \varepsilon_3\left[e^{-\delta_1(t-t_0)} - e^{-\delta_2(t-t_0)}\right]\|\tilde{\eta}(t_0)\|,\end{aligned}$$

which gives $x(t) \to 0$ as $t \to \infty$. □

Lemma 4.3.2 and 4.3.3 demonstrate that the closed loop system (4.16) can be made exponentially stable when $w = 0$. Thus the first condition in Definition 4.2.1 is satisfied. We consider the following Theorem to approach the second condition in the definition.

Theorem 4.3.4. *Under Assumptions 2.3.1, 2.3.2, 2.3.3, 4.2.1, the CORP is solvable by the distributed dynamic state feedback control law* (4.3)*, with suitable gains G_i's as described in Remarks 4.3.1 and a scaling factor $\mu > 0$, if $\tilde{\eta}_i$ is exponentially stable.*

Proof. The linear regulator equation in (2.3) corresponding to the follower agents can be rewritten as

$$\begin{aligned} X(I_N \otimes S) &= (A+BK_1)X + (\bar{E}+B\bar{K}_2), \\ 0 &= (C+DK_1)X + (\bar{F}+D\bar{K}_2), \end{aligned} \tag{4.21}$$

where X follows the notation in (2.7). Let us define a new state variable in the form $\tilde{x}_i = x_i - X_i w, i = 1,2,\cdots,N$. Then by (4.21) we get the following state equation for the follower agents

$$\dot{\tilde{x}} = (A+BK_1)\tilde{x} + BK_2\tilde{\eta}. \tag{4.22}$$

By combining (4.22), (4.5), the overall state space equation for the follower agents can be rewritten as $\dot{\tilde{x}}_c = \mathbf{A}_c\tilde{x}_c$, where $\tilde{x}_c = \mathrm{col}(\tilde{x},\tilde{\eta})$. From Lemma 4.3.3, $\lim_{t\to\infty}\tilde{x}_c(t) = 0$.

Now, it yields from (4.21), that the regulated outputs for all the follower agents equal

$$e = (C+DK_1)\tilde{x} + DK_2\tilde{\eta}. \tag{4.23}$$

Therefore the regulated output for all the follower agents can be combined as $e = C_c\tilde{x}_c$. Since $\tilde{x}_c$ exponentially converges to zero, $\lim_{t\to\infty} e_i(t) = 0$ for all agent i. Thus the CORP is solved. □

4.4 Distributed Output Feedback Control

Building upon our results on the state feedback control, we study the CORP by distributed measurement output feedback control. Let the measured output $y_i = y_i(\sigma(t),t) \in \mathbb{R}^{p_i}$ from the i^{th} subsystem be defined as

$$y_i = C_{x_i}x_i, \ i = 1,2,3,\cdots,N. \tag{4.24}$$

We consider that the Assumption 2.5.1 holds. Additionally, we note that while $a_{i0}(\sigma(t),t) \neq 0$, the signal y_{mi} from the exosystem is available to agent i through their communication to determine their cooperative estimation $\eta_i(t)$ (4.2) of the leader's state $w(t)$ in (2.2). For the MAS satisfying the problem assumptions, we consider the distributed dynamic output feedback controller as

$$u_i = K_{1_i}\hat{x}_i + K_{2_i}\eta_i,\ i = 1, 2, \cdots, N, \tag{4.25}$$

where K_{1_i}, K_{2_i} are defined as in (4.3) and (4.4), and the estimation $\hat{x}_i \in \mathbb{R}^{n_i}$ of the state vector x_i by the i^{th} agent is defined as

$$\dot{\hat{x}}_i = A_i\hat{x}_i + B_iu_i + E_i\eta_i + H_i(C_{x_i}\hat{x}_i - y_i), \tag{4.26}$$

where the observer gain matrix $H_i \in \mathbb{R}^{n_i \times p_i}$ is selected such that $A_i + H_iC_{x_i}$ is Hurwitz. The error equation corresponding to (4.26) can then be found as

$$\dot{\tilde{\hat{x}}}_i = (A_i + H_iC_{x_i})\tilde{\hat{x}}_i + E_i\tilde{\eta}_i, \tag{4.27}$$

where $\tilde{\hat{x}}_i = \hat{x}_i - x_i,\ i = 1, 2, 3, \cdots, N$. Since $\lim_{t\to\infty}\tilde{\eta}_i(t) = 0$ by Lemma 4.3.2, then from (4.27) $\lim_{t\to\infty}\tilde{\hat{x}}_i(t) = 0$ by virtue of $A_i + H_iC_{x_i}$ being a Hurwitz matrix.

Under the measurement feedback distributed control (4.25), (4.26), define the overall closed-loop system state and the regulated output of the overall system as $x_c = \text{col}(x, \tilde{\psi})$ and e, where $\tilde{\psi} = \text{col}(\tilde{\hat{x}}, \tilde{\eta})$. The dynamics of the overall closed loop system then follows the state space equation (4.16) with

$$\mathbf{A}_{c_{\sigma(t)}} = \left[\begin{array}{c|c} \mathbf{A}_{c_1} & \mathbf{A}_{c_2} \\ \hline 0 & \mathbf{A}_{c_4}(\sigma(t),t) \end{array}\right], \ \mathbf{A}_{c_1} = A + BK_1,$$

$$\mathbf{A}_{c_4}(\sigma,t) = \begin{bmatrix} A+HC_x & E \\ 0 & M_{\sigma,t} \end{bmatrix}, \mathbf{A}_{c_2} = B\begin{bmatrix} K_1 & K_2 \end{bmatrix},$$

$$\mathbf{B}_c = \mathrm{col}(\bar{E}+B\bar{K}_2, 0), \mathbf{C}_c = \begin{bmatrix} \mathbf{C}_{c_1} & \mathbf{C}_{c_2} \end{bmatrix},$$

$$\mathbf{C}_{c_1} = C + DK_1, \mathbf{C}_{c_2} = D\begin{bmatrix} K_1 & K_2 \end{bmatrix}, \mathbf{D}_c = \bar{F} + D\bar{K}_2.$$

Since $\tilde{\eta}_i(t)$ is exponentially stable, then from Lemma 4.3.3 the origin of the switched system $\dot{x}_c = \mathbf{A}_{c_{\sigma(t)}} x_c$ can be shown to be exponentially stable by virtue of $A+BK_1$ and $A+HC_x$ being Hurwitz matrices for suitable selection of gain matrices K_1 and H.

Remark 4.4.1. *It is clear from the proof of Lemma 4.3.3 that, unperturbed* $(w=0)$ *closed loop system* (4.16) *is exponentially stable, provided* $\tilde{\eta}_i(t)$ *is exponentially stable and the controller gains* $K_{1_i}, K_{2_i},\ i=1,2,\cdots,N$ *being selected in such a way that the matrix* $\mathbf{A}_{c_1}$ *is Hurwitz. Thus the first condition in Definition 4.2.1 is satisfied.*

Next, we consider the following Theorem to satisfy the second condition in Definition 4.2.1.

Theorem 4.4.1. *Under Assumptions 2.3.1, 2.3.2, 2.3.3, 4.2.1, 2.5.1, the CORP is solvable by the distributed dynamic measurement feedback control law* (4.25) *with observer gains* H_i*, controller gains in Remark 4.4.1 and a scaling factor* $\mu > 0$*, if* $\tilde{\eta}_i$ *is exponentially stable.*

Proof. The proof of this theorem follows directly from the proof of Theorem 1. With $\tilde{x}_i = x_i - X_i w,\ i=1,2,\cdots,N$, and by virtue of (4.16), (4.21), we obtain $\lim_{t\to\infty}\tilde{x} = 0$

and consequently $\lim_{t\to\infty} e(t) = 0$. Therefore the second condition of Definition 4.2.1 is satisfied, and the output regulation problem is solved. $\square$

4.5 Illustrative Example

In this section we present a numerical example to illustrate the design process of our proposed solution. The follower agents are considered to be double integrator systems, and the exosystem is assumed to be an unforced dual-frequency harmonic oscillator. The system dynamics as given in (2.1) have the following state space matrices

$$
\begin{aligned}
&A_i = \begin{bmatrix} 0 & 1 \\ 0 & 0 \end{bmatrix},\ B_i = \begin{bmatrix} 0 \\ 1 \end{bmatrix},\ C_i = \begin{bmatrix} 1 & 0 \end{bmatrix},\ D_i = 0, \\
&E_1 = \begin{bmatrix} 0 & 0 & 0 & 0 \\ 1 & 0 & 0 & 0 \end{bmatrix},\ E_2 = \begin{bmatrix} 0 & 0 & 0 & 0 \\ 0 & 0 & 1 & 0 \end{bmatrix}, \\
&E_3 = 0_{2\times 4},\ F_i = \begin{bmatrix} 1 & 0 & 1 & 0 \end{bmatrix},\ i = 1,2,3.
\end{aligned}
$$

The leader dynamics is captured in the form (2.2) with $S = \text{blk diag}(S_1, S_2)$, where

$$
S_1 = \begin{bmatrix} 0 & -1 \\ 1 & 0 \end{bmatrix},\ S_2 = \begin{bmatrix} 0 & -2 \\ 2 & 0 \end{bmatrix}. \tag{4.28}
$$

It is easy to verify that the Assumptions 2.3.1, 2.3.2, 2.3.3 are all satisfied. Next we introduce the switching signal $\sigma(t)$ which generates the switching network topology $\mathcal{G}_{\sigma(t)}$ as shown in Figure 4.1, where the leader is designated by node 0. The switching signal is defined as follows

$$
\sigma(t) = mod_6(i-1)+1,\ \text{for}\ \frac{i-1}{6}T^* \le t < \frac{i}{6}T^*, \tag{4.29}
$$

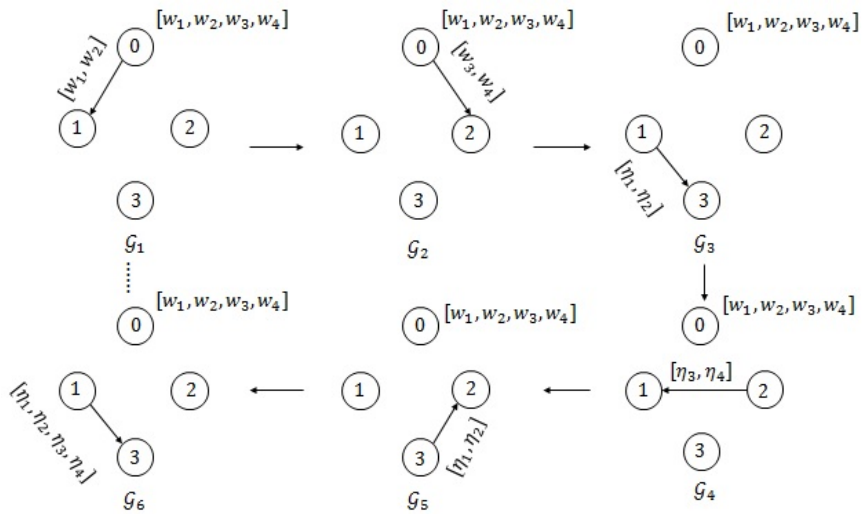

Figure 4.1: Switching network topology $\mathcal{G}_{\sigma(t)}$ with $\mathcal{P} = \{1,2,3,4,5,6\}$

where $i = 1,2,\cdots,\infty$. The switching period T^* is 1s. The notations written side by side of the network graph in Figure 4.1 indicates the information exchange during a non-switching interval. Union of the communication graphs, taken over a switching period T^* is depicted in Figure 4.2, which satisfies the connectivity assumption of agents.

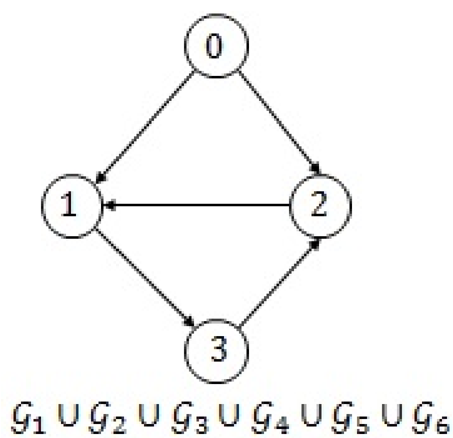

Figure 4.2: Joint communication network of agents over one switching period

From the available information, the measurement output matrix of all the agents are as follows

$$\begin{aligned} C_{w_1}(\sigma(t),t) &= \begin{cases} \begin{bmatrix} I_2 \; 0_{2\times 2} \end{bmatrix} & \text{if } \sigma(t)=1 \\ 0, \text{ otherwise}, \end{cases} \\ C_{w_2}(\sigma(t),t) &= \begin{cases} \begin{bmatrix} 0_{2\times 2} \; I_2 \end{bmatrix} & \text{if } \sigma(t)=2 \\ 0, \text{ otherwise} \end{cases}, \\ C_{w_3}(\sigma(t),t) &= 0_{2\times 4}. \end{aligned} \tag{4.30}$$

It is easy to verify the strongly connected partition of the joint communication network $\mathcal{G}_1 \cup \mathcal{G}_2 \cup \mathcal{G}_3 \cup \mathcal{G}_4 \cup \mathcal{G}_5 \cup \mathcal{G}_6$. From the above measurement output matrices C_{w_i} and the exosystem matrix S, we are able to verify the combined detectability condition. The dynamic state feedback control law yields the form (4.2), (4.3) with

$$\begin{aligned} K_{2_1} &= \begin{bmatrix} -8 & 4 & -4 & 8 \end{bmatrix}, \; K_{1_i} = \begin{bmatrix} -8 & -4 \end{bmatrix}, \\ K_{2_2} &= \begin{bmatrix} -7 & 4 & -5 & 8 \end{bmatrix}, \; G_1 = \begin{bmatrix} I_2 \; 0_{2\times 2} \end{bmatrix}, \\ K_{2_3} &= \begin{bmatrix} -7 & 4 & -4 & 8 \end{bmatrix}, \; G_2 = \begin{bmatrix} 0_{2\times 2} \; I_2 \end{bmatrix}, \\ G_3 &= 0_{4\times 2}, \; \mu = 1.5. \end{aligned} \tag{4.31}$$

The discussion in Section 4.3 on $V_1(t)$ not being uniformly decreasing is further illustrated in Figure 4.3, where the energy function $V_1(t)$ satisfies Lemma 4.3.1.

The asymptotic convergence of $\tilde{\eta}(t)$ to 0 results in $\lim_{t\to\infty} V_1(t) = 0$. The selection of G_i as above renders matrix $\boldsymbol{\mathcal{R}}$ in (4.8) Hurwitz. Applying the control law (4.3) to the MAS composed of (2.1) and (2.2), we obtain the simulation result in Figure 4.4, which shows the regulated output e_i of the follower agents in (2.1) asymptotically converging to zero. Thus the objectives of the CORP are achieved. Next we approach the same problem using an output feedback distributed control law (4.25) to the subsystems with the additional measured output matrices in (4.24) and controller

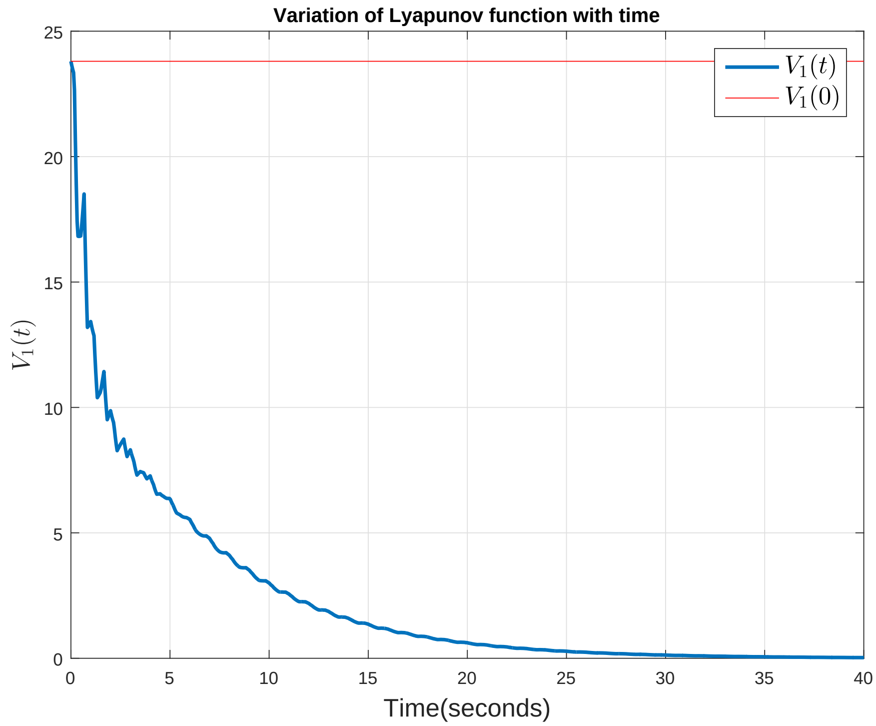

Figure 4.3: Variation of the energy function $V_1 = \tilde{\eta}^{\mathrm{T}}\tilde{\eta}$ with time

gain matrices as follows

$$C_{x_i} = \begin{bmatrix} 0 & 0 \\ 0.5 & 1 \end{bmatrix}, \; H_i = \begin{bmatrix} -8 & 0 \\ 0 & -4 \end{bmatrix}, \; K_{1_i} = \begin{bmatrix} -8 & -4 \end{bmatrix}, \; i = 1, 2, 3,$$

$$\mu = 1.5, \; K_{2_1} = \begin{bmatrix} -8 & 4 & -4 & 8 \end{bmatrix}, \; K_{2_2} = \begin{bmatrix} -7 & 4 & -5 & 8 \end{bmatrix},$$

$$K_{2_3} = \begin{bmatrix} -7 & 4 & -4 & 8 \end{bmatrix}.$$

By applying an output feedback distributed control law (4.25) to the subsystems, we obtain the simulation result of the regulated output e_i in Figure 4.5, which shows that the tracking errors for all the follower agents asymptotically converge to zero in the presence of dynamic communication protocol as long as the conditions in Assumption 4.2.1 are satisfied.

To understand the implications of Assumption 4.2.1, we consider a case with the value of the switching signal $\sigma(t)$ repeating the sequence $\{1, 2, 4, 6\}$ uniformly

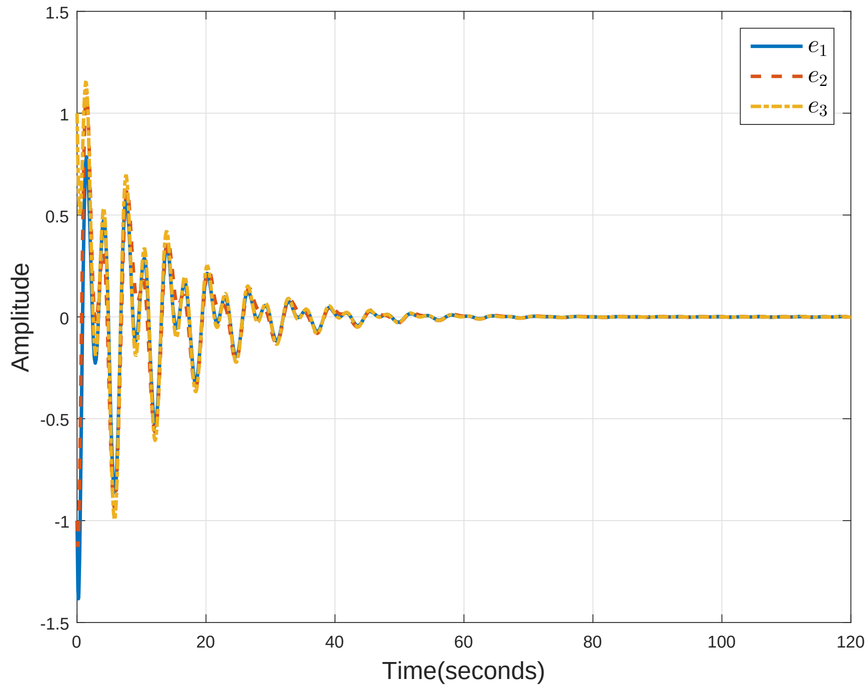

Figure 4.4: Tracking error of the three followers in $\mathcal{G}_{\sigma(t)}$ under the distributed state feedback control

over the switching period T^*. With all the other parameters unchanged, the joint communication network $\mathcal{G}_1 \cup \mathcal{G}_2 \cup \mathcal{G}_4 \cup \mathcal{G}_6$ does not satisfy Assumption 4.2.1. If the control law (4.3) with the controller parameters in (4.31) is applied to (2.1) where the subsystems are interconnected through the dynamic digraph $\mathcal{G}_{\sigma(t)}$, we obtain the simulation result in Figure 4.6. Since $\boldsymbol{\mathcal{R}}$ in (4.8) is not Hurwitz, $\lim_{t\to\infty} \eta_i(t) - w(t) \neq 0$ and therefore $\lim_{t\to\infty} e_i(t) \neq 0$, as depicted in Figure 4.6.

4.6 Conclusion

In this chapter we studied the CORP for MASs in a switching network where no subsystem received enough information to independently reconstruct the exosystem states. We proposed a distributed control law that achieves the objectives of the CORP under switching network. We demonstrated that the objectives of the studied

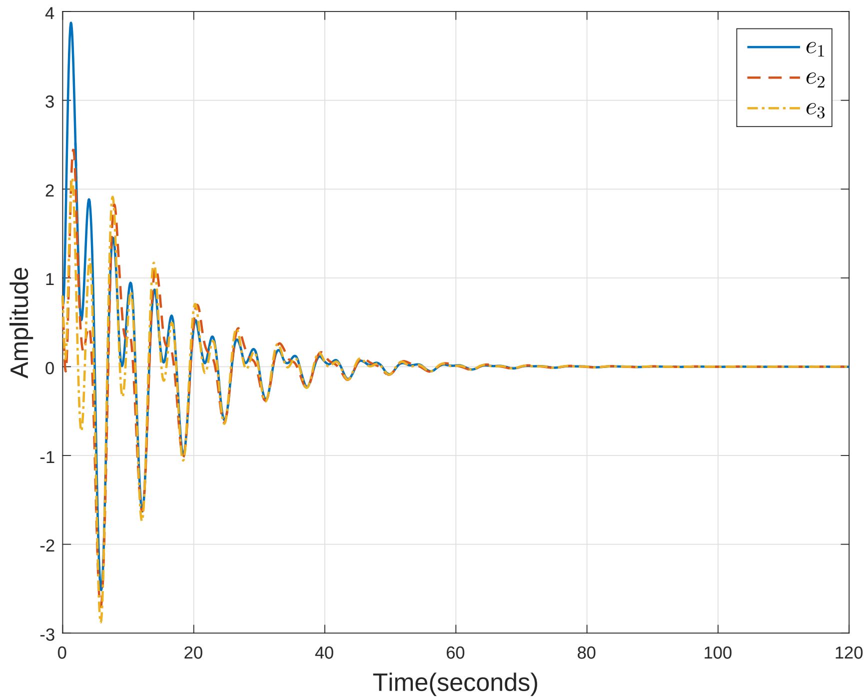

Figure 4.5: Tracking error of the three followers in $\mathcal{G}_{\sigma(t)}$ under the distributed output feedback control

control problem are achieved under relaxed detectability and connectivity assumptions when compared to previous results in the literature.

An illustrative numerical example was presented to verify the theoretical results developed in this chapter. The simulation results showed that the regulated outputs of the subsystems are synchronized, and the regulation error approaches zero. This is true even when none of the subsystems received sufficient information through their measurements to estimate the exosystem states during any switching instant.

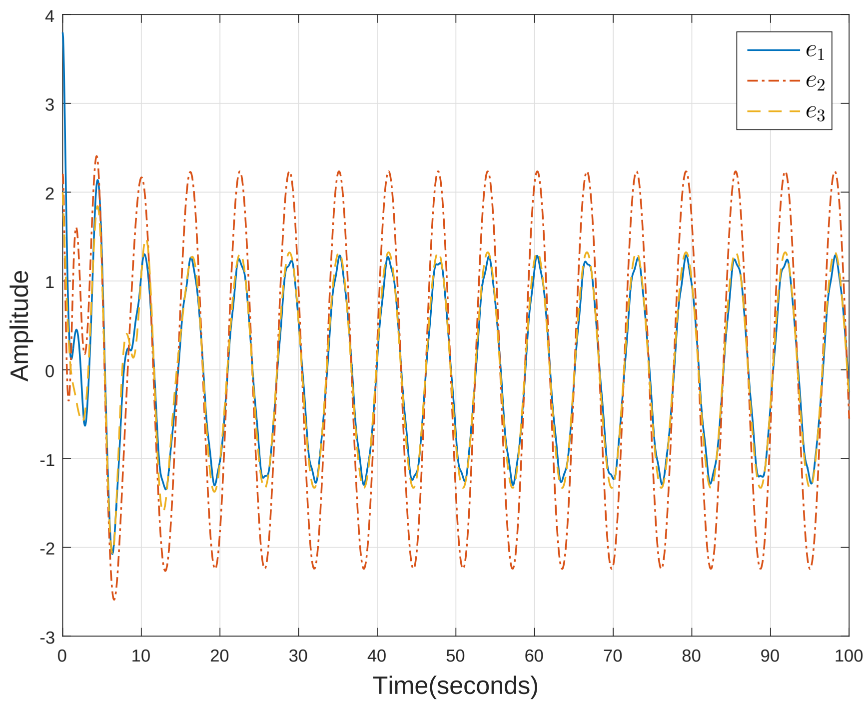

Figure 4.6: Tracking error of the three followers in $\mathcal{G}_{\sigma(t)}, \sigma(t) = \{1, 2, 4, 6\}$ under the distributed state feedback control

Chapter 5

Position Synchronization of Networked Motors- A Case Study

In this chapter we aim to experimentally validate the theoretical developments of the previous chapter through a case study. Experimental testing is an important aspect in the design of any distributed control algorithm. The first and foremost step towards successful application of the derived control algorithm is to suitably design the experiment which is regarded as the most accurate and unequivocal standard for testing the proposed hypothesis.

In particular we apply our derived theoretical results for the CORP to the position synchronization problem of networked motors under a time-varying communication network, and with restricted access to the synchronization signal. This scenario is very common in the applications of product handling machines, textile industries [56, 57], multi-conveyor belt systems and industrial manufacturing systems where the position of several electrical motors ("slave") are required to follow the position of the "master" motor. The objective of the multi-motor synchronization problem is to derive a distributed control algorithm for each motor to synchronize its shaft angular position to an external reference trajectory, while also compensating for disturbances that perturbs the motor tracking performance [58]. In this work we consider the accessibility of the synchronization signal to the motors is restricted, and communication in the distributed system is intermittent. Such network conditions have become more common in manufacturing environments, where equipment with large reflective surfaces adds significant challenges to wireless communication. Similar limitations to the access of shared measurement signals are also often encountered in distributed observation problems.

5.1 Experimental Setup

The experimental setup, as shown in Figure 5.1 consists of servomotors and PC's associated to each servomotor for implementation of the control algorithm. The details on the switching signal $\sigma(t)$ dictating the communication topology is provided in Section 5.3. In the framework of cooperative control problem each of these servomotors can be regarded as follower agents while the leader trajectories are assumed to be generated by a computer.

The goals of this experiment are stated as follows:

- Set up a communication between the PC's associated to each servomotor.
- Implement the decentralized control algorithm in the computers to stabilize the respective servomotor dynamics while synchronizing their positions to the leader trajectory.

The rest of the chapter is organized in the following manner. In Section 5.2 we briefly present the linearized servomotor dynamics along with the interaction between its different components. The implementation of the communication network between the follower servomotors is provided in Section 5.3. The design of controller and observer parameters are given in Section 5.4 and the experimental results and a

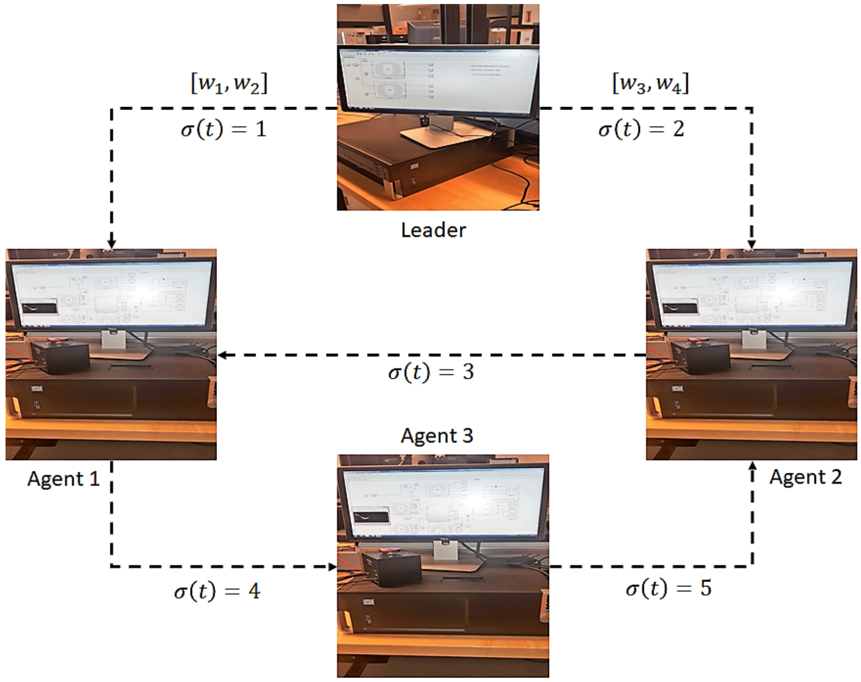

Figure 5.1: Experimental setup

qualitative analysis with respect to the existing control methods are given in Section 5.5. Finally some concluding remarks are presented in Section 5.6.

5.2 Servo Motor

The servomotors used in this experiment are *Qube-Servo 2* model from *Quanser*. A single-ended rotary encoder is used to measure the angular position of the DC motor. In each revolution the encoder outputs 2048 counts on angular position. A digital tachometer is also available to read the angular velocity of the motor. The servomotor also includes a data acquisition device with two 24-bit encoder channels with quadrature decoding and one PWM analog output channel. The DAQ also incorporates a 12-bit ADC. A schematic diagram of the *Qube Servo 2* model is shown in Figure 5.2 with the motor parameters being listed in Table 1.

The DC motor shaft is connected to a load hub with inertia J_h. A disk load with moment of inertia being J_d is mounted on the load hub. The back-emf voltage $e_b(t)$,

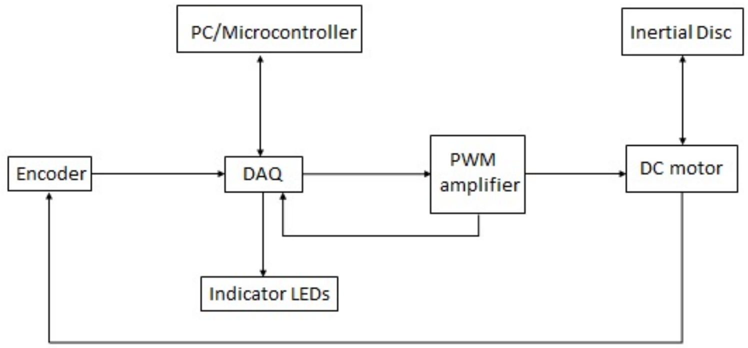

Figure 5.2: Interaction between servomotor components

Table 5.1: Model parameters for the experimental servomotor system

Parameter	**Symbol**	**Unit**	**Value**
Terminal resistance	R_m	Ω	8.4
Torque constant	k_t	N.m/A	0.042
Motor back emf constant	k_m	V/rad/s	0.042
Rotor inductance	L_m	mH	1.16
Load hub mass	m_h	kg	0.0106
Radius of the load hub mass	r_h	m	0.0111
Rotor inertia	J_m	kg.m^2	4.0×10^{-6}
Load hub inertia	J_h	kg.m^2	0.6×10^{-6}
Mass of disk load	m_d	kg	0.053
Radius of disk load	r_d	m	0.0248

dependent on the angular velocity ω_m of the motor shaft, opposes the current flow and is given by $e_b = k_m \omega_w$, where k_m denotes the motor back-emf constant. The identified transfer function indicating the relation from input voltage V_m to output angular position θ_i is given as follows

$$P(s) = \frac{\theta_i(s)}{V_m(s)} = \frac{k_t}{s(sR_m J_{eq} + k_t k_m)} = \frac{23}{s(0.13s+1)},$$

where $J_{eq} = J_m + J_h + 0.5 m_d r_d^2$. This input-output relation can be further expressed into the state-space form as follows

$$\begin{aligned} A_i &= \begin{bmatrix} 0 & 1 \\ 0 & -7.6932 \end{bmatrix}, \; B_i = \begin{bmatrix} 0 \\ 176.9231 \end{bmatrix}, \\ C_i &= \begin{bmatrix} 1 & 0 \end{bmatrix}, D_i = 0, \; i = 1,2,3. \end{aligned} \tag{5.1}$$

5.3 Communication Network

The Qube servomotors are controlled in a decentralized manner by separate Windows based computers. The real-time digital control is implemented using Simulink and Quarc, at a sampling rate of 1 KHz. Quarc supports a variety of communication protocols through the Quanser stream API. We set up communication between the multiple *Qube* servomotors through a TCP/IP protocol. The switching communication network is dictated by the switching signal $\sigma(t)$ repeating the sequence $\{1,2,3,4,5\}$ in Figure 5.3 with switching period $T^* = 0.005$s. The dashed lines in the figure represent the communication links that are active for a given value of switching signal $\sigma(t)$. A leader computer generates the reference trajectory, which are to be tracked by follower servomotors, and all motors are subjected to external disturbances. In the output regulation framework as in Figure 5.3, the reference and disturbance inputs are considered as exogenous signals from an external leader. The dynamics of the reference signal generator is associated with the vector $\begin{bmatrix} w_1 & w_2 \end{bmatrix}^{\mathrm{T}}$, while the disturbance vector is $\begin{bmatrix} w_3 & w_4 \end{bmatrix}^{\mathrm{T}}$. The union of the repeating sequence of switching communication digraphs $\{\mathcal{G}_1,\mathcal{G}_2,\mathcal{G}_3,\mathcal{G}_4,\mathcal{G}_5\}$ yields the joint communication network in Fig. 4.2, where node 0 denotes the leader and the follower nodes are numbered from 1 to 3. Each motor, designated as a follower agent in a MAS, is required to track the reference signal from the leader while rejecting the disturbance signals. The exosystem

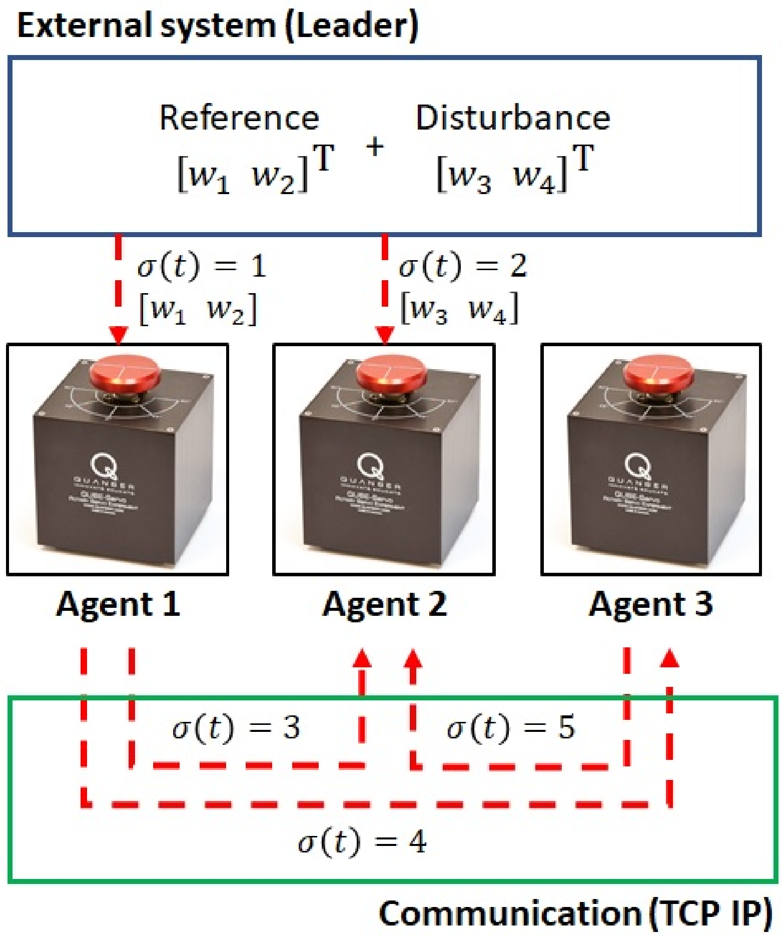

Figure 5.3: Experimental Setup

is defined as in (2.2) with

$$S = \text{blk diag}(S_1, S_2),\ S_1 = \begin{bmatrix} 0 & -1 \\ 1 & 0 \end{bmatrix},\ S_2 = \begin{bmatrix} 0 & -10 \\ 10 & 0 \end{bmatrix}.$$

The signal w_1 from the leader is viewed as a reference position of the follower motors need to track, and w_3 represent disturbances such as electrical noise that enters the agent dynamics through the control input u_i for all agent i, thereby resulting in $E_i = B_i \begin{bmatrix} 0 & 0 & 1 & 0 \end{bmatrix}$.

The information that the follower motors receive on the leader states is specified by the matrices C_{w_i} in (4.30). It is to note that agent 1 only receives from the leader node the reference signals $\begin{bmatrix} w_1 & w_2 \end{bmatrix}^{\mathrm{T}}$, while agent 2 can only measure the disturbance signal $\begin{bmatrix} w_3 & w_4 \end{bmatrix}^{\mathrm{T}}$ as shown in Fig. 5.3. Since the sensed information by any agent is not enough for reconstructing the entire vector $w(t)$, the distributed observer in (4.2) is required to propagate the estimation of exosystem signals among the agents. The objective is to make all the agents track the signal $w_1(t)$, *i.e.* $\lim_{t\to\infty}\theta_i(t) - w_1(t) = 0,\ i = 1,2,3$, while keeping all the states of the agents bounded. The regulated error e_i is now defined as the difference of the motor position θ_i and w_1 and therefore F_i in (2.1) becomes $F_i = \begin{bmatrix} -1 & \mathbf{0}_{1\times 3} \end{bmatrix}$.

5.4 Controller Design

The distributed control for the synchronization problem is designed with the suitable observer gains and controller gains as noted in Remarks 4.3.1 and 4.4.1. We verify that Assumptions 2.3.1, 2.3.2, 2.3.3, 4.2.1, and 2.5.1 are satisfied, and thus the control law (4.25) is found with $K_{1_i} = \begin{bmatrix} -8 & -4 \end{bmatrix}$, $K_{2_i} = \begin{bmatrix} -7.994 & 4.043 & -1 & 0 \end{bmatrix}$ and G_i's as in (4.31).

5.5 Experimental Results

Figure 5.4 shows the regulated error of the motors e_i. The servomotors track the reference trajectory with a 4.7% tracking error, which is primarily caused by the modeling uncertainty and the time delay in the network communication.

The results in Fig. 5.4 is compared to equivalent results obtained with the distributed control solutions in [41, 49, 51]. Let $\sigma(t) = \{1,2,4\}$ to be the switching sequence repeating uniformly over every T^* interval. The union of the associated digraphs $\mathcal{G}_1 \cup \mathcal{G}_2 \cup \mathcal{G}_4$, as shown in Figure 5.5, satisfies the uniform connectivity of leader node 0 to the rest of the nodes in each T^* interval, as prescribed for the solutions

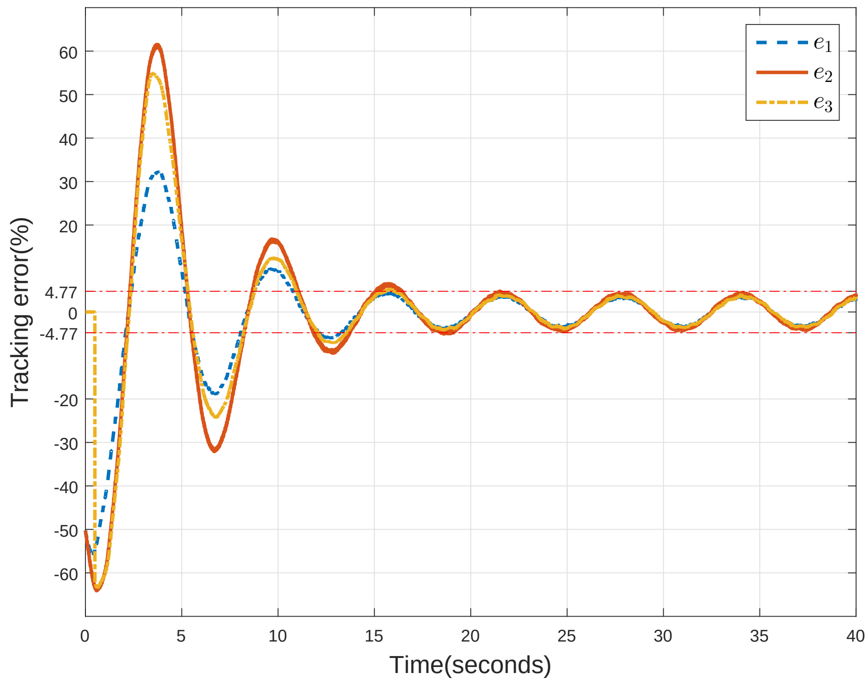

Figure 5.4: Tracking error(%) of the follower servomotors

in [41, 49, 51]. Under this connectivity requirement, a control solution to the output regulation problem was offered in [41, 49], in which $w(t)$ was required to be completely detectable from y_i for some agent i in the digraph $\mathcal{G}_{\sigma(t)}$. This is clearly no longer true from Figure 5.5 and (4.30). When the control algorithm from [41, 49] is applied to the agents in the current problem, the tracking error responses are as shown in Figure 5.6. This figure shows that agents 1 and 3 can track the reference w_1, while the tracking error for agent 2 is significantly larger. This is because agent 2 is no longer updated on the reference signal w_1. Similar observations can be made for the disturbance signal w_3 in agents 1 and 3. The comparative analysis thus shows the uniqueness of our control solution which solves the output regulation problem under the detectability constraint, which is otherwise not possible to be solved by the results in [41, 49].

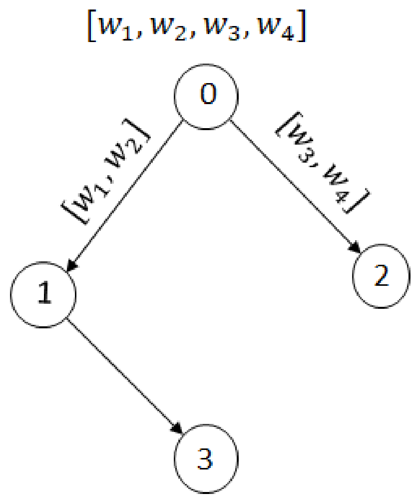

Figure 5.5: Joint comunication network $\mathcal{G}_1 \cup \mathcal{G}_2 \cup \mathcal{G}_4$ over a switching period T^*

5.6 Conclusion

The theoretical results developed in former chapters were tested experimentally on the position synchronization problem of networked motors under considered detectability constraint and switching communication topology. By applying the proposed control algorithm, it was observed that the tracking error for the follower servomotors incurs a small error in comparison to the existing control methods. The experimental test results also revealed the uniqueness of our proposed control solution by successfully solving the output regulation problem under the relaxed detectability condition, which is otherwise not possible to be solved by the existing control techniques in the literature.

As mentioned in the text, the tracking error resulted from the experiment was caused mainly by the presence of time delay in the communication between servomotors. To mitigate such effects, in our next chapter we develop a theory for distributed estimation of exosystem states in the face of measurement and communication delays.

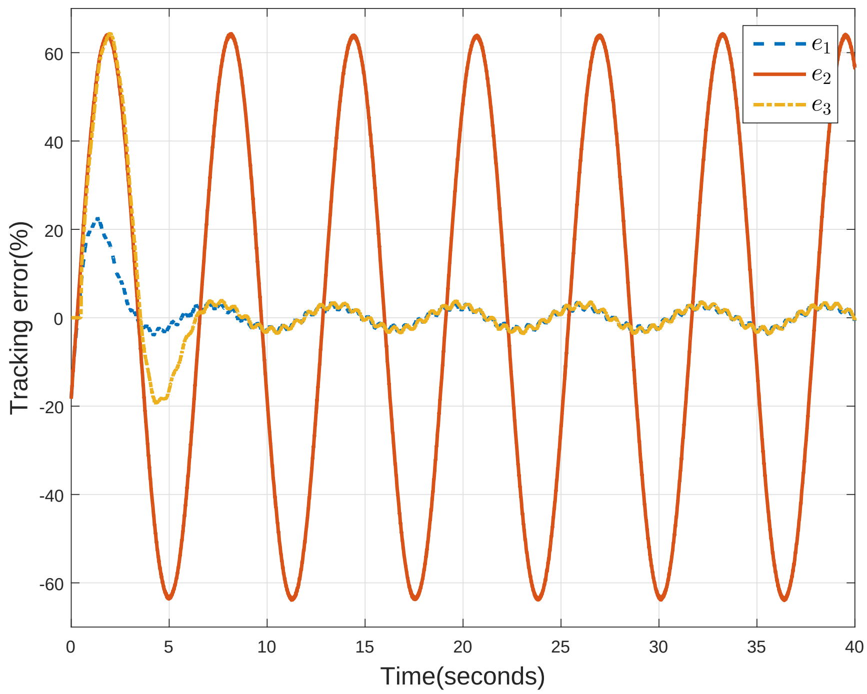

Figure 5.6: Tracking error(%) of the follower servomotors by the implementation of distributed control algorithm in earlier litearture

Chapter 6

Distributed State Estimation by a Network of Observers under Communication and Measurement Delays

In the last decade, the research on distributed sensing and estimation have received considerable attention due to its wide range of applications in areas that include electrical power systems [59], energy management [60, 61], wide-area monitoring [62], fault tolerant control [63], sensor networks, health care, military and surveillance control [64]. To estimate and track the target state evolving from a dynamic process, distributed Kalman filtering [65–67] and distributed observers [68–70] have been studied extensively.

The objective of the distributed state estimation for a dynamic plant is to reconstruct the plant state vector by a network of observers using limited local plant measurements and the communication shared between the observers. In contrast to the decentralized estimation scheme [29, 30], where at least one observer must independently estimate the entire plant state vector and the estimation must then propagated to the remaining observers through a consensus protocol, each observer in the distributed observation framework receives only a portion of the plant output measurement needed for the estimation of the system states. The limited plant output information is not sufficient for independently reconstructing the entire state vector. Instead, observers disseminate their local information over a communication network, and collaborate to jointly synthesize an estimation of the plant dynamics. Under the framework of the distributed observation problem, each observer can be viewed as a follower agent, and the plant to be observed as the leader agent. The design of distributed observers can then be regarded as a special case of a leader-follower consensus problem, where each follower cannot independently reconstruct the leader's trajectory [2, 3, 53, 71].

The design of distributed discrete LTI observers subject to a scalability constraint was studied in [68], while [69] investigated the design of continuous LTI distributed observers with a preassigned observer spectrum. In case of packet dropouts and abrupt changes of the network topology over time, a hybrid observer comprising of a local observer and a local parameter estimator was designed in [70].

In this work we study the distributed state estimation problem by a network of observers under arbitrarily large communication and measurement delays. First, we consider the case when the communication delay and measurement delay are equal, and we construct a distributed solution following the low gain approach. Sufficient conditions for the stability of the observation error dynamics, including an upper bound for the low gain parameter, are found for arbitrary large delays. Next, we extend our solution to the general case when the communication and measurement delays are different, and we derive equivalent conditions for the convergence of the observation error as in the initial simpler case. Finally, with the solution to the distributed state estimation problem, we aim to solve a leader-follower synchronization problem for the case where leader trajectory cannot be independently estimated by the followers. A version of the leader-follower synchronization problem with similar estimation constraints appears in [2, 3, 71]. In contrast to these papers, this work introduces latency in the measurements from the leader and the communication between the followers. With the help of an illustrative example and a comparative analysis, we demonstrate the effectiveness of our derived results.

The remainder of the chapter is organized in the following way. The problem formulation and algebraic graph theoretic properties are briefly revisited in Section 6.1. Next we derive the stability condition for the distributed observer dynamics coupled with communication and measurement delays in Section 6.2. Under the presence of noisy plant measurements, the distributed state estimation problem for the group of observers is revisited in Section 6.3. In Section 6.4, we present the leader-follower synchronization problem as an application to the studied distributed state estimation problem. An illustrative example to verify the effectiveness of the proposed approach is presented in Section 6.5. Lastly, conclusions are reported in Section 6.6.

Notations. We now briefly introduce some notations and symbols, which will be used throughout the chapter. The Kronecker product of matrices is denoted by $\otimes$. A vector $\mathbf{1}_N$ is a column vector in $\mathbb{R}^N$ of all ones. $\mathbb{Z}^+$ is the set of all positive integers. I_q and 0_q respectively denote the identity matrix and zero matrix of dimension $q \times q$. Unless mentioned otherwise, for matrices $A_i, i = 1, 2, \cdots, N$, $\bar{A} = \mathrm{col}(A_1, A_2, \cdots, A_N) = \begin{bmatrix} A_1^{\mathrm{T}} & A_2^{\mathrm{T}} & \cdots, A_N^{\mathrm{T}} \end{bmatrix}^{\mathrm{T}}$ and $A = \mathrm{blk\ diag}(A_1, A_2, \cdots, A_N)$ represents a block diagonal matrix with the i^{th} block being A_i. For a non-zero vector x, and matrix X, $\|x\|$, and $\|X\|$ respectively stand for the $\mathbf{L}^2$ norm for vectors and the spectral norm for matrices. For a square matrix $\mathcal{X}$, $\lambda_i(\mathcal{X})$ denotes the i^{th} eigenvalue, while the minimum, maximum and sum of eigenvalues are respectively denoted by $\lambda_{\min}(\mathcal{X})$, $\lambda_{\max}(\mathcal{X})$ and $\mathrm{Tr}(\mathcal{X})$. For the positive scalar τ, let $\mathcal{C}([-\tau, 0], \mathbb{R}^m)$ denote the Banach space of all continuous functions mapping the interval $[-\tau, 0]$ into $\mathbb{R}^m$ endowed with the supremum norm.

6.1 Problem Formulation

Consider a continuous linear time-invariant plant with dynamics

$$\dot{w} = Sw, \tag{6.1}$$

where $w \in \mathbb{R}^q$. The output of the plant denoted by $y_m = \mathrm{col}(y_{m_1}, y_{m_2}, \cdots, y_{m_N})$ is measured by a group of N distributed autonomous observers with an objective to provide an asymptotic estimation of the plant state vector $w(t)$. However, each of these observers receives only a small part of the measurement signal $y_m(t)$, namely $y_{m_i}(t) \in \mathbb{R}^{p_i}$ for the i^{th} observer defined as

$$y_{m_i}(t) = C_{w_i} w(t - \tau_2), i = 1, 2, \cdots, N, \tag{6.2}$$

where τ_2 denotes the measurement delay. These observers are connected with each other through a communication network to jointly provide an estimation for $w(t)$. The observers along with the plant model in (6.1) can be viewed as a multi-agent system with the plant being the leader agent and the observers being the followers.

6.1.1 Problem Statement

Let the connections between the plant (6.1) and the N distributed observers be described by the graph $\mathcal{G} = (\mathcal{V}, \mathcal{E})$, $\mathcal{V} = \{0, 1, 2, \cdots, N\}$. Under the multi-agent system representation, the leader agent (6.1) is the zeroth node of $\mathcal{V}$, while the follower agents are the remaining N nodes. The dynamics of the distributed observers in the presence of communication and measurement delays are given as

$$\begin{aligned}\dot{\eta}_i = S\eta_i + \mu \sum_{j\in\mathcal{N}_i} a_{ij} e^{\tau_1 S}(\eta_j(t-\tau_1) - \eta_i(t-\tau_1)) \\ + \mu a_{i0} e^{\tau_2 S} G_i C_{w_i}\left(w(t-\tau_2) - \eta_i(t-\tau_2)\right),\end{aligned} \tag{6.3}$$

where η_i is the state estimation by the i^{th} observer, $i = 1, 2, \cdots, N$, τ_1 is the inter-agent communication delay, and G_i and μ are respectively the observer gain and the low-gain to be designed.

Suppose $w(\theta) = w_\theta \in \mathcal{C}([-\tau, 0], \mathbb{R}^q)$, $\eta_i(\theta) = \eta_{i\theta} \in \mathcal{C}([-\tau, 0], \mathbb{R}^q)$, $\tau = \max(\tau_1, \tau_2)$, and denote the estimation error by $\tilde{\eta}_i = \eta_i - w$, with $\tilde{\eta}_i(\theta) = \tilde{\eta}_{i\theta} \in \mathcal{C}([-\tau, 0], \mathbb{R}^q), \theta \in [-\tau, 0]$. The estimation error dynamics obtained from (6.1) and (6.3) is given as

$$\dot{\tilde{\eta}}_i = S\tilde{\eta}_i + \mu \sum_{j\in\mathcal{N}_i} a_{ij} e^{\tau_1 S}(\tilde{\eta}_j(t-\tau_1) - \tilde{\eta}_i(t-\tau_1)) - \mu a_{i0} e^{\tau_2 S} G_i C_{w_i} \tilde{\eta}_i(t-\tau_2). \tag{6.4}$$

We consider that the assumptions 2.3.1, 2.3.4 hold. The condition in 2.3.4 is referred to as the "combined detectability" property in [2, 3, 53]. An equivalent observability condition appears in [46, 68–70]. As noted in [46, 68], the "source components" or equivalently "active agents" in [71] of digraph $\mathcal{G}$ are responsible for estimating the leader dynamics and disseminating that estimation to other passive followers in the network. Due to this reason, in the current work we only take into account the active observer agents with the connectivity requirement in Assumption 2.3.5 being reinstated as follows:

Assumption 6.1.1. *All N follower agents form a strongly connected partition of the digraph $\mathcal{G}$, and for at least one agent $i \in \{1, 2, \cdots, N\}$, $C_{w_i} \neq 0$.*

Remark 6.1.1. *The strongly connected partition of $\mathcal{G}$ in Assumption 6.1.1 can be seen as a way for an observer agent i to collect information on modes that may not be detectable by the pair (S, C_{w_i}). In such case, Assumption 2.3.4 guarantees that* *information on such mode is indeed collected by some observer agents in the system, and Assumption 6.1.1 provides a path for the information to travel to the i agent.*

Now we are ready to define the problem statement as follows.

Definition 6.1.1. Distributed state estimation problem: Design observer gains G_i, $i = 1,2,\cdots,N$, and feedback gain μ such that the estimation error dynamics (6.4) is exponentially stable, *i.e.*, for given $\tau_1, \tau_2 > 0$ and $\tilde{\eta}_{i\theta} \in \mathcal{C}([-\tau,0],\mathbb{R}^q)$, $\lim_{t\to\infty} \tilde{\eta}_i(t) = 0$ for $i = 1,2,\cdots,N$.

Before we present the main contributions of this work, we first establish the following results, which will be used in the next section.

Proposition 1. Given the plant dynamics (6.1) with the state matrix S satisfying Assumption 2.3.1, it holds that

$$e^{-S^{\mathrm{T}}t}e^{-St} \geq e^{-\omega\gamma^* t} I_q, \tag{6.5}$$

for a positive scalar $\boldsymbol{\gamma}^* = \min\{\boldsymbol{\gamma} > 0 : \mathbf{Q} = S^{\mathrm{T}} + S + \boldsymbol{\gamma} I > 0\}$, and $\omega = q-1$.

Proof. Select a positive scalar $\boldsymbol{\gamma}^*$ such that $\mathbf{Q}$ is positive definite. Then by using Cholesky decomposition $\mathbf{Q} = WW^{\mathrm{T}}$ we obtain

$$S^{\mathrm{T}} + S - WW^{\mathrm{T}} = -\boldsymbol{\gamma}^* I_q, \tag{6.6}$$

and thus Lemma 1 of [72] yields that

$$e^{S^{\mathrm{T}}t}e^{St} \leq e^{\omega\gamma^* t} I_q,\ \omega = q-1. \tag{6.7}$$

Since $e^{\omega\gamma^* t} I_q - e^{S^{\mathrm{T}}t}e^{St} \geq 0$, then

$$e^{-St}e^{-S^{\mathrm{T}}t} \geq e^{-\omega\gamma^* t} I_q. \tag{6.8}$$

By multiplying the left hand side of (6.8) by e^{St} and its right hand side by e^{-St} we obtain (6.5). This concludes the proof. $\square$

Lemma 6.1.2. *For any positive semi-definite matrix $M_0 \geq 0$, two scalars $\boldsymbol{\gamma}_1$ and $\boldsymbol{\gamma}_2$ with $\boldsymbol{\gamma}_2 \geq \boldsymbol{\gamma}_1$, and a vector valued function $\omega : [\boldsymbol{\gamma}_1, \boldsymbol{\gamma}_2] \to \mathbb{R}^n$, the inequality*

$$\left(\int_{\boldsymbol{\gamma}_1}^{\boldsymbol{\gamma}_2} \omega^T(\boldsymbol{\beta})\ d\boldsymbol{\beta}\right)\ M_0\ \left(\int_{\boldsymbol{\gamma}_1}^{\boldsymbol{\gamma}_2} \omega(\boldsymbol{\beta})\ d\boldsymbol{\beta}\right) \leq (\boldsymbol{\gamma}_2 - \boldsymbol{\gamma}_1) \int_{\boldsymbol{\gamma}_1}^{\boldsymbol{\gamma}_2} \omega^T(\boldsymbol{\beta})\ M_0\ \omega(\boldsymbol{\beta})\ d\boldsymbol{\beta} \quad (6.9)$$

holds if the integrals are well defined.

Proof. A version of this lemma appears in [72–75], where M_0 was considered to be strictly positive definite. Here we extend the result to semi-definite matrices.

For a real symmetric matrix M_0, it can be orthogonally decomposed as $M_0 = \mathbf{J} D_{M_0} \mathbf{J}^{-1}$ where $\mathbf{J}^{\mathrm{T}} = \mathbf{J}^{-1}$, and D_{M_0} is a real diagonal matrix with all diagonal elements being the eigenvalues of M_0. Then the integral on the right hand side of (6.9) yields the following form

$$\begin{aligned}(\boldsymbol{\gamma}_2 - \boldsymbol{\gamma}_1) \int_{\boldsymbol{\gamma}_1}^{\boldsymbol{\gamma}_2} \omega^{\mathrm{T}}(\boldsymbol{\beta}) M_0 \omega(\boldsymbol{\beta}) d\boldsymbol{\beta} &= (\boldsymbol{\gamma}_2 - \boldsymbol{\gamma}_1) \int_{\boldsymbol{\gamma}_1}^{\boldsymbol{\gamma}_2} \omega^{\mathrm{T}}(\boldsymbol{\beta}) \mathbf{J} D_{M_0} \mathbf{J}^{\mathrm{T}} \omega(\boldsymbol{\beta}) d\boldsymbol{\beta}, \\ &= (\boldsymbol{\gamma}_2 - \boldsymbol{\gamma}_1) \int_{\boldsymbol{\gamma}_1}^{\boldsymbol{\gamma}_2} \boldsymbol{\omega}^T(\boldsymbol{\beta}) D_{M_0} \boldsymbol{\omega}(\boldsymbol{\beta}) d\boldsymbol{\beta}, \qquad (6.10)\end{aligned}$$

where $\boldsymbol{\omega}(\boldsymbol{\beta}) = \mathbf{J}^{\mathrm{T}} \omega(\boldsymbol{\beta})$, $D_{M_0} = \text{blk diag}(\lambda_1, \lambda_2, \cdots, \lambda_n)$. Suppose M_0 has r non-zero eigenvalues, *i.e.*, with no loss of generality let $\lambda_i = 0$, $i = r+1, r+2, \cdots, n$ and $\boldsymbol{\omega}(\boldsymbol{\beta}) = \text{col}(\boldsymbol{\omega}_1(\boldsymbol{\beta}), \boldsymbol{\omega}_2(\boldsymbol{\beta}), \cdots, \boldsymbol{\omega}_n(\boldsymbol{\beta}))$. Then by virtue of the result in [75], the integral expression in (6.10) reduces to the form

$$\begin{aligned}&(\boldsymbol{\gamma}_2 - \boldsymbol{\gamma}_1) \int_{\boldsymbol{\gamma}_1}^{\boldsymbol{\gamma}_2} \omega^{\mathrm{T}}(\boldsymbol{\beta}) M_0 \omega(\boldsymbol{\beta}) d\boldsymbol{\beta} = (\boldsymbol{\gamma}_2 - \boldsymbol{\gamma}_1) \int_{\boldsymbol{\gamma}_1}^{\boldsymbol{\gamma}_2} \sum_{i=1}^{r} \left[\lambda_i \boldsymbol{\omega}_i^{\mathrm{T}}(\boldsymbol{\beta}) \boldsymbol{\omega}_i(\boldsymbol{\beta})\right] d\boldsymbol{\beta}, \\ &= \sum_{i=1}^{r} \lambda_i \left[(\boldsymbol{\gamma}_2 - \boldsymbol{\gamma}_1) \int_{\boldsymbol{\gamma}_1}^{\boldsymbol{\gamma}_2} \boldsymbol{\omega}_i^{\mathrm{T}}(\boldsymbol{\beta}) \boldsymbol{\omega}_i(\boldsymbol{\beta}) d\boldsymbol{\beta}\right] \geq \sum_{i=1}^{r} \lambda_i \left(\int_{\boldsymbol{\gamma}_1}^{\boldsymbol{\gamma}_2} \boldsymbol{\omega}_i^{\mathrm{T}}(\boldsymbol{\beta}) d\boldsymbol{\beta}\right) \left(\int_{\boldsymbol{\gamma}_1}^{\boldsymbol{\gamma}_2} \boldsymbol{\omega}_i(\boldsymbol{\beta}) d\boldsymbol{\beta}\right), \\ &= \sum_{i=1}^{n} \lambda_i \left(\int_{\boldsymbol{\gamma}_1}^{\boldsymbol{\gamma}_2} \boldsymbol{\omega}_i^{\mathrm{T}}(\boldsymbol{\beta}) d\boldsymbol{\beta}\right) \left(\int_{\boldsymbol{\gamma}_1}^{\boldsymbol{\gamma}_2} \boldsymbol{\omega}_i(\boldsymbol{\beta}) d\boldsymbol{\beta}\right) = \left[\int_{\boldsymbol{\gamma}_1}^{\boldsymbol{\gamma}_2} \boldsymbol{\omega}^{\mathrm{T}}(\boldsymbol{\beta}) d\boldsymbol{\beta}\right] D_{M_0} \left[\int_{\boldsymbol{\gamma}_1}^{\boldsymbol{\gamma}_2} \boldsymbol{\omega}(\boldsymbol{\beta}) d\boldsymbol{\beta}\right],\end{aligned}$$

$$= \left[\int_{\gamma_1}^{\gamma_2} \omega^{\mathrm{T}}(\boldsymbol{\beta})d\boldsymbol{\beta}\right] \mathbf{J} D_{M_0} \mathbf{J}^{\mathrm{T}} \left[\int_{\gamma_1}^{\gamma_2} \omega(\boldsymbol{\beta})d\boldsymbol{\beta}\right]$$
$$= \left[\int_{\gamma_1}^{\gamma_2} \omega^{\mathrm{T}}(\boldsymbol{\beta})d\boldsymbol{\beta}\right] M_0 \left[\int_{\gamma_1}^{\gamma_2} \omega(\boldsymbol{\beta})d\boldsymbol{\beta}\right]. \tag{6.11}$$

This concludes the proof for this lemma. □

Next, we present the Lyapunov-Krasovskii stability theorem which will be frequently used in deriving the stability of the estimation error dynamics (6.4).

Theorem 6.1.3. *Lyapunov-Krasovskii Stability Theorem [76]: Consider the system*

$$\dot{\tilde{\eta}} = f(t, \tilde{\eta}(t+\theta)),\ \theta \in [-\tau, 0], \tag{6.12}$$

where $f \in \mathbb{R} \times \mathcal{C}[-\tau, 0] \to \mathbb{R}^{Nq}$ *maps* $\mathbb{R} \times$ (*bounded sets in* $\mathcal{C}[-\tau, 0]$) *into bounded sets of* $\mathbb{R}^{Nq}$. *Suppose that* $u, v, \mathbf{w} : \mathbb{R}^+ \to \mathbb{R}^+$ *are continuous non-decreasing functions,* $u(s)$, *and* $v(s)$ *are positive for* $s > 0$, *and* $u(0) = v(0) = 0$. *The trivial solution of the system* (6.12) *is uniformly stable if there exists a continuous functional* $\mathbb{V} : \mathbb{R} \times \mathcal{C}[-\tau, 0] \to \mathbb{R}^+$, *which is positive-definite,* i.e.

$$u(|\tilde{\eta}(t)|) \le \mathbb{V}(t, \tilde{\eta}(\theta)) \le v(\|\tilde{\eta}(\theta)\|_{\mathcal{C}}),\ \theta \in [-\tau, 0], \tag{6.13}$$

and such that its derivative along the system trajectory (6.12) *is non-positive in the sense that*

$$\dot{\mathbb{V}}(t, \tilde{\eta}(\theta)) \le -\mathbf{w}(|\tilde{\eta}(t)|). \tag{6.14}$$

If $\mathbf{w}(s) > 0$ *for* $s > 0$, *then the trivial solution is uniformly asymptotically stable. If in addition* $\lim_{s\to\infty} u(s) = \infty$, *then it is globally asymptotically stable.*

6.2 Main Result

In this section, we will present the stability results for the estimation error dynamics in (6.4), which will eventually lead to the design of observer gains G_i and low gain parameter μ. The current work also provides an upper bound for μ to ensure stability of the error dynamics.

To demonstrate the convergence of the estimation error dynamics (6.4) with communication and measurement delays τ_1 and τ_2, first we evaluate the boundedness of the response for $t \leq \bar{\tau}$, before the delayed measurements are available for feedback correction. After the boundedness of the initial response is established, we then proceed to evaluate the asymptotic stability of $\tilde{\eta}(t)$, for $t \geq \bar{\tau}$. For the first part, we will check the boundedness of $\tilde{\eta}(t)$, $\forall t \in [0, \bar{\tau}]$, driven by the initial conditions $\tilde{\eta}(\theta)$ for $\theta \in [-\bar{\tau}, 0]$. With no loss of generality, we assume that $\bar{\tau} = m\underline{\tau} + \in$ where $m \in \mathbb{Z}^+, \in < \underline{\tau}$. In a step-by-step manner we will evaluate the bounds of $\tilde{\eta}(t)$ across each such sub-intervals.

From (6.4) we obtain

$$
\begin{aligned}
\tilde{\eta}(t) = & \left(I_N \otimes e^{St}\right)\tilde{\boldsymbol{\eta}}(0) - \mu \int_0^t I_N \otimes e^{S(t-s+\tau_2)} G C_w \tilde{\boldsymbol{\eta}}(s-\tau_2) ds \\
& - \mu \int_0^t I_N \otimes e^{S(t-s+\tau_1)} (\boldsymbol{\mathcal{L}} \otimes I_q) \tilde{\boldsymbol{\eta}}(s-\tau_1) ds, \forall t < \underline{\tau} \\
\|\tilde{\eta}\| \leq & \|e^{St}\| \|\tilde{\boldsymbol{\eta}}(0)\| + \mu \int_0^t \|e^{(t-s+\tau_2)S}\| \sqrt{\sigma_G} \|\tilde{\boldsymbol{\eta}}(s-\tau_2)\| ds \\
& + \mu \int_0^t \|e^{(t-s+\tau_1)S}\| \sqrt{\sigma_{\mathcal{L}}} \|\tilde{\boldsymbol{\eta}}(s-\tau_1)\| ds, \\
& \leq \max_{\theta \in [0, \underline{\tau}]} \Big(\|e^{S\theta}\| + \mu \underline{\tau} \Big(\|e^{S(\tau_2+\theta)}\| \sqrt{\sigma_G} \\
& \qquad + \|e^{S(\tau_1+\theta)}\| \sqrt{\sigma_{\mathcal{L}}} \Big) \Big) \|\tilde{\boldsymbol{\eta}}\|_{\mathcal{C}},
\end{aligned}
\tag{6.15}
$$

where $\|\tilde{\boldsymbol{\eta}}\|_{\mathcal{C}} = \max_{\theta \in [-\bar{\tau}, 0]} \|\tilde{\boldsymbol{\eta}}(\theta)\|$. It follows that $\tilde{\eta}(t)$, $\forall t \in [0, \underline{\tau}]$ is bounded as $\tilde{\boldsymbol{\eta}} \in \mathcal{C}([-\tau, 0], \mathbb{R}^{Nq})$.

For the subsequent intervals with $t > \underline{\tau}$, we obtain from (6.4),

$$\tilde{\eta}(t) = \left(I_N \otimes e^{S\underline{\tau}}\right)\tilde{\eta}(t-\underline{\tau}) - \mu\int_{t-\underline{\tau}}^{t}(\pi_1(s)+\pi_2(s))ds, \tag{6.16}$$

where $\pi_1 = I_N \otimes e^{S(t-s+\tau_2)}GC_w\tilde{\eta}(s-\tau_2)ds$, $\pi_2 = I_N \otimes e^{S(t-s+\tau_1)}(\mathcal{L}\otimes I_q)\tilde{\eta}(s-\tau_1)ds$. Since $\tilde{\eta}(t), t \in [0,\underline{\tau}]$ and $\tilde{\boldsymbol{\eta}}(\theta), \forall\theta \in [-\underline{\tau},0]$ are bounded, it follows from (6.16) that $\tilde{\eta}(t)$, $\forall t \in [\underline{\tau}, 2\underline{\tau}]$ is bounded.

In a similar manner, we can evaluate $\|\tilde{\eta}(t)\|$, $\forall t \in [j\underline{\tau},(j+1)\underline{\tau}]$, $j \geq 2$, and by using the method of induction we can show $\tilde{\eta}(t)$ is bounded for $t \in [0, m\underline{\tau}]$. Again for $t \geq m\underline{\tau}$, from (6.4) it yields

$$\tilde{\eta}(t) = \left(I_N \otimes e^{Sm\underline{\tau}}\right)\tilde{\eta}(t-m\underline{\tau}) - \mu\int_{t-\mu\underline{\tau}}^{t}(\pi_1(s)+\pi_2(s))ds,$$

which also implies that $\tilde{\eta}(t)$, $\forall t \in [0,\bar{\tau}]$ is bounded as $\tilde{\boldsymbol{\eta}}(\theta), \forall\theta \in [-\bar{\tau},0]$ and $\tilde{\eta}(t), \forall t \in [0, m\underline{\tau}]$ are bounded.

Since we obtained that $\tilde{\eta}(t)$ is bounded $\forall t \in [0,\bar{\tau}]$, we now need to show the stability of the error dynamics (6.4) for $t \geq \bar{\tau}$.

6.2.1 Case 1: $\tau_1 = \tau_2$

First we consider the case when $\tau_1 = \tau_2 = \tau$. As $\tilde{\eta}(t)$ is shown to be bounded for $\forall t \in [0,\tau]$, in the following discussion we then proceed to show the asymptotic stability of $\tilde{\eta}(t)$ for $t > \tau$. Let $\tilde{\eta} = \mathrm{col}(\tilde{\eta}_1, \tilde{\eta}_2, \cdots, \tilde{\eta}_N)$ and thus the composite error vector $\tilde{\eta}$ evolves as follows

$$\dot{\tilde{\eta}} = (I_N \otimes S)\tilde{\eta} - \mu\left(e^{\tau(I_N\otimes S)}GC_w\right)\tilde{\eta}(t-\tau) - \mu\left(\mathcal{L}\otimes e^{\tau S}\right)\tilde{\eta}(t-\tau), \tag{6.17}$$

where $\mathcal{L} \in \mathbb{R}^{N\times N}$ is the Laplacian matrix corresponding to the strongly connected partition of the network of N observer agents, $G = \text{blk diag}(G_1, G_2, \cdots, G_N)$, and

$C_w = \text{blk diag}(C_{w_1}, C_{w_2}, \cdots, C_{w_N})$. From (6.17), we obtain $\tilde{\eta}(t)$ as

$$\tilde{\eta}(t) = e^{(I_N \otimes S)\tau}\tilde{\eta}(t-\tau) - \mu(\pi_1(t) + \pi_2(t)), \tag{6.18}$$

where

$$\begin{aligned} \pi_1(t) &= \int_{t-\tau}^{t} e^{(I_N \otimes S)(t-s)} \left(\mathcal{L} \otimes e^{\tau S}\right) \tilde{\eta}(s-\tau)\ ds, \\ \pi_2(t) &= \int_{t-\tau}^{t} e^{(I_N \otimes S)(t-s+\tau)} G C_w\ \tilde{\eta}(s-\tau) ds. \end{aligned} \tag{6.19}$$

The substitution of $\tilde{\eta}(t-\tau)$ from (6.18) into (6.17) results in

$$\dot{\tilde{\eta}} = \left(I_N \otimes e^{\tau S}\right) M \left(I_N \otimes e^{-\tau S}\right) \tilde{\eta} - \mu^2 \left(\mathcal{L} \otimes e^{\tau S} + (I_N \otimes e^{\tau S}) G C_w\right) (\pi_1^* + \pi_2^*), \tag{6.20}$$

where

$$\begin{aligned} M &= \left[(I_N \otimes S) - \mu\left(\mathcal{L} \otimes I_q\right) - \mu G C_w\right], \\ \pi_1^*(t) &= \left(I_N \otimes e^{-\tau S}\right) \pi_1(t),\ \pi_2^*(t) = \left(I_N \otimes e^{-\tau S}\right) \pi_2(t). \end{aligned}$$

Let us now introduce some notations which will be used throughout this section. Denote $\bar{C}_w = \text{col}\left(C_{w_1}, C_{w_2}, \cdots, C_{w_N}\right)$, $\sigma_G = \|GC_w\|^2$, $\sigma_{\mathcal{L}} = \|\mathcal{L}\|^2$, $\mathbf{G} = [G_1'\ G_2'\ \cdots\ G_N']$, $G_i' = \zeta_i G_i$ where ζ_i is the i^{th} entry of the left eigenvector $\zeta = [\zeta_1\ \zeta_2\ \cdots\ \zeta_N]^{\text{T}}$ of $\mathcal{L}$ corresponding to zero eigenvalue. Without loss of generality, let $\sum_i \zeta_i = 1$. Note that for the Laplacian matrix $\mathcal{L}$ of a strongly connected communication network, the results in [46, 77] states that the positive-definite diagonal matrix $\Sigma = \text{diag}(\zeta)$ makes $\hat{\mathcal{L}} = \Sigma\mathcal{L} + \mathcal{L}^{\text{T}}\Sigma$ positive semi-definite. Additionally, $\hat{\mathcal{L}}$ has zero row sum and zero column sum, and thus it can be viewed as the Laplacian matrix of an undirected communication network.

To analyze the stability of (6.17), we construct a Lyapunov function of the form $V(\tilde{\eta}) = \tilde{\eta}^{\text{T}}(t)\left(\Sigma \otimes e^{-\tau S^{\text{T}}} P e^{-\tau S}\right)\tilde{\eta}(t)$ where P is a positive definite matrix. Since the matrix $\left(\Sigma \otimes e^{-\tau S^{\text{T}}} P e^{-\tau S}\right)$ is symmetric and have all positive eigenvalues, $V(\tilde{\eta}) >$

0, $\forall \tilde{\eta} \neq 0$. By differentiating $V(\tilde{\eta})$ along the trajectories of (6.20), we obtain

$$\begin{aligned}
\dot{V}(\tilde{\eta}) &= \tilde{\eta}_d^{\mathrm{T}} \left[M^{\mathrm{T}} (\Sigma \otimes P) + (\Sigma \otimes P) M \right] \tilde{\eta}_d \\
&- 2\mu^2 \left(\pi_1^{*^{\mathrm{T}}} + \pi_2^{*^{\mathrm{T}}} \right) \left(\mathcal{L}^{\mathrm{T}} \otimes I_q \right) \left(\Sigma \otimes P e^{-\tau S} \right) \tilde{\eta} \\
&- 2\mu^2 \left(\pi_1^{*^{\mathrm{T}}} + \pi_2^{*^{\mathrm{T}}} \right) C_w^{\mathrm{T}} G^{\mathrm{T}} \left(\Sigma \otimes P e^{-\tau S} \right) \tilde{\eta}, \\
&\leq \dot{V}_0 + 4\mu^2 V + \mu^2 \sum_i^2 \pi_i^{*^{\mathrm{T}}} \left[\mathcal{L}^{\mathrm{T}} \Sigma \mathcal{L} \otimes P + C_w^{\mathrm{T}} G^{\mathrm{T}} (\Sigma \otimes P) G C_w \right] \pi_i^*,
\end{aligned} \tag{6.21}$$

where $V_0 = \int_0^t \tilde{\eta}_d^{\mathrm{T}}(s) \left[M^{\mathrm{T}} (\Sigma \otimes P) + (\Sigma \otimes P) M \right] \tilde{\eta}_d(s)\ ds$, $\tilde{\eta}_d(t) = \left(I_N \otimes e^{-\tau S} \right) \tilde{\eta}(t)$. We consider the following Lemma to evaluate (6.21).

Lemma 6.2.1. *Consider the distributed observers* (6.17) *satisfying Assumptions 2.3.1-6.1.1, and gains G_i selected such that the matrix $\mathcal{R} = S - \mu \mathbf{G} \bar{C}_w$ is a Hurwitz matrix for any $\mu \in (0,1)$. Let then $P \in \mathbb{R}^{q \times q} > 0$ be a solution to the inequality*

$$\mathcal{R}^T P + P \mathcal{R} < 0, \tag{6.22}$$

such that the matrix $P(S - \mu G_i C_{w_i}) + (S - \mu G_i C_{w_i})^T P$ has non-positive eigenvalues for all follower agents i. Then for the identical communication and measurement delays $\tau_1 = \tau_2 = \tau$ the observer states $\eta_i(t)$ converges to $w(t)$ asymptotically, i.e.,

$$\lim_{t \to \infty} (\eta_i(t) - w(t)) = 0,\ i = 1, 2, \cdots, N,$$

if the low gain parameter μ satisfies $\mu < \bar{\mu}$, where

$$\bar{\mu} = \sqrt{\frac{\alpha}{\lambda_{\max}(P)\ \zeta_{\max} \left(4\varepsilon_d + \tau^2 (\sigma_{\mathcal{L}} + \sigma_G)^2 e^{2\omega\gamma^*\tau} \right)}}, \tag{6.23}$$

with $\alpha > 0$ such that $M^T(\Sigma \otimes P) + (\Sigma \otimes P)M < -\alpha I$ and $\varepsilon_d = \|e^{-\tau S}\|^2 e^{\omega\gamma^*\tau}$.

Proof. Let $\mathcal{G}$ satisfy Assumption 6.1.1 with at least one agent being the child node of the leader. Now, we evaluate the first term on the right-hand side of the inequality in (6.21). In this regard, we have

$$\begin{aligned}\dot{V}_0 &= \tilde{\eta}_d^{\mathrm{T}}\left[M^{\mathrm{T}}(\Sigma\otimes P)+(\Sigma\otimes P)M\right]\tilde{\eta}_d,\\ &= \tilde{\eta}_d^{\mathrm{T}}\left[\Sigma\otimes(S^{\mathrm{T}}P+PS)-\mu C_w^{\mathrm{T}}G^{\mathrm{T}}(\Sigma\otimes P)-\mu(\Sigma\otimes P)GC_w-\mu(\hat{\mathcal{L}}\otimes I_q)\right]\tilde{\eta}_d. \quad (6.24)\end{aligned}$$

It is inferred from Assumption 6.1.1 that the matrix $(\hat{\mathcal{L}}\otimes I_q)$ is positive semi-definite, and the lemma assumes that $P(S-\mu G_iC_{w_i})+(S-\mu G_iC_{w_i})^{\mathrm{T}}P$ is negative semi-definite. These assumptions then yield that $\dot{V}_0\leq 0$. We will now investigate the invariant set of $\tilde{\eta}_d$ on which $\dot{V}_0=0$. Assumption 6.1.1 yields $\hat{\mathcal{L}}$ has zero row sum, and thus the term $-\mu\tilde{\eta}_d^{\mathrm{T}}\left(\hat{\mathcal{L}}\otimes I_q\right)\tilde{\eta}_d$ in (6.24) becomes zero non-trivially only when $\tilde{\eta}_d=\mathbf{1}_N\otimes\tilde{\eta}_f$, for any $\tilde{\eta}_f\in\mathbb{R}^q$. Replacing this $\tilde{\eta}_d$ into (6.24) then yields that

$$\dot{V}_0=\tilde{\eta}_f\left[\mathcal{R}^{\mathrm{T}}P+P\mathcal{R}\right]\tilde{\eta}_f<0. \quad (6.25)$$

Therefore,

$$\dot{V}_0=\tilde{\eta}_d^{\mathrm{T}}\left(M^{\mathrm{T}}(\Sigma\otimes P)+(\Sigma\otimes P)M\right)\tilde{\eta}_d<0,$$

must be true for any non-zero $\tilde{\eta}_d$, and $\dot{V}_0=0$ only when $\tilde{\eta}_d=0$.

Because $\tilde{\eta}_d^{\mathrm{T}}\left(M^{\mathrm{T}}(\Sigma\otimes P)+(\Sigma\otimes P)M\right)\tilde{\eta}_d$ is continuous and finite over $\mu\in(0,1)$, there must exist a positive scalar $\alpha>0$ such that

$$\tilde{\eta}_d^{\mathrm{T}}\left(M^{\mathrm{T}}(\Sigma\otimes P)+(\Sigma\otimes P)M\right)\tilde{\eta}_d<-\alpha\|\tilde{\eta}_d\|^2.$$

It is then inferred from Proposition 1 that the following holds,

$$\dot{V}_0<-\alpha e^{-\omega\gamma^*\tau}\|\tilde{\eta}\|^2. \quad (6.26)$$

Substituting (6.24), (6.26) into (6.21) then yields

$$\begin{aligned}\dot{V}(\tilde{\eta}) \leq & -\alpha e^{-\omega\gamma^*\tau}\|\tilde{\eta}\|^2 + 4\mu^2 V + \mu^2 {\pi_1^*}^{\mathrm{T}}\left(\mathcal{L}^{\mathrm{T}}\Sigma\mathcal{L}\otimes P\right)\pi_1^* \\ & + \mu^2 {\pi_2^*}^{\mathrm{T}}\left(\mathcal{L}^{\mathrm{T}}\Sigma\mathcal{L}\otimes P\right)\pi_2^* + \mu^2 {\pi_1^*}^{\mathrm{T}} C_w^{\mathrm{T}} G^{\mathrm{T}}(\Sigma\otimes P) G C_w \pi_1^* \\ & + \mu^2 {\pi_2^*}^{\mathrm{T}} C_w^{\mathrm{T}} G^{\mathrm{T}}(\Sigma\otimes P) G C_w \pi_2^*. \end{aligned} \tag{6.27}$$

Now each of the terms in (6.27) are evaluated separately as follows. By virtue of Lemma 6.1.2, ${\pi_1^*}^{\mathrm{T}}\left(\mathcal{L}^{\mathrm{T}}\Sigma\mathcal{L}\otimes P\right)\pi_1^*$ can be rewritten as

$$\begin{aligned} & {\pi_1^*}^{\mathrm{T}}\left(\mathcal{L}^{\mathrm{T}}\Sigma\mathcal{L}\otimes P\right)\pi_1^* \\ & = \left[\int_{t-\tau}^{t} \tilde{\eta}^{\mathrm{T}}(s-\tau)\left(\mathcal{L}^{\mathrm{T}}\otimes e^{S^{\mathrm{T}}(t-s)}\right)ds\right]\left[\mathcal{L}^{\mathrm{T}}\Sigma\mathcal{L}\otimes P\right] \\ & \qquad \left[\int_{t-\tau}^{t}\left(\mathcal{L}\otimes e^{S(t-s)}\right)\tilde{\eta}(s-\tau)ds\right], \\ & \leq \tau\int_{t-\tau}^{t}\tilde{\eta}^{\mathrm{T}}(s-\tau)\left(\mathcal{L}^{\mathrm{T}}\otimes e^{S^{\mathrm{T}}(t-s)}\right)\left(\mathcal{L}^{\mathrm{T}}\Sigma\mathcal{L}\otimes P\right) \\ & \qquad \left(\mathcal{L}\otimes e^{S(t-s)}\right)\tilde{\eta}(s-\tau)ds, \\ & \leq \tau\zeta_{\max}\lambda_{\max}(P)\sigma_{\mathcal{L}}^2\int_{t-\tau}^{t}\tilde{\eta}^{\mathrm{T}}(s-\tau) \\ & \qquad \left[I_N\otimes e^{S^{\mathrm{T}}(t-s)}e^{S(t-s)}\right]\tilde{\eta}(s-\tau)\ ds. \end{aligned} \tag{6.28}$$

By using the results of Proposition 1 and the inequality in (6.5), Equation (6.28) reduces to

$$\begin{aligned} {\pi_1^*}^{\mathrm{T}}\left(\mathcal{L}^{\mathrm{T}}\Sigma\mathcal{L}\otimes P\right)\pi_1^* & \leq \tau\zeta_{\max}\lambda_{\max}(P)\sigma_{\mathcal{L}}^2\int_{t-\tau}^{t} e^{\omega\gamma^*(t-s)}\tilde{\eta}^{\mathrm{T}}(s-\tau)\tilde{\eta}(s-\tau)ds, \\ & \leq \tau\zeta_{\max}\lambda_{\max}(P)\sigma_{\mathcal{L}}^2\ e^{\omega\gamma^*\tau}\int_{t-2\tau}^{t-\tau}\tilde{\eta}^{\mathrm{T}}(s)\tilde{\eta}(s)ds, \\ & = \tau\zeta_{\max}\lambda_{\max}(P)\sigma_{\mathcal{L}}^2\ e^{\omega\gamma^*\tau}\left[\tau\tilde{\eta}^{\mathrm{T}}(t)\tilde{\eta}-\dot{V}_1\right], \end{aligned} \tag{6.29}$$

where $V_1 = \int_{\tau}^{2\tau}\int_{t-s}^{t}\tilde{\eta}^{\mathrm{T}}(\boldsymbol{\sigma})\tilde{\eta}(\boldsymbol{\sigma})d\boldsymbol{\sigma}\ ds$. Similarly for ${\pi_2^*}^{\mathrm{T}}\left(\mathcal{L}^{\mathrm{T}}\Sigma\mathcal{L}\otimes P\right)\pi_2^*(t)$ in (6.27), we obtain

$$ {\pi_2^*}^{\mathrm{T}}\left(\mathcal{L}^{\mathrm{T}}\Sigma\mathcal{L}\otimes P\right)\pi_2^*(t) \le \tau\zeta_{\max}\lambda_{\max}(P)\sigma_{\mathcal{L}}\sigma_G\ e^{\omega\gamma^*\tau}\left[\tau\|\tilde{\eta}\|^2 - \dot{V}_1\right]. \tag{6.30} $$

On the same note, the evaluation of ${\pi_1^*}^{\mathrm{T}}C_w^{\mathrm{T}}G^{\mathrm{T}}(\Sigma\otimes P)GC_w\pi_1^*$ in (6.27) yields the same bound as in (6.30). Lastly ${\pi_2^*}^{\mathrm{T}}C_w^{\mathrm{T}}G^{\mathrm{T}}(\Sigma\otimes P)GC_w\pi_2^*$ is evaluated as follows

$$ {\pi_2^*}^{\mathrm{T}}C_w^{\mathrm{T}}G^{\mathrm{T}}(\Sigma\otimes P)GC_w\pi_2^* \le \tau\zeta_{\max}\lambda_{\max}(P)\sigma_G^2\ e^{\omega\gamma^*\tau}\left[\tau\|\tilde{\eta}\|^2 - \dot{V}_1\right]. \tag{6.31} $$

Define a new Lyapunov function V_ϕ as

$$ V_\phi = V + \mu^2\tau e^{\omega\gamma^*\tau}\zeta_{\max}\lambda_{\max}(P)(\sigma_{\mathcal{L}}+\sigma_G)^2 V_1 $$

for the system (6.17), which is positive definite since $V > 0$. The substitution of the results of (6.29)-(6.31) into (6.27) yields

$$ \dot{V}_\phi \le -\alpha e^{-\omega\gamma^*\tau}\|\tilde{\eta}\|^2 + 4\mu^2 V + \mu^2\tau^2 e^{\omega\gamma^*\tau}\zeta_{\max}\lambda_{\max}(P)\left(\sigma_{\mathcal{L}}+\sigma_G\right)^2\|\tilde{\eta}\|^2, \tag{6.32} $$

where $V \le \zeta_{\max}\lambda_{\max}(P)\|e^{-\tau S}\|^2\|\tilde{\eta}\|^2$. As a result, we obtain from (6.32)

$$ \begin{aligned} \dot{V}_\phi \le \Big(&-\alpha e^{-\omega\gamma^*\tau} + 4\lambda_{\max}(P)\mu^2\zeta_{\max}\|e^{-\tau S}\|^2 \\ &+\lambda_{\max}(P)\mu^2\tau^2\zeta_{\max}e^{\omega\gamma^*\tau}(\sigma_{\mathcal{L}}+\sigma_G)^2\Big)\|\tilde{\eta}\|^2 < 0, \end{aligned} \tag{6.33} $$

for all μ bounded by

$$ \bar{\mu} = \sqrt{\frac{\alpha}{\lambda_{\max}(P)\ \zeta_{\max}\left(4\varepsilon_d + \tau^2\left(\sigma_{\mathcal{L}}+\sigma_G\right)^2 e^{2\omega\gamma^*\tau}\right)}}. $$

Finally, from Theorem 6.1.3 and V_ϕ we obtain that (6.4) is stable and $\lim_{t\to\infty}\tilde{\eta}(t)=0$. This concludes the proof. □

Remark 6.2.1. *Assumption 2.3.4 guarantees the existence of a matrix* $\mathbf{G}$ *so that* $\mathcal{R}$ *in Lemma 6.2.1 is Hurwitz. While the conditions of Lemma 6.2.1 allows for any such* $\mathbf{G}$ *that makes* $\mathcal{R}$ *Hurwitz, the selection of the equivalent observer gain in [46] is limited to the solution of a parametric Riccati equation. Furthermore, any observer gain* $\mathbf{G}$ *obtained from the solution to the parametric Riccati equation in [46] will result in a Hurwitz matrix* $\mathcal{R}$*, but the opposite may not necessarily hold.*

Remark 6.2.2. *Let us consider the case where the state matrix* S *in* (2.3.1) *has all semi-simple eigenvalues on the imaginary axis. Then* S *be transformed into a block-diagonal real Jordan form, with each block having a structure* $\begin{bmatrix} 0 & l \\ -l & 0 \end{bmatrix}$ *corresponding to the eigenvalue pair* $0\pm jl$*. Such* S *matrix can be found to be a normal matrix and thus unitarily diagonalizable,* i.e., $S=UD_SU^{-1}$, $S^H=UD_S^HU^{-1}$*, where* U *is a unitary matrix. This also implies that* $S^T+S=S^H+S=U(D_S+D_S^H)U^{-1}=0$*, and as a result* $e^{S+S^T}=I_q$*. Thus,* $e^{S^Tt}e^{St}$ *in the computation for* (6.27) *can be replaced by* I_q *instead of the bound in* (6.7)*, and the low gain bound in* (6.23) *reduces to*

$$\bar{\mu}=\sqrt{\frac{\alpha}{\lambda_{\max}(P)\ \zeta_{\max}(4+\tau^2\ (\sigma_{\mathcal{L}}+\sigma_G)^2)}}.$$

6.2.2 Case 2: $\tau_1\neq\tau_2$

We now consider the case when the measurement delays and inter-agent communication delays are not the same, *i.e.*, $\tau_1\neq\tau_2$. The composite estimation error dynamics is then obtained as

$$\dot{\tilde{\eta}}=(I_N\otimes S)\tilde{\eta}-\mu\left(e^{(I_N\otimes\tau_2 S)}GC_w\right)\tilde{\eta}(t-\tau_2)-\mu\left(\mathcal{L}\otimes e^{\tau_1 S}\right)\tilde{\eta}(t-\tau_1),t>0, \tag{6.34}$$

with the initial conditions $\tilde{\eta}(\theta) = \tilde{\boldsymbol{\eta}}(\theta)$, $\tilde{\boldsymbol{\eta}} \in \mathcal{C}([-\bar{\tau},0],\mathbb{R}^{Nq}), \forall\theta \in [-\bar{\tau},0]$. Since we obtained that $\tilde{\eta}(t)$ is bounded for $t \in [0,\bar{\tau}]$, we now need to show the stability of the closed-loop system (6.34) for $t \geq \bar{\tau}$. In this regard, from (6.34) we evaluate $\tilde{\eta}(t-\tau_1)$ and $\tilde{\eta}(t-\tau_2)$ as

$$\tilde{\eta}(t-\tau_1) = e^{-(I_N \otimes S\tau_1)}\tilde{\eta}(t) + \mu(\boldsymbol{\pi}_1^* + \boldsymbol{\pi}_2^*), \tag{6.35}$$

$$\tilde{\eta}(t-\tau_2) = e^{-(I_N \otimes S\tau_2)}\tilde{\eta}(t) + \mu(\boldsymbol{\pi}_3^* + \boldsymbol{\pi}_4^*), \tag{6.36}$$

where

$$\begin{aligned}
\boldsymbol{\pi}_1^* &= \int_{t-\tau_1}^{t} e^{(I_N \otimes S)(t-s)}(\mathcal{L} \otimes I_q)\tilde{\eta}(s-\tau_1)\, ds,\\
\boldsymbol{\pi}_2^* &= \int_{t-\tau_1}^{t} e^{(I_N \otimes S)(t-s)} \left(I_N \otimes e^{(\tau_2-\tau_1)S}\right) GC_w\tilde{\eta}(s-\tau_2)\, ds,\\
\boldsymbol{\pi}_3^* &= \int_{t-\tau_2}^{t} e^{(I_N \otimes S)(t-s)}(\mathcal{L} \otimes e^{(\tau_1-\tau_2)S})\tilde{\eta}(s-\tau_1)\, ds,\\
\boldsymbol{\pi}_4^* &= \int_{t-\tau_2}^{t} e^{(I_N \otimes S)(t-s)} GC_w\tilde{\eta}(s-\tau_2)\, ds.
\end{aligned}$$

By substituting (6.35) and (6.36) in (6.34), we obtain

$$\dot{\tilde{\eta}} = \left(I_N \otimes e^{\tau_2 S}\right) M \left(I_N \otimes e^{-\tau_2 S}\right)\tilde{\eta}(t) - \mu^2\left(\boldsymbol{\pi}_1 + \boldsymbol{\pi}_2 + \boldsymbol{\pi}_3 + \boldsymbol{\pi}_4\right), \tag{6.37}$$

where $\boldsymbol{\pi}_i = \left(\mathcal{L} \otimes e^{\tau_1 S}\right)\boldsymbol{\pi}_i^*$, $i = 1,2$, $\boldsymbol{\pi}_j = \left(I_N \otimes e^{\tau_2 S}\right) GC_w \boldsymbol{\pi}_j^*$, $j = 3,4$.

To analyze the stability of (6.37), we consider a Lyapunov function of the form

$$\mathbf{V}(\tilde{\eta}) = \tilde{\eta}^{\mathrm{T}}(\Sigma \otimes e^{-\tau_2 S^{\mathrm{T}}} P e^{-\tau_2 S})\tilde{\eta},$$

where P is a positive definite matrix as in Lemma 6.2.1. Denote $\tilde{\eta}_{\mathbf{d}} = (I_N \otimes e^{-\tau_2 S})\tilde{\eta}(t)$ and thus by differentiating $\mathbf{V}$ along the trajectory of (6.37) we obtain

$$\begin{aligned}
\dot{\mathbf{V}}(\tilde{\eta}) = {}& \tilde{\eta}_{\mathbf{d}}^{\mathrm{T}}\left[M^{\mathrm{T}}(\Sigma \otimes P) + (\Sigma \otimes P)M\right]\tilde{\eta}_{\mathbf{d}} - 2\mu^2(\boldsymbol{\pi}_1^{\mathrm{T}} + \boldsymbol{\pi}_2^{\mathrm{T}})(\Sigma \otimes e^{-\tau_2 S^{\mathrm{T}}} P e^{-\tau_2 S})\tilde{\eta}\\
& - 2\mu^2\left(\boldsymbol{\pi}_3^{\mathrm{T}} + \boldsymbol{\pi}_4^{\mathrm{T}}\right)(\Sigma \otimes e^{-\tau_2 S^{\mathrm{T}}} P e^{-\tau_2 S})\tilde{\eta},
\end{aligned}$$

$$\leq -\alpha e^{-\omega\gamma^{*}\tau_2}\|\tilde{\eta}\|^2 + 4\mu^2\mathbf{V}(\tilde{\eta}) + \mu^2\sum_{i=1}^{2}\boldsymbol{\pi}_i^{*\mathrm{T}}\left(\mathcal{L}^{\mathrm{T}}\Sigma\mathcal{L}\otimes e^{(\tau_1-\tau_2)S^{\mathrm{T}}}Pe^{(\tau_1-\tau_2)S}\right)\boldsymbol{\pi}_i^{*}$$
$$+\mu^2\sum_{i=3}^{4}\boldsymbol{\pi}_i^{*\mathrm{T}}C_w^{\mathrm{T}}G^{\mathrm{T}}(\Sigma\otimes P)GC_w\boldsymbol{\pi}_i^{*}. \tag{6.38}$$

In a similar manner to the proof of Lemma 6.2.1, we evaluate each term on the right-hand side of the inequality (6.38) separately. From the second term in (6.38), we obtain

$$\mu^2\boldsymbol{\pi}_1^{*\mathrm{T}}\left(\mathcal{L}^{\mathrm{T}}\Sigma\mathcal{L}\otimes e^{(\tau_1-\tau_2)S^{\mathrm{T}}}Pe^{(\tau_1-\tau_2)S}\right)\boldsymbol{\pi}_1^{*}$$
$$\leq \lambda_{\max}(P)\mu^2\tau_1\zeta_{\max}\sigma_{\mathcal{L}}^2 e^{\omega\gamma^{*}(2*\tau_1-\tau_2)}\left[\tau_1\|\tilde{\eta}\|^2-\dot{\mathbf{V}}_1\right], \tag{6.39}$$

where $\mathbf{V}_1 = \int_{\tau_1}^{2\tau_1}\int_{t-s}^{t}\tilde{\eta}^{\mathrm{T}}(\boldsymbol{\sigma})\tilde{\eta}(\boldsymbol{\sigma})d\boldsymbol{\sigma}\ ds$. Similarly, by evaluating the third term in (6.38), we obtain

$$\mu^2\boldsymbol{\pi}_2^{*\mathrm{T}}\left(\mathcal{L}^{\mathrm{T}}\Sigma\mathcal{L}\otimes e^{(\tau_1-\tau_2)S^{\mathrm{T}}}Pe^{(\tau_1-\tau_2)S}\right)\boldsymbol{\pi}_2^{*}$$
$$\leq \lambda_{\max}(P)\mu^2\tau_1\zeta_{\max}\sigma_{\mathcal{L}}\sigma_G e^{\omega\gamma^{*}\tau_1}\left[\tau_1\|\tilde{\eta}\|^2-\dot{\mathbf{V}}_2\right], \tag{6.40}$$

where $\mathbf{V}_2 = \int_{\tau_2}^{\tau_1+\tau_2}\int_{t-s}^{t}\tilde{\eta}^{\mathrm{T}}(\boldsymbol{\sigma})\tilde{\eta}(\boldsymbol{\sigma})d\boldsymbol{\sigma}\ ds$. Next from $\mu^2\boldsymbol{\pi}_3^{*\mathrm{T}}C_w^{\mathrm{T}}G^{\mathrm{T}}(\Sigma\otimes P)GC_w\boldsymbol{\pi}_3^{*}$ in (6.38) we obtain,

$$\mu^2\boldsymbol{\pi}_3^{*\mathrm{T}}C_w^{\mathrm{T}}G^{\mathrm{T}}(\Sigma\otimes P)GC_w\boldsymbol{\pi}_3^{*}$$
$$\leq \lambda_{\max}(P)\mu^2\tau_2\zeta_{\max}e^{\omega\gamma^{*}\tau_1}\sigma_G\sigma_{\mathcal{L}}\left[\tau_2\|\tilde{\eta}\|^2-\dot{\mathbf{V}}_3\right], \tag{6.41}$$

where $\mathbf{V}_3 = \int_{\tau_1}^{\tau_1+\tau_2}\int_{t-s}^{t}\tilde{\eta}^{\mathrm{T}}(\boldsymbol{\sigma})\tilde{\eta}(\boldsymbol{\sigma})d\boldsymbol{\sigma}\ ds$. Lastly $\mu^2\boldsymbol{\pi}_4^{*\mathrm{T}}C_w^{\mathrm{T}}G^{\mathrm{T}}(\Sigma\otimes P)GC_w\boldsymbol{\pi}_4^{*}$ in (6.38) is evaluated to yield the following upper bound

$$\mu^2\boldsymbol{\pi}_4^{*\mathrm{T}}C_w^{\mathrm{T}}G^{\mathrm{T}}(\Sigma\otimes P)GC_w\boldsymbol{\pi}_4^{*}$$
$$\leq \lambda_{\max}(P)\mu^2\tau_2\zeta_{max}\sigma_G^2 e^{\omega\gamma^{*}\tau_2}\left[\tau_2\|\tilde{\eta}\|^2-\dot{\mathbf{V}}_4\right], \tag{6.42}$$

with $\mathbf{V}_4 = \int_{\tau_2}^{2\tau_2} \int_{t-s}^{t} \tilde{\eta}^{\mathrm{T}}(\boldsymbol{\sigma})\tilde{\eta}(\boldsymbol{\sigma})d\boldsymbol{\sigma}\ ds$. Now we introduce the following lemma to prove the asymptotic convergence of $\tilde{\eta}(t)$ in (6.34).

Lemma 6.2.2. *Consider the distributed observers* (6.34) *satisfying Assumptions 2.3.1-6.1.1, and G_i and P selected from the conditions in Lemma 6.2.1 for any $\mu \in (0,1)$. Then for the non-identical communication and measurement delays $\tau_1 \neq \tau_2$, the observer states $\eta_i(t)$ converges to $w(t)$ asymptotically,* i.e.,

$$\lim_{t\to\infty} (\eta_i(t) - w(t)) = 0, \ i = 1, 2, \cdots, N,$$

if the low gain parameter μ satisfies $\mu < \bar{\boldsymbol{\mu}}$, with

$$\bar{\boldsymbol{\mu}} = \sqrt{\frac{\alpha}{\lambda_{\max}(P)\zeta_{\max}(4\varepsilon_{\mathbf{d}} + c_1c_2)}}, \varepsilon_{\mathbf{d}} = e^{\omega\gamma^*\tau_2}\|e^{-\tau_2 S}\|^2, \tag{6.43}$$

where $c_1 = \sigma_G e^{\omega\gamma^*\tau_2} + \sigma_{\mathcal{L}} e^{\omega\gamma^*\tau_1}$, and
$c_2 = \tau_1^2\sigma_{\mathcal{L}} e^{\omega\gamma^*\tau_1} + \tau_2^2\sigma_G e^{\omega\gamma^*\tau_2}$.

Proof. We define a new Lyapunov function $\mathbf{V}_\phi$ as

$$\begin{aligned} \mathbf{V}_\phi = \mathbf{V} + \lambda_{\max}(P)\mu^2\zeta_{\max}\Big(&\tau_1\sigma_{\mathcal{L}}^2 e^{\omega\gamma^*(2\tau_1-\tau_2)}\mathbf{V}_1 \\ &+ \sigma_{\mathcal{L}}\sigma_G e^{\omega\gamma^*\tau_1}(\tau_1\mathbf{V}_2 + \tau_2\mathbf{V}_3) + \tau_2\sigma_G^2 e^{\omega\gamma^*\tau_2}\mathbf{V}_4\Big), \end{aligned} \tag{6.44}$$

where $\mathbf{V} \leq \lambda_{\max}(P)\ \zeta_{\max}\|e^{-\tau_2 S}\|^2\|\tilde{\eta}\|^2$. Since $\mathbf{V} > 0$, the Lyapunov function $\mathbf{V}_\phi$ is also positive. Then by substituting the results from (6.39), (6.40), (6.41) and (6.42) into (6.38), we obtain

$$\begin{aligned} \dot{\mathbf{V}}_\phi \leq \Big[&-\alpha e^{-\omega\gamma^*\tau_2} + 4\lambda_{\max}(P)\mu^2\zeta_{\max}\|e^{-\tau_2 S}\|^2 \\ &+ \lambda_{\max}(P)\mu^2\zeta_{\max}\Big(\tau_1^2\sigma_{\mathcal{L}}^2 e^{2\omega\gamma^*(2\tau_1-\tau_2)} + \tau_2^2\sigma_G^2 e^{\omega\gamma^*\tau_2} \\ &+ (\tau_1^2 + \tau_2^2)\sigma_{\mathcal{L}}\sigma_G e^{\omega\gamma^*\tau_1}\Big)\Big]\|\tilde{\eta}\|^2 < 0, \end{aligned} \tag{6.45}$$

for $\mu < \bar{\boldsymbol{\mu}}$ with $\bar{\boldsymbol{\mu}}$ in (6.43). Therefore, by Theorem 6.1.3 and $\mathbf{V}_\phi$, $\lim_{t\to\infty}\tilde{\eta}_i(t) = 0$, $i = 1,2,\cdots,N$. This concludes the proof. $\square$

In case when $\tau_1 = \tau_2 = \tau$, then $c_1 = e^{\omega\gamma^*\tau}(\sigma_G + \sigma_{\mathcal{L}})$ and $\bar{\boldsymbol{\mu}}$ reduces to $\bar{\mu}$ in (6.23). On the other hand, if S has all semi-simple eigenvalues on the imaginary axis, then by using Remark 6.2.2 and Lemma 6.2.2 we obtain the bound on the low gain parameter μ as

$$\bar{\boldsymbol{\mu}} = \sqrt{\frac{\alpha}{\lambda_{\max}\zeta_{\max}\left(4 + (\sigma_{\mathcal{L}} + \sigma_G)(\tau_1^2\sigma_{\mathcal{L}} + \tau_2^2\sigma_G)\right)}}. \tag{6.46}$$

6.3 Distributed State Estimation Problem under Noisy Plant Measurements

In the previous discussions, we considered the distributed state estimation problem for an accurately known plant model by a network of observers. However, in reality, the plant model may incorporate some uncertainties in the dynamics and so is the information received by the observers. In such cases, the local estimation errors between adjacent agents may not converge to zero. Based on the vector dissipativity property of uncertain systems, in [78, 79] authors designed a group of H_∞ robust filters by solving some LMI conditions. For a stochastic uncertain plant model with the plant measurements by the distributed sensors being subject to bounded external disturbances, an event-triggered robust distributed state estimators was addressed in [80]. However, the results in [78–80] do not account for the communication delay in the network.

In this section, we assume that the plant measurements received by the observers are subject to bounded external disturbances, and the incoming measurement signal y_{m_i} to each observer agent $i \in 1,2\cdots,N$ in (6.2) is rewritten as

$$y_{m_i} = C_{w_i} w(t - \tau_2) + \xi_i(t), \tag{6.47}$$

where $\xi_i(t)$ is any measurable, essentially bounded function over $[0,\infty)$. For non-identical communication and measurement delays, the distributed estimation error dynamics under the redefined plant measurements (6.47) becomes

$$\begin{aligned}\dot{\tilde{\eta}} = (I_N \otimes S)\tilde{\eta} - \mu\left(I_N \otimes e^{\tau_2 S} G C_w\right)\tilde{\eta}(t-\tau_2)\\ -\mu\left(\mathcal{L}\otimes e^{\tau_1 S}\right)\tilde{\eta}(t-\tau_1) + \mu\left(I_N \otimes e^{\tau_2 S}\right) G C_w \xi,\end{aligned} \tag{6.48}$$

where $\xi = \mathrm{col}(\xi_1, \xi_2, \cdots, \xi_N)$. By defining $M_0 = (I_N \otimes S), M_1 = -\mu\left(I_N \otimes e^{\tau_2 S} G C_w\right)$, $M_2 = -\mu\left(\mathcal{L}\otimes e^{\tau_1 S}\right)\tilde{\eta}(t-\tau_1)$ we can rewrite (6.48) in the form as

$$\dot{\tilde{\eta}} = M_0\tilde{\eta} + \sum_{i=1}^{2} M_i \tilde{\eta}(t-\tau_i) - M_1\xi, \tag{6.49}$$

with initial conditions $\tilde{\eta}(\theta) = \tilde{\boldsymbol{\eta}}(\theta),\ \forall\theta \in [-\bar{\tau}, 0]$. Since the unforced estimation error dynamics ($\xi = 0$) was shown to be asymptotically stable by a suitable selection of observer gains G_i and low gain parameter μ following the conditions in Lemma 6.2.2, Proposition 2.5 from [81] then determines that the error dynamics (6.49) is also input-to-state stable (ISS). In other words, there exists a KL function β_0 and K function β_1 such that

$$\|\tilde{\eta}(t)\| \leq \beta_0(\|\tilde{\eta}\|_\infty, t) + \beta_1(\|\xi\|_\infty), \tag{6.50}$$

where $\|\xi\|_\infty = \sup_{t\geq 0}\|\xi(t)\|$.

For the input-to-state stable error dynamics and the bound in (6.50), using the results in [24] yields that

$$\sup_{t\in[0,\infty)}\|\tilde{\eta}(t)\| \leq \beta_1\left(\sup_{t\in[0,\infty)}\|\xi(t)\|\right).$$

Furthermore, from the results of [24,81], the solution to (6.49) for $t > \bar{\tau}$ can be bounded as follows

$$\begin{aligned} \|\tilde{\eta}(t)\| &\leq \alpha_1 e^{-\sigma_1(t-\bar{\tau})}\sqrt{(1+\bar{\tau})}\|\tilde{\boldsymbol{\eta}}\|_\infty + \int_{\bar{\tau}}^{t} \alpha_1 e^{-\sigma_1(t-s)}\|M_1\|\|\xi(s)\|\ ds, \\ &\leq \alpha_1 \int_{\bar{\tau}}^{t} e^{-\sigma_1(t-s)}\|M_1\|\|\xi(s)\|\ ds, \end{aligned} \tag{6.51}$$

where α_1 and σ_1 are real positive scalars. The bound in (6.51) represents the β_0 and β_1 functions introduced in (6.50). Finally, for the special case of a decaying disturbance $\lim_{t\to\infty}\xi(t) = 0$, from [24] we find that $\lim_{t\to\infty}\tilde{\eta}(t) = 0$.

6.4 Application to a Leader-Follower Synchronization Problem

In this section, we present a leader-follower synchronization problem under network latency, and a detectability constraint that none of the followers can independently reconstruct the leader dynamics from its measurements. Due to the presence of time delays in the measurement and communication between followers, the results from [2,3,71] are not applicable. Thus, with the proposed results from the distributed state estimation problem studied in this work, we proceed to tackle the leader-follower synchronization problem in face of measurement and network latency.

To study this problem, let us first consider N heterogeneous follower agents with the dynamics

$$\dot{x}_i = A_i x_i + B_i u_i, \tag{6.52}$$

where $x_i \in \mathbb{R}^{n_i}, u_i \in \mathbb{R}^{m_i}$ are respectively the state vector and control input for the agent i. The distributed control problem then consists for all agents to synchronize their states to a leader, given as (6.1), by regulating the error signal $e_i \in \mathbb{R}^{\mathbf{p}_i}$,

$$e_i = C_i x_i - F_i w,\ i = 1, 2, \cdots, N. \tag{6.53}$$

It is assumed that e_i is not available as a measurement for control, but follower agents collect delayed leader measurements $y_{m_i} \in \mathbb{R}^{p_i}$

$$y_{m_i} = C_{w_i} w(t - \tau_2). \tag{6.54}$$

It is also assumed that the follower agents are connected under a communication network described by the digraph $\mathcal{G}$, and inter-agent communications are subject to the communication delay τ_1. The objective of this synchronization problem is to design a distributed control law $u_i(t)$ such that the regulated error signals $e_i(t)$ asymptotically converge to zero.

As noted in [23, 29, 30], the solvability of the synchronization problem requires Assumption 2.3.2 and an additional assumption stated as follows.

Assumption 6.4.1. *There exists a unique solution pair* (X_i, U_i) *to the linear regulator equations, given below.*

$$\begin{aligned} X_i S &= A_i X_i + B_i U_i, \\ 0 &= C_i X_i - F_i. \end{aligned} \tag{6.55}$$

Given that the Assumptions 2.3.1-6.4.1 hold, the distributed state feedback control law u_i takes the form [2]

$$u_i = K_{1_i} x_i + K_{2_i} \eta_i, \tag{6.56}$$

where $\eta_i(t)$ is the distributed observer state with the dynamics given in (6.3). The controller gains K_{1_i}, K_{2_i} are selected such a way that $(A_i + B_i K_{1_i})$ is Hurwitz and $K_{2_i} = U_i - K_{1_i} X_i$. Since $\lim_{t\to\infty} \eta_i(t) = w(t)$ by Lemma 6.2.2, the control solution to the aforementioned synchronization problem can be summarized in the following theorem.

Theorem 6.4.1. *Given the leader* (6.1)*, N followers* (6.52)*, and the digraph $\mathcal{G}$, the distributed control law u_i in* (6.56) *solves the leader-follower synchronization problem if the sufficient conditions of Lemma 6.2.2 are satisfied.*

The proof of Theorem 6.4.1 follows similar procedure as in [2], with the results of Lemma 6.2.2 to guarantee the stability of the leader state estimation error dynamics. Under the constraint that (S, C_{w_i}) is not detectable for any $i = 1, 2, \cdots, N$, the control solution (6.56), based on the proposed observation protocol (6.3) is unique in a sense that it can solve the output regulation problem for multi-agent system while the comparable results in [24, 25, 29, 30, 49, 82] do not, even with the Assumptions 2.3.1, 2.3.2, 6.4.1, 2.3.4, and 6.1.1 being put in place.

6.5 Illustrative Example

In this section we consider an illustrative example to evaluate the effectiveness of our proposed algorithm. Let the plant (6.1) have state vector $w = \begin{bmatrix} w_1 & w_2 & w_3 & w_4 \end{bmatrix}^{\mathrm{T}}$ and state matrix

$$S = \text{blk diag}(S_1, S_2), S_1 = \begin{bmatrix} 0 & -1 \\ 1 & 0 \end{bmatrix}, S_2 = \begin{bmatrix} 0 & -2 \\ 2 & 0 \end{bmatrix}. \tag{6.57}$$

The measured output matrices $C_{w_i},\ i = 1, 2, 3$, are given as follows:

$$C_{w_1} = \begin{bmatrix} I_2 & 0_2 \end{bmatrix},\ C_{w_2} = \begin{bmatrix} 0_2 & I_2 \end{bmatrix},\ C_{w_3} = 0_{2\times 4},$$

from which we verify that none of the pairs $(S, C_{w_i}),\ i = 1, 2, 3$, are detectable. Instead, the combined detectability property in Assumption 2.3.4 is satisfied for the given C_{w_i}.

Clearly, the follower agent 1 can directly receive the signal $\begin{bmatrix} w_1 & w_2 \end{bmatrix}^{\mathrm{T}}$ from the plant measurement $y_{m_1}(t)$, while agent 2 receives the signal $\begin{bmatrix} w_3 & w_4 \end{bmatrix}^{\mathrm{T}}$.

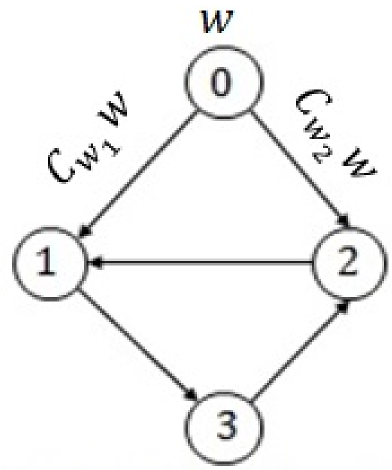

Figure 6.1: Communication network $\mathcal{G}$ for the observer agents $1, 2, 3$

The communication network between the observers is represented by the digraph $\mathcal{G}$ satisfying Assumption 6.1.1, as illustrated in Figure 6.1, with the Laplacian matrix $\mathcal{L}$ given as follows

$$\mathcal{L} = \begin{bmatrix} 1 & -1 & 0 \\ 0 & 1 & -1 \\ -1 & 0 & 1 \end{bmatrix}.$$

The strongly connected partition of $\mathcal{G}$ in Figure 6.1 allows the exchange of estimated states between agents, and complements for the incomplete measurements that each agent receives from the plant. Even though a single observer cannot independently reconstruct the exosystem state vector $w(t)$, the strongly connected communication network between the observer agents enables them to jointly synthesize an estimate of the plant state.

We first consider the case when measurement delays and inter-agent communication delays are the same, and let $\tau = 1.2$. Given the Laplacian matrix $\mathcal{L}$, we find $\zeta_i = 1/3 =$

$\zeta_{\max}$, $i = 1,2,3$. Next, we select the observer gains as

$$G_1 = \begin{bmatrix} I_2 & 0_2 \end{bmatrix}^{\mathrm{T}}, G_2 = \begin{bmatrix} 0_2 & I_2 \end{bmatrix}^{\mathrm{T}}, G_3 = 0_{4\times 2} \tag{6.58}$$

such that the matrix

$$\mathcal{R} = \text{blk diag}\left(\begin{bmatrix} -\mu/3 & -1 \\ 1 & -\mu/3 \end{bmatrix}, \begin{bmatrix} -\mu/3 & -2 \\ 2 & -\mu/3 \end{bmatrix}\right)$$

in (6.22) is Hurwitz with the eigenvalues located at $-\mu/3 \pm j, -\mu/3 \pm 2j$. We note here that $\mathcal{R}^{\mathrm{T}} + \mathcal{R} = -\frac{2\mu}{3} I$ and $\mathcal{R}\mathcal{R}^{\mathrm{T}} = \mathcal{R}^{\mathrm{T}}\mathcal{R}$. Next, from the Lyapunov equation $\mathcal{R}^{\mathrm{T}} P + P\mathcal{R} = -\mu I$, we find the solution P as

$$P = \int_0^\infty e^{\mathcal{R}^{\mathrm{T}} s} e^{\mathcal{R}s}\, ds = \int_0^\infty e^{\mathcal{R}^{\mathrm{T}} + \mathcal{R}s}\, ds = 1.5I.$$

We also verify that the matrices $(S - \mu G_i C_{w_i})^{\mathrm{T}} P + P(S - \mu G_i C_{w_i}), i = 1,2$ has eigenvalues at $-3,-3,0,0$ and $(S - \mu G_3 C_{w_3})^{\mathrm{T}} P + P(S - \mu G_3 C_{w_3}) = 0$. Thus P satisfies the LMI conditions in Lemma 6.2.1. Next, by substituting P in (6.26), we find that $M^{\mathrm{T}}(\Sigma \otimes P) + (\Sigma \otimes P)M < -0.2\mu$. Then by using (6.33) directly, we find a tighter bound on μ in comparison to (6.23) as follows

$$\bar{\mu} = \frac{0.2}{\zeta_{\max}\lambda_{\max}(P)(4+\tau^2(\sigma_{\mathcal{L}}+\sigma_G))^2} = \frac{0.1}{1+4\tau^2} = 0.0147.$$

The simulated response of the distributed observers with $\mu = 0.014$ and G_i as given in (6.58) are presented in Figure 6.2 through the sum of the observation errors $\delta_i(t) = \sum_{q=1}^{4} \|\tilde{\eta}_{iq}(t)\|$, where $\tilde{\eta}_i = \begin{bmatrix} \tilde{\eta}_{i1} & \tilde{\eta}_{i2} & \tilde{\eta}_{i3} & \tilde{\eta}_{i4} \end{bmatrix}^{\mathrm{T}}$ and $i = 1,2,3$. The simulated response shows that $\delta_i(t)$ and $\tilde{\eta}_i$ converges asymptotically to zero, and thus the objectives of the distributed observation problem are achieved.

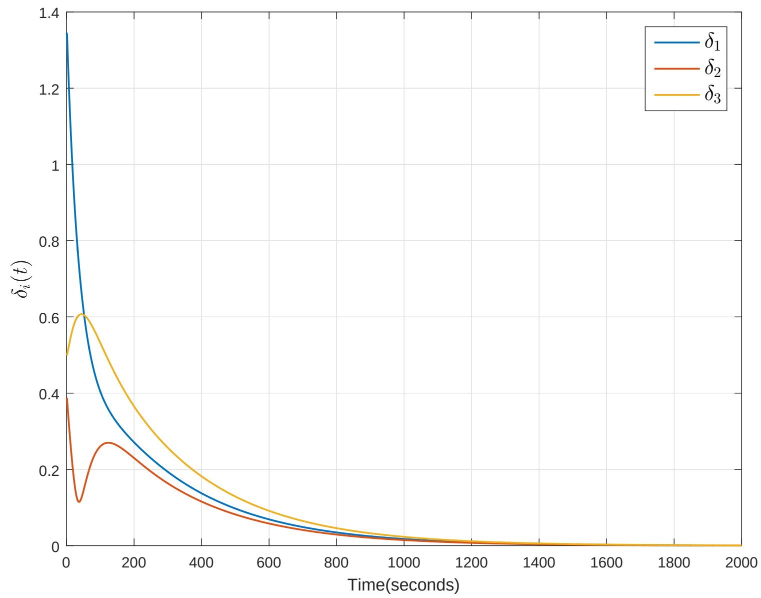

Figure 6.2: Observation error of three observers for the case when $\tau_1 = \tau_2 = 1.2$

Let us now consider a second case, where $\tau_1 = 0.8$ and $\tau_2 = 1.2$. Since the observer gains G_i do not account for the delay, we proceed with the same G_i's as in (6.58). Therefore with the same $P, \alpha, \zeta_{\max}, \sigma_{\mathcal{L}}, \sigma_G$ as in the previous case, we obtain the upper bound $\bar{\boldsymbol{\mu}}$ from satisfying the inequality in (6.45) as

$$\bar{\boldsymbol{\mu}} = \frac{0.1}{1 + 1.5\tau_1^2 + \tau_2^2} = 0.029. \tag{6.59}$$

We select $\mu = 0.022 < \bar{\boldsymbol{\mu}}$. With these designed parameters, the simulation results are obtained as in Figure 6.3, which shows that $\delta_i(t)$ converges to zero. From the observation errors in Figs. 6.2 and 6.3, it is evident that the plant states w_1 and w_2 are accurately estimated by the observer agent 2. Although these plant states are undetectable from the measurement $y_{m_2}(t)$, the strongly connected communication network and the collaboration between the observer agents enable the follower agent 2 to successfully estimate the plant states.

With the designed observers and scalar feedback gain for the distributed state estimation problem, let us now apply our results to a leader-follower synchronization

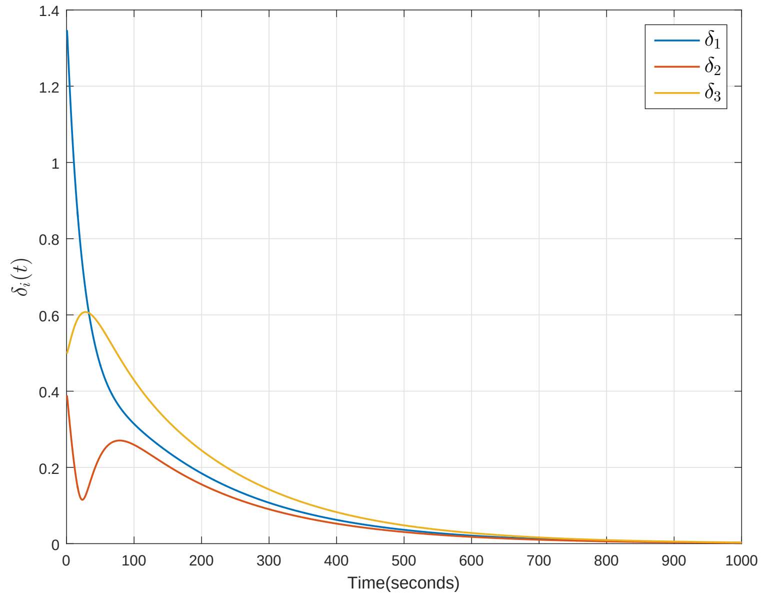

Figure 6.3: Observation error of three observers for $\tau_1 = 0.8$ and $\tau_2 = 1.2$

problem under measurement delay $\tau_1 = 0.8$ and $\tau_2 = 1.2$. The leader system matrix S is given in (6.57) and the dynamics of the follower agent i are described by a double integrator as given below

$$\dot{x}_{1_i} = x_{2_i},\ \dot{x}_{2_i} = u_i,\ e_i = x_{1_i} - (w_1 + w_3). \tag{6.60}$$

From (6.60), the subsystem matrices are found to be

$$A_i = \begin{bmatrix} 0 & 1 \\ 0 & 0 \end{bmatrix}, B_i = \begin{bmatrix} 0 \\ 1 \end{bmatrix}, C_i = [1 \;\; 0], F_i = [1 \;\; 0 \;\; 1 \;\; 0].$$

It is easy to verify that the Assumptions 2.3.1-6.4.1 hold. The controller gains in (6.56) are obtained as $K_{1_i} = \begin{bmatrix} -8 & -4 \end{bmatrix}$, $K_{2_i} = \begin{bmatrix} 7 & -4 & 4 & -8 \end{bmatrix}$ while the observer gains G_i are given in (6.58) and $\mu = 0.022$. By applying the distributed control law (6.56) to the subsystem dynamics (6.60), we observe in Fig. 6.4 that all the followers are synchronized with the desired leader trajectory $w_1 + w_3$. Thus, the leader-follower synchronization problem in the presence of measurement and communication delay is solved by a dynamic control method that relies on our proposed distributed state estimation algorithm.

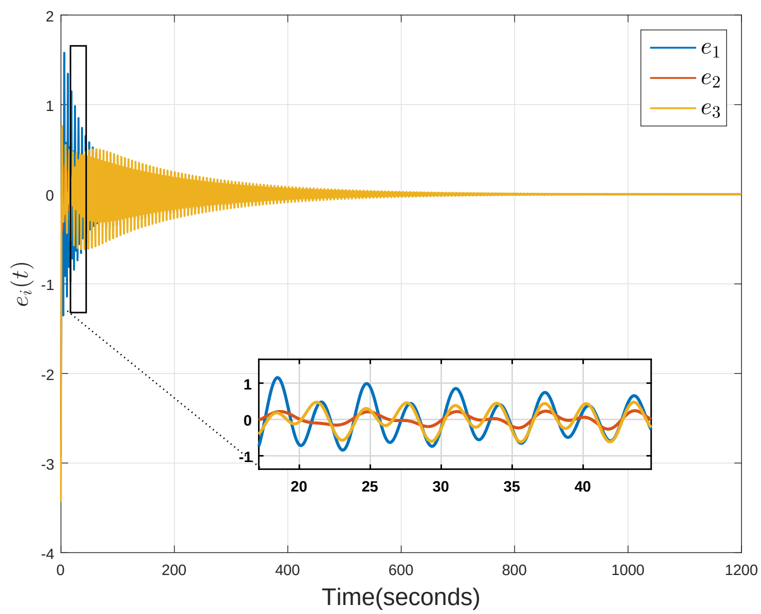

Figure 6.4: Tracking error of the followers under the distributed dynamic control law (6.3), (6.56)

To highlight the importance of considering the delay in the synchronization problem, we now apply the control law u_i in (6.56) with the observer dynamics given in [2,3,71] to the subsystems (6.60). The corresponding simulation results are observed in Fig. 6.5, from which it is evident that none of the followers are synchronized with the leader by the resulting control solution.

Next, we consider that the measurements from the plant received by the i^{th} observer are subject to a time-varying perturbation $\xi_i(t) = 0.3|\sin(t)|^2,\ i = 1,2,3$ with an L_2 norm bound 0.3. Thus from the results in Section 6.3, we can easily verify that the local estimation error $\|\tilde{\eta}(t)\|$ under this perturbation will also remain bounded within $[0,3]$.

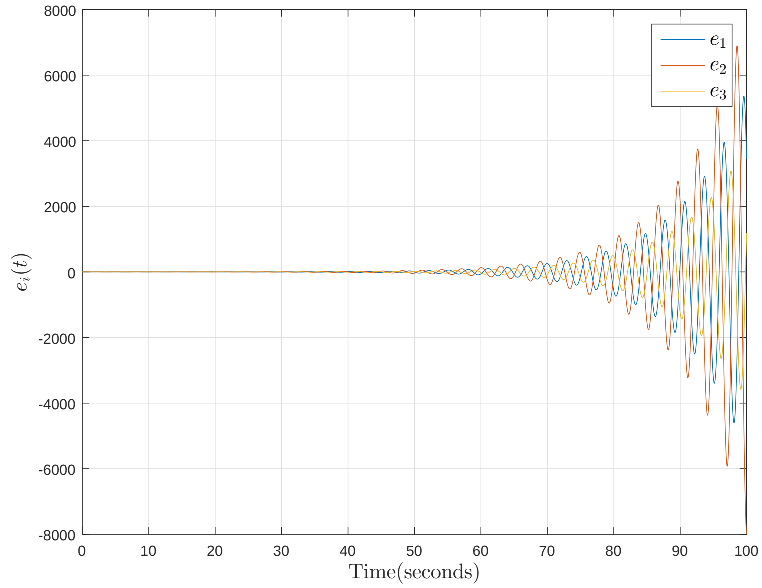

Figure 6.5: Tracking error of the followers under the distributed control law [2, 3]

6.6 Conclusion

In this work we studied the distributed state estimation problem for autonomous dynamic systems, and under arbitrarily large communication and measurement delays. The proposed observer framework relies on the strongly connected communication network between the observer agents and the combined detectability property of the system, to guarantee that the local state estimation of all agents converges to the states of the observed plant, including states that may not be detectable through local measurements. Our current work considered the presence of arbitrarily large time delays in the communication and measurements of the observer agents, and a distributed observer framework was developed for the estimation problem. Sufficient conditions for the stability of the corresponding observation error dynamics were derived, including an upper bound for the low gain parameter of the observer equations.

Furthermore, we investigated the distributed state estimation problem with heterogeneous time-delays and external disturbances in the measurements. As the nominal system was shown to be asymptotically stable, we noted that under bounded external perturbations, the distributed estimation error dynamics is ISS. Additionally, we derived a bound on the local estimation errors of the observer agents in terms of the supremum norm of the disturbance signals.

The results of the distributed state estimation problem was also applied to solve the leader-follower synchronization problem in the case when the measurements from the leader and the communication between the followers are subjected to arbitrarily large time delays. Illustrative simulation examples were offered to verify our mathematical analysis and the theoretical results in this work. By comparing our results to the existing approaches, we demonstrated the advantages of our estimation algorithm.

Chapter 7

Distributed State Estimation under Heterogeneous Time-Varying Communication Delays

In this chapter we study the distributed leader state estimation problem in leader-follower multi-agent systems over a deterministic network and under time-varying communication delays. In this work we propose a distributed estimation technique that allows the follower agents to collectively reconstruct the leader agent states by communicating their estimates with neighboring agents. Additionally, we assume that the communications between the leader and followers are subject to heterogeneous time-varying delays. By using the low gain methodology, sufficient stability conditions of the estimation error dynamics in the presence of network latency are derived, including an upper bound for the delay magnitude. Lastly, the proposed distributed state estimation method is applied to develop a solution to the leader tracking problem in leader-follower multi-agent systems. An illustrative example is also presented to verify the effectiveness of our theoretical results.

Multi-agent consensus problems with time-varying communication delays was studied by the authors of [83–86]. In [87], the consensus problem was studied for first order integrator systems with constant communication delays and bounded time-varying self delays. In [85], authors studied a nonlinear consensus problem for first order multi-agent systems under fixed and switching communication networks. With the Lyapunov-Razumikhin stability analysis, local stability results of the consensus problem was presented in [85]. In [86], a leader-follower consensus problem was studied for nonlinear agents in an undirected network with identical communication delays. For high order multi-agent systems, consensus problem with identical agents and large communication delays was studied in [88].

In this work, we study the distributed leader state estimation problem of a leader-follower multi-agent system over a deterministic network with non-identical time-varying communication latencies. Motivated by the results in [89], we offer a solution to the distributed state estimation problem with a truncated predictor feedback approach which allows us to design our delay-independent observer gains. By applying the Lyapunov-Krasovskii stability analysis, sufficient conditions for the stability of the observation error dynamics, including an upper bound for the delay, are derived. Next, the states estimation solution is applied to offer a distributed solution to the leader-follower synchronization control problem, in which we considered limited observability of the leader states. Finally, with the help of an illustrative example and a comparative analysis, we demonstrate the uniqueness of our derived results. Compared to the works in [46, 90], where distributed state estimation problem was studied for heterogeneous time-invariant communication delays, in this paper we extend our results in [91] to the time-varying counterpart. Differently from the works of [84–88], our current work presents a solution to the distributed state estimation problem for higher order heterogeneous multi-agent systems, connected on a directed communication network, and under time-varying network delays.

The remainder of the chapter is organized in the following way. The problem formulation and algebraic graph theoretic properties are briefly revisited in Section 7.1. Next we derive the stability condition for the distributed observer dynamics coupled with communication in Section 7.2. In Section 7.3, we present the result of the leader-follower synchronization problem and offer a distributed control solution. An illustrative example to verify the effectiveness of the proposed approach is presented in Section 7.4. Lastly, conclusions are reported in Section 7.5.

7.1 Problem Formulation

Consider a system of N heterogeneous agents with the dynamics

$$\dot{x}_i = A_i x_i + B_i u_i, \tag{7.1a}$$

$$y_i(t) = C_i w(t - \tau_{i0}(t)),\ i = 1, 2, \cdots, N, \tag{7.1b}$$

where $x_i \in \mathbb{R}^{n_i}, u_i \in \mathbb{R}^{m_i}, y_i \in \mathbb{R}^{p_i}$, and $\tau_{i0}(t) \geq 0$ are respectively the state, control input, output vectors and the measurement delay of agent i. The agents are connected over a deterministic network with latency $\tau_{i0}(t) \in [0, D]$, where D represents the range of delays. Deterministic networks enable agents to record the time delay introduced by the communication over the network [92]. The measurement signal y_i of agent i receives a part of the delayed leader state vector $w \in \mathbb{R}^q$ that evolves as follows

$$\dot{w}(t) = Sw(t), \tag{7.2}$$

In the context of a leader-follower synchronization problem, Eqs. (7.1a) and (7.2) constitute a multi-agent system of order $N+1$ with (7.2) as a leader and N agents in (7.1a) as followers.

The objective of the group of N distributed observers is to provide an asymptotic estimation of the plant state vector $w(t)$. When the pair (S, C_i) is detectable for some agent i, the distributed estimation problem becomes a well studied decentralized state observation problem under measurement delay. On the other hand, when the previous detectability condition is not satisfied, a cooperative effort is required by the observers over the communication network to jointly provide an estimation for $w(t)$. The estimation of the states $w(t)$ is more challenging when we include the latency in the communication between the distributed observers to the formulation of the cooperative observation problem.

7.1.1 Problem Statement

Let the connections between the leader (7.2) and the N followers be described by the graph $\mathcal{G} = (\mathcal{V}, \mathcal{E})$, $\mathcal{V} = \{0, 1, 2, \cdots, N\}$. Under the multi-agent system representation, the leader agent (7.2) is the zeroth node of $\mathcal{V}$, while the follower agents are the remaining N nodes. The relative importance of the communication between two nodes i and j are designated by a weighting factor a_{ij}, which is positive if there exists a directed edge from j to i, and zero otherwise. The in-degree of a node i is defined as $d_i = \sum_{j \in \mathcal{N}_i} a_{ij}$, where $\mathcal{N}_i$ is the neighborhood set of node i.

The distributed observer equation for i^{th} agent in the presence of known inter-agent communication delays and delayed measurement y_i in (7.1b), are given as

$$\begin{aligned} \dot{\eta}_i = S\eta_i + \mu \sum_{j \in \mathcal{N}_i} a_{ij} \Big(\eta_j(t - \tau_{ij}(t)) - \eta_i(t - \tau_{ij}(t)) \Big) \\ + \mu a_{i0} G_i C_i \Big(w(t - \tau_{i0}(t)) - \eta_i(t - \tau_{i0}(t)) \Big), \end{aligned} \tag{7.3}$$

where η_i is the state estimation by the i^{th} observer, $\tau_{ij}(t) : \mathbb{R}^+ \to \mathbb{R}$ is a continuous time-varying communication delay with a delay range D such that $\tau_{ij}(t) \in [0, D]$, G_i and μ are respectively the observer gain and the low gain parameter to be determined.

The "low gain" parameter is commonly found in the Truncated Predictor Feedback (TPF) control solution, studied by [55].

For the sake of brevity, we will use τ_{ij} and τ_{i0} in place of $\tau_{ij}(t)$ and $\tau_{i0}(t)$ throughout the text. Since τ_{i0} is the delay resulted in the communication between the leader and agent i, τ_{i0} can also be viewed as a communication delay. Therefore in the rest of the text both τ_{ij} and τ_{i0} will be referred to as communication delays unless otherwise mentioned.

Remark 7.1.1. *For convenience with the predictor based approach, in the works of [72, 73], the time varying delay function was denoted by $\phi(t) = t - \tau(t)$, with $\tau(t)$ being the time delay. Such formalism also required to use the inverse function of ϕ, namely ϕ^{-1} for the stability analysis. As shown in Remark 2.1 of [55], the existence of ϕ^{-1} is guaranteed by assuming that $\phi(t)$ is continuously differentiable and its derivative is bounded. In other words, $\dot{\tau}$ was assumed to be bounded. However, in this paper we will represent the time-varying delay function as it appears in* (7.3) *without substituting them by $\phi(t)$ and due to this we do not need to explicitly assume the bounds on the derivative of the delay $\dot{\tau}$. Consequently, the results presented here will also hold for discontinuous delays $\tau(t)$.*

For $D = \max(\tau_{ij}, \tau_{i0}),\ i = 1, 2, \cdots, N$, and $\theta \in [-D, 0]$, let the initial conditions $w(\theta) = \mathbf{w}(\theta)$ and $\eta_i(\theta) = \boldsymbol{\eta}_i(\theta)$, where $\mathbf{w}, \boldsymbol{\eta}_i \in \mathcal{C}([-D, 0], \mathbb{R}^q)$. Denote the estimation error $\tilde{\eta}_i = \eta_i - w$, $\tilde{\eta}_i(\theta) = \tilde{\boldsymbol{\eta}}_i(\theta)$ with $\tilde{\boldsymbol{\eta}}_i \in \mathcal{C}([-D, 0], \mathbb{R}^q)$. The estimation error dynamics obtained from (7.2) and (7.3) is given as

$$\dot{\tilde{\eta}}_i = S\tilde{\eta}_i + \mu \sum_{j\in\mathcal{N}_i} a_{ij}\Big(\tilde{\eta}_j(t-\tau_{ij}) - \tilde{\eta}_i(t-\tau_{ij})\Big) - \mu a_{i0} G_i C_i \tilde{\eta}_i(t-\tau_{i0}). \tag{7.4}$$

To guarantee the solvability of the distributed state estimation problem we consider the Assumptions 2.3.1, 2.3.4 and 6.1.1 with $\bar{C}_{w_a}$ in 2.3.4 replaced with $\bar{C} = \mathrm{col}(C_1, C_2, \cdots, C_N)$.

Definition 7.1.1. Distributed state estimation problem: Design observer gains $G_i,\ i=1,2,\cdots,N$, feedback gain μ such that the estimation error dynamics (7.4) is exponentially stable, *i.e.*, for a constant delay bound $D>0$ and $\tilde{\boldsymbol{\eta}}_i \in \mathcal{C}([-D,0],\mathbb{R}^q)$, $\lim_{t\to\infty}\tilde{\eta}_i(t)=0$ for $i=1,2,\cdots,N$.

7.2 Stability of the Estimation Error Dynamics

In this section, we will present the stability results for the estimated error dynamics in (7.4), which will eventually lead to the design of observer gains G_i and low gain μ. The current work also provides an upper bound for D to ensure stability of the error dynamics.

To demonstrate the convergence of the estimation error dynamics (7.4) with communication delays τ_{ij}, τ_{i0}, $\forall i,j=1,2,\cdots,N$, $i\neq j$, first we evaluate the boundedness of the response for $t\leq D$, before the delayed measurements are available for feedback correction. After the boundedness of the initial response is established, we then proceed to evaluate the exponential stability $\tilde{\eta}(t)$, for $t>D$. For the first part, we will check the boundedness of $\tilde{\eta}(t)$, for $\forall t\in[0,D]$, driven by the initial conditions $\tilde{\boldsymbol{\eta}}(\theta)$ for $\theta\in[-D,0]$.

For $t=0$, from (7.4) we obtain,

$$\begin{aligned}\|\dot{\tilde{\eta}}_i(0)\| &\leq \|S\|\|\tilde{\boldsymbol{\eta}}_i(0)\|+\mu\Big(\sum_{j\in\mathcal{N}_i}\|\tilde{\boldsymbol{\eta}}_j(-\tau_{ij})\|+\mathcal{N}_i\|\tilde{\boldsymbol{\eta}}_i(-\tau_{ij})\|+\sqrt{\sigma_{G_i}}\|\tilde{\boldsymbol{\eta}}_i(-\tau_{i0})\|\Big)\\ &\leq \Big(\|S\|+2\mu\mathcal{N}_i+\mu\sqrt{\sigma_{G_i}}\Big)\|\tilde{\boldsymbol{\eta}}_0\|_{\mathcal{C}},\end{aligned} \tag{7.5}$$

where $i=1,2,\cdots,N$, $\sigma_{G_i}=\|G_iC_i\|^2$, and $\|\tilde{\boldsymbol{\eta}}_0\|_{\mathcal{C}}=\max\limits_{\theta\in[-D,0],i=1,\cdots,N}\|\tilde{\boldsymbol{\eta}}_i\|$. Since $\dot{\tilde{\eta}}_i|_{t=0}$ is found to be bounded, we have an arbitrarily small $\varepsilon>0$ such that for $t\in[0,\varepsilon]$, $\tilde{\eta}_i(t)$ also remains bounded. By using this result and the boundedness of $\tilde{\boldsymbol{\eta}}_i(\theta),\theta\in[-D,0]$, next we verify that $\dot{\tilde{\eta}}_i|_{t=\varepsilon}$ is bounded and so is $\tilde{\eta}_i(t)$ for $i=1,2,\cdots,N$ and

$t \in [\varepsilon, 2\varepsilon]$. In a similar manner we will find that across each sub-intervals $[k\varepsilon, (k+1)\varepsilon]$, $k = 0, 1, \cdots, m-1$ with $m \in \mathbb{Z}^+, m\varepsilon = D$, $\tilde{\eta}_i(t)$ is bounded.

As we obtained that $\tilde{\eta}_i(t)$ is bounded for $t \in [0, D]$, we now need to show the exponential stability of (7.4) for $t > D$. To do this, let us first introduce three auxiliary variables $\bar{\delta}_{ij}(t)$, $\hat{\delta}_{ij}(t)$, and $\hat{\delta}_{i0}$ as follows

$$\begin{aligned}
\bar{\delta}_{ij}(t) &= \tilde{\eta}_j(t-\tau_{ij}) - \tilde{\eta}_j(t) = -\int_{t-\tau_{ij}}^{t} \dot{\tilde{\eta}}_j(s)\ ds,\ j \neq i \\
\hat{\delta}_{ij}(t) &= \tilde{\eta}_i(t) - \tilde{\eta}_i(t-\tau_{ij}) = \int_{t-\tau_{ij}}^{t} \dot{\tilde{\eta}}_i(s)\ ds, \\
\hat{\delta}_{i0}(t) &= \tilde{\eta}_i(t) - \tilde{\eta}_i(t-\tau_{i0}) = \int_{t-\tau_{i0}}^{t} \dot{\tilde{\eta}}_i(s)\ ds.
\end{aligned} \tag{7.6}$$

By substituting $\tilde{\eta}_j(t-\tau_{ij})$, $\tilde{\eta}_i(t-\tau_{ij})$ and $\tilde{\eta}_i(t-\tau_{i0})$ in (7.4) with $\bar{\delta}_{ij}(t)$, $\hat{\delta}_{ij}(t)$, $\hat{\delta}_{i0}$ from (7.6), we obtain

$$\dot{\tilde{\eta}}_i = S\tilde{\eta}_i + \mu \sum_{j=1}^{N} a_{ij}(\tilde{\eta}_j - \tilde{\eta}_i) - \mu a_{i0} G_i C_i \tilde{\eta}_i + \mu(\bar{\delta}_i + \hat{\delta}_i + a_{i0} G_i C_i \hat{\delta}_{i0}), \tag{7.7}$$

where $\bar{\delta}_i(t) = \sum_{j=1}^{N} a_{ij} \bar{\delta}_{ij}(t)$, $\hat{\delta}_i(t) = \sum_{j=1}^{N} a_{ij} \hat{\delta}_{ij}(t)$.

Let $\bar{\delta} = \mathrm{col}(\bar{\delta}_1, \bar{\delta}_2, \cdots, \bar{\delta}_N)$, $\hat{\delta} = \mathrm{col}(\hat{\delta}_1, \hat{\delta}_2, \cdots, \hat{\delta}_N)$, and $\hat{\delta}_0 = \mathrm{col}(\hat{\delta}_{10}, \hat{\delta}_{20}, \cdots, \hat{\delta}_{N0})$ and thus the composite error vector $\tilde{\eta}$ evolves as follows

$$\dot{\tilde{\eta}} = M\tilde{\eta} + \mu(\bar{\delta} + \hat{\delta} + GC\hat{\delta}_0), \tag{7.8}$$

where $M = [(I_N \otimes S) - \mu(\mathcal{L} \otimes I_q) - \mu GC]$, $\mathcal{L} \in \mathbb{R}^{N \times N}$ is the Laplacian matrix corresponding to the strongly connected partition of the network of N observer agents, $G = \text{blk diag}(G_1, \cdots, G_N)$, and $C = \text{blk diag}(C_1, \cdots, C_N)$.

We now introduce some additional notations which will be used throughout the text. Let d_{out}^i and d_{in}^i be the out-degree and in-degree of a node i. Denote $d_{\text{out,max}} = \max\limits_{i=1,2,\cdots,N} d_{\text{out}}^i$, $d_{\text{in,max}} = \max\limits_{i=1,2,\cdots,N} d_{\text{in}}^i$, $\sigma_M = \|M\|^2, \sigma_G = \|GC\|^2$, $\bar{C} =$

$\mathrm{col}(C_1, C_2, \cdots, C_N)$, $\mathbf{G} = [G'_1\ G'_2\ \cdots\ G'_N]$, $G'_i = \zeta_i G_i$ where ζ_i is the i^{th} entry of the left eigenvector $\zeta = [\zeta_1, \zeta_2, \cdots, \zeta_N]^{\mathrm{T}}$ of $\mathcal{L}$ corresponding to zero eigenvalue. Without loss of generality, let $\sum_i \zeta_i = 1$. Note that for the Laplacian matrix $\mathcal{L}$ of a strongly connected communication network, the results in [46,77] states that the positive-definite diagonal matrix $\Sigma = \mathrm{diag}(\zeta)$ makes $\hat{\mathcal{L}} = \Sigma\mathcal{L} + \mathcal{L}^{\mathrm{T}}\Sigma$ positive semi-definite. Additionally, $\hat{\mathcal{L}}$ has zero row sum and zero column sum, and thus it can be viewed as the Laplacian matrix of an undirected communication network.

To analyze the stability of (7.8), we construct a Lyapunov function of the form $V(\tilde{\eta}) = \tilde{\eta}^{\mathrm{T}}(t)\,(\Sigma \otimes P)\,\tilde{\eta}(t)$ where P is a positive definite matrix and $\Sigma = \mathrm{diag}(\zeta)$ is a diagonal matrix with the i^{th} diagonal entry being ζ_i. Since the matrix $(\Sigma \otimes P)$ is symmetric and have all positive eigenvalues, $0 \leq \zeta_{min}\lambda_{min}(P)\|\tilde{\eta}\|^2 \leq V(\tilde{\eta}) \leq \zeta_{\max}\lambda_{\max}(P)\|\tilde{\eta}\|^2$, $\forall \tilde{\eta} \neq 0$, where $\zeta_{\min} = \min(\zeta_i)$, $\zeta_{\max} = \max(\zeta_i)$, $i = 1, 2, \cdots, N$. By differentiating $V(t)$ along the trajectories of (7.8), we obtain

$$\begin{aligned}
\dot{V}(\tilde{\eta}) &= \tilde{\eta}^{\mathrm{T}}\left[M^{\mathrm{T}}(\Sigma \otimes P) + (\Sigma \otimes P)\,M\right]\tilde{\eta} + 2\mu\tilde{\eta}^{\mathrm{T}}(\Sigma \otimes P)(\bar{\delta} + \hat{\delta}) + 2\mu\tilde{\eta}^{\mathrm{T}}GC(\Sigma \otimes P)\hat{\delta}_0^{\mathrm{T}} \\
&\leq \dot{V}_0 + \bar{\delta}^{\mathrm{T}}(\Sigma^2 \otimes P^2)\bar{\delta} + \hat{\delta}^{\mathrm{T}}(\Sigma^2 \otimes P^2)\hat{\delta} + \hat{\delta}_0^{\mathrm{T}}(\Sigma^2 \otimes P^2)\hat{\delta}_0 + \mu^2(2 + \sigma_G)\|\tilde{\eta}\|^2 \\
&\leq \dot{V}_0 + \lambda_{\max}^2(P)\zeta_{\max}^2\left[\bar{\delta}^{\mathrm{T}}\bar{\delta} + \hat{\delta}^{\mathrm{T}}\hat{\delta} + \hat{\delta}_0\hat{\delta}_0\right] + \mu^2(2 + \sigma_G)\|\tilde{\eta}\|^2,
\end{aligned} \tag{7.9}$$

where $V_0 = \int_0^t \tilde{\eta}^{\mathrm{T}}(s)\left[M^{\mathrm{T}}(\Sigma \otimes P) + (\Sigma \otimes P)\,M\right]\tilde{\eta}(s)\,ds$. Next, we consider the following Lemma to evaluate the first term of (7.9).

Theorem 7.2.1. *Consider the distributed observers* (7.3) *satisfying Assumptions 2.3.1, 2.3.4, 6.1.1, and gains G_i selected such that $\mathcal{R} = S - \mu\mathbf{G}\bar{C}$ is a Hurwitz matrix for any $\mu \in (0, 1)$. Let then $P \in \mathbb{R}^{q \times q} > 0$ be a solution to the inequality*

$$\mathcal{R}^T P + P\mathcal{R} < 0, \tag{7.10}$$

such that the matrix $P(S-\mu G_iC_i)+(S-\mu G_iC_i)^TP$ *has non-positive eigenvalues for all follower agents* i. *Then for the time-varying communication delays* $\tau_{ij}, j=0,1,\cdots,N$, $i=1,2,\cdots,N,\ i\neq j$, *the observer states* $\eta_i(t)$ *converges to* $w(t)$ *asymptotically,* i.e.,

$$\lim_{t\to\infty}(\eta_i(t)-w(t))=0,\ i=1,2,\cdots,N,$$

if the upper bound for the delay D *satisfies* $D<\bar{D}$, *where*

$$\bar{D}=\frac{1}{2}\sqrt{\frac{\alpha\mu-\mu^2(2+\sigma_G)}{c_0\Big(\zeta_{\max}^2\lambda_{\max}^2(P)\sigma_M+\alpha\mu^3-\mu^4(2+\sigma_G)\Big)}}, \tag{7.11}$$

with $\alpha>0$ *such that* $M^T(\Sigma\otimes P)+(\Sigma\otimes P)M<-\alpha I$ *and* $c_0=(N-1)d_{out,\max}^2+(N-1)d_{in,\max}^2+1$.

Proof. Let $\mathcal{G}$ satisfy Assumption 6.1.1 with at least one agent being the child node of the leader. Now, we evaluate the first term on the right-hand side of the inequality in (7.9). In this regard, we have

$$\begin{aligned}\dot{V}_0&=\tilde{\eta}^{\mathrm{T}}\left[M^{\mathrm{T}}(\Sigma\otimes P)+(\Sigma\otimes P)M\right]\tilde{\eta},\\ &=\tilde{\eta}^{\mathrm{T}}\left[\Sigma\otimes(S^{\mathrm{T}}P+PS)-\mu C^{\mathrm{T}}G^{\mathrm{T}}(\Sigma\otimes P)-\mu(\Sigma\otimes P)GC-\mu(\hat{\mathcal{L}}\otimes I_q)\right]\tilde{\eta}.\end{aligned} \tag{7.12}$$

It is inferred from Assumption 6.1.1 that the matrix $(\hat{\mathcal{L}}\otimes I_q)$ is positive semi-definite, and the lemma assumes that $P(S-\mu G_iC_i)+(S-\mu G_iC_i)^{\mathrm{T}}P$ is negative semi-definite. These assumptions then yield that $\dot{V}_0\leq 0$. We will now investigate the invariant set of $\tilde{\eta}$ on which $\dot{V}_0=0$. Assumption 6.1.1 yields $\hat{\mathcal{L}}$ has zero row sum, and thus the term $-\mu\tilde{\eta}^{\mathrm{T}}\left(\hat{\mathcal{L}}\otimes I_q\right)\tilde{\eta}$ in (7.12) becomes zero non-trivially only when $\tilde{\eta}=\mathbf{1}_N\otimes\tilde{\eta}_f$, for any $\tilde{\eta}_f\in\mathbb{R}^q$. Replacing this $\tilde{\eta}$ into (7.12) then yields that

$$\dot{V}_0=\tilde{\eta}_f\left[\mathcal{R}^{\mathrm{T}}P+P\mathcal{R}\right]\tilde{\eta}_f<0. \tag{7.13}$$

Therefore,

$$\dot{V}_0 = \tilde{\eta}^{\mathrm{T}} \left[M^{\mathrm{T}}(\Sigma \otimes P) + (\Sigma \otimes P) M \right] \tilde{\eta} < 0,$$

must be true for any non-zero $\tilde{\eta}$, and $\dot{V}_0 = 0$ only when $\tilde{\eta} = 0$.

Because $\tilde{\eta}^{\mathrm{T}} \left[M^{\mathrm{T}}(\Sigma \otimes P) + (\Sigma \otimes P] M \right) \tilde{\eta}$ is continuous and finite over $\mu \in (0,1)$, there must exist a positive scalar $\alpha > 0$ such that

$$\tilde{\eta}^{\mathrm{T}} \left(M^{\mathrm{T}}(\Sigma \otimes P) + (\Sigma \otimes P) M \right) \tilde{\eta} < -\alpha \mu \|\tilde{\eta}\|^2. \tag{7.14}$$

Substituting (7.14) into (7.9) we obtain

$$\dot{V}(\tilde{\eta}) \leq -\alpha \mu \|\tilde{\eta}\|^2 + \mu^2 (2 + \sigma_G) \|\tilde{\eta}\|^2 + \lambda_{\max}^2(P) \zeta_{\max}^2 \left[\bar{\delta}^{\mathrm{T}} \bar{\delta} + \hat{\delta}^{\mathrm{T}} \hat{\delta} + \hat{\delta}_0 \hat{\delta}_0 \right]. \tag{7.15}$$

Now we evaluate the rest of the terms in (7.15) as follows. Since

$$\bar{\delta}^{\mathrm{T}} \bar{\delta} = \sum_{i=1}^{N} \bar{\delta}_i^{\mathrm{T}} \bar{\delta}_i \leq (N-1) \sum_{i=1}^{N} \sum_{j=1, j \neq i}^{N} a_{ij}^2 \bar{\delta}_{ij}^{\mathrm{T}} \bar{\delta}_{ij},$$

then from (7.6) and Lemma 6.1.2, we obtain

$$\bar{\delta}^{\mathrm{T}} \bar{\delta} \leq (N-1) D d_{\mathrm{out,max}}^2 \int_{t-D}^{t} \dot{\tilde{\eta}}^{\mathrm{T}}(s) \dot{\tilde{\eta}}(s) \, ds. \tag{7.16}$$

In a similar manner the bounds on the terms $\hat{\delta}^{\mathrm{T}} \hat{\delta}$ and $\hat{\delta}_0^{\mathrm{T}} \hat{\delta}_0$ can be deduced as follows,

$$\begin{aligned} \hat{\delta}^{\mathrm{T}} \hat{\delta} &\leq (N-1) D d_{\mathrm{in,max}}^2 \int_{t-D}^{t} \dot{\tilde{\eta}}^{\mathrm{T}}(s) \dot{\tilde{\eta}}(s) \, ds, \\ \hat{\delta}_0^{\mathrm{T}} \hat{\delta}_0 &\leq D \int_{t-D}^{t} \dot{\tilde{\eta}}^{\mathrm{T}}(s) \dot{\tilde{\eta}}(s) \, ds. \end{aligned} \tag{7.17}$$

Let us take $V_1 = \int_0^D \int_{t-s}^{t} \dot{\tilde{\eta}}^{\mathrm{T}}(s) \dot{\tilde{\eta}}(s) \, ds$ and thus from Eqs. (7.16), (7.17) we obtain

$$\bar{\delta}^{\mathrm{T}} \bar{\delta} + \hat{\delta}^{\mathrm{T}} \hat{\delta} + \hat{\delta}_0^{\mathrm{T}} \hat{\delta}_0 \leq c_0 D^2 \dot{\tilde{\eta}}^{\mathrm{T}} \dot{\tilde{\eta}} - c_0 D \dot{V}_1. \tag{7.18}$$

Next, by using (7.8), we evaluate $\dot{\tilde{\eta}}^{\mathrm{T}}(t)\dot{\tilde{\eta}}(t)$ as follows

$$\dot{\tilde{\eta}}^{\mathrm{T}}(t)\dot{\tilde{\eta}}(t) \leq 4\sigma_M\|\tilde{\eta}\|^2 + 4\mu^2\left(\bar{\delta}^{\mathrm{T}}\bar{\delta} + \hat{\delta}^{\mathrm{T}}\hat{\delta} + \hat{\delta}_0^T\hat{\delta}_0^{\mathrm{T}}\right). \tag{7.19}$$

Substituting the results of (7.19) in (7.18) yields

$$\bar{\delta}^{\mathrm{T}}\bar{\delta} + \hat{\delta}^{\mathrm{T}}\hat{\delta} + \hat{\delta}_0^{\mathrm{T}}\hat{\delta}_0 \leq \frac{c_0 D}{1-4\mu^2 c_0 D^2}\left[4D\sigma_M\|\tilde{\eta}\|^2 - \dot{V}_1\right], \tag{7.20}$$

and therefore from (7.15) we obtain

$$\dot{V} \leq (-\alpha\mu + \mu^2(2+\sigma_G))\|\tilde{\eta}\|^2 + \frac{c_0\lambda_{\max}^2(P)\zeta_{\max}^2}{1-4\mu^2 c_0 D^2}\left[4D^2\sigma_M\|\tilde{\eta}\|^2 - D\dot{V}_1\right]. \tag{7.21}$$

Let us define $V_\phi = V + \lambda_{\max}^2(P)\zeta_{\max}^2\dfrac{c_0 D}{1-4\mu^2 c_0 D^2}V_1$ which is positive everywhere except when $\tilde{\eta} = 0$ and $\dot{\tilde{\eta}}(t+\theta) = 0, \theta \in [-D, 0]$. Additionally, from (7.19), (7.20), V_ϕ can easily be shown to be bounded between two non-decreasing functions. Then by rearranging the terms in (7.21) we obtain

$$\dot{V}_\phi \leq \left(-\alpha\mu + \mu^2(2+\sigma_G) + \frac{4c_0\lambda_{\max}^2(P)\zeta_{\max}^2 D^2\sigma_M}{1-4\mu^2 c_0 D^2}\right)\|\tilde{\eta}\|^2.$$

As a result, $\dot{V}_\phi < 0$ for $D < \bar{D}$ with

$$\bar{D} = \frac{1}{2}\sqrt{\frac{\alpha\mu - \mu^2(2+\sigma_G)}{c_0\left(\zeta_{\max}^2\lambda_{\max}^2(P)\sigma_M + \mu^2(\alpha\mu - \mu^2(2+\sigma_G))\right)}}.$$

Therefore, according to the Lyapunov-Krasovskii stability theorem 6.1.3, the estimation error dynamics (7.4) is globally asymptotically stable and $\lim_{t\to\infty}\tilde{\eta}(t) = 0$. This concludes the proof. □

Remark 7.2.1. *$\mathcal{R}$ can be rewritten as*

$$\mathcal{R} = S - \mu \mathbf{G}\bar{C}. \tag{7.22}$$

By Assumption 2.3.4, there exists a matrix $\mathbf{G}$ so that $\mathcal{R}$ in (7.22) is Hurwitz. While Theorem 7.2.1 allows for any $\mathbf{G}$ such that $\mathcal{R}$ is Hurwitz, the equivalent observer gain in [46] is tied to the solution of a parametric Riccati equation. It is also true that any solution to the parametric Riccati equation in [46] and the corresponding observer gain $\mathbf{G}$ results in $\mathcal{R}$ being Hurwitz, but the opposite may not necessarily hold.

Remark 7.2.2. *From the delay bound $\bar{D}$ in (7.11), we observe that the stability of the estimation error dynamics is independent of the rate of change of delay $\dot{\tau}_{ij}(t)$ and $\dot{\tau}_{i0}(t)$. Hence, (7.11) can also be applied to the distributed state estimation problems with fast time-varying delays, indicating that the proposed estimation algorithm is robust with respect to the time variation of the delays. Furthermore, from (7.11), we also obtain the upper bound of the low gain parameter $\mu \in (0, \mu^*)$ as*

$$\mu^* = \frac{\alpha}{2 + \sigma_G}. \tag{7.23}$$

7.3 Application to a Leader-Follower Synchronization Problem

In this section, we present a leader-follower synchronization problem under network latency, and a detectability constraint that none of the followers can independently reconstruct the leader dynamics from its measurements. Due to the presence of time delays in the measurement and communication between followers, the results from [2, 3, 71] are not applicable. Thus, with the proposed results from the distributed state estimation problem studied in this work, we proceed to tackle the leader-follower synchronization problem in face of time-varying measurement and network latency.

The distributed control problem then consists for all agents to synchronize their states to a leader, given as (7.2), by regulating the error signal $e_i \in \mathbb{R}^{\mathbf{p}_i}$,

$$e_i = C_{x_i} x_i - F_i w, \; i = 1, 2, \cdots, N. \tag{7.24}$$

It is assumed that e_i is not available as a measurement for control, but follower agents collect delayed leader measurements $y_i \in \mathbb{R}^{p_i}$

$$y_i = C_i w(t - \tau_{i0}). \tag{7.25}$$

It is also assumed that the follower agents are connected under a communication network described by the digraph $\mathcal{G}$, and communications between agent i with the other agents are subject to the communication delay $\tau_i(t)$. The objective of this synchronization problem is to design a distributed control law $u_i(t)$ such that the regulated error signals $e_i(t)$ asymptotically converge to zero.

As noted in [29, 30], the solvability of the synchronization problem requires the assumptions 2.3.2, and 6.4.1 while the following regulator equation to yield a unique solution pair (X_i, U_i).

$$\begin{aligned} X_i S &= A_i X_i + B_i U_i, \\ 0 &= C_{x_i} X_i - F_i. \end{aligned} \tag{7.26}$$

Given that the Assumptions 2.3.1, 2.3.2, 6.4.1 hold, the distributed state feedback control law u_i takes the form [2]

$$u_i = K_{1_i} x_i + K_{2_i} \eta_i, \tag{7.27}$$

where $\eta_i(t)$ is the distributed observer state with the dynamics given in (7.3). The controller gains K_{1_i}, K_{2_i} are selected such a way that $(A_i + B_i K_{1_i})$ is Hurwitz and $K_{2_i} = U_i - K_{1_i} X_i$. Since $\lim_{t\to\infty} \eta_i(t) = w(t)$ by Theorem 7.2.1, the control solution to the aforementioned synchronization problem can be summarized in the following Theorem.

Theorem 7.3.1. *Given the leader* (7.2)*, N followers* (7.1a)*, and the digraph $\mathcal{G}$, the distributed control law u_i in* (7.27) *solves the leader-follower synchronization problem if Assumptions 2.3.1, 2.3.2, 6.4.1, 2.3.4 and 6.1.1 are satisfied.*

The proof of Theorem 7.3.1 follows similar procedure as in [2], with the results of Theorem 7.2.1 to guarantee the stability of the leader state estimation error dynamics.

7.4 Illustrative Example

In this section we consider an illustrative example to evaluate the effectiveness of our proposed algorithm. Let the plant (7.2) have state vector $w = \begin{bmatrix} w_1 & w_2 & w_3 & w_4 \end{bmatrix}^{\mathrm{T}}$ and state matrix

$$S = \text{blk diag}(S_1, S_2), S_1 = \begin{bmatrix} 0 & -1 \\ 1 & 0 \end{bmatrix}, S_2 = \begin{bmatrix} 0 & -2 \\ 2 & 0 \end{bmatrix}. \tag{7.28}$$

The measured output matrices $C_i,\ i = 1,2,3$, are given as follows:

$$C_1 = \begin{bmatrix} I_2 & 0_2 \end{bmatrix},\ C_2 = \begin{bmatrix} 0_2 & I_2 \end{bmatrix},\ C_3 = 0_{2\times 4},$$

from which we verify that none of the pairs $(S, C_i),\ i = 1,2,3$, are detectable. Instead, the combined detectability property in Assumption 2.3.4 is satisfied for the given C_i. Clearly, the follower agent 1 can directly receive the signal $\begin{bmatrix} w_1 & w_2 \end{bmatrix}^{\mathrm{T}}$ from the plant measurement $y_1(t)$, while agent 2 receives the signal $\begin{bmatrix} w_3 & w_4 \end{bmatrix}^{\mathrm{T}}$.

The communication network between the observers is represented by the digraph $\mathcal{G}$ satisfying Assumption 6.1.1, as illustrated in Figure 6.1, with the Laplacian matrix $\mathcal{L}$ given as follows

$$\mathcal{L} = \begin{bmatrix} 1 & -1 & 0 \\ 0 & 1 & -1 \\ -1 & 0 & 1 \end{bmatrix}. \tag{7.29}$$

The strongly connected partition of $\mathcal{G}$ in Figure 6.1 allows the exchange of estimated states between agents, and complements for the incomplete measurements that each agent receives from the plant. Even though a single observer cannot independently reconstruct the exosystem state vector $w(t)$, the strongly connected communication network between the observer agents enables them to jointly synthesize an estimate of the plant state.

We now introduce the communication delay functions for the example problem as follows.

$$\begin{aligned} \tau_{12}(t) &= 0.005\Big(1+\sin^2(1000t)\Big) = \tau_{21}(t), \\ \tau_{23}(t) &= 0.01\cos^2(500t) = \tau_{32}(t), \\ \tau_{31}(t) &= 0.01\Big(1-\sin^2(1000t)\Big) = \tau_{13}(t), \\ \tau_{10}(t) &= 0.006\cos^2(1000t) = \tau_{20}(t). \end{aligned}$$

From the given time-varying functions of the communication delays, the delay bound D for this simulation can be chosen to be $D = 0.01$.

From the Laplacian matrix $\mathcal{L}$ in (7.29), we obtain $\zeta_{max} = 1/3$ and $c_0 = 5$. We select the design parameters as follows:

$$G_1 = \begin{bmatrix} I_2 & 0_2 \end{bmatrix}^{\mathrm{T}}, G_2 = \begin{bmatrix} 0_2 & I_2 \end{bmatrix}^{\mathrm{T}}, G_3 = 0_{4\times 2},$$

which make the matrix

$$\mathcal{R} = \text{blk diag}\left(\begin{bmatrix} -\mu/3 & -1 \\ 1 & -\mu/3 \end{bmatrix}, \begin{bmatrix} -\mu/3 & -2 \\ 2 & -\mu/3 \end{bmatrix}\right)$$

in (7.22) Hurwitz with the eigenvalues located at $-\mu/3 \pm j, -\mu/3 \pm 2j$. We note here that $\mathcal{R}^{\mathrm{T}} + \mathcal{R} = -\dfrac{2\mu}{3}I$ and $\mathcal{R}\mathcal{R}^{\mathrm{T}} = \mathcal{R}^{\mathrm{T}}\mathcal{R}$. Next, from the Lyapunov equation $\mathcal{R}^{\mathrm{T}}P + P\mathcal{R} = -\mu I$, we find the solution P as

$$P = \int_0^\infty e^{\mathcal{R}^{\mathrm{T}}s}e^{\mathcal{R}s}\, ds = \int_0^\infty e^{(\mathcal{R}^{\mathrm{T}}+\mathcal{R})s}\, ds = 1.5I.$$

We also verify that the matrices $(S - \mu G_i C_{w_i})^{\mathrm{T}}P + P(S - \mu G_i C_{w_i}), i = 1,2$ has eigenvalues at $-3\mu, -3\mu, 0, 0$ and $(S - \mu G_3 C_{w_3})^{\mathrm{T}}P + P(S - \mu G_3 C_{w_3}) = 0$. Thus P satisfies the LMI conditions in Theorem 7.2.1. Next, by substituting P in (7.14), we find that $M^{\mathrm{T}}(\Sigma \otimes P) + (\Sigma \otimes P)M < -0.2\mu I$. As a result, from (7.11) and Remark 7.2.2 the upper bound of μ is found to be $\mu^* = 0.0731$. For simulation purpose, we select $\mu = 0.06$.

With these parameters, we obtain from (7.11) that $\bar{D} = 0.0106$ and $D < \bar{D}$. The simulated response of the distributed observers are presented in Figure 7.1 through the sum of the observation errors $\delta_i(t) = \|\tilde{\eta}_i(t)\|$, where $i = 1,2,3$. The simulated response shows that $\delta_i(t)$ or equivalently $\tilde{\eta}_i$ converges asymptotically to zero, and thus the objectives of the distributed observation problem are achieved.

With the designed observers and scalar feedback gain for the distributed state estimation problem, let us now apply our results to a leader-follower synchronization problem. The leader system matrix S is given in (7.28) and the dynamics of the follower agent i are described by a double integrator as given below

$$\dot{x}_{1_i} = x_{2_i},\ \dot{x}_{2_i} = u_i,\ e_i = x_{1_i} - (w_1 + w_3). \tag{7.30}$$

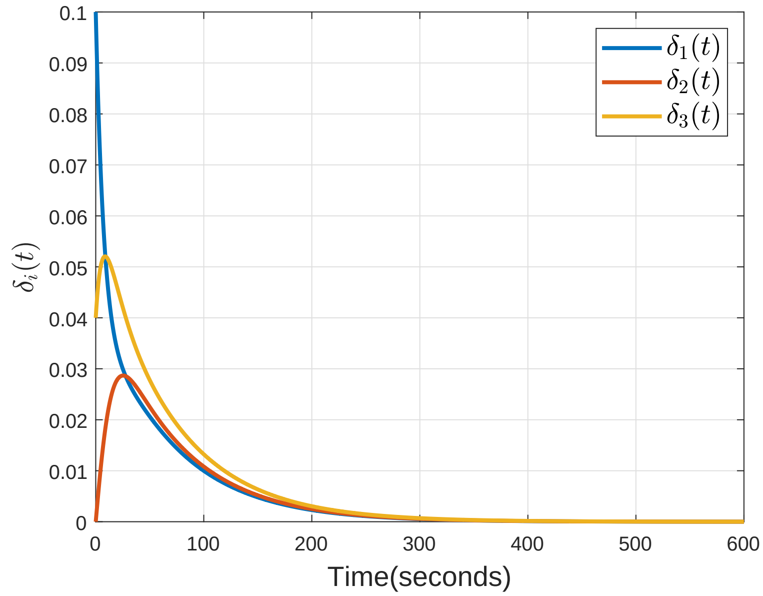

Figure 7.1: Observation error of three observers for the case under time-varying communication and measurement delay within the delay bound $\bar{D} = 0.0106$

From (7.30), the subsystem matrices are found to be

$$A_i = \begin{bmatrix} 0 & 1 \\ 0 & 0 \end{bmatrix}, B_i = \begin{bmatrix} 0 \\ 1 \end{bmatrix}, C_{x_i} = [1 \quad 0], F_i = [1 \quad 0 \quad 1 \quad 0].$$

It is easy to verify that the Assumptions 2.3.1, 2.3.2, 6.4.1 hold. The controller gains in (7.27) are obtained as $K_{1_i} = \begin{bmatrix} -8 & -4 \end{bmatrix}$, $K_{2_i} = \begin{bmatrix} 7 & -4 & 4 & -8 \end{bmatrix}$. By applying the distributed control law (7.27) to the subsystem dynamics (7.30), we observe in Fig. 7.2 that all the followers are synchronized with the desired leader trajectory $w_1 + w_3$. Thus, the leader-follower synchronization problem in the presence of time-varying measurement and communication delay is solved by a dynamic control method that relies on our proposed distributed state estimation algorithm.

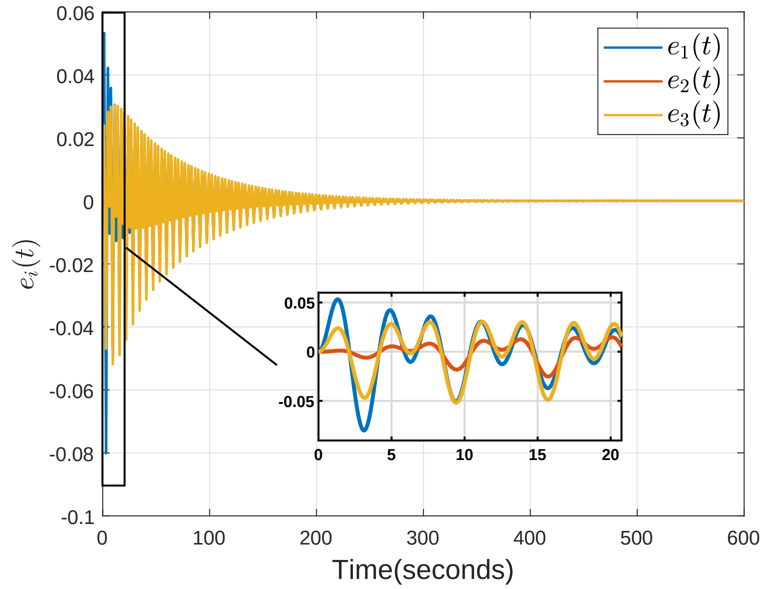

Figure 7.2: Tracking error of the followers under the distributed dynamic control law (7.3), (7.27)

7.5 Conclusion

In this work we studied the distributed state estimation problem for autonomous dynamic systems, and under time-varying communication and measurement delays. The proposed observer framework relies on the strongly connected communication network between the observer agents and the combined detectability property of the system, to guarantee that the local state estimation of all agents converges to the states of the observed plant, including states that may not be detectable through local measurements. Our current work considered the presence of time delays in the communication and measurements of the observer agents, and a distributed observer framework was developed for the considered estimation problem. Sufficient conditions for the stability of the corresponding observation error dynamics were derived, including an upper bound for the delay and low gain parameter of the observer equations. It was also demonstrated that the stability results for the estimation error dynamics is independent of the variation of the delay and thus the proposed estimation technique is unperturbed by the fast varying delays.

Compared with similar results in the literature, the results presented in this work provided generalization of the sufficient conditions to guarantee the convergence of the observer estimation errors to zero, only prescribing a Hurwitz condition for the selection of the observer correction gain. Such general results are obtained without requiring solutions to extensive matrix inequalities conditions.

The results of the distributed state estimation problem was also applied to solve the leader-follower synchronization problem in the case when the measurements from the leader and the communication between the followers are subjected to time delays. Illustrative simulation examples were offered to verify our mathematical analysis and the theoretical results in this work.

In this current work we assumed that the communication and measurement delays were known to the agents. However, there are some practical situations where this may not be the case. With this as motivation, in our future research we aim to extend our current work to the case for unknown time delays.

Chapter 8

Synchronization of Distributed Generators in a Microgrid under Communication Latency- A Case Study

Electrical power grids over the last decade have undergone a rapid transformation from a traditional generation and transmission infrastructure to an automated intelligent control, sensing and communication network based technology, known as "smart grid". One of the basic building blocks of this smart grid technology are microgrids (MG) which are typically small scale electrical power networks comprised of distributed energy resources, controllable load and storage units. In normal conditions, MGs operate synchronously with the main utility grid but they are also able to operate autonomously when disconnected from the main grid in the event of faults, black outs and natural disasters [93].

The distributed power generation in microgrids are supported by renewable sources such as solar PV cells, biomass fuel cells, wind and microturbines [94]. These renewable energy resources in the MG are connected with the main grid at the point of common coupling (PCC) through parallelly connected voltage source inverters (VSI) shown in Figure 8.1.

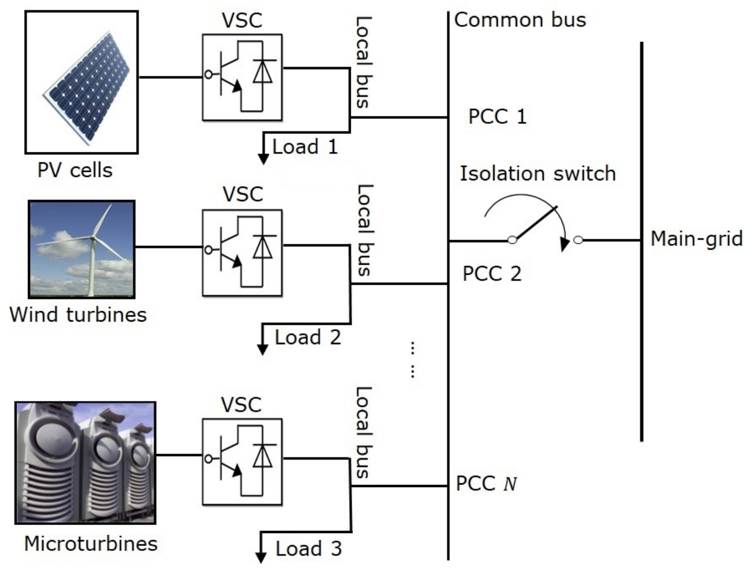

Figure 8.1: Typical microgrid structure with inverter based generators

The main control objective of distributed generator (DG) units is to synchronize their terminal voltage and VSI frequency with the reference grid set points. Hierarchical control [95] is one of the basic control strategies, which consists of primary, secondary and tertiary control layers. The primary control, also known as droop control [96] maintains the transient voltage and frequency stability of the MG, and enables balanced power sharing once it goes to the islanded mode. The current standard is to use proportional droop controller locally at each inverter, while quadratic voltage droop controllers can also be found in [97, 98].

With the application of the droop control, the frequency and voltage magnitude of the VSIs deviate from their nominal values, which is restored with another layer of control called secondary control [96]. The objective of the secondary control is to generate the voltage and frequency reference signals for the primary controller of each DG unit. While centralized and decentralized techniques [99] were used in the secondary control, these methods suffer from limitations such as dense communication network, single point of failure, and large transmission power loss. Therefore, a distributed cooperative control structure in [93, 96, 100, 100, 101] was offered as an efficient alternative. The final level of control is tertiary control, which is concerned with global economic dispatch over the network, and depends on current energy markets and prices. In most cases, this control structure is centralized and occurs offline.

This work primarily focuses on the secondary control layer which has a consensus based cooperative control structure. But compared to the works of [96], we consider that the communication between the agents are now subject to heterogeneous delays. In microgrid applications where maintaining data integrity is of paramount importance, authentication of the data prior to propagation into the network is viewed as an effective control theoretic approach to maintain data integrity and prevent malicious cyber attacks [102]. The verification of the message being transferred between the DG units in a deterministic network [103] then introduces bounded communication delays. For the known time varying communication delays, a distributed cooperative control solution to the synchronization problem was offered in [104, 105].

In [106], the authors studied the stability of an inverter based MG systems under time invariant input delay caused by the differing bandwidth of internal controllers. The MG was represented in Lure form and the Lyapunov-Krasovskii stability method was invoked to investigate the local stability of the MG with delay. The authors in [104, 105] proposed a cooperative control strategy to regulate terminal DG voltages under time varying delay. In [104], it was assumed that the communication delay was identical for all networked agents while in [105], the outgoing information from a particular DG was subject to the same delay regardless of the recipient DG units it was connected to. Moreover, the communication topology of the DG units was assumed to be balanced in [105] and strongly connected in [104].

Motivated by the works of [96, 101] we extend the results in [93] to study the voltage and frequency synchronization of networked DG units in an islanded MG under heterogeneous communication time delays. With the use of low-gain feedback, we offer a delay tolerant robust distributed coordination and control protocol for the networked DGs. Using the low-gain methodology and Lyapunov-Krasovskii based large signal stability analysis, we derive the sufficient stability conditions with an upper bound for the low gain parameter. Lastly we validate our theoretical results with some simulation examples.

The contribution of this work can be summarized as follows. Here we study the voltage and frequency synchronization of inverter based autonomous DGs in an islanded MG under arbitrarily large, yet bounded time varying communication delays. In contrast with [104, 105, 107, 108] we consider that the communication delays between the DGs are heterogeneous. By using the low gain techniques we offer a robust distributed control solution to the problem for both known and unknown latencies. Next, with the Lyapunov-Krasovskii large signal stability analysis, we derive delay dependent sufficient stability conditions to ensure the synchronization. Such delay dependent stability conditions avoid the conservatism associated with the delay independent results found in [105]. Moreover, to synchronize the terminal voltage and frequency of DGs while proportionally sharing the active and reactive power among themselves, the solvability conditions of the problem in [104, 105, 107, 108] require that the communication topology between the DGs is either balanced or strongly connected. In contrast, the control solution offered in this work rather prescribes a more relaxed spanning tree assumption.

The remainder of the chapter can be organized as follows. First we describe the parallel operation of inverter based DGs in Section 8.1. Then, we formulate our problem, present necessary assumptions, review some hierarchical control methods and define our problem objective in Section 8.2. In Section 8.3, we derive our stability results for both the known and unknown communication delays. Next, we verify our theoretical developments of the earlier sections with the help of a numerical example in Section 8.4. Finally some conclusions of the chapter appear in Section 8.5.

Notation. We now define the following notations which will be used throughout the chapter. A column vector $\mathbf{1}_N \in \mathbb{R}^N$ is a vector in $\mathbb{R}^N$ with all ones. For scalars $d_i,\ i=1,2,\cdots,N$, $D=\text{blk diag}(d_1,d_2,\cdots,d_N)$ represents a block diagonal matrix with the diagonal elements being d_i. For two non-negative integers a,b, $I[a,b]$ denotes the set of all intermediate positive integers in the closed interval $[a,b]$. For two symmetric matrices $A,\ B$ of identical dimensions, let us denote by $A<B$ that the matrix $A-B$ is negative definite.

8.1 Parallel Operation of Inverter Based Microgrids

MG operates in both grid connected and as well as in the islanded mode. In the grid connected mode, the DG units are controlled to act as a constant power source which supplies the demanded power by the main grid. This is enabled by the grid-feeding inverters [109] in the DG unit, which acts as a current source with a high impedance in parallel to control the power exchange between the main grid and the DG. Since the DG units now operate in tandem with the main grid, it has identical operating frequency and terminal voltage as the main grid.

However, when the MG undergoes a planned or unplanned isolation from the main grid, the DG units of the islanded MG are then required to pick up all the local loads while synchronizing the terminal voltage and frequency. The grid-forming inverters in the DG unit play an important role in regulating the voltage and the frequency in an islanded MG operation. The grid forming inverters in the MG act as a voltage source with a low impedance in series and set the reference voltage and frequency set points for other grid feeding generators in the islanded MG. The parallel operation of these grid-froming inverters and their control techniques has been reviewed in the works of [94, 110].

The schematic diagram of two parallel DGs connected to the main grid at a PCC is shown in Figure 8.2 where V_{oi} is the terminal voltage magnitude of the i^{th} DG, Z_{Load} and Z_i are respectively the load impedance and transmission line impedance between the i^{th} DG and PCC. Acccordingly, as stated in [94] the model of an MG can be divided into three major submodules such as DGs, electrical power network and loads. A DG model includes a power sharing controller, VSI, output LC filter, and internal voltage and current controllers. The dynamics of these sub-modules and their components will be discussed later in greater details.

In case of a medium or low voltage distribution network with a purely inductive impedance Z_i, *i.e.* $Z_i = jX_i$, and small power angle δ_i, from [110] the injected active power P_i and reactive power Q_i between the DGs and the PCC are obtained as follows.

$$P_i = \frac{V_{oi} V \delta_i}{X_i}, \; Q_i = \frac{V(V_{oi} - V)}{X_i}. \tag{8.1}$$

It is clear from (8.1) that the active power injected to the main grid by a DG

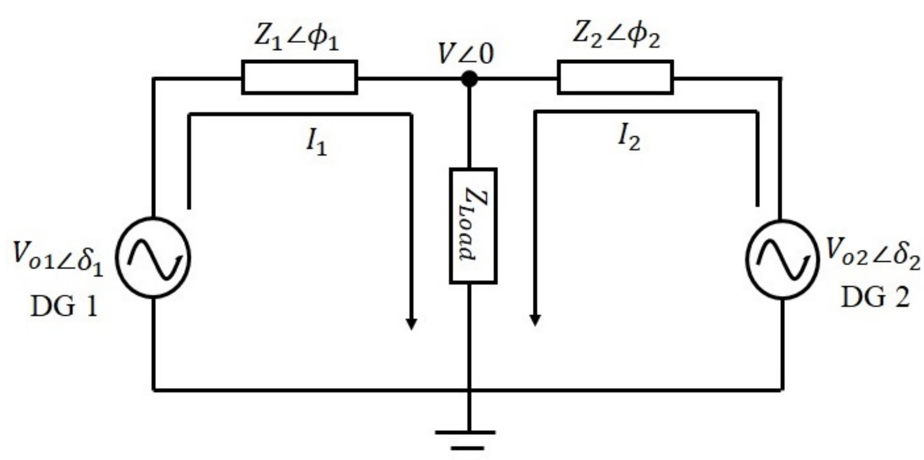

Figure 8.2: Equivalent schematic diagram of parallel inverter based microgrid

depends on the power angle or consequently the frequency, while the reactive power depends on the difference in amplitude between the terminal voltage of the DG and the grid reference voltage at the PCC. As a result of this, the output power of a DG can be controlled directly by what is known as frequency and voltage droop controllers [110, 111].

8.2 Problem Formulation

8.2.1 Hierarchical Control of Distributed Generators

Consider a network of VSI operated N DG units with the primary, secondary and other internal controllers shown in Fig. 8.3. We note here that the nonlinear dynamics of the DG units are formulated in its own direct-quadrature reference frame $d-q$ of the inverter, which rotates anticlockwise with an angular frequency ω_i. One of the inverter reference frames is chosen to be a common reference frame and let ω_{com} be its frequency of rotation. Then the relative angle of the i^{th} inverter reference frame is calculated with respect to the common reference frame as follows

$$\dot{\delta}_i = \omega_i - \omega_{\text{com}}. \tag{8.2}$$

The primary controller inside the power controller block in Fig. 8.3 implements two droop based feedback control laws (8.3) to set the reference terminal voltage V_{oi}^* and inverter frequency ω_i as follows

$$\omega_i = \omega_{n_i} - m_{P_i} P_i,\ V_{oi}^* = V_{n_i} - n_{Q_i} Q_i, \tag{8.3}$$

where ω_{n_i} and V_{n_i} are respectively the nominal frequency and voltage set points, m_{P_i} and n_{Q_i} are the droop coefficients selected in such a way that

$$m_{P_i} P_{\max,i} = m_{P_j} P_{\max,j},\ n_{Q_i} Q_{\max,i} = n_{Q_j} Q_{\max,j} \tag{8.4}$$

with $P_{\max,i}$, $Q_{\max,i}$ being respectively the rated active and reactive power capacities of i^{th} DG. From the droop characteristics in (8.3), it is clear that an increase in load demand results in a corresponding decrease in ω_i and V_{oi}^* from their prespecified nominal values. This droop based control techniques enable a balanced power sharing among the DGs, yet without requiring any direct communication from one to the other.

This droop technique emulates the governor characteristics of a synchronous generator in traditional power systems where an increased load demand is met by reducing the rotational frequency (speed) of the generator. This droop characteristic then allows the synchronous generators or the VSIs, running in parallel, to share the additional load in proportion to their power rating (8.4).

With no loss of generality, let V_{ni} be the nominal set point output voltage along its own direct axis, then the primary voltage control strategy aligns $V_{oi}^* = V_{ni} - n_{Q_i} Q_i$ along the direct axis of the inverter reference frame as follows

$$\begin{aligned} \omega_i &= \omega_{n_i} - m_{P_i} P_i, \\ V_{odi}^* &= V_{oi}^* = V_{ni} - n_{Q_i} Q_i,\ V_{oqi}^* = 0. \end{aligned} \tag{8.5}$$

As shown in Fig. 8.3, the voltage controller receives this reference voltage set points $\begin{bmatrix} V_{odi}^* & V_{oqi}^* \end{bmatrix}^{\mathrm{T}}$ from the power controller and generates the reference current set points $\begin{bmatrix} I_{Ldi}^* & I_{Lqi}^* \end{bmatrix}^{\mathrm{T}}$ to be tracked by the current controller [94,96,112]. The current controller receives the unfiltered feedback current signal $\begin{bmatrix} I_{Ldi} & I_{Lqi} \end{bmatrix}^{\mathrm{T}}$ from the VSI, their respective reference set points from the voltage controller as inputs and produces the reference DC voltage $\begin{bmatrix} V_{Idi}^* & V_{Iqi}^* \end{bmatrix}^{\mathrm{T}}$ for the DC to AC converter shown in Figure 8.3.

As noted in [93, 104], the voltage and current controller works much faster as compared to the power controller and therefore we can neglect the fast dynamics of the voltage and current controller and rewrite (8.5) as follows

$$\begin{aligned} \omega_i &= \omega_{n_i} - m_{P_i} P_i, \\ V_{odi} &= V_{ni} - n_{Q_i} Q_i, \ V_{oqi} = 0. \end{aligned} \tag{8.6}$$

The downside of this droop control is that the voltage V_{odi} and frequency ω_i of the DG unit deviate from their respective grid reference points V_{ref} and ω_{ref} and thus to restore the MG to the normal operating condition, another layer of control called secondary control is required [96, 101, 112]. Secondary control changes the auxillary input variable ω_{ni} and V_{ni} such that ω_i and V_{odi} synchronizes with the respective reference values ω_{ref} and V_{ref}. To avoid the single point of failure associated with the centralized control structure [113], a distributed cooperative control and coordination protocol was developed for the secondary control layer in the works of [112] which allows the DG units to rely only on the local communication from their neighbors as depicted in Figure 8.3.

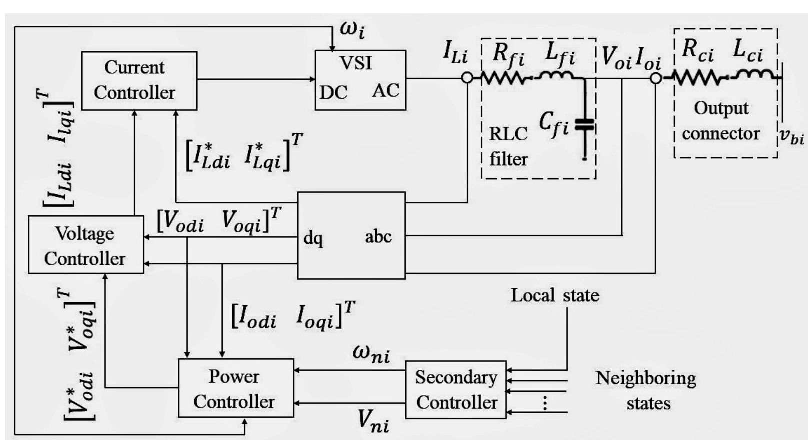

Figure 8.3: Block diagram of a DG with VSI and other internal controllers

8.2.2 Dynamic Model of Inverter Based DGs

In this work we consider the large signal nonlinear dynamical models of the DG, network and loads unlike [94, 112]. Similar to [96], we assume that the DC voltage source of the inverter is ideal. Furthermore, for simplicity we also neglect the switching processes involved with the pulse width modulation (PWM) in an inverter, as the switching frequency of PWM is much larger (4 kHz-10 kHz) as compared to the other control processes in the DG.

We also note here that the nonlinear dynamics of the DG units are formulated in its own $(d-q)_i$ reference frame of the inverter, which rotates anticlockwise with an angular frequency ω_i shown in Figure 8.4. One of the inverter reference frames is chosen to be a common reference frame $(D-Q)$ and let ω_{com} be its frequency of rotation. The inputs/outputs to a DG, network and load dynamics expressed in local $(d-q)_i$ coordinates can then be translated to the $(D-Q)$ coordinate by the transformation

$$T_i = \begin{bmatrix} \cos(\delta_i) & -\sin(\delta_i) \\ \sin(\delta_i) & \cos(\delta_i) \end{bmatrix}, \tag{8.7}$$

where δ_i, as shown in Fig. 8.4 is the shifted angle of the $(d-q)_i$ coordinate frame relative to $(D-Q)$.

Next we will revisit the dynamical models of the various components of the MG namely DG, networks, loads and their submodules.

8.2.3 Power Controller

Power controller calculates the instantaneous active and reactive power output P_i and Q_i as follows

$$\begin{aligned} \dot{P}_i &= -\omega_{ci} P_i + \omega_{ci} \left[V_{odi} I_{odi} + V_{oqi} I_{oqi} \right], \\ \dot{Q}_i &= -\omega_{ci} Q_i + \omega_{ci} \left[V_{oqi} I_{odi} - V_{odi} I_{oqi} \right], \end{aligned} \tag{8.8}$$

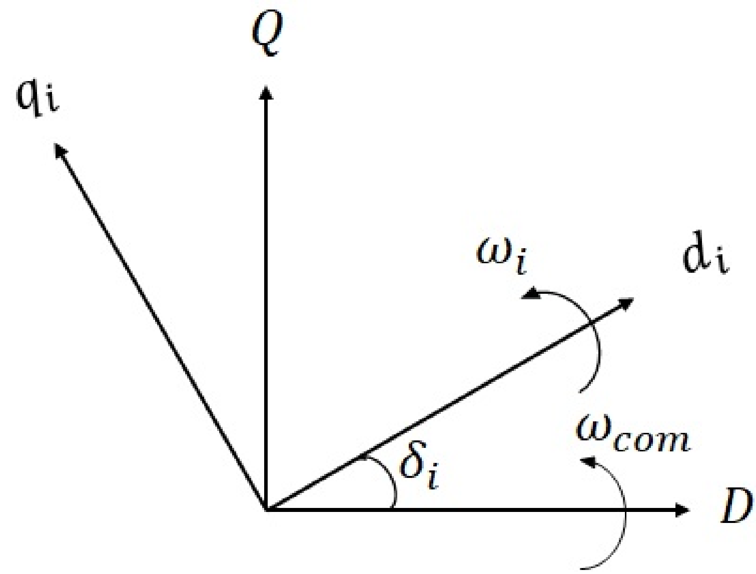

Figure 8.4: local $(d-q)_i$ to common $(D-Q)$ coordinate frame transformation

where ω_{ci} is the cut-off frequency of the low pass filters to remove the high frequency distortion by PWM switching, $V_{odi}, V_{oqi}, I_{odi}, I_{oqi}$ are respectively the direct and quadrature components of the three phase inverter voltage V_{oi} and current I_{oi}.

As noted earlier, the primary controller inside the power controller block implements two droop based feedback control laws (8.3) to set the reference terminal voltage V_{oi}^* and inverter frequency ω_i.

8.2.4 Voltage and Current Controller

The voltage controller receives the reference voltage set points $\begin{bmatrix} V_{odi}^* & V_{oqi}^* \end{bmatrix}^{\mathrm{T}}$ from the power controller. A traditional output voltage control ($V_{odi} \rightarrow V_{odi}^*$) as noted in [94, 96, 112] is achieved with a proportional-integral (PI) control structure and generates the reference current set points $\begin{bmatrix} I_{Ldi}^* & I_{Lqi}^* \end{bmatrix}^{\mathrm{T}}$ to be tracked by the current controller.

The current controller on the other hand receives the unfiltered feedback current signal $\begin{bmatrix} I_{Ldi} & I_{Lqi} \end{bmatrix}^{\mathrm{T}}$ from the VSI, their respective reference set points noted above from the voltage controller as inputs and produces the reference DC voltage $\begin{bmatrix} V_{Idi}^* & V_{Iqi}^* \end{bmatrix}^{\mathrm{T}}$

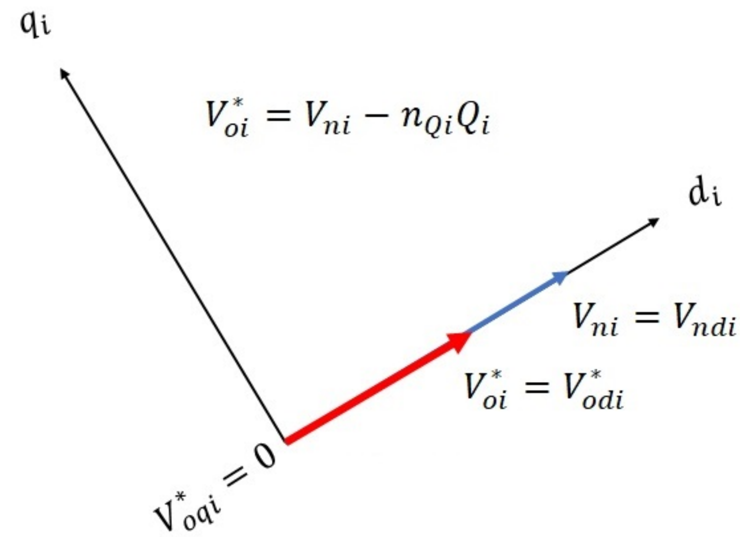

Figure 8.5: Reference terminal voltage V_{oi}^* aligned on d_i axis

for the DC to AC converter shown in Figure 8.3. Just like the voltage controller, the current controller also adopts a PI control structure to achieve the current regulation ($I_{Li} \to I_{Li}^*$).

To get a complete dynamical state space model of the voltage and current controllers, interested readers are referred to [94, 96]. Since we also do not consider the VSI switching dynamics because of its negligible time constant compared to that of the internal controllers and output filters, in the dynamics of coupling RLC filers and output connectors we can safely use $V_{Idi} = V_{Idi}^*$ and $V_{Iqi} = V_{Iqi}^*$.

8.2.5 Output Filters and Connectors

Output LC filters and connectors at the DG terminal yield the following differential equations

$$\dot{I}_{Ldi} = -\frac{R_{fi}}{L_{fi}} I_{Ldi} + \omega_i I_{Lqi} + \frac{1}{L_{fi}}(V_{Idi} - V_{odi}), \tag{8.9}$$

$$\dot{I}_{Lqi} = -\frac{R_{fi}}{L_{fi}} I_{Lqi} - \omega_i I_{Ldi} + \frac{1}{L_{fi}}(V_{Iqi} - V_{oqi}), \tag{8.10}$$

$$\dot{V}_{odi} = \omega_i V_{oqi} + \frac{1}{C_{fi}}(I_{Ldi} - I_{odi}), \tag{8.11}$$

$$\dot{V}_{oqi} = -\omega_i V_{odi} + \frac{1}{C_{fi}}(I_{Lqi} - I_{oqi}), \tag{8.12}$$

$$\dot{I}_{odi} = -\frac{R_{ci}}{L_{ci}} I_{odi} + \omega_i I_{oqi} + \frac{1}{L_{ci}}(V_{odi} - V_{bdi}), \tag{8.13}$$

$$\dot{I}_{oqi} = -\frac{R_{ci}}{L_{ci}} I_{oqi} - \omega_i I_{odi} + \frac{1}{L_{ci}}(V_{oqi} - V_{bqi}), \tag{8.14}$$

where $R_{ci}, L_{ci}, V_{bdi}, V_{bqi}$ are respectively the coupling resistance, inductance, direct and quadrature components of the bus voltage. By defining the state vector $x_i = \begin{bmatrix} \delta_i & P_i & Q_i & I_{Ldi} & I_{Lqi} & V_{odi} & V_{oqi} & I_{odi} & I_{oqi} \end{bmatrix}^{\mathrm{T}}$ the Eqs. (8.2), (8.8), (8.6) - (8.14) can be augmented to obtain the large signal dynamical model of a DG in compact state space form as follows

$$\begin{aligned} \dot{x}_i &= f_i(x_i) + g_i u_i^{\text{dist}} + k_i(x_i) u_i, \\ y_i &= h_i(x_i) + D_i u_i, \end{aligned} \tag{8.15}$$

where $u_i^{\text{dist}} = \begin{bmatrix} \omega_{\text{com}} & V_{bdi} & V_{bqi} \end{bmatrix}^{\mathrm{T}}$, u_i and y_i are respectively the control input and output vectors, and the detailed expressions for $f_i(x_i), g_i, k_i(x_i), h_i(x_i)$ and D_i can be deduced directly from Eqs. (8.2) - (8.14).

To connect a DG with other neighboring DGs, networks and loads we first need to transform the inputs and outputs to a DG expressed in local coordinates to that in the common $(D-Q)$ coordinate by the transformation T_i in (8.7).

8.2.6 Network Model and Loads

The schematic diagram for the network model and loads is shown in Figure 8.6 where the bus voltages, injected current to the i^{th} PCC, line current between buses i and j, injected current into load $Z_{\text{Load},i} = R_{\text{Load},i} + j\omega_{\text{com}} L_{\text{Load},i}$ are respectively denoted by $V_{bi}, I_{oi}, I_{\text{Line},ij}, I_{\text{Load},i}$. The state equations of the line current $I_{\text{Line},ij}$ between the buses i and j and the load current $I_{\text{Load},i}$ expressed on a common reference frame are given as follows

$$\dot{I}_{\text{LineD},ij} = \omega_{\text{com}} I_{\text{LineQ},ij} + \frac{\Delta\tilde{V}_{bD,ij}}{L_{\text{Line},ij}}, \tag{8.16}$$

$$\dot{I}_{\text{LineQ},ij} = -\omega_{\text{com}} I_{\text{LineD},ij} + \frac{\Delta\tilde{V}_{bQ,ij}}{L_{\text{Line},ij}}, \tag{8.17}$$

$$\dot{I}_{\text{LoadD},i} = \omega_{\text{com}} I_{\text{LoadQ},i} - \frac{R_{\text{Load},i}}{L_{\text{Load},i}} I_{\text{LoadD},i} + \frac{V_{bDi}}{L_{\text{Load},i}}, \tag{8.18}$$

$$\dot{I}_{\text{LoadQ},i} = -\omega_{\text{com}} I_{\text{LoadD},i} - \frac{R_{\text{Load},i}}{L_{\text{Load},i}} I_{\text{LoadQ},i} + \frac{V_{bQi}}{L_{\text{Load},i}}, \tag{8.19}$$

with $\Delta V_{bD,ij} = V_{bDi} - V_{bDj}$, $\Delta V_{bQ,ij} = V_{bQi} - V_{bQj}$, $\Delta\tilde{V}_{bD,ij} = \Delta V_{bD,ij} - R_{\text{Line},ij} I_{\text{LineD},ij}$ and $\Delta\tilde{V}_{bQ,ij} = \Delta V_{bQ,ij} - R_{\text{Line},ij} I_{\text{LineQ},ij}$.

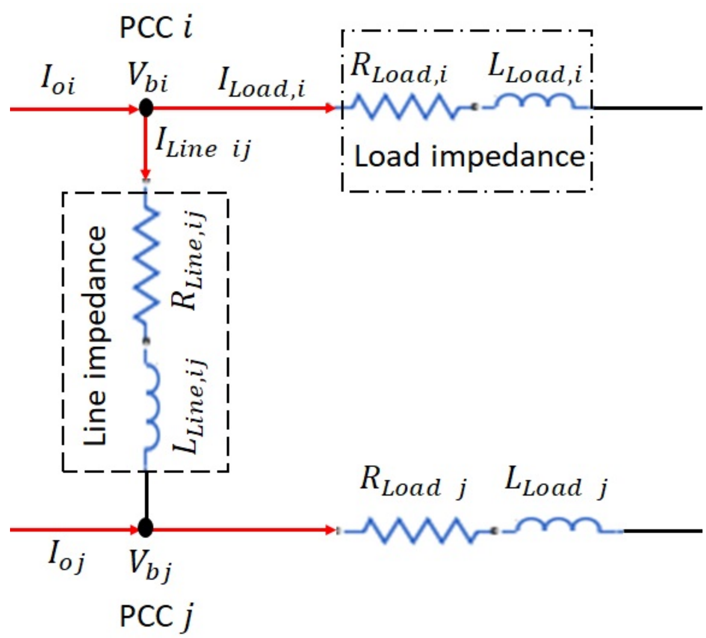

Figure 8.6: Network representation between two adjoining buses i and j

The objective of this synchronization problem is to design a cooperative secondary control law $u_i = V_{ni}$ (or ω_{ni}) in (8.3) such that $V_{odi} \to V_{\text{ref}}$ (or $\omega_i \to \omega_{\text{ref}}$). By using the feedback linearization method in [93] we obtain a desired linear relation between

$\dot{V}_{odi}$ (or $\dot{\omega}_i$) and auxiliary control inputs u_{Vi} (or $u_{\omega i}$) as follows

$$\dot{V}_{odi} = u_{Vi}, \; \dot{\omega}_i = u_{\omega i}. \tag{8.20}$$

Once we design the control law u_{Vi} (or $u_{\omega i}$) to render $V_{odi} \to V_{\text{ref}}$ (or $\omega_i \to \omega_{\text{ref}}$), then from (8.20) we can compute the required form of V_{ni} (or ω_{ni}) as

$$V_{ni}(t) = \int_0^t (u_{Vi}(s) + n_{Q_i}\dot{Q}_i(s)) \; ds, \tag{8.21}$$

$$\omega_{ni}(t) = \int_0^t (u_{\omega i}(s) + m_{P_i}\dot{P}_i(s)) \; ds. \tag{8.22}$$

A consensus based distributed cooperative control algorithm for constructing u_{Vi} (or $u_{\omega i}$) was developed in [93, 96, 112] to achieve a satisfactory synchronization performance for the delay free communication between the DGs. In this work we consider that the communication from the DG units is subject to an arbitrary large heterogeneous time-varying latency unlike [104, 105, 107].

8.2.7 Latency in Synchronization over a Deterministic Network

Let $\mathcal{G}$ be the digraph representing the communication topology of the DGs and $\tau_{ij}(t)$ be the latency in the communication between DG i and DG $j \in \mathcal{N}_i$. In the context of multi-agent cooperative control, N DGs along with the grid set-points can be viewed as a leader-follower multi-agent system with the reference grid operating point being the leader signal and N DGs as followers. Let the leader node be designated as zeroth node and the followers as $i = I[1, N]$, then the digraph $\bar{\mathcal{G}} = \mathcal{G} \cup (0, \{e_{i0}\})$ represents the network of $N+1$ agents.

Since the local communication between the DG units is now inflicted with some latencies, our proposed cooperative control structure explicitly accounts for the delay in the coordination and control protocol. For a deterministic network where the communication latencies can be precisely recorded, the distributed control law u_{Vi} (or $u_{\omega i}$) for N DGs can be designed as follows

$$\begin{aligned} u_{Vi} = \mu \sum_{j\in\mathcal{N}_i} a_{ij} \left[V_{odj}(t-\tau_{ij}(t)) - V_{odi}(t-\tau_{ij}(t))\right] \\ + \mu a_{i0}\left[V_{\text{ref}}(t-\tau_{i0}(t)) - V_{odi}(t-\tau_{i0}(t))\right], \end{aligned} \tag{8.23}$$

$$\begin{aligned} u_{\omega i} = \mu \sum_{j\in\mathcal{N}_i} a_{ij} \left[\omega_j(t-\tau_{ij}(t)) - \omega_i(t-\tau_{ij}(t))\right] \\ + \mu a_{i0}\left[\omega_{\text{ref}}(t-\tau_{i0}(t)) - \omega_i(t-\tau_{i0}(t))\right], \end{aligned} \tag{8.24}$$

where $a_{ij} > 0$ is the weighting factor for the communication link between nodes j and i, a_{i0} is the pinning gain of the edge connecting the node i to the reference, $\tau_{ij}(t) : \mathbb{R}^+ \to \mathbb{R},\ j = I[0,N]$ is continuous time varying communication delay with the delay range $\bar{\tau}$ such that $\tau_{ij}(t) \in [0,\bar{\tau}]$ and μ is the low gain parameter to be determined. The "low gain" parameters are commonly found in the Truncated Predictor Feedback (TPF) control solution for time delayed systems [72]. For the sake of brevity, we will use $\tau_{ij},\ j = 0,1,\cdots,N$ in place for $\tau_{ij}(t)$ for the rest of the text.

For $\bar{\tau} = \max(\tau_{ij}),\ i = I[1,N],\ j = I[0,N]$ with $j \neq i$, and $\theta \in [-\bar{\tau},0]$ let the initial conditions $V_{\text{ref}}(\theta) = \mathbf{V}_{\text{ref}}(\theta)$ and $V_{odi}(\theta) = \mathbf{V}_i(\theta)$, where $\mathbf{V}_{\text{ref}}, \mathbf{V}_i \in \mathcal{C}([-\bar{\tau},0],\mathbb{R})$. Denote the disagreement error $\tilde{V}_i = V_{odi} - V_{\text{ref}}$, $\tilde{\omega}_i = \omega_i - \omega_{\text{ref}}$ with $\tilde{V}_i(\theta) = \tilde{\mathbf{V}}_i(\theta)$, $\tilde{\omega}_i(\theta) = \tilde{\boldsymbol{\omega}}_i(\theta)$ where $\tilde{\mathbf{V}}_i(\theta),\ \tilde{\boldsymbol{\omega}}_i(\theta) \in \mathcal{C}([-\bar{\tau},0],\mathbb{R})$. By substituting (8.23) (or (8.24)) into (8.20), the voltage (or frequency) error dynamics can then be obtained as follows

$$\dot{\tilde{V}}_i = \mu \sum_{j=1}^{N} a_{ij}[\tilde{V}_j(t-\tau_{ij}) - \tilde{V}_i(t-\tau_{ij})] - \mu a_{i0}\tilde{V}_i(t-\tau_{i0}), \tag{8.25}$$

$$\dot{\tilde{\omega}}_i = \mu \sum_{j=1}^{N} a_{ij}[\tilde{\omega}_j(t-\tau_{ij}) - \tilde{\omega}_i(t-\tau_{ij})] - \mu a_{i0}\tilde{\omega}_i(t-\tau_{i0}), \tag{8.26}$$

We need the following assumption to guarantee the solvability of the consensus problem.

Assumption 8.2.1. *The digraph $\bar{\mathcal{G}}$ contains a spanning tree with the leader node being the root.*

Remark 8.2.1. *The Laplacian matrix $\bar{\mathcal{L}}$ of $\bar{\mathcal{G}}$ can be partitioned as*

$$\bar{\mathcal{L}} = \left[\begin{array}{c|c} 0 & [0]_{1\times N} \\ \hline G\mathbf{1}_N & H \end{array}\right], \tag{8.27}$$

where $H = \mathcal{L} + G$ with $\mathcal{L}$ being the Laplacian matrix corresponding to the digraph $\mathcal{G}$ and G being a diagonal matrix with the diagonal elements a_{i0}, $i = I[1,N]$. By Assumption 8.2.1 and Lemma 2 of [114], $\bar{\mathcal{L}}$ has a simple zero eigenvalue. Furthermore, by Assumption 8.2.1 and Lemma 1 of [29], the matrix H is nonsingular and has eigenvalues with positive real parts. Therefore $-H$ is a Hurwitz matrix.

Let us denote $\tilde{V} = \mathrm{col}(\tilde{V}_1, \tilde{V}_2, \cdots, \tilde{V}_N)$, $\tilde{\mathbf{V}} = \mathrm{col}(\tilde{\mathbf{V}}_1, \tilde{\mathbf{V}}_2, \cdots, \tilde{\mathbf{V}}_N)$, $\tilde{\omega} = \mathrm{col}(\tilde{\omega}_1, \tilde{\omega}_2, \cdots, \tilde{\omega}_N)$, and $\tilde{\boldsymbol{\omega}} = \mathrm{col}(\tilde{\boldsymbol{\omega}}_1, \tilde{\boldsymbol{\omega}}_2, \cdots, \tilde{\boldsymbol{\omega}}_N)$. Now we are ready to define the problem statement as follows.

Given a digraph $\mathcal{G}$ of N networked agents with linearized dynamics (8.20) and the auxiliary control u_{Vi} (or $u_{\omega i}$) in (8.23) (or (8.24)), the objective of the studied synchronization problem is to design a feedback gain μ such that the error dynamics (8.25) (or (8.26)) is globally asymptotically stable, *i.e.*, for a constant delay bound $\bar{\tau} > 0$ and $\tilde{\mathbf{V}}(\theta)$ (or $\tilde{\boldsymbol{\omega}}(\theta)$) $\in \mathcal{C}([-\bar{\tau}, 0], \mathbb{R}^N)$, $\lim_{t\to\infty} \tilde{V}(t) = 0$ (or $\lim_{t\to\infty} \tilde{\omega}(t) = 0$).

8.3 Main Result

In this section, we present the stability results of the synchronization error dynamics in (8.25) and (8.26), which will eventually lead to the design of our low gain parameter μ. The current work provides an upper bound of μ to ensure the stability of the error dynamics. The stability results are also extended to the case where τ_{ij} and τ_{i0} are not known in the control.

To demonstrate the convergence of the error dynamics (8.25) (or (8.26)) with communication delays $\tau_{ij},\ i = I[1,N], j = I[0,N], i \neq j$, first we evaluate the boundedness of the response for $t \leq \bar{\tau}$ before the delayed measurements are available for feedback correction.

For $t = 0^+$, from (8.25) we obtain

$$\begin{aligned}
\|\dot{\tilde{V}}_i\|_{t=0^+} &\leq \mu \left(\sum_{j=1}^{N} a_{ij} |\tilde{\mathbf{V}}_j(-\tau_{ij})\| \right) + \mu |\mathcal{N}_i| \|\tilde{\mathbf{V}}_i(-\tau_{ij})\| \\
&\quad + \mu \|\tilde{\mathbf{V}}_i(-\tau_{i0})\|, \\
&\leq \mu \sum_{j=1}^{N} \|\tilde{\mathbf{V}}_j(-\tau_{ij})\| + \mu |\mathcal{N}_i| \|\tilde{\mathbf{V}}_i(-\tau_{ij})\| + \mu \|\tilde{\mathbf{V}}_i(-\tau_{i0})\|, \\
&\leq \mu (2|\mathcal{N}_i| + 1) \|\tilde{\mathbf{V}}_0\|_{\mathcal{C}}
\end{aligned} \tag{8.28}$$

where $\|\tilde{\mathbf{V}}_0\|_{\mathcal{C}} = \max_{\theta \in [-\bar{\tau}, 0]} \|\tilde{\boldsymbol{V}}_i(\theta)\|,\ i = I[1,N]$ and $|\mathcal{N}_i|$ is the cardinality of the set $\mathcal{N}_i$. Since $\dot{\tilde{V}}_i$ is bounded at $t = 0^+$, then for an arbitrarily small positive scalar ε, the error vector $\tilde{V}_i$ also remains bounded in the interval $[0, \varepsilon]$. By using this result and exploiting the boundedness of $\tilde{\mathbf{V}}_i(\theta),\ \theta \in [-\bar{\tau}, 0]$, from (8.25) we can again find that $\|\dot{\tilde{V}}_i\|_{t=\varepsilon^+}$ is bounded and so is $\tilde{V}_i(t)$ for $t \in [\varepsilon, 2\varepsilon]$. In an inductive manner, we find that $\tilde{V}_i(t)$ is bounded across each subintervals $[(k-1)\varepsilon, k\varepsilon],\ k = I[0,m]$ with $m \in \mathbb{Z}^+,\ m\varepsilon = \bar{\tau}$. Following the steps shown above, $\tilde{\omega}_i(t)$ in (8.26) can also be shown to be bounded within the interval $[0, \bar{\tau}]$.

Once the boundedness of the initial response is obtained, we then proceed to derive the asymptotic stability conditions of (8.25) in Section 8.3.1 and (8.26) in Section 8.3.2 for $t > \bar{\tau}$.

8.3.1 Stability of the Voltage Synchronization Error Dynamics

Let us define two auxiliary variables $\bar{\delta}_{ij}(t), j = I[1,N]$, and $\hat{\delta}_{ij}(t),\ j = I[0,N]$, $i \neq j$ as follows

$$\bar{\delta}_{ij}(t) = \tilde{V}_j(t-\tau_{ij}) - \tilde{V}_j(t) = -\int_{t-\tau_{ij}}^{t} \dot{\tilde{V}}_j(s)\ ds, \tag{8.29}$$

$$\hat{\delta}_{ij}(t) = \tilde{V}_i(t) - \tilde{V}_i(t-\tau_{ij}) = \int_{t-\tau_{ij}}^{t} \dot{\tilde{V}}_i(s)\ ds. \tag{8.30}$$

By substituting $\tilde{V}_j(t-\tau_{ij})$, $\tilde{V}_i(t-\tau_{ij})$, $\tilde{V}_i(t-\tau_{i0})$ in (8.25) with $\bar{\delta}_{ij}(t)$ and $\hat{\delta}_{ij}(t)$ defined above, we can rewrite (8.25) as

$$\dot{\tilde{V}}_i = \mu \sum_{j=1}^{N} a_{ij}(\tilde{V}_j - \tilde{V}_i) - \mu a_{i0}\tilde{V}_i + \mu(\bar{\delta}_i + \hat{\delta}_i + a_{i0}\hat{\delta}_{i0}), \tag{8.31}$$

where $\bar{\delta}_i = \sum_{j=1}^{N} a_{ij}\bar{\delta}_{ij},\ \hat{\delta}_i = \sum_{j=1}^{N} a_{ij}\hat{\delta}_{ij}$. The augmented error dynamics then becomes

$$\dot{\tilde{V}} = -\mu H \tilde{V} + \mu(\bar{\delta} + \hat{\delta}) + \mu G \hat{\delta}_0, \tag{8.32}$$

with $\bar{\delta} = \mathrm{col}(\bar{\delta}_1, \bar{\delta}_2, \cdots, \bar{\delta}_N),\ \hat{\delta} = \mathrm{col}(\hat{\delta}_1, \hat{\delta}_2, \cdots, \hat{\delta}_N)$, and $\hat{\delta}_0 = \mathrm{col}(\hat{\delta}_{10}, \hat{\delta}_{20}, \cdots, \hat{\delta}_{N0})$.

To analyze the stability of (8.32), we construct an energy function of the form $\mathbb{V}_0 = \tilde{V}^{\mathrm{T}} P \tilde{V}$ where $P \in \mathbb{R}^{N\times N}$ is a positive definite matrix. Since P is symmetric and has all positive eigenvalues,

$$0 \leq \lambda_{\min}(P)\|\tilde{V}\|^2 \leq \mathbb{V}_0 \leq \lambda_{\max}(P)\|\tilde{V}\|^2,\ \tilde{V} \neq 0.$$

By differentiating $\mathbb{V}_0$ along the trajectories of (8.32) we obtain

$$\dot{\mathbb{V}}_0 = \dot{\tilde{V}}^{\mathrm{T}} P \tilde{V} + \tilde{V}^{\mathrm{T}} P \dot{\tilde{V}} = -\mu \tilde{V}^{\mathrm{T}}[H^{\mathrm{T}} P + P H]\tilde{V} + 2\mu(\bar{\delta}^{\mathrm{T}} P \tilde{V} + \hat{\delta}^{\mathrm{T}} P \tilde{V} + \hat{\delta}_0^{\mathrm{T}} G P \tilde{V}),$$

$$\leq \mu \tilde{V}^{\mathrm{T}}(H_1^{\mathrm{T}}P + PH_1 + 3)\tilde{V} + \mu\lambda_{\max}^2(P)(\bar{\delta}^{\mathrm{T}}\bar{\delta} + \hat{\delta}^{\mathrm{T}}\hat{\delta} + \hat{\delta}_0^{\mathrm{T}}G^2\hat{\delta}_0). \tag{8.33}$$

The positive definite matrix P in (8.33) is obtained to satisfy the following Lyapunov equation

$$H_1^{\mathrm{T}}P + PH_1 = -\beta I_N,\ \beta > 0. \tag{8.34}$$

For any $\beta > 0$, a corresponding positive definite solution P in (8.34) can always be found since $H_1 = -H$ is a Hurwitz matrix by Remark 8.2.1. Furthermore, the matrix G^2 in (8.33) is a diagonal matrix with elements a_{i0}^2 and therefore $\lambda_{\max}(G^2) = d_0^2$, where $d_0 = \max(a_{10}, a_{20}, \cdots, a_{N0})$. By substituting these results into Equation (8.33) we obtain

$$\dot{\mathbb{V}}_0 \leq \mu(-\beta+3)\tilde{V}^{\mathrm{T}}\tilde{V} + \mu\lambda_{\max}^2(P)(\bar{\delta}^{\mathrm{T}}\bar{\delta} + \hat{\delta}^{\mathrm{T}}\hat{\delta} + d_0^2\hat{\delta}_0^{\mathrm{T}}\hat{\delta}_0). \tag{8.35}$$

Since $\bar{\delta}^{\mathrm{T}}\bar{\delta} = \sum_{i=1}^{N}\bar{\delta}_i^{\mathrm{T}}\bar{\delta}_i$ with $\bar{\delta}_i$ defined in (8.31), then by using the Young's inequality for products

$$2\bar{\delta}_{ij}a_{ij}a_{ik}\bar{\delta}_{ik} \leq \frac{1}{\alpha_0}a_{ij}^2\|\bar{\delta}_{ij}\|^2 + \alpha_0 a_{ik}^2\|\bar{\delta}_{ik}\|^2,\ \alpha_0 > 0 \tag{8.36}$$

we obtain $\bar{\delta}^{\mathrm{T}}\bar{\delta} \leq (N-1)\sum_{i=1}^{N}\sum_{j=1}^{N}a_{ij}^2\|\bar{\delta}_{ij}\|^2$. Next, with an extension of the Jensen inequality presented in Lemma 1 of [115] we obtain

$$\bar{\delta}^{\mathrm{T}}\bar{\delta} \leq (N-1)\bar{\tau}d_{\mathrm{out}}^2\left[\int_{t-\bar{\tau}}^{t}\dot{\tilde{V}}^{\mathrm{T}}(s)\dot{\tilde{V}}(s)\ ds\right], \tag{8.37}$$

where d_{out} is the maximum out-degree of nodes in digraph $\mathcal{G}$. In a similar manner $\hat{\delta}^{\mathrm{T}}\hat{\delta}$ and $\hat{\delta}_0^{\mathrm{T}}\hat{\delta}_0$ in (8.35) yields

$$\begin{aligned} \hat{\delta}^{\mathrm{T}}\hat{\delta} &\leq (N-1)\bar{\tau}d_{\mathrm{in}}^2\left[\int_{t-\bar{\tau}}^{t}\dot{\tilde{V}}^{\mathrm{T}}(s)\dot{\tilde{V}}(s)\right], \\ \hat{\delta}_0^{\mathrm{T}}\hat{\delta}_0 &\leq \bar{\tau}\int_{t-\bar{\tau}}^{t}\dot{\tilde{V}}^{\mathrm{T}}(s)\dot{\tilde{V}}(s)ds, \end{aligned} \tag{8.38}$$

with d_{in} be the maximum in-degree of nodes in $\mathcal{G}$. Let us now consider a functional of the form $\mathbb{V}_1 = \int_0^{\bar{\tau}} \int_{t-s}^{t} \dot{\tilde{V}}^{\mathrm{T}}(\sigma)\dot{\tilde{V}}(\sigma)\, d\sigma\, ds$. Then from (8.37) and (8.38), we obtain

$$\bar{\delta}^{\mathrm{T}}\bar{\delta} + \hat{\delta}^{\mathrm{T}}\hat{\delta} + d_0^2\hat{\delta}_0^{\mathrm{T}}\hat{\delta}_0 \leq c_0\bar{\tau}^2\dot{\tilde{V}}^{\mathrm{T}}\dot{\tilde{V}} - c_0\bar{\tau}\dot{\mathbb{V}}_1, \tag{8.39}$$

where $c_0 = (N-1)d_{\text{out}}^2 + (N-1)d_{\text{in}}^2 + d_0^2$. By using an inequality similar to (8.36), from (8.32) we deduce $\dot{\tilde{V}}^{\mathrm{T}}\dot{\tilde{V}}$ as follows

$$\dot{\tilde{V}}^{\mathrm{T}}\dot{\tilde{V}} \leq 4\mu^2\Big(\tilde{V}^{\mathrm{T}}H^{\mathrm{T}}H\tilde{V} + \big(\bar{\delta}^{\mathrm{T}}\bar{\delta} + \hat{\delta}^{\mathrm{T}}\hat{\delta} + d_0^2\hat{\delta}_0^{\mathrm{T}}\hat{\delta}_0\big)\Big), \tag{8.40}$$

which after substitution in (8.39) yields

$$\bar{\delta}^{\mathrm{T}}\bar{\delta} + \hat{\delta}^{\mathrm{T}}\hat{\delta} + d_0^2\hat{\delta}_0^{\mathrm{T}}\hat{\delta}_0 \leq \frac{-c_0\bar{\tau}\dot{\mathbb{V}}_1 + 4\mu^2c_0\bar{\tau}^2\sigma_H\tilde{V}^{\mathrm{T}}\tilde{V}}{1 - 4\mu^2c_0\bar{\tau}^2}, \tag{8.41}$$

with $\sigma_H = \|H\|^2$. From (8.35), we thus obtain

$$\dot{\mathbb{V}}_0 \leq \mu(-\beta+3)\tilde{V}^{\mathrm{T}}\tilde{V} + \mu\lambda_{\max}^2(P)\left[\frac{-c_0\bar{\tau}\dot{\mathbb{V}}_1 + 4\mu^2c_0\bar{\tau}^2\sigma_H\tilde{V}^{\mathrm{T}}\tilde{V}}{1 - 4\mu^2c_0\bar{\tau}^2}\right]. \tag{8.42}$$

Next we present the main stability theorem of this work to derive an upper bound of the low gain parameter μ that in turn ensures the asymptotic convergence of $\tilde{V}(t)$ in face of arbitrary time varying communication delays τ_{ij} within the bound $[0, \bar{\tau}]$.

Theorem 8.3.1. *Consider the linearized subsystem dynamics* (8.20) *with the control protocol in* (8.23) *satisfying Assumption 8.2.1. For a scalar $\beta > 3$, let $P > 0$ be a solution to* (8.34). *Then for any arbitrary time-varying latency $\tau_{ij},\ j = I[0,N], j \neq i$ within the bound $[0, \bar{\tau}]$, the controlled subsystem state V_{odi} converges to V_{ref} asymptotically,* i.e., $\lim_{t\to\infty}(V_{odi}(t) - V_{ref}) = 0,\ i = I[1,N]$ *if the low gain parameter μ satisfies*

$\mu < \bar{\mu}$, *where*

$$\bar{\mu} = \frac{1}{2\bar{\tau}\sqrt{c_0}}\sqrt{\frac{\beta-3}{\sigma_H \lambda_{\max}^2(P)+(\beta-3)}},\ \beta > 3. \tag{8.43}$$

Proof. Let us consider a Lyapunov-Krasovskii functional of the form

$$\mathbb{V}_2 = \mathbb{V}_0 + \frac{\mu c_0 \lambda_{\max}^2(P)\bar{\tau}}{1-4\mu^2 c_0 \bar{\tau}^2}\mathbb{V}_1. \tag{8.44}$$

Then by differentiation and little rearrangement of terms in (8.42) we obtain

$$\dot{\mathbb{V}}_2 \le \mu\left[-\beta+3+\frac{4\mu^2 c_0 \bar{\tau}^2 \sigma_H \lambda_{\max}^2(P)}{1-4\mu^2 c_0 \bar{\tau}^2}\right]\|\tilde{V}\|^2. \tag{8.45}$$

Therefore $\dot{\mathbb{V}}_2 < 0$ if $\mu < \bar{\mu}$ with $\bar{\mu}$ defined in (8.43). Moreover for any $\beta > 3$, from (8.43) we notice that

$$4c_0\mu^2\bar{\tau}^2 < \frac{(\beta-3)}{\sigma_H \lambda_{\max}^2(P)+(\beta-3)} < 1$$

and as a result $\mathbb{V}_2$ in (8.44) is always positive except when $\tilde{V} = 0$ and $\dot{\tilde{V}}(t+\theta) = 0$, $\theta \in [-\bar{\tau}, 0]$. Furthermore, from (8.40) and (8.41), $\mathbb{V}_2$ is bounded between two non-decreasing functions thereby satisfying the first condition of the Lyapunov-krasovskii stability theorem [115]. Hence the synchronization error dynamics in (8.32) is globally asymptotically stable, *i.e.*, $\lim_{t\to\infty}\tilde{V}(t) = 0$. This concludes the proof. □

Remark 8.3.1. *From* (8.43) *we notice that a higher delay bound* $\bar{\tau}$ *will result in a corresponding lower gain* μ. *In other words, for any arbitrarily large* $\bar{\tau} > 0$, *there exists a unique upper bound* $\bar{\mu}$ *on* μ *such that for any* $\mu \in [0, \bar{\mu})$ (8.43) *is satisfied. This conclusion is same as that of the low gain based TPF control for time delayed systems [89].*

8.3.2 Stability of the Frequency Synchronization Error Dynamics

Given the linearized subsystem dynamics (8.20) with the cooperative frequency controller (8.26), by virtue of Theorem 8.3.1, the inverter frequency ω_i can be shown to be synchronized with ω_{ref} analogously. For the subsequent discussion in the chapter, we present only the stability results for the voltage synchronization as the analogous results for the frequency counterpart can be straightforwardly deduced.

8.3.3 Voltage Synchronization of Networked DGs under Unknown Communication Latency

Although deterministic networks enable nodes to synchronize their clocks and accurately track communication latencies, there are some practical instances where the communication delay may be unknown. In the following we consider such general case and demonstrate the effectiveness of a low gain based control to withhold stability even in the case of unknown time varying latencies. To do this, let us redefine the control protocol u_{Vi} as follows

$$u_{Vi} = \mu \sum_{j=1}^{N} a_{ij}[V_{odj}(t-\tau_{ij}) - V_{odi}(t)] + \mu a_{i0}[V_{\text{ref}}(t-\tau_{i0}) - V_{odi}(t)], \tag{8.46}$$

and from (8.20) the closed loop dynamics thus becomes

$$\begin{aligned}\dot{V}_{odi} &= \mu \sum_{j=1}^{N} a_{ij}[V_{odj}(t-\tau_{ij}) - V_{odi}(t)] + \mu a_{i0}[V_{\text{ref}}(t-\tau_{i0}) - V_{odi}(t)],\\ &= \mu \sum_{j=1}^{N} a_{ij}(V_{odj} - V_{odi}) + \mu \sum_{j=1}^{N} a_{ij}(V_{odj}(t-\tau_{ij}) - V_{odj})\\ &\quad + \mu a_{i0}(V_{\text{ref}}(t-\tau_{i0}) - V_{\text{ref}}) + \mu a_{i0}(V_{\text{ref}} - V_{odi}).\end{aligned} \tag{8.47}$$

By substituting $\tilde{V}_i = V_{odi} - V_{\mathrm{ref}}$, from (8.47), the synchronization error dynamics yields the following result,

$$\dot{\tilde{V}}_i = \mu\sum_{j=1}^{N} a_{ij}(\tilde{V}_j - \tilde{V}_i) + \mu\sum_{j=1}^{N} a_{ij}(\tilde{V}_j(t-\tau_{ij}) - \tilde{V}_j)$$
$$- \mu a_{i0}\tilde{V}_i + \mu\sum_{j=1}^{N} a_{ij}(V_{\mathrm{ref}}(t-\tau_{ij}) - V_{\mathrm{ref}}) + \mu a_{i0}(V_{\mathrm{ref}}(t-\tau_{i0}) - V_{\mathrm{ref}}). \tag{8.48}$$

Similar to the case in Section 8.3.1, first we evaluate the boundedness of $\tilde{V}_i(t)$ for $t \in [0, \bar{\tau}]$. With a little abuse of notation, let $\|\mathbf{V}_{\bar{\mathrm{ref}}}\|_{\mathcal{C}} = \max_{\theta\in[-\bar{\tau},0]} \|\mathbf{V}_{\mathrm{ref}}(\theta)\|$ and then from (8.48) we obtain

$$\|\dot{\tilde{V}}_i\|_{t=0} \leq \mu(4\mathcal{N}_i + 1)\|\tilde{\mathbf{V}}_0\|_{\mathcal{C}} + 2\mu(\mathcal{N}_i + 1)\|\mathbf{V}_{\bar{\mathrm{ref}}}\|_{\mathcal{C}}, \tag{8.49}$$

which shows that $\|\dot{\tilde{V}}_i\|$ is bounded at $t = 0$, and thus for an arbitrarily small scalar $\varepsilon > 0$, $\tilde{V}_i(t)$ is bounded within the interval $[0, \varepsilon]$. Continuing in same manner as in the previous case, we inductively evaluate that across each subintervals $[(k-1)\varepsilon, k\varepsilon],\ k = I[0, m]$, with $m\varepsilon = \bar{\tau}$, $\tilde{V}_i(t)$ is bounded. Next we investigate the asymptotic stability of the error dynamics (8.48) for $t > \bar{\tau}$.

Since V_{ref} is a constant DC signal for any $t > \bar{\tau}$, then regardless of the delay $\tau_{ij},\ j = I[0, N],\ i \neq j$, $V_{\mathrm{ref}}(t - \tau_{ij}) = V_{\mathrm{ref}}(t)$ and consequently from (8.48) we obtain

$$\dot{\tilde{V}}_i = \mu\sum_{j=1}^{N} a_{ij}(\tilde{V}_j - \tilde{V}_i) - \mu a_{i0}\tilde{V}_i + \mu\bar{\delta}_i, \tag{8.50}$$

with $\bar{\delta}_i$ being defined in (8.31). The composite error dynamics thus becomes

$$\dot{\tilde{V}} = \mu H_1\tilde{V} + \mu\bar{\delta}, \tag{8.51}$$

where $H_1 = -(\mathcal{L} + G)$. To analyze the stability, let us take an energy function of the form $\mathbb{V}_3 = \tilde{V}^{\mathrm{T}}\mathbf{P}\tilde{V}$ with $\mathbf{P} \in \mathbb{R}^{N\times N} > 0$ being a positive definite matrix solution to the equation

$$H_1^{\mathrm{T}}\mathbf{P}+\mathbf{P}H_1=-\beta_0 I_N, \beta_0>0. \tag{8.52}$$

Such a solution always exists since H_1 is a Hurwitz matrix. By differentiation of $\mathbb{V}_3$ along the trajectories of (8.51) we thus obtain

$$\begin{aligned}\dot{\mathbb{V}}_3 &= -\mu\beta_0\tilde{V}^{\mathrm{T}}\tilde{V}+2\mu\tilde{V}^{\mathrm{T}}P\bar{\delta} \le \mu(-\beta_0+1)\tilde{V}^{\mathrm{T}}\tilde{V}+\mu\bar{\delta}^{\mathrm{T}}\mathbf{P}^2\bar{\delta},\\ &\le \mu(-\beta_0+1)\tilde{V}^{\mathrm{T}}\tilde{V}+\mu\lambda_{\max}^2(\mathbf{P})\bar{\delta}^{\mathrm{T}}\bar{\delta}. \end{aligned}\tag{8.53}$$

With an upperbound of $\bar{\delta}^{\mathrm{T}}\bar{\delta}$ in (8.37) and the definition of $\mathbb{V}_1$ in (8.39), we can further evaluate $\bar{\delta}^{\mathrm{T}}\bar{\delta}$ in (8.53) as follows

$$\bar{\delta}^{\mathrm{T}}\bar{\delta} \le c_1\bar{\tau}^2\dot{\tilde{V}}^{\mathrm{T}}\dot{\tilde{V}}-c_1\bar{\tau}\dot{\mathbb{V}}_1, \tag{8.54}$$

where $c_1=(N-1)d_{\mathrm{out}}^2$. Similar to (8.40), along the trajectory of (8.51) we compute

$$\dot{\tilde{V}}^{\mathrm{T}}\dot{\tilde{V}} \le 2\mu^2(\sigma_H\tilde{V}^{\mathrm{T}}\tilde{V}+\bar{\delta}^{\mathrm{T}}\bar{\delta}),$$

which after substitution in (8.54) yields

$$\bar{\delta}^{\mathrm{T}}\bar{\delta} \le \frac{2c_1\mu^2\sigma_H\bar{\tau}^2}{1-2c_1\mu^2\bar{\tau}^2}\tilde{V}^{\mathrm{T}}\tilde{V}-\frac{c_1\bar{\tau}}{1-2c_1\mu^2\bar{\tau}^2}\dot{\mathbb{V}}_1. \tag{8.55}$$

Let us define

$$\mathbb{V}_4=\mathbb{V}_3+\frac{c_1\mu\lambda_{\max}^2(\mathbf{P})\bar{\tau}}{1-2c_1\mu^2\bar{\tau}^2}\mathbb{V}_1. \tag{8.56}$$

Then by substituting the results of (8.55) into (8.53) and a little rearrangement of terms, we obtain

$$\dot{\mathbb{V}}_4 \le \mu\Big(-\beta_0+1+\frac{2\mu^2\lambda_{\max}^2(\mathbf{P})\sigma_H\bar{\tau}^2c_1}{1-2\mu^2\bar{\tau}^2c_1}\Big)\|\tilde{V}\|^2. \tag{8.57}$$

We now present the following stability theorem which prescribes an upper bound for the low gain parameter μ to ensure the asymptotic convergence of the error state $\tilde{V}$ in (8.51).

Theorem 8.3.2. *Consider the linearized subsystem dynamics* (8.20) *with the control protocol in* (8.46) *satisfying Assumption 8.2.1. For a scalar $\beta_0 > 1$, let $\mathbf{P} > 0$ be a solution to* (8.52)*. Then for any arbitrary unknown time-varying latency τ_{ij}, $j = I[0,N], j \neq i$ within the bound $[0,\bar{\tau}]$, the controlled subsystem state V_{odi} in* (8.47) *converges to V_{ref} asymptotically,* i.e., $\lim_{t\to\infty}(V_{odi}(t) - V_{ref}) = 0,\ i = I[1,N]$ *if the low gain parameter μ satisfies $\mu < \bar{\boldsymbol{\mu}}$, where*

$$\bar{\boldsymbol{\mu}} = \frac{1}{\sqrt{2c_1}\bar{\tau}}\sqrt{\frac{\beta_0 - 1}{\sigma_H \lambda_{\max}^2(\mathbf{P}) + \beta_0 - 1}},\ \beta_0 > 1. \tag{8.58}$$

Proof. Given the energy functional $\mathbb{V}_4$ in (8.56) with its derivative in (8.57), by virtue of $\mu < \bar{\mu}$ with $\bar{\mu}$ in (8.58) and Lyapunov-Krasovskii stability theorem [115], the proof of Theorem 8.3.1 can be replicated with a very slight modification to obtain $\lim_{t\to\infty}\tilde{V}(t) = 0$. This concludes the proof. □

8.4 Illustrative Example

Consider a network of 4 DGs from [96] with the communication topology and per phase circuit diagram shown in Figure 8.7 and the DG, networks and load parameters listed below.

$$m_{P_i} = 9.4\times 10^{-5}, i = 1,2, m_{P_j} = 12.5\times 10^{-5},$$

$$n_{Q_i} = 1.3\times 10^{-3}, i = 1,2, n_{Q_j} = 1.5\times 10^{-3}, j = 3,4,$$

$$R_{c_i} = 0.3, L_{c_i} = 35.35\times 10^{-3}, R_{f_i} = 0.1, L_{f_i} = 2.25\times 10^{-3},$$

$$C_{f_i} = 50\times 10^{-6}, R_{Line,ij} = 0.23, L_{Line,21} = 318\times 10^{-6},$$

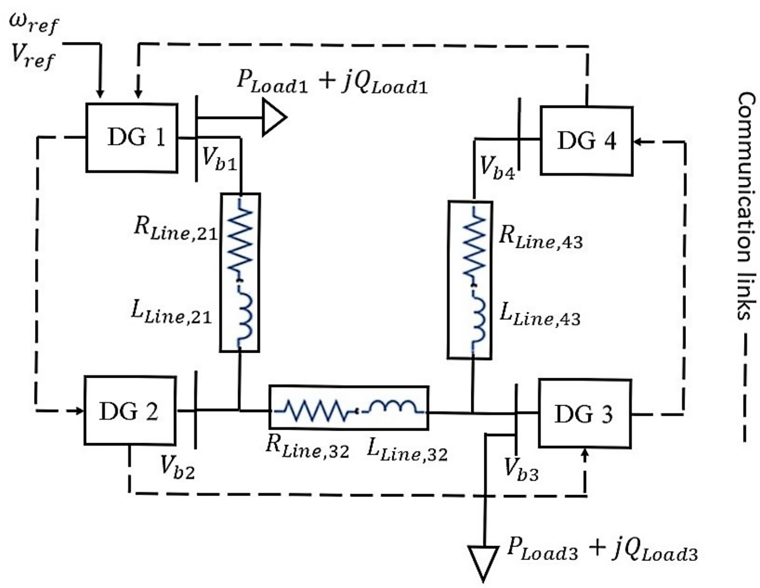

Figure 8.7: Network of 4 DGs with communication links and per phase line impedances

$$\begin{aligned}
&L_{Line,32} = 1847 \times 10^{-6}, L_{Line,43} = 318 \times 10^{-6},\\
&P_{Load1} = 12 \times 10^{3}, P_{Load3} = 15.3 \times 10^{3},\\
&Q_{Load1} = 12 \times 10^{3}, Q_{Load3} = 7.6 \times 10^{3}.
\end{aligned} \tag{8.59}$$

As shown in Fig. 8.7, we assume that DG 1 receives the grid reference set points

Table 8.1: Communication delays between the DGs

t	$\tau_{10}(t)$	$\tau_{21}(t) = \tau_{32}(t)$	$\tau_{43}(t)$
$i \leq t < i+0.2T$	0.1	0.48	0.3
$i+0.2T \leq t < i+0.3T$	0.1	0.3	0.4
$i+0.3T \leq t < i+0.4T$	0.33	0.3	0.2
$i+0.4T \leq t < i+0.5T$	0.33	0.1	0.2
$i+0.5T \leq t < i+0.7T$	0.48	0.2	0.2
$i+0.7T \leq t < i+0.9T$	0.24	0.2	0.48
$i+0.9T \leq t < i+T$	0.3	0.4	0.1

$V_{\text{ref}} = 380$ V and $\omega_{\text{ref}} = 60$ Hz. Now we introduce the communication delays between the DGs as shown in Table 8.1, where $i = 1, 2, \cdots,$ and $T = 10$. From the data in Table 8.1, we find $\bar{\tau} = 0.5$. Moreover, from the communication topology of the DG units in

Fig. 8.7 we obtain

$$H = \begin{bmatrix} 1 & 0 & 0 & 0 \\ -1 & 1 & 0 & 0 \\ 0 & -1 & 1 & 0 \\ 0 & 0 & -1 & 1 \end{bmatrix} \tag{8.60}$$

and consequently $\sigma_H = 3.5321$, $c_1 = 3$. With $\beta_0 = 2$, from (8.58) we evaluate $\bar{\mu} = 0.1164$. For simulation purpose, we select $\mu = 0.1153$ and after applying the control protocol (8.46) to the linearized subsystems (8.20) with this μ the simulation results are obtained in Figure 8.8.

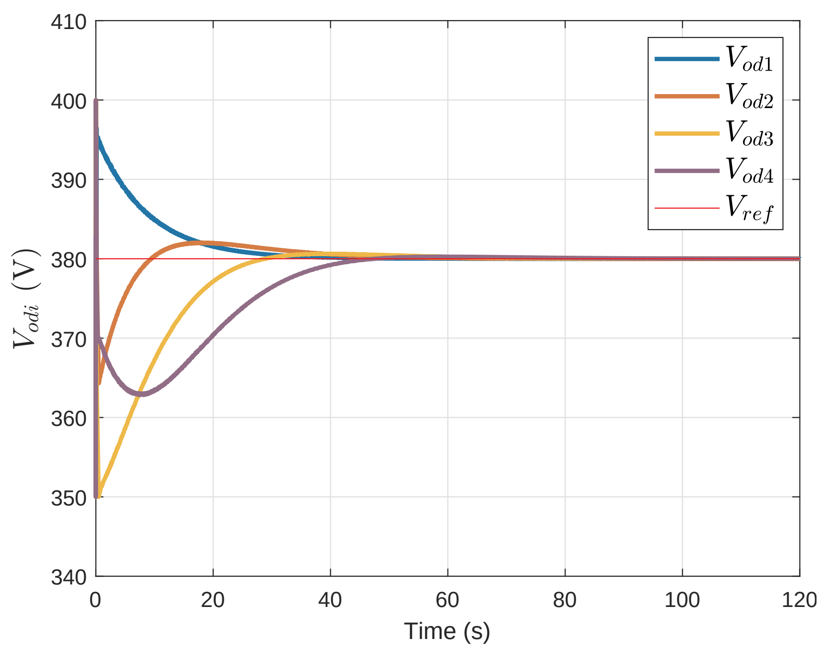

Figure 8.8: Filtered DG output voltage regulation

From Fig. 8.8 we observe that the DG output voltage magnitudes V_{odi} asymptotically converge to $V_{\text{ref}} = 380$ in the presence of unknown communication delays bounded within $[0, 0.5]$. However, for larger delay, a corresponding low gain bound can always be found from (8.58) to asymptotically stabilize the DG subsystems (8.20). We note here that the convergence will be slower as the delay goes larger but the proposed control protocol (8.46) can always guarantee asymptotic stability of (8.20)

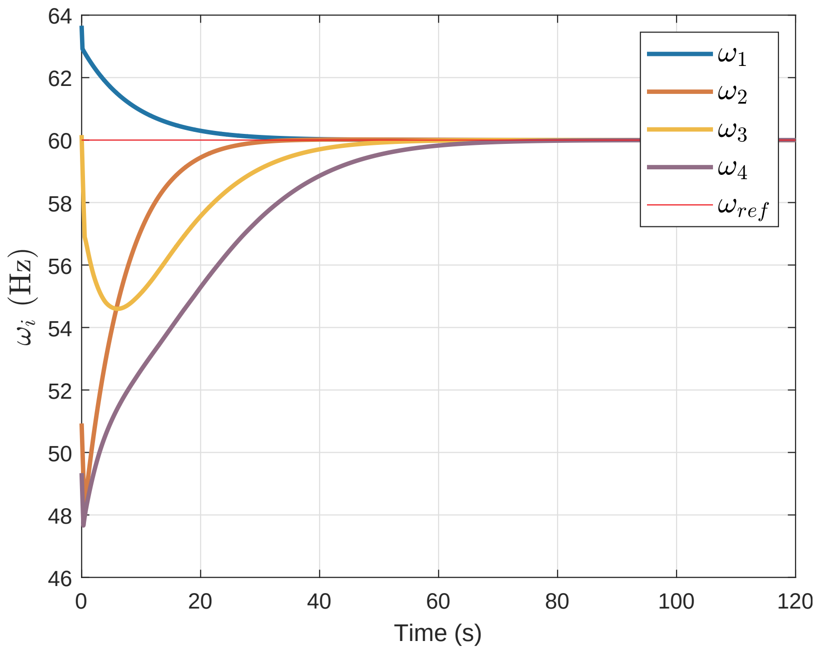

Figure 8.9: DG inverter frequency regulation

even when the delays are large enough. A similar control protocol for frequencies can achieve frequency synchronization, as observed from Fig. 8.9.

8.5 Conclusion

In this chapter we studied the voltage and frequency synchronization problem of inverter based islanded DG units under known or unknown arbitrary time varying communication delays. By linearizing the nonlinear DG dynamics with input output linearization and then by applying the proposed low gain based cooperative control protocol on the linearized subsystems we have shown that the DG terminal voltage and inverter frequencies are synchronized to the grid reference points in the presence of network latencies. We derived sufficient delay dependent conditions in terms of the upper bound of the low gain parameter to guarantee the stability of the synchronization. We also noted that the solution to this synchronization problem does not require any restrictive assumptions on the network topology when compared to the previous results.

With the help of an illustrative example we highlighted the effectiveness of our theoretical results. We demonstrated that the proposed low gain based control protocol can always render asymptotic stability to the DG units, although the speed of convergence is dictated by the delay bounds. The objectives of the DG synchronization problem are thus achieved with a low gain cooperative controller under arbitrary heterogeneous time delays and mild communication requirements. In future, we will explore the critical load restoration problem of islanded microgrids under time delays and switching network topologies.

Chapter 9

Conclusions and Future Work

In this dissertation we explored the CORP for MASs under the detectability constraint that none of the follower members were capable of independently estimating the leader trajectory from their individual measurements. As a result none of the followers could solve the output regulation problem by itself. In our proposed solution, we devised a novel distributed estimation algorithm based on the collective measurements by all the followers. This was achieved by issuing a "combined detectability" condition and a mild connectivity assumption to ensure the propagation of measurement signals among followers. With the estimated leader state, a distributed controller was designed for the followers and shown to solve the ORP under the assumptions and constraints considered in this thesis.

The motivations and the objectives of the research effort presented in this thesis were discussed in Chap. 1. Starting with the fundamental cooperative control problems, the discussion was extended to the traditional CORP. It was also noted that the objective for any classical cooperative control problem is to synthesize a distributed control law for the followers using the local information available to them from their neighbors. The challenges to the ORP under various constraints were described in greater detail along with the different approaches adopted to solve such problems. Furthermore, a brief overview of the subsequent chapters was also presented.

In Chapter 2, the CORP for linear MASs was studied under the detectability constraint discussed above. By proposing a novel estimation technique relying on the collective measurements of the followers, distributed state feedback and output feedback control solutions were offered. The design procedure for constructing the controller and observer gains were also depicted. With the help of a numerical example, the theoretically derived results were validated. Simulation results showed how the followers were able to successfully track the leader states, and the regulated output of the followers converged to zero asymptotically under the proposed control solution.

In Chapter 3, the solution to the CORP for nominal agent dynamics was extended to the problem when the dynamics of the agents are subject to additive paramateric uncertainties. It was also assumed that the local regulated error signals were not available to the followers for control. With the estimated leader states from Chap 2, an estimated regulated error signal was constructed and used as a feedback to the local control. The proposed distributed control solution incorporated an internal model of the leader to allow for norm-bounded uncertainties in the agents' dynamics. Additionally, a bound to the norm of the error in the regulated output is theoretically derived as a function of the uncertain parameters. A numerical example was presented, which showed that all the followers had the regulated outputs converged to zero asymptotically even in the presence of uncertainties in the dynamics.

In Chapter 4, we studied the CORP of MASs in a switching network, where the agents group do not have enough information to independently reconstruct the leader states at any single switching configuration. Extending the results from Chap. 2 to the case for dynamic network, we offered a novel distributed estimation algorithm to reconstruct the leader trajectory. Necessary conditions for the stability of the estimation error dynamics was derived, and the observer design procedure was also outlined. Based on the observed states, a distributed control law was constructed for the MASs with underlying switching communication. An illustrative example showed that the objectives of the CORP were achieved under given communication and detectability constraints.

In Chap. 5, the theoretical results developed in the former chapters were tested experimentally on the position synchronization problem of networked motors under the considered detectability constraint and switching communication topology. Firstly, we introduced the experimental setup consisting of a group of servomotors, a leader computer for generating the reference trajectory to be tracked by the follower motors, the communication between the networked motors through the TCP/IP protocol, and the PC's for implementing the estimation and control algorithms for each motors. Next, the control law was designed by suitably selecting the controller, observer gains and a scaling factor. By implementing the proposed control algorithm, it was observed that the tracking error for the follower servomotors incurs a small tracking error while other existing techniques were not applicable. Finally some discussions on the experimental results were presented along with a comparative analysis with respect to other existing methods in the literature.

In Chapters 6 and 7, we studied the distributed state estimation problem of a network of observers under heterogeneous time-invariant and time-varying communication delays. With the use of low-gain methodologies, we offer sufficient stability conditions of the estimation error dynamics in terms of the upper bound of the delay magnitude or the low gain parameter. The proposed distributed state estimation method is applied to then develop a control solution of the leader tracking problem in a leader-follower multi-agent system. Furthermore, in the presence of communication delays, we also investigated the distributed state estimation of an autonomous plant by a multi-observer systems for the case when the plant measurements are inflicted with noise. We found that the bounds on the local estimation errors are dictated by the supremum norm bounds of the disturbance signals.

In Chapter 8, we studied the voltage and frequency synchronization problem of inverter based islanded distributed generators under known or unknown arbitrary time-varying communication delays. With a low gain parameter in the consensus based control protocol, we derived sufficient delay dependent conditions for the stability of the synchronization.

9.1 Future Research

This dissertation addresses various cooperative control problems namely CORP, distributed state estimation and synchronization control of multi-agent systems under detectability constraints, uncertainty in agent dynamics, switching communication topologies and network latencies. While working on these research areas, we recognized several potential open problems which we would like to pursue in future research endeavors.

9.1.1 Task 1

One possible research direction is to study CORP for the case when the plant measurements are only available intermittently. Since the proposed control techniques rely on the continuous measurements from the exosystem, they do not apply when the exosystem measurement is only available sporadically. For non-minimum SISO systems, tracking of intermittent periodic output for a single agent system was studied by [116]. For intermittent aperiodic measurements, output regulation problem for nonlinear minimum phase systems was studied by the authors of [117]. However, to the best of authors' knowledge, there have been no analogous results available for the CORP of multi-agent system in case when "informed" agents receive only an insufficient measurement from the exosystem aperiodically. Therefore, studying the CORP with aperiodic exosystem measurements with the considered detectability constraint is an interesting future research endeavor.

9.1.2 Task 2

The implementation of a control algorithm in practical applications inevitably suffers from the challenge of actuator saturation. Control input saturation is probably the most usual nonlinearity encountered in control engineering because of the hardware constraints of sensors and actuators. If the effects of saturation are ignored in the design, a controller may "wind up" the actuator, possibly resulting in degraded performance or even instability. A classical approach to avoiding such undesirable behaviors is to add an anti-windup compensator to the original controller. Recently, in [118], a Riccati equation based design approach was adopted to deal with this problem. For a general linear system with the open-loop poles being located in the closed left half plane, a low-gain design method [119] relying on a parametric Lyapunov equation [120] was developed to achieve semi-global stabilization.

While the effects of actuator saturation were considered for the synchronization problem [121], there have been no analogous results available for the CORP. With this as motivation, we would like to extend the results for CORP under detectability constraints to the case when the control input for the follower agents is limited by actuator saturation.

Bibliography

[1] L. Garattoni and M. Birattari. Autonomous task sequencing in a robot swarm. *Sci. Robot*, 3(20):1–12, 2018.

[2] H. Basu and S. Y. Yoon. Cooperative output regulation of multi-agent systems with incomplete exosystem measurement. In *55th IEEE Conf. on Decision and Control*, pages 951–956, Las Vegas, USA, December 2016.

[3] H. Basu and S. Y. Yoon. Robust cooperative output regulation of a linear multi-agent system with incomplete exosystem measurement. In *IEEE Int. Conf. Advanced Intelligent Mechatronics*, pages 1406–1411, Munich, Germany, 2017.

[4] J. A. Fax and R. M. Murray. Information flow and cooperative control of vehicle formations. *IEEE Trans. Autom. Control*, 49(9):1465–1476, 2014.

[5] H. Kim, H. Shim, and J. H. Seo. Output consensus of heterogeneous uncertain linear multi-agent systems. *IEEE Trans. Autom. Control*, 56(1):200–206, Jan. 2011.

[6] F. Xiao, L. Wang, J. Chen, and Y. Gao. Finite-time formation control for multi-agent systems. *Automatica*, 45(11):2605–2611, 2009.

[7] M. Porfiri, D. Robertson, and D. Stilwell. Tracking and formation control of multiple autonomous agents: A two level consensus approach. *Automatica*, 43:1318–1328, 2007.

[8] R. Ramaithitima, M. Whitzer, S. Bhattacharya, and V. Kumar. Sensor coverage robot swarms using local sensing without metric information. In *2015 IEEE International Conference on Robotics and Automation (ICRA)*, pages 3408–3415, Washington, USA, 2015.

[9] Y. Wang, E. Garcia, D. Casbeer, and F. Zhang. *Cooperative Control of Multi-Agent Systems: Theory and Applications*. Wiley, 2017.

[10] W. Ren, R. Beard, and E. Atkins. Information consensus in multivehicle cooperative control. *IEEE Control Syst. Mag.*, 27(2):71–82, 2007.

[11] W. Ren and R. Beard. *Distributed consensus in multivehicle cooperative control*. Communication and Control Engineering. Springer-Verlag, London,UK, 2008.

[12] W. Ren and Y. Cao. *Distributed Coordination of Multi-agent Networks*. Communications and Control Engineering. Springer-Verlag, London, 2011.

[13] W. Ren, R. Beard, and E. Atkins. A suvey of consensus problems in multi-agent coordination. In *Proc. Amer. Control. Conf.*, pages 1859–1864, Portland, OR, 2005.

[14] S. Sundaram and C. N. Hadjicostis. Finite-time distributed consensus in graphs with time-invariant topologies. In *Proceedings of the 2007 American Control Conference*, pages 711–716, New York City, USA, 2007.

[15] W. Ren and R. Beard. Consensus seeking in multiagent systems under dynamically changing interaction topologies. *IEEE Trans. Autom. Control*, 50(5):655–661, May 2005.

[16] A. Jadbabaie, J. Lin, and A. Morse. Coordination of groups of mobile autonomous agents using nearest neighbor rules. *IEEE Trans. Autom. Control*, 48(6):988–1001, Jun. 2003.

[17] R. Olfati-Saber and R. Murray. Consensus problems in networks of agents with switching topology and time delays. *IEEE Trans. Autom. Control*, 49(9):1520–1533, Sep. 2004.

[18] Y.-P. Tian and Y. Zhang. High-order consensus of heterogeneous multi-agent systems with unknown communication delays. *Automatica*, 48(6):1205–1212, Jun. 2012.

[19] L. Zeng and G. Hu. Consensus of linear multi-agent systems with communication and input delays. *Acta Automatica Sinica*, 39(7), July 2013.

[20] W. Zhenzua, X. Juanjuan, Z. Huanshui, and L. Shengtao. Consensus of first-order agents with time-varying communication delay. In *Proc. of the 35th Chinese Control Conf.*, pages 8120–8124, Chengdu, China, July 2016.

[21] B. A. Francis. Linear multivariable regulator problem. *SIAM J. Control Optim.*, 15:486–505, 1977.

[22] A. Isidori and C. I. Byrnes. Output regulation of nonlinear systems. *IEEE Trans. Autom. Control*, 35:131–140, 1990.

[23] J. Huang. *Nonlinear Output Regulation: Theory and Applications*. Advances in Design and Control. SIAM, Philadelphia, 2004.

[24] M. Lu and J. Huang. Cooperative output regulation problem for linear time-delay multi-agent systems under switching network. *Neurocomputing*, 190:132–139, 2016.

[25] M. Lu and J. Huang. Cooperative output regulation problem for linear time-delay multi-agent systems under switching network. In *in proc. 30th Chinese Control Conf.*, Yantai, China, July 2011.

[26] A. Loria, J. Dasdemir, and N. A. Jarquin. Leader–follower formation and tracking control of mobile robots along straight paths. *IEEE Trans. Control Syst. Technol.*, 24(2):727–732, 2016.

[27] J. Hu and Y. Hong. Leader following coordination of multiagent system with coupling time delays. *Physica A: stat. Mech. Appl.*, 374(2):853–863, 2007.

[28] X. Wang, Y. Hong, J. Huang, and Z. Jiang. A distributed control approach to a robust output regulation problem for multi agent linear systems. *IEEE Trans. Autom. Control*, 55(12):2891–2895, Dec. 2010.

[29] Y. Su and J. Huang. Cooperative output regulation of linear multiagent systems. *IEEE Trans. Autom. Control*, 57(4):1062–1066, 2012.

[30] Y. Su and J. Huang. Cooperative output regulation of linear multiagent systems by output feedback. *Syst. and Control Lett.*, 61(12):1248–1253, 2012.

[31] J. Xiang, W. Wei, and Y. Li. Synchronized output regulation of linear networked systems. *IEEE Trans. Autom. Control*, 54(6):1336–1341, 2009.

[32] J. Huang. Remarks on synchronized output regulation of linear networked systems. *IEEE Trans. Autom. Control*, 56(3):630–631, 2011.

[33] Y. Su, Y. Hong, and J. Huang. A result on the cooperative robust output regulation for linear uncertain multi-agent systems. In *Proc. 9th IEEE Int. Conf. on Control and Autom.*, pages 639–643, Santiago, Chile, Dec 2011.

[34] Y. Su and J. Huang. Cooperative robust output regulation of linear uncertain multi-agent systems. In *Proc. of the 10th World Congress on Intelligent Control and Autom.*, pages 1299–1304, Beijing, China, Jul. 2012.

[35] Y. Su. Cooperative output regulation for linear uncertain multi-agent systems with nonidentical relative degrees. In *proc. 34th Chinese Control Conf.*, pages 2836–2841, Hangzhou, China, July 2015. IEEE.

[36] Y. Su and J. Huang. Cooperative robust output regulation of a class of heterogenous linear uncertain multi-agent systems. *Int. J. Robust. Nonlinear Control*, 24:2819–2839, June 2013.

[37] W. Liu and J. Huang. Cooperative global robust output regulation for a class of nonlinear multi-agent systems with switching networks. *IEEE trans. Autom. Control*, 60:1963–1968, July 2015.

[38] Y. Su and J. Huang. Cooperative adaptive output regulation for a class of nonlinear uncertain multi-agent systems with unknown leader. *Syst. and Control Lett.*, 62:461–467, 2013.

[39] H. Zhang, F. L. Lewis, and A. Das. Optimal design for synchronization of cooperative systems: State feedback, observer and output feedback. *IEEE Trans. Autom. Control*, 56(8):1948–1952, 2011.

[40] I. Pan, A. Mukherjee, S. Das, and A. Gupta. Simulation studies on multiple control loops over a bandwidth limited shared communication network with packet dropouts. In *Proceeding of the 2011 IEEE Students' Technology Symposium*, pages 113–118, Kharagpur, India, 2011.

[41] Y. Su and J. Huang. Cooperative output regulation with application to multi-agent consensus under switching network. *IEEE Trans. Sys., Man, and Cybern.B.l*, 42(3):864–875, June 2012.

[42] S. Wang and J. Huang. Cooperative output regulation of singular multi-agent systems under switching network by standard reduction. *IEEE Trans. Circuits Syst. I, Reg. Papers*, 65(4):1377–1385, 2018.

[43] J. Liang, B. Shen, H. Dong, and J. Lam. Robust distributed state estimation for sensor networks with multiple stochastic communication delays. *Int. J. Syst. Sci.*, 42(9):1459–1471, 2011.

[44] H. Li, X. Liao, X. Lei, T. Huang, and W. Zhu. Second-order consensus seeking in multi-agent systems with nonlinear dynamics over random switching directed networks. *IEEE Trans. Circuits Syst. I, Reg. Papers*, 60(6):1595–1607, June 2013.

[45] B. Zhou and Z. Lin. Consensus of high-order multi-agent systems with input and communication delays- state feedback case. In *2013 American Control Conf.*, pages 4027–4032, Washington DC, USA, 2013.

[46] K. Liu, J. Lu, and Z. Lin. Design of distributed observers in the presence of arbitrarily large communication delays. *IEEE Trans. Neural Netw. Learn Syst.*, 29(9):4447–4461, 2018.

[47] W. Yu, G. Chen, J. Lu, and J. Kurths. Synchronization via pinning control on general complex networks. *SIAM J. CONTROL OPTIM.*, 51(2):1395–1416, 2013.

[48] L. Yu and J. Wang. Robust cooperative control for multi-agent systems via distributed output regulation. *Syst. and Control Lett.*, 62:1049–1056, 2013.

[49] Y. Yan and J. Huang. Cooperative output regulation of discrete-time linear time-delay multi-agent systems under switching network. *Neurocomputing*, 241:108–114, 2017.

[50] Q. Jia and W. K. S. Tang. Consensus of nonlinear agents in directed network with switching topology and communication delay. *IEEE Trans. on Circuits and Systems*, 59(12):3015–3023, 2012.

[51] W. Ni and D. Cheng. Leader-following consensus of multi-agent systems under fixed and switching topologies. *Syst. and Control Lett*, 59:209–217, 2010.

[52] G. Casadei, L. Marconi, and A. Isidori. About disconnected topologies and synchronization of homogeneous nonlinear agents over switching networks. *International Journal of Robust and Nonlinear Control*, 28(3):901–917, 2018.

[53] H. Basu and S. Y. Yoon. Cooperative output regulation of multi-agent systems in a switching network with incomplete exosystem measurement. In *Proc. of 2018 Annual American Control Conference (ACC)*, pages 5195–5200, Wisconsin, USA, June 2018.

[54] D. Aeyels and J. Peuteman. On exponential stability of nonlinear time-varying differntial equations. *Automatica*, 35:1091–1100, 1999.

[55] B. Zhou. *Truncated Predictor Feedback for Time-Delay Systems*. Springer, 2014.

[56] F. Perez-Pinal, C. Nunez, R. Alvarez, and I. Cervantes. Comparison of multi-motor synchronization techniques. In *30th Annual Conference of IEEE Industrial Electronics Society (IECON 2004)*, Busan, South Korea, 2004.

[57] V. Chauhan and V. P. Patel. Multi-motor synchronization techniques. *International Journal of Science, Engineering and Technology Research*, 3(2):319–322, 2014.

[58] S. J. Yague, G. R. Carmenaty, A. R. Blanco, and A. G. Cerrada. Distributed cooperative control for stepper motor synchronization. *MATEC Web of Conferences*, 167(02001):1–10, 2018.

[59] S.-Y. Lin. A distributed state estimator for electric power systems. *IEEE Trans. Power Syst*, 7(2):551–557, 1992.

[60] S. Kar, G. Hug, J. Mohammadi, and J. M. F. Maura. Distributed state estimation and energy management in smart grids: A consensus+innovations approach. *IEEE J. Sel. Topics Signal Process.*, 8(6):1022–1038, 2014.

[61] W. Jiang, V. Vittal, and G. T. Heydt. A distributed state estimator utilizing synchronized phasor measurements. *IEEE Trans. Power Syst.*, 22(2):563–571, 2017.

[62] L. Xie, D-H. Choi, S. Kar, and H. V. Poor. Fully distributed state estimation for wide-area monitoring systems. *IEEE Trans. Smart Grid*, 3(3):1154–1169, 2012.

[63] K. Menighed, C. Aubrun, and J-J. Yame. Distributed state estimation and model predictive control : Application to fault tolerant control. In *2009 IEEE Int. Conf. on Control and autom.*, pages 936–941, Christchurch, New Zealand, Dec. 2009.

[64] H. Leung, S. Chandana, and S. Wei. Distributed sensing based on intelligent sensor networks. *IEEE Circuits Syst. Mag.*, 8(2):38–52, 2008.

[65] R. Olfati-Saber. Kalman-consensus filter : Optimality, stability, and performance. In *Joint 48th IEEE Conf. on Decision and Control and 28th Chinese Control Conf.*, pages 7036–7042, Shanghai, China, Dec. 2009.

[66] R. Olfati-Saber. Distributed kalman filtering for sensor networks. In *Proc. of the 46th IEEE Conf. on Decision and Control*, pages 5492–5498, New Orleans, LA, USA, Dec. 2007.

[67] U. A. Khan and J. M. F. Moura. Distributing the kalman filter for large-scale systems. *IEEE Trans. Signal Process.*, 56(10):4919–4935, Oct. 2008.

[68] S. Park and N. C. Martins. Design of distributed lti observers for state omniscience. *IEEE Trans. Autom. Control*, 62(2):561–576, 2017.

[69] L. Wang and A. S. Morse. A distributed observer for a time-invariant linear system. In *Proc. of 2017 American Control Conf.*, pages 2020–2025, Seattle, WA, USA, 2017. IEEE.

[70] L. Wang, A. S. Morse, D. Fullmer, and J. Liu. A hybrid observer for a distributed linear system with a changing neighbor graph. In *Proc. of 2017 IEEE 56th Annual Conf. on Decision and Control*, pages 1024–1029, Melbourne, Australia, December 2017.

[71] H. Basu and S. Y. Yoon. Robust cooperative output regulation under exosystem detectability constraint. *Int. J. Control*, 2018. accepted.

[72] B. Zhou, Z. Lin, and G. Duan. Truncated predictor feedback for linear systems with long time-varying input delays. *Automatica*, 48:2387–2399, 2012.

[73] S. Y. Yoon and Z. Lin. Truncated predictor feedback control for exponentially unstable linear systems with time-varying input delay. *Syst. and Control Lett.*, 62:837–844, 2013.

[74] B. Zhou, Z. Lin, and G. Duan. Stabilization of linear systems with input delay and saturation- a parametric lyapunov equation approach. *Int. J. Robust Nonlinear Control*, 20:1502–1519, 2010.

[75] K. Gu. An integral inequality in the stability problem of time-delay systems. In *Proc. of the 39th IEEE Conf. on Decision and Control*, pages 2805–2810, Sydney, Australia, Dec. 2000.

[76] E. Fredman. Tutorial on lyapunov-based methods for time-delay systems. *European Journal of Control*, 20:271–283, 2014.

[77] W. Yu, G. Chen, J. Lu, and J. Kurths. Synchronization via pinning control on general complex networks. *SIAM J. CONTROL OPTIM.*, 51(2):1395–1416, 2013.

[78] V. A. Ugrinovskii. Distributed robust filtering with h_∞ consensus of estimates. In *Proc. of the 2010 American Control Conference*, pages 1374–1379, Baltimore, MD, USA, 2010.

[79] V. A. Ugrinovskii. Distributed robust filtering with h_∞ consensus of estimates. *Automatica*, 47(1):1–13, 2011.

[80] H. Dong, Z. Wang, F. E. Alsaadi, and B. Ahmad. Event-triggered robust distributed state estimation for sensor networks with state-depndent noises. *Int. J. Gen. Syst.*, 44(2):254–266, 2015.

[81] P. Pepe and Z. P. Ziang. A lyapunov–krasovskii methodology for iss and iiss of time-delay systems. *Syst. Control Lett.*, 55:1006–1014, 2006.

[82] Z. Liu, W. Yan, H. Li, and M. Small. Cooperative output regulation problem of multi-agent systems with stochastic packet dropout and time-varying communication delay. *J. FRANKLIN I.*, 355(17):8664–8682, 2018.

[83] Z. Wang, J. Xu, and H. Zhang. Consenusability of multi-agent systems with time-varying communication delay. *Syst. & Control Lett.*, 65:37–42, 2014.

[84] Z-J. Tang, T-Z. Huang, J-L. Shao, and J-P. Hu. Consensus of second-order multi-agent systems with nonuniform time-varying delays. *Neurocomputing*, 97:410–414, 2012.

[85] U. Munz, A. Papachristodoulou, and F. Allgower. Nonlinear multi-agent system consensus with time-varying delays. In *In Proc. of the International Federation of Automatic Control*, pages 1522–1527, Seoul, Korea, 2008.

[86] Q. Jia, W. K. S. Tang, and W. A. Halang. Leader following of nonlinear agents with switching connective network and coupling delay. *IEEE Trans. Circuits Syst. I, Reg. Papers*, 58(10):2508–2519, 2011.

[87] J. Wei and H. Fang. Multi-agent consensus with time-varying delays and switching topologies. *Journal of Systems Engineering and Electronics*, 25(3):489–495, 2014.

[88] B. Zhou and Z. Lin. Consensus of high-order multi-agent systems with large input and communication delays. *Automatica*, 50:452–464, 2014.

[89] Y. Wei and Z. Lin. Delay independent truncated predictor feedback for stabilization of linear systems with multiple time-varying input delays. In *Proc. of the 2017 American Control Conference*, pages 5732–5737, Seattle, USA, 2017.

[90] H. Basu and S. Y. Yoon. Distributed state estimation by a network of observers under communication and measurement delays. *IFAC PapersOnLine*, 52(20):13–18, 2019.

[91] H. Basu and S. Y. Yoon. Distributed state estimation by a network of observers under communication and measurement delays. *Syst. and Control Lett.*, 133:1045–1054, 2019.

[92] Norm Finn. Deterministic networking. In *IETF IEEE Retreat I*, Newark, USA, 2014.

[93] A. Bidram, A. Davoudi, F. L. Lewis, and Z. Qu. Secondary control of microgrids based on distributed cooperative control of multi-agent systems. *IET Gener. Transm. Distrib.*, 7(8):822–831, 2013.

[94] N. Pogaku, M. Prodanovic, and T. C. Green. Modeling, analysis and testing of autonomous operation of an inverter-based microgrid. *IEEE Trans. Power Electron.*, 22(2):613–625, 2007.

[95] A. Bidram and A. Davoudi. Hierarchical structure of microgrids control system. *IEEE Trans. Smart Grid*, 3(4):1963–1976, 2012.

[96] A. Bidram, A. Davoudi, F. L. Lewis, and J. M. Guerrero. Distributed cooperative secondary control of microgrids using feedback linearization. *IEEE Trans. Power Syst.*, 28(3):3462–3470, 2013.

[97] M. Ma and A. Lahmedi. On the impact of synchronization attacks on distributed and cooperative control in microgrid systems. In *Proc. of s. IEEE Int. Conf. on Communications, Control, and Computing Technologies for Smart Grids*, Aalborg, Denmark, 2018.

[98] J. W. S.-Porco, F. Dorfler, and F. Bullo. Synchronization and power sharing for droop-controlled inverters in islanded microgrids. *Automatica*, 49(9):2603–2611, 2013.

[99] J. A. P. Lopes, C. L. Moreira, and A. G. Madureira. Defining control strategies for microgrids islanded operation. *IEEE Trans. Power Syst.*, 21(2):916–924, 2006.

[100] J. W. S.-Porco, Q. Shafiee, F. Dörfler, J. C. Vasquez, J. M. Guerrero, and F. Bullo. Secondary frequency and voltage control of islanded microgrids via distributed averaging. *IEEE Trans. Ind. Electron.*, 62(11):7025–7038, 2005.

[101] S. Shah, H. Sun, D. Nikovski, and J. Zhang. Consensus-based synchronization of microgrids at multiple points of interconnection. In *Proc. of the 2018 IEEE Power & Energy Society General Meeting (PESGM)*, Portland, OR, USA, 2018.

[102] V. Kounev, D. Tipper, A. A. Yavuz, B. M. Grainger, and G. F. Reed. A secure communication architecture for distributed microgrid control. *IEEE Trans. Smart Grid*, 6(5):2484–2492, 2015.

[103] Cisco. Time-sensitive networking: A technical introduction, 2017.

[104] J. Lai, H. Zhou, W. Hu, and L. Zhong. Synchronization of hybrid microgrids with communication latency. *Mathematical Problems in Engineering*, 2015(10):1–11, 2015.

[105] J. Lai, X. Lu, R-Li. Tang, X. Li, and Z. Dong. Delay-tolerant distributed voltage control for multiple smart loads in ac microgrids. *ISA Transactions*, 86:181–191, 2019.

[106] S. Kotpalliwar, S. Satpute, S. Meshram, F. Kazi, and N. Singh. Modelling and stability of time-delayed microgrid systems. In *Proc. of the 9th IFAC Symposium on Control of Power and Energy Systems CPES*, pages 294–299, New Delhi, India, 2015.

[107] X. Lu, N. Chen, Y. Wang, L. Qu, and J. Lai. Distributed impulsive control for islanded microgrids with variable communication delays. *IET CONTROL THEORY A.*, 10(14):1732–1739, 2016.

[108] X. Lu, X. Yu, J. Lai, Y. Wang, and J. M. Guerrero. A novel distributed secondary coordination control approach for islanded microgrids. *IEEE Trans. Smart Grid*, 9(4):2726–2740, 2018.

[109] C.-K. Nguyen, T.-T. Nguyen, H.-J. Yoo, and H.-M. Kim. Improving transient response of power converter in a stand-alone microgrid using virtual synchronous generator. *Energies*, 11(27):1–17, 2018.

[110] U. B. Tayab, M. A. B. Roslan, L. J. Hwai, and M. Kashif. A review of droop control techniques for microgrid. *Renew. Sust. Energ. Rev.*, 76:717–727, 2017.

[111] H. R. Pota. Droop control for islanded microgrids. In *Proc. IEEE Power Eng. Soc. Gen. Meet.*, pages 1–4, Vancouver, Canada, 2013.

[112] A. D. Banadaki, F. D. Mohammadi, and A. Feliachi. State space modeling of inverter based microgrids considering distributed secondary voltage control. In *2017 North American Power Symposium (NAPS)*, Morgantown, WV, USA, 2017.

[113] Q. Shafiee, J. M. Guerrero, and J. C. Vasquez. Distributed secondary control for islanded microgrids—a novel approach. *IEEE Trans. Power Electron.*, 29(2):1018–1031, 2014.

[114] Z. Li, Z. Duan, G. Chen, and L. Huang. Consensus of multiagent systems and synchronization of complex networks: A unified viewpoint. *IEEE Trans. Circuits Syst. I, Reg. Papers*, 57(1):213–224, 2010.

[115] H. Basu and S. Y. Yoon. Distributed state estimation by a network of observers under communication and measurement delays. *Syst. Control Lett.*, 133, 2019.

[116] R. Jafari and R. Mukherjee. Intermittent output tracking for linear single-input single-output non-minimum-phase systems. In *Proc. of the 2012 American Control Conference (ACC)*, Montreal, Canada, 2012.

[117] D. Astolfi, G. Casadei, and R. Postoyan. Emulation-based semiglobal output regulation of minimum phase nonlinear systems with sampled measurements. In *Proc. of the 16th European Control Conference*, Limassol, Cyprus, 2018.

[118] Z. Lin and A. Saberi. Semi-global exponential stabilization of linear discrete-time systems subject to input saturation via linear feedbacks. *Syst. and Control Lett.*, 24:125–132, 1995.

[119] Z. Lin. *Low Gain Feedback*. Springer, London, 1998.

[120] B. Zhou, G. Duan, and Z. Lin. A parametric lyapunov equation approach to the design of low gain feedback. *IEEE Trans. Autom. Control*, 53(6):1548–1554, July 2008.

[121] K. Takaba. Synchronization of linear multi-agent systems under input saturation. In *21st International Symposium on Mathematical Theory of Networks and Systems*, pages 1076–1079, Groningen, Netherlands, 2014.